

**WestminsterResearch**

<http://www.westminster.ac.uk/westminsterresearch>

**Investigating Microbial Quorum Sensing Potential for Enhanced  
Production of Biodegradable Polymers**

**Aziz, Z.**

This is an electronic version of a PhD thesis awarded by the University of Westminster.

© Mr Zain Aziz, 2021.

The WestminsterResearch online digital archive at the University of Westminster aims to make the research output of the University available to a wider audience. Copyright and Moral Rights remain with the authors and/or copyright owners.

# **Investigating Microbial Quorum Sensing Potential for Enhanced Production of Biodegradable Polymers**

Zain Aziz

A thesis submitted in partial fulfilment of the requirements  
of the University of Westminster for the degree of Doctor  
of Philosophy

March 2021

## Abstract

Polyhydroxyalkanoates (PHA) are a type of biopolymer that can be biosynthesised and accumulated by several specialised bacterial species. Their favourable mechanical properties coupled with their ability to naturally biodegrade within the environment make PHAs a potential candidate to replace traditional plastics, which cause harm to our environment, our wildlife and ourselves. One of the main drawbacks associated with PHAs, is the difficulty of producing them in large quantities, which hinders their potential usage. However, the manipulation of quorum sensing circuits has yet to be explored in the context of increasing the amount of PHA produced by bacterial species. Quorum sensing is a process of cell-to-cell communication, that allows for bacteria to share information about cell densities and coordinate gene expression, such as altering the production of secondary metabolites like PHAs.

During this study two Gram-negative bacterial species (*Cupriavidus necator* H16 and *Pseudomonas putida* KT2440) were grown in specific production media and supplemented with three different exogenous quorum molecules sensing ( $C_4$ -HSL,  $C_6$ -HSL and 3-oxo- $C_{12}$ -HSL), to study if there was a change in the amount of PHA produced. It was observed that *C. necator* H16 increased production of PHAs, specifically small chain length PHA (SCL PHA) poly(3-hydroxybutyrate) (P(3HB)), by 13.03% and 17.85% when grown in shake flasks and bioreactors, when supplemented with the quorum sensing molecule 3-oxo- $C_{12}$ -HSL. Whilst PHA production increased in culture of *P. putida* KT2440, when supplemented with  $C_4$ -HSL. PHA production of the medium chain length polymer (MCL PHA) of poly(3-hydroxyoctanoate-co-3-hydroxydecanoate-co-3-hydroxydodecanoate) (P(3HO-co-3HD-co-3HDD)) increased by 7.24% and 10.89% when grown in shake flasks and bioreactors, respectively.

To understand as to why there was a change in production of PHAs produced by the two species of bacteria, qPCR was used to measure the expression of two key *Pha* genes (*PhaC1* and *PhaZ*) when exposed to exogenous quorum sensing molecules in bioreactors. *C. necator* H16 displayed an increase in regulation of the *PhaC1* gene, within 24 hours of fermentation by 2.53-fold when supplemented with 3-oxo- $C_{12}$ -HSL. Alternatively, *PhaZ* displayed an increase in transcription at the same time point, but by 1.48-fold. *P. putida* KT2440 cultures displayed a significant increase in regulation of *PhaC1* at 48 hours of fermentation when supplemented with both  $C_4$ -HSL and 3-oxo- $C_{12}$ -HSL. Although an increase of *PhaZ* was also observed, it was less than *PhaC1*.

## **Acknowledgements**

To begin I would like to take this opportunity to thank everyone that has supported me throughout this PhD journey.

First, I would like to express my sincerest gratitude to my supervisor Professor Tajalli Keshavarz without whom this project would never have taken place. Thank you for identifying something in me and helping to nurture and develop me not only as a researcher, but as a person too. Your guidance throughout this project has been invaluable. I am under no illusion that at times I have been difficult to work with, however you consistently persisted with me, and ultimately the result is this piece of research. I hope you enjoyed these last few years as much as I did. I'd also like to thank Dr Godfrey Kyazze for his continuous support throughout this PhD.

Thank you to all the technical staff at the University of Westminster within the Faculty of Science and Technology for their assistance, particularly, Thakor Tandel and Neville Antonio.

I would also like to thank all my friends and colleagues from Lab C6.06 at the University of Westminster for their friendship and support, with special recognition to Dr Nasim Farahmand.

I would also like to make special acknowledgment to my very good friend, Dr Mahek Merchant. I truly do not think I would have ever been able to complete this journey without you by my side. I cannot thank you enough for the encouragement and support you have provided over all these years, which you did from when I first met you during my undergraduate degree as your student up until this very moment of writing my acknowledgments. I am so appreciative of the friendship we have developed as I know you have always been my biggest supporter and wanted the absolute best for me. Thank you for everything.

Finally, I would like to thank my entire family, especially my parents for their unconditional love and support. You have all supported me throughout this process and always believed I could achieve great things. I hope this makes you all proud, because it was always for you.

## Table of Contents

<b>Abstract</b> .....	II
<b>Acknowledgements</b> .....	III
<b>Table of Contents</b> .....	IV
<b>List of Figures</b> .....	X
<b>List of Tables</b> .....	XVIII
<b>List of Equations</b> .....	XXIII
<b>List of Appendices</b> .....	XXIII
<b>List of Abbreviations</b> .....	XXV
<b>Chapter 1: Introduction</b> .....	1
1.1    Plastics .....	2
1.1.1    Fossil-fuel derived plastics .....	3
1.1.1.1    Disposal Methods .....	5
1.1.1.1.1    Landfill.....	5
1.1.1.1.2    Incineration.....	7
1.1.1.1.3    Recycling.....	8
1.1.2    Biopolymers.....	11
1.2    Polyhydroxyalkanoates (PHAs) .....	13
1.2.1    Discovery of PHAs.....	14
1.2.2    Types and characteristics of PHAs.....	16
1.2.2.1    Short-chain-length PHAs (SCL PHAs).....	17
1.2.2.2    Medium-chain-length PHAs (MCL PHAs) .....	17
1.2.3    Biosynthesis and metabolism of PHAs .....	18
1.2.3.1    Biosynthesis of SCL PHAs.....	19
1.2.3.2    Biosynthesis of MCL PHAs .....	20
1.2.3.3    Classification of PHA synthases and their genes.....	22
1.2.4    Biodegradability of PHAs.....	25
1.2.5    Production strategies.....	26
1.2.5.1    Raw materials .....	26

1.2.5.2	Batch fermentation.....	27
1.2.5.3	Fed-batch fermentation.....	28
1.2.5.4	Continuous fermentation.....	29
1.3	Microbial production of PHAs .....	30
1.3.1	Gram-negative bacteria .....	30
1.3.2	Gram-positive bacteria .....	33
1.3.3	<i>Archaea</i> .....	34
1.3.4	Detection of PHA.....	36
1.3.4.1	Downstream recovery process methods.....	40
1.4	Global markets and economics of PHAs .....	43
1.5	Applications of PHAs .....	45
1.5.1	Biomedical applications of PHAs.....	45
1.5.1.1	PHAs as the scaffold materials in wound management .....	45
1.5.1.2	PHAs as drug delivery systems .....	46
1.6	Quorum sensing .....	47
1.6.1	Quorum sensing in bacteria.....	48
1.6.1.1	Mechanisms of quorum sensing molecules in Gram-negative bacteria .....	48
1.6.1.2	Mechanisms of quorum sensing molecules in Gram-positive bacteria .....	50
1.6.1.3	Interspecies Quorum Sensing.....	54
1.6.2	Quorum Sensing applications.....	55
1.6.2.1	Quorum sensing inhibition - Quorum quenching.....	55
1.6.2.2	Biosensors and quorum sensing.....	56
1.6.2.3	Quorum sensing and PHA production.....	58
1.7	Hypothesis.....	60
1.8	Aim and objectives.....	60
<b>Chapter 2:</b>	<b>Materials and method .....</b>	<b>62</b>
2.1	Materials, chemicals and reagents .....	63

2.2	Bacterial strains .....	63
2.2.1	Long-term storage of bacterial strains .....	63
2.2.2	Preparation of working stock .....	64
2.3	Media.....	64
2.3.1	Inoculum medium .....	66
2.3.2	PHA production media.....	66
2.3.2.1	<i>C. necator</i> H16 PHA production medium .....	66
2.3.2.2	<i>P. putida</i> KT2440 PHA production medium .....	67
2.4	Experimental setup.....	68
2.4.1	Preparation of quorum sensing molecules .....	68
2.4.2	Preparation of inoculum for shaken flask fermentation.....	69
2.4.3	Shake flask fermentation process.....	69
2.4.4	Preparation of inoculum for bioreactor fermentation.....	71
2.4.5	Bioreactor fermentation .....	72
2.5	Analytical methods.....	74
2.5.1	Optical density (OD) measurements.....	74
2.5.2	pH measurements .....	74
2.5.3	Dry cell weight (DCW) .....	75
2.5.4	Quantification of total carbohydrates .....	75
2.5.5	Estimation of nitrogen concentration .....	76
2.5.6	PHA extraction.....	77
2.5.6.1	Solvent dispersion/Sodium hypochlorite digestion method .	77
2.5.6.2	Soxhlet extraction .....	78
2.5.7	Crotonic acid method for PHA concentration determination ...	79
2.6	Kinetic growth parameters calculations .....	80
2.6.1	Growth yield .....	80
2.6.2	Product yields.....	80
2.6.3	Specific production rate .....	81
2.7	Identification and structural characterisation of PHAs .....	81
2.7.1	Phase contrast microscopy .....	81
2.7.2	Macroscopic observation of PHAs via Sudan Black B colony staining	82

2.7.3	Fluorescence microscopy and Nile red staining .....	82
2.7.4	Fourier Transform Infrared Spectroscopy (FTIR).....	83
2.7.5	Gas Chromatography – Mass spectroscopy (GC-MS) .....	84
2.8	Molecular biology techniques .....	85
2.8.1	Isolation and extraction of DNA .....	85
2.8.2	Measurement of nucleic acid concentration .....	86
2.8.3	Primers .....	87
2.8.3.1	Polymerase chain reaction (PCR).....	88
2.8.3.1.1	Agarose gel electrophoresis.....	89
2.8.4	Isolation and extraction of RNA .....	90
2.8.5	Complementary DNA (cDNA) synthesis .....	91
2.8.6	Quantitative PCR (qPCR).....	93
2.8.6.1	Analysis and quantification of qPCR data .....	94
2.9	Statistical analysis .....	95
<b>Chapter 3:</b>	<b>SCL PHA production via <i>C. necator</i> H16.....</b>	<b>96</b>
3.1	Introduction.....	97
3.2	PHA production by <i>C. necator</i> H16 in shake flasks with the addition of exogenous quorum sensing molecules at 2 $\mu$ M concentration .....	97
3.3	PHA production by <i>C. necator</i> H16 in shake flasks with the addition of exogenous quorum sensing molecules at 10 $\mu$ M concentration .....	98
3.3.1	Characterisation and identification of SCL PHAs produced in shaken flask fermentation .....	109
3.3.1.1	Sudan Black B staining .....	110
3.3.1.2	Nile red dye staining .....	110
3.3.1.3	FTIR.....	112
3.3.1.4	GC-MS.....	115
3.4	Growth profile bioreactors.....	117
3.4.1	Characterisation and identification of SCL PHAs produced in 2 L bioreactor fermentation .....	126
3.4.1.1	FTIR analysis .....	126
3.4.1.2	GC-MS.....	128

3.5	Molecular biology.....	129
3.5.1	PCR for the confirmation of <i>Pha</i> genes in <i>C. necator</i> H16 ...	129
3.5.2	qPCR for the measurement of the expression levels of <i>Pha</i> genes in <i>C. necator</i> H16 .....	130
3.6	Discussion .....	132
3.6.1	Growth profile analysis .....	132
3.6.2	Characterisation and identification of SCL PHAs produced by <i>C. necator</i> H16.....	138
3.6.3	Molecular Biology .....	141
<b>Chapter 4:</b>	<b>MCL PHA production by <i>P. putida</i> KT2440 .....</b>	<b>143</b>
4.1	Introduction.....	144
4.2	PHA production by <i>P. putida</i> KT2440 in shake flasks with the addition of exogenous quorum sensing molecules at 2 $\mu$ M concentration 144	
4.3	PHA production by <i>P. putida</i> KT2440 in shake flasks with the addition of exogenous quorum sensing molecules at 10 $\mu$ M concentration 145	
4.3.1	Characterisation and identification of MCL PHAs produced in shaken flask fermentation .....	156
4.3.1.1	Sudan Black B staining of <i>P. putida</i> KT2440 .....	157
4.3.1.2	Nile red dye staining of <i>P. putida</i> KT2440.....	157
4.3.1.3	FTIR analysis of MCL PHA produced at shake flask level	159
4.3.1.4	GC-MS analysis of MCL PHA produced at shake flask level 161	
4.4	PHA production in bioreactors with the addition of exogenous quorum sensing molecules at 10 $\mu$ M concentration .....	165
4.4.1	Characterisation and identification of MCL PHAs produced in 2 L bioreactor fermentation .....	174
4.4.1.1	FTIR analysis of MCL PHA produced at bioreactor level ..	175
4.4.1.2	GC-MS analysis of MCL PHA produced at bioreactor level 176	
4.5	Molecular biology.....	178

4.5.1	PCR for the confirmation of <i>Pha</i> genes in <i>P. putida</i> KT2440	179
4.5.2	qPCR for the measurement of the expression levels of <i>Pha</i> genes in <i>P. putida</i> KT2440	179
4.6	Discussion	181
4.6.1	Growth profile analysis	181
4.6.2	Characterisation and identification of MCL PHAs produced by <i>P. putida</i> KT2440	189
4.6.3	Molecular biology	195
<b>Chapter 5:</b>	<b>General Discussion and conclusions</b>	<b>200</b>
<b>Chapter 6:</b>	<b>Future Works</b>	<b>205</b>
6.1	Optimisation of fermentations for the production of PHAs	206
6.2	Further characterisation of PHAs	207
6.3	Analysis of alternative <i>Pha</i> gene expressions via qPCR	208
6.4	Increasing production of secondary metabolites from other species of bacteria when supplemented with exogenous quorum sensing molecules	209
6.5	Production and addition of “crude” quorum sensing molecules	210
6.6	Effect of PHA production on Gram-positive bacteria when in the presence of exogenous quorum sensing molecules	210
<b>Chapter 7:</b>	<b>References</b>	<b>212</b>
Appendix		229
	Calibration curves	230

## List of Figures

<b>Figure 1.1</b> Proportions of different industries' plastics usage worldwide in 2015, (Geyer, Jambeck and Law, 2017) .....	3
<b>Figure 1.2</b> Chemical structures of fossil-fuel derived plastics: <b>(A)</b> PET <b>(B)</b> PS .....	5
<b>Figure 1.3</b> Global primary waste generation by polymer type measured in million tonnes (MT) per year. Polymer types are as follows: LDPE (Low-density polyethylene), HDPE (High-density polyethylene), PP (Polypropylene), PS (Polystyrene), PVC (Polyvinyl chloride), PET (Polyethylene terephthalate), PUR (polyurethane) and PP&A fibres (Polyphthalamide fibres) (Geyer, Jambeck and Law, 2017) .....	10
<b>Figure 1.4</b> Chemical structures of biopolymers: <b>(A)</b> PHA and <b>(B)</b> PLA .....	13
<b>Figure 1.5</b> TEM image of intracellular PHA granules in <i>Marichromatium bheemicum</i> (Higuchi-Takeuchi <i>et al.</i> , 2016) .....	15
<b>Figure 1.6</b> Pathway for the biosynthesis and metabolism of PHAs in bacteria produced from sugars and fatty acids. ....	21
<b>Figure 1.7</b> Schematic diagram of the organisation of synthase genes encoding various classes of enzymes. ....	24
<b>Figure 1.8</b> Chemical structures of quorum sensing molecules (AHLs) produced by Gram-negative bacteria: <b>(A)</b> C <sub>4</sub> -HSL, <b>(B)</b> C <sub>6</sub> -HSL and <b>(C)</b> 3-oxo-C <sub>12</sub> -HSL .....	50
<b>Figure 1.9</b> Simplified scheme of quorum sensing networks in Gram-negative bacteria (left) and Gram-positive bacteria (right) .....	53
<b>Figure 2.1</b> Diagrammatic representation of the shaken flask fermentation set up .....	71
<b>Figure 2.2</b> Diagrammatic representation of the bioreactor fermentation setup. (i) represents pre-inoculum. ....	73
<b>Figure 3.1</b> Fermentation profile of <i>C. necator</i> H16 grown in 1 L shake flasks over a 72 hour period without the addition of exogenous quorum sensing molecules (control). Samples were taken every 6 hours throughout the fermentation run, which was run in batch mode fermentation. MSM medium was used as the production medium, containing fructose as the sole carbon source. Error bars represent $\pm$ SD values (n = 9). ....	99

**Figure 3.2** Fermentation profile of *C. necator* H16 grown in 1 L shake flasks over a 72 hour period with addition of DMSO at a final concentration of 10  $\mu$ M. Samples were taken every 6 hours throughout the fermentation run, which was run in batch mode fermentation. MSM medium was used as the production medium, containing fructose as the sole carbon source. Error bars represent  $\pm$  SD values (n = 9). ..... 101

**Figure 3.3** Fermentation profile of *C. necator* H16 grown in 1 L shake flasks over a 72 hour period with addition of C<sub>4</sub>-HSL at a final concentration of 10  $\mu$ M. Samples were taken every 6 hours throughout the fermentation run, which was run in batch mode fermentation. MSM medium was used as the production medium, containing fructose as the sole carbon source. Error bars represent  $\pm$  SD values (n = 9). ..... 103

**Figure 3.4** Fermentation profile of *C. necator* H16 grown in 1 L shake flasks over a 72 hour period with addition of C<sub>6</sub>-HSL at a final concentration of 10  $\mu$ M. Samples were taken every 6 hours throughout the fermentation run, which was run in batch mode fermentation. MSM medium was used as the production medium, containing fructose as the sole carbon source. Error bars represent  $\pm$  SD values (n = 9). ..... 105

**Figure 3.5** Fermentation profile of *C. necator* H16 grown in 1 L shake flasks over a 72 hour period with addition of 3-oxo-C<sub>12</sub>-HSL at a final concentration of 10  $\mu$ M. Samples were taken every 6 hours throughout the fermentation run, which was run in batch mode fermentation. MSM medium was used as the production medium, containing fructose as the sole carbon source. Error bars represent  $\pm$  SD values (n = 9). ..... 107

**Figure 3.6** Percentage change of PHA produced from *C. necator* H16 grown in 1 L shake flasks (batch mode fermentation) containing production media and exogenous quorum sensing molecules with a final concentration of 10  $\mu$ M. Results shown are expressed as mean percentage changes of PHA produced when compared to an untreated control (grown in the absence of exogenous quorum sensing molecules) with  $\pm$  SD values (n = 9). ..... 109

**Figure 3.7** Representative positive result of *C. necator* H16 culture grown on a nutrient agar plate and stained with Sudan Black B dye to indicate the presence of inclusion bodies. Samples of cultures were collected 48 hours

post inoculation. The image shown is that of a *C. necator* H16 sample grown in the presence of the quorum sensing molecule 3-oxo-C<sub>12</sub>-HSL. .... 110

**Figure 3.8** Microscopic images of *C. necator* H16 cultures grown in 1 L shake flasks and stained with Nile red dye to indicate the presence of inclusion bodies containing PHAs. Cultures were visualised using a fluorescence microscope at X40 magnification. Images were taken of cultures 48 hours post inoculation. The images are labelled as follows: **(A)** Control, **(B)** DMSO, **(C)** C<sub>4</sub>-HSL, **(D)** C<sub>6</sub>-HSL and **(E)** 3-oxo-C<sub>12</sub>-HSL..... 111

**Figure 3.9** FTIR spectra of SCL PHA produced by *C. necator* H16 grown in shaken flasks. The following spectra are labelled as follows: **(A)** Standard P(3HB) **(B)** Control, **(C)** DMSO, **(D)** C<sub>4</sub>-HSL, **(E)** C<sub>6</sub>-HSL and **(F)** 3-oxo-C<sub>12</sub>-HSL..... 114

**Figure 3.10** Combined FTIR spectra of SCL PHA produced by *C. necator* H16 within shaken flasks and in the presence of different quorum sensing molecules. The graph also includes the spectrum of a commercial standard P(3HB). .... 114

**Figure 3.11** Representative GC-MS analysis of the polymer produced when *C. necator* H16 was grown in shaken flasks. The TIC above displays the methanolysis product of the PHAs produced when grown in the presence of DMSO. Methyl Benzoate was used as an internal standard. .... 116

**Figure 3.12** Mass spectrum of the peak generated from GC of the methanolysis product of the PHA produced by *C. necator* H16 when grown in shaken flasks with a R<sub>t</sub> of 4.1 minutes was identified using the NIST library as methyl ester of 3HB. .... 116

**Figure 3.13** Fermentation profile of *C. necator* H16 grown in 2 L bioreactors over a 72 hour period without the addition of exogenous quorum sensing molecules (control). Samples were taken every 6 hours throughout the fermentation run, which was run in batch mode fermentation. MSM medium was used as the production medium, containing fructose as the sole carbon source. Error bars represent ± SD values (n = 3). .... 118

**Figure 3.14** Fermentation profile of *C. necator* H16 grown in 2 L bioreactors over a 72 hour period with addition of C<sub>4</sub>-HSL at a final concentration of 10 µM. Samples were taken every 6 hours throughout the fermentation run, which was run in batch mode fermentation. MSM medium was used as the

production medium, containing fructose as the sole carbon source. Error bars represent  $\pm$  SD values (n = 3). ..... 120

**Figure 3.15** Fermentation profile of *C. necator* H16 grown in 2 L bioreactors over a 72 hour period with addition of C<sub>6</sub>-HSL at a final concentration of 10  $\mu$ M. Samples were taken every 6 hours throughout the fermentation run, which was run in batch mode fermentation. MSM medium was used as the production medium, containing fructose as the sole carbon source. Error bars represent  $\pm$  SD values (n = 3). ..... 122

**Figure 3.16** Fermentation profile of *C. necator* H16 grown in 2 L bioreactors over a 72 hour period with addition of 3-oxo-C<sub>12</sub>-HSL at a final concentration of 10  $\mu$ M. Samples were taken every 6 hours throughout the fermentation run, which was run in batch mode fermentation. MSM medium was used as the production medium, containing fructose as the sole carbon source. Error bars represent  $\pm$  SD values (n = 3). ..... 124

**Figure 3.17** Percentage change of PHA produced from *C. necator* H16 grown in 2 L bioreactors (batch mode fermentation) containing production media and exogenous quorum sensing molecules with a final concentration of 10  $\mu$ M. Results shown are expressed as mean percentage changes of PHA produced when compared to an untreated control (grown in the absence of exogenous quorum sensing molecules) with error bars  $\pm$  SD values (n = 3). ..... 126

**Figure 3.18** Combined FTIR spectra of SCL PHA produced by *C. necator* H16 grown within bioreactors and in the presence of different quorum sensing molecules. The graph also includes the spectrum of a commercial standard P(3HB). ..... 127

**Figure 3.19** Representative GC-MS analysis of the polymer produced when *C. necator* H16 was grown in bioreactors. The TIC above displays the methanolysis products of the PHAs produced when grown in the absence of quorum sensing molecules. Methyl Benzoate was used as an internal standard. .... 128

**Figure 3.20** Normalised fold change expression of **(A) *PhaC*** and **(B) *PhaZ*** in *C. necator* H16 when grown with the addition of different exogenous quorum sensing molecules, compared with an untreated control (grown without the addition of exogenous quorum sensing molecules *C. necator* H16 cells were sampled over a 72 hour period from a 2 L bioreactor in batch mode

fermentation. Results are expressed as mean fold change (control being standardised to 1.0) with error bars representing SD (n = 9). Data was analysed using a two-way ANOVA with *post hoc*. Tukey's multiple comparisons test (\**p* < 0.05)..... 131

**Figure 4.1** Fermentation profile of *P. putida* KT2440 grown in 1 L shake flasks over a 72 hour period without the addition of exogenous quorum sensing molecules (control). Samples were taken every 6 hours throughout the fermentation run, which was run in batch mode fermentation. E2 medium was used as the production medium, containing glucose as the sole carbon source. Error bars represent ± SD values (n = 9). ..... 146

**Figure 4.2** Fermentation profile of *P. putida* KT2440 grown in 1 L shake flasks over a 72 hour period with addition of DMSO at a final concentration of 10 µM. Samples were taken every 6 hours throughout the fermentation run, which was run in batch mode fermentation. E2 medium was used as the production medium, containing glucose as the sole carbon source. Error bars represent ± SD values (n = 9). ..... 148

**Figure 4.3** Fermentation profile of *P. putida* KT2440 grown in 1 L shake flasks over a 72 hour period with addition of C<sub>4</sub>-HSL at a final concentration of 10 µM. Samples were taken every 6 hours throughout the fermentation run, which was run in batch mode fermentation. E2 medium was used as the production medium, containing glucose as the sole carbon source. Error bars represent ± SD values (n = 9). ..... 150

**Figure 4.4** Fermentation profile of *P. putida* KT2440 grown in 1 L shake flasks over a 72 hour period with addition of C<sub>6</sub>-HSL at a final concentration of 10 µM. Samples were taken every 6 hours throughout the fermentation run, which was run in batch mode fermentation. E2 medium was used as the production medium, containing glucose as the sole carbon source. Error bars represent ± SD values (n = 9). ..... 152

**Figure 4.5** Fermentation profile of *P. putida* KT2440 grown in 1 L shake flasks over a 72 hour period with addition of 3-oxo-C<sub>12</sub>-HSL at a final concentration of 10 µM. Samples were taken every 6 hours throughout the fermentation run, which was run in batch mode fermentation. E2 medium was used as the production medium, containing glucose as the sole carbon source. Error bars represent ± SD values (n = 9). ..... 154

**Figure 4.6** Percentage change of PHA produced from *P. putida* KT2440 grown in 1 L shake flasks (batch mode fermentation) containing production media and exogenous quorum sensing molecules with a final concentration of 10  $\mu$ M. Results shown are expressed as mean percentage changes of PHA produced when compared to an untreated control (grown in the absence of exogenous quorum sensing molecules) with  $\pm$  SD values (n = 9). ..... 156

**Figure 4.7** Representative positive result of *P. putida* KT2440 culture grown on a nutrient agar plate and stained with Sudan Black B dye to indicate the presence of inclusion bodies. Samples of cultures were collected 48 hours post inoculation. The image shown is that of a *P. putida* KT2440 sample grown in the presence of the quorum sensing molecule C<sub>6</sub>-HSL..... 157

**Figure 4.8** Microscopic images of *P. putida* KT2440 cultures grown in 1 L shake flasks and stained with Nile red dye to indicate the presence of inclusion bodies. Cultures were visualised using a fluorescence microscope at X40 magnification. Images were taken of cultures 48 hours post inoculation. The images are labelled as follows: **(A)** Control, **(B)** DMSO, **(C)** C<sub>4</sub>-HSL, **(D)** C<sub>6</sub>-HSL and **(E)** 3-oxo-C<sub>12</sub>-HSL..... 158

**Figure 4.9** FTIR spectra of MCL PHA produced by *P. putida* KT2440 grown within 1 L shake flasks and in the presence of exogenous quorum sensing molecules. The following spectra are labelled as follows: **(A)** Control, **(B)** DMSO, **(C)** C<sub>4</sub>-HSL, **(D)** C<sub>6</sub>-HSL and **(E)** 3-oxo-C<sub>12</sub>-HSL..... 160

**Figure 4.10** Combined FTIR spectra of MCL PHA produced by *P. putida* KT2440 grown within 1 L shake flasks and in the presence of exogenous quorum sensing molecules. .... 161

**Figure 4.11** Representative GC-MS analysis of the polymer produced when *P. putida* KT2440 was grown in 1 L shake flasks. The TIC above displays the methanolysis products of the PHAs produced when grown in the presence of 3-oxo-C<sub>12</sub>-HSL. Methyl Benzoate was used as an internal standard. .... 162

**Figure 4.12** Mass spectra of the peaks generated from GC of the methanolysis product of the PHA produced by *P. putida* KT2440 grown in shaken flasks with R<sub>t</sub> of **(A)** 7.7 minutes, **(B)** 9.3 minutes and **(C)** 10.7 minutes were identified using the NIST library as methyl esters of 3HO, 3HD and 3HDD respectively. .... 163

**Figure 4.13** Fermentation profile of *P. putida* KT2440 grown in 2 L bioreactors over a 72 hour period without the addition of exogenous quorum sensing molecules (control). Samples were taken every 6 hours throughout the fermentation run, which was run in batch mode fermentation. E2 medium was used as the production medium, containing glucose as the sole carbon source. Error bars represent  $\pm$  SD values (n = 3). ..... 166

**Figure 4.14** Fermentation profile of *P. putida* KT2440 grown in 2 L bioreactors over a 72 hour period with addition of C<sub>4</sub>-HSL at a final concentration of 10  $\mu$ M. Samples were taken every 6 hours throughout the fermentation run, which was run in batch mode fermentation. E2 medium was used as the production medium, containing glucose as the sole carbon source. Error bars represent  $\pm$  SD values (n = 3). ..... 168

**Figure 4.15** Fermentation profile of *P. putida* KT2440 grown in 2 L bioreactors over a 72 hour period with addition of C<sub>6</sub>-HSL at a final concentration of 10  $\mu$ M. Samples were taken every 6 hours throughout the fermentation run, which was run in batch mode fermentation. E2 medium was used as the production medium, containing glucose as the sole carbon source. Error bars represent  $\pm$  SD values (n = 3). ..... 170

**Figure 4.16** Fermentation profile of *P. putida* KT2440 grown in 2 L bioreactors over a 72 hour period with addition of 3-oxo-C<sub>12</sub>-HSL at a final concentration of 10  $\mu$ M. Samples were taken every 6 hours throughout the fermentation run, which was run in batch mode fermentation. E2 medium was used as the production medium, containing glucose as the sole carbon source. Error bars represent  $\pm$  SD values (n = 3). ..... 172

**Figure 4.17** Percentage change of PHA produced from *P. putida* KT2440 grown in 2 L bioreactors (batch mode fermentation) containing production media and exogenous quorum sensing molecules with a final concentration of 10  $\mu$ M. Results shown are expressed as mean percentage changes of PHA produced when compared to an untreated control (grown in the absence of exogenous quorum sensing molecules) with  $\pm$  SD values (n = 3). ..... 174

**Figure 4.18** Combined FTIR spectra of MCL PHA produced by *P. putida* KT2440 grown within 2 L bioreactors and in the presence of exogenous quorum sensing molecules. .... 175

**Figure 4.19** Representative GC-MS analysis of the polymer produced when *P. putida* KT2440 was grown in 2 L bioreactors. The TIC above displays the methanolysis products of the PHAs produced when grown in the presence of C<sub>4</sub>-HSL. Methyl Benzoate was used as an internal standard..... 176

**Figure 4.20** Comparison of the monomeric composition of PHAs (Mol %) produced when supplemented with exogenous quorum sensing molecules in shake flasks and bioreactors. Data was analysed using a two-way ANOVA with *post hoc*. Tukey's multiple comparisons test (ns > 0.05). ..... 178

**Figure 4.21** Normalised fold change expression of **(A) *PhaC1*** and **(B) *PhaZ*** in *P. putida* KT2440 when grown with the addition of different exogenous quorum sensing molecules, compared with an untreated control (grown without the addition of exogenous quorum sensing molecules). *P. putida* KT2440 cells were sampled over a 72 hour period from a 2 L bioreactor in batch mode fermentation. Results are expressed as mean fold change (control being standardised to 1.0) with error bars representing ± SD (n = 9). Data was analysed using a two-way ANOVA with *post hoc*. Tukey's multiple comparisons test (\**p* < 0.05)..... 180

## List of Tables

<b>Table 1.1</b> Uses of different fossil-fuel derived plastics.....	5
<b>Table 1.2</b> Summary of toxic pollutants released during the incineration of plastics and their effects (Verma <i>et al.</i> , 2016).....	8
<b>Table 1.3</b> Raw materials to produce and uses of different biopolymers .....	13
<b>Table 1.4</b> Summary of physical and chemical properties of SCL PHA and MCL PHA against PP (Zinn and Hany, 2005).....	18
<b>Table 1.5</b> The four classes of PHA synthases (Rehm, 2003). .....	23
<b>Table 1.6</b> Methods of detection of PHAs (Tan <i>et al.</i> , 2014) .....	37
<b>Table 1.7</b> Comparison of the advantages and disadvantages of various PHA extraction methods (Kunasundari and Sudesh, 2011) .....	41
<b>Table 1.8</b> List of commercial companies producing PHAs (Dufour <i>et al.</i> , 2019). .....	44
<b>Table 2.1</b> Nutrient Broth No. 2 composition (Sigma-Aldrich, Dorset, UK)....	65
<b>Table 2.2</b> Nutrient agar composition (Sigma-Aldrich, Dorset, UK).....	65
<b>Table 2.3</b> Modified minimal salts medium (MSM) composition for <i>C. necator</i> H16 (Rai <i>et al.</i> , 2011).....	65
<b>Table 2.4</b> Trace element stock solution for modified MSM composition in 1 M hydrochloric acid (HCl) (Rai <i>et al.</i> , 2011). .....	65
<b>Table 2.5</b> E2 medium composition for <i>P. putida</i> KT2440 (Le Meur <i>et al.</i> , 2012). .....	66
<b>Table 2.6</b> Trace element stock solution for E2 medium composition in 1 M hydrochloric acid (HCl) (Le Meur <i>et al.</i> , 2012).....	66
<b>Table 2.7</b> Magnesium sulphate heptahydrate stock solution composition (Le Meur <i>et al.</i> , 2012).....	66
<b>Table 2.8</b> Inoculum growth conditions for each bacterial species.....	69
<b>Table 2.9</b> Concentrations of the quorum sensing molecules throughout this project. ....	70
<b>Table 2.10</b> Shaken flask fermentation conditions for each bacterial species. .....	70
<b>Table 2.11</b> Bioreactor fermentation conditions for each bacterial species...	73
<b>Table 2.12</b> Phenol-nitroprusside buffer (Rai <i>et al.</i> , 2011). .....	77
<b>Table 2.13</b> Alkaline hypochlorite reagent (Rai <i>et al.</i> , 2011). .....	77

<b>Table 2.14</b> Primers used for <i>C. necator</i> H16 .....	87
<b>Table 2.15</b> Primers used for <i>P. putida</i> KT2440.....	87
<b>Table 2.16</b> Primers for reference gene used during qPCR.....	87
<b>Table 2.17</b> PCR reaction components.....	88
<b>Table 2.18</b> PCR cycling protocol .....	89
<b>Table 2.19</b> gDNA removal reaction components .....	92
<b>Table 2.20</b> Reverse transcription reaction components.....	92
<b>Table 2.21</b> gDNA elimination and reverse transcription temperature protocol using a thermal cyclers .....	93
<b>Table 2.22</b> qPCR reaction components.....	94
<b>Table 2.23</b> qPCR cycling protocol .....	94
<b>Table 3.1</b> Summary of key growth parameters in relation to PHA production of <i>C. necator</i> H16 grown in 1 L shake flasks (batch mode fermentation) containing production media and exogenous quorum sensing molecules with a final concentration of 2 $\mu$ M. Results shown are from samples collected 48 hours post inoculation and expressed as means with $\pm$ SD values (n = 9) .	98
<b>Table 3.2</b> Kinetic growth parameters of <i>C. necator</i> H16 grown in 1 L shake flasks, batch mode fermentation without the addition of exogenous quorum sensing molecules. Data from time points 24 and 48 hours were used to calculate the following parameters.....	100
<b>Table 3.3</b> Kinetic growth parameters of <i>C. necator</i> H16 grown in 1 L shake flasks, batch mode fermentation with the addition of DMSO. Data from time points 24 and 48 hours were used to calculate the following parameters ..	102
<b>Table 3.4</b> Kinetic growth parameters of <i>C. necator</i> H16 grown in 1 L shake flasks, batch mode fermentation with the addition of C <sub>4</sub> -HSL. Data from time points 24 and 48 hours were used to calculate the following parameters. .	104
<b>Table 3.5</b> Kinetic growth parameters of <i>C. necator</i> H16 grown in 1 L shake flasks, batch mode fermentation with the addition of C <sub>6</sub> -HSL. Data from time points 24 and 48 hours were used to calculate the following parameters. .	106
<b>Table 3.6</b> Kinetic growth parameters of <i>C. necator</i> H16 grown in 1 L shake flasks, batch mode fermentation with the addition of 3-oxo-C <sub>12</sub> -HSL. Data from time points 24 and 48 hours were used to calculate the following parameters. .....	108

<b>Table 3.7</b> PHA monomer composition of SCL PHAs synthesised by <i>C. necator</i> H16 when grown in shaken in the presence of different exogenous quorum sensing molecules. ....	117
<b>Table 3.8</b> Kinetic growth parameters of <i>C. necator</i> H16 grown in 2 L bioreactors, batch mode fermentation without the addition of exogenous quorum sensing molecules. Data from time points 24 and 48 hours were used to calculate the following parameters.....	119
<b>Table 3.9</b> Kinetic growth parameters of <i>C. necator</i> H16 grown in 2 L bioreactors, batch mode fermentation with the addition of C <sub>4</sub> -HSL. Data from time points 24 and 48 hours were used to calculate the following parameters. ....	121
<b>Table 3.10</b> Kinetic growth parameters of <i>C. necator</i> H16 grown in 2 L bioreactors, batch mode fermentation with the addition of C <sub>6</sub> -HSL. Data from time points 24 and 48 hours were used to calculate the following parameters. ....	123
<b>Table 3.11</b> Kinetic growth parameters of <i>C. necator</i> H16 grown in 2 L bioreactors, batch mode fermentation with the addition of 3-oxo-C <sub>12</sub> -HSL. Data from time points 24 and 48 hours were used to calculate the following parameters.....	125
<b>Table 3.12</b> PHA monomer composition of SCL PHAs synthesised by <i>C. necator</i> H16 when grown in bioreactors in the presence of different exogenous quorum sensing molecules. ....	129
<b>Table 3.13</b> PHA productions of <i>C. necator</i> H16 in batch mode fermentation using 1 L shake flasks containing production media with the addition of exogenous quorum sensing molecules at a concentration of 10 µM. Productions were calculated using data of samples collected at 24 and 48 hours.....	135
<b>Table 3.14</b> PHA productions of <i>C. necator</i> H16 in batch mode fermentation using 2 L bioreactors containing production media with the addition of exogenous quorum sensing molecules at a concentration of 10 µM. Productions were calculated using data of samples collected at 24 and 48 hours.....	137
<b>Table 4.1</b> Summary of key growth parameters in relation to PHA production of <i>P. putida</i> KT2440 grown in 1 L shake flasks (batch mode fermentation)	

containing production media and exogenous quorum sensing molecules with a final concentration of 2  $\mu$ M. Results shown are from samples collected 48 hours post inoculation and expressed as means with  $\pm$  SD values (n = 9). 145

**Table 4.2** Kinetic growth parameters of *P. putida* KT2440 grown in 1 L shake flasks, batch mode fermentation without the addition of exogenous quorum sensing molecules. Data from time points 24 and 48 hours were used to calculate the following parameters. .... 147

**Table 4.3** Kinetic growth parameters of *P. putida* KT2440 grown in 1 L shake flasks, batch mode fermentation with the addition of DMSO. Data from time points 24 and 48 hours were used to calculate the following parameters. . 149

**Table 4.4** Kinetic growth parameters of *P. putida* KT2440 grown in 1 L shake flasks, batch mode fermentation with the addition of C<sub>4</sub>-HSL. Data from time points 24 and 48 hours were used to calculate the following parameters. . 151

**Table 4.5** Kinetic growth parameters of *P. putida* KT2440 grown in 1 L shake flasks, batch mode fermentation with the addition of C<sub>6</sub>-HSL. Data from time points 24 and 48 hours were used to calculate the following parameters. . 153

**Table 4.6** Kinetic growth parameters of *P. putida* KT2440 grown in 1 L shake flasks, batch mode fermentation with the addition of 3-oxo-C<sub>12</sub>-HSL. Data from time points 24 and 48 hours were used to calculate the following parameters. .... 155

**Table 4.7** PHA monomer composition of MCL PHAs synthesised by *P. putida* KT2440 when grown in 1 L shake flasks in the presence of exogenous quorum sensing molecules. .... 165

**Table 4.8** Kinetic growth parameters of *P. putida* KT2440 grown in 2 L bioreactors, batch mode fermentation without the addition of exogenous quorum sensing molecules. Data from time points 24 and 48 hours were used to calculate the following parameters. .... 167

**Table 4.9** Kinetic growth parameters of *P. putida* KT2440 grown in 2 L bioreactors, batch mode fermentation with the addition of C<sub>4</sub>-HSL. Data from time points 24 and 48 hours were used to calculate the following parameters. .... 169

**Table 4.10** Kinetic growth parameters of *P. putida* KT2440 grown in 2 L bioreactors, batch mode fermentation with the addition of C<sub>6</sub>-HSL. Data from

time points 24 and 48 hours were used to calculate the following parameters.  
..... 171

**Table 4.11** Kinetic growth parameters of *P. putida* KT2440 grown in 2 L bioreactors, batch mode fermentation with the addition of 3-oxo-C<sub>12</sub>-HSL. Data from time points 24 and 48 hours were used to calculate the following parameters..... 173

**Table 4.12** PHA monomer composition of MCL PHAs synthesised by *P. putida* KT2440 when grown in bioreactors in the presence of exogenous quorum sensing molecules. .... 177

**Table 4.13** PHA productions of *P. putida* KT2440 in batch mode fermentation using 1 L shake flasks containing production media with the addition of exogenous quorum sensing molecules at a concentration of 10 µM. Productions were calculated using data of samples collected at 24 and 48 hours..... 183

**Table 4.14** PHA productions of *P. putida* KT2440 in batch mode fermentation using 2 L bioreactors containing production media with the addition of exogenous quorum sensing molecules at a concentration of 10 µM. Productions were calculated using data of samples collected at 24 and 48 hours..... 187

## List of Equations

<b>Equation 1:</b> $VVM (L/L/min) = \text{Volume of air} / \text{Volume of media} / \text{Time (minutes)}$ .....	73
<b>Equation 2:</b> $DCW (g) = \text{Weight of tube containing freeze dried cells} - \text{Initial weight of the tube (g)}$ .....	75
<b>Equation 3:</b> $PHA \text{ yield (\% DCW)} = \text{PHA extracted} / DCW \times 100$ .....	78
<b>Equation 4:</b> $YXS (g/g) = \Delta X / \Delta S = (X_2 - X_1) / (S_1 - S_2)$ .....	80
<b>Equation 5:</b> $YPS (g/g) = \Delta P / \Delta S = (P_2 - P_1) / (S_1 - S_2)$ .....	80
<b>Equation 6:</b> $YPX (g/g) = \Delta P / \Delta X = (P_2 - P_1) / (X_2 - X_1)$ .....	80
<b>Equation 7:</b> $Q_p (g/L.H) = 1/X \times \Delta P / \Delta T = 1/X \times (P_2 - P_1) / (T_2 - T_1)$ .....	81
<b>Equation 8:</b> $\text{Monomer composition Mol \%} = (\text{Height of monomer peak} \times 100) / \text{Total height of all monomers' peaks}$ .....	85
<b>Equation 9:</b> $\Delta CT_{Control} = CT_{GOI, Control} - CT_{Reference, Control}$ .....	95
<b>Equation 10:</b> $\Delta CT_{Test} = CT_{GOI, Test} - CT_{Reference, Test}$ .....	95
<b>Equation 11:</b> $\Delta \Delta CT = \Delta CT_{GOI} - \Delta CT_{Control}$ .....	95
<b>Equation 12:</b> $2 - \Delta \Delta CT = \text{Normalised expression ratio}$ .....	95

## List of Appendices

<b>Appendix 1:</b> Total carbohydrates calibration curve .....	230
<b>Appendix 2:</b> Nitrogen concentration calibration curve .....	230
<b>Appendix 3:</b> Crotonic acid calibration curve .....	231

## Publication:

**Aziz, Z., Kyazze, G. and Keshavarz, T. (2020).** Recycling and the Environment: A Comparative Review Between Mineral-Based Plastics and Bioplastics. *Chemical Engineering Transactions*, 79, 355-360.

## **Author's Declaration**

I declare that the present work was carried out in accordance with the Guidelines and Regulations of the University of Westminster. The work is original except where indicated by special reference in the text.

The submission as a whole or part is not substantially the same as any that I previously or am currently making, whether in published or unpublished form, for a degree, diploma or similar qualification at any university or similar institution.

Until the outcome of the current application to the University of Westminster is known, the work will not be submitted for any such qualification at another university or similar institution.

Any views expressed in this work are those of the author and in no way represent those of the University of Westminster.

Signed:

Date:

## List of Abbreviations

( <i>R</i> )-3-HA-CoA	( <i>R</i> )-3-hydroxyacyl-CoA
( <i>R</i> )-3-HB-CoA	( <i>R</i> )-3-hydroxybutyryl-CoA
( <i>R</i> )-3-HButDH	( <i>R</i> )-3-hydroxybutyrate dehydrogenase
°C	Degrees Celsius
<sup>1</sup> H NMR	Proton nuclear magnetic resonance
3-OH-C <sub>14</sub> -HSL	<i>N</i> -(3-hydroxy-tetradecanoyl)-L- homoserine lactone
3-OH-C <sub>14</sub> -HSL	<i>N</i> -(3-hydroxy-tetradecanoyl)-L-homoserine lactone
3-oxo-C <sub>12</sub> -HSL	<i>N</i> -(3-oxododecanoyl)-L-homoserine lactone
3-oxo-C <sub>6</sub> -HSL	<i>N</i> -(3-oxohexanoyl)-L-homoserine lactone
3HB	3-hydroxybutyrate/3-hydroxybutanoic acid
3HD	3-hydroxydecanoate
3HDD	3-hydroxydodecanoate/3-hydroxydodecanoic acid
3HHp	3-hydroxyheptanoate
3HHx	3-hydroxyhexanoate/3-hexanoic acid
3HO	3-hydroxyoctanoate/3-hydroxyoctanoic acid
3HV	3-hydroxyvalerate
ABC	ATP-Binding cassette
ACP	Acyl carrier protein
AHL	<i>N</i> -acyl homoserine lactone
AI-2	Autoinducer 2
AI-2-P	AI-2 phosphate
AIPs	Autoinducer peptides
ANOVA	Analysis of variance
bp	Base pairs
BTEX	Benzene, toluene, ethylbenzene and xylene
C <sub>4</sub> -HSL	<i>N</i> -butanoyl-L-homoserine lactone
C <sub>6</sub> -HSL	<i>N</i> -hexanoyl-L-homoserine
cDNA	Complementary DNA
CFU/mL	Colony forming units per millilitre
CoA	Coenzyme A
CoA	Coenzyme A
D	Aspartate

DCW	Dry cell weight
DMSO	Dimethyl sulfoxide
DPD	4,5-dihydroxy-2,3-pentanedione
DSC	Differential scanning calorimetry
EDTA	Ethylenediaminetetraacetic acid
FTIR	Fourier transformed infrared technique
g	Gram
g/g	Gram per gram
g/L	Grams per litre
g/L.H	Gram per litre per hour
g/mol	Grams per mole
GC	Gas Chromatography
GC-MS	Gas Chromatography – Mass Spectroscopy
gDNA	Genomic DNA
GOI	Gene of interest
H	Histidine
HDPE	High-density polyethylene
kb	Kilobase
kDa	Kilodalton
kg	Kilogram
KSs	Ketoacyl synthase
LC-MS	Liquid Chromatography - Mass Spectroscopy
LCL PHAs	Long-chain-length PHAs
LDPE	Low-density polyethylene
LPS	Lipopolysaccharide
LTA	Lipoteichoic acids
<i>M</i>	Molar concentration
m/z	Mass-to-charge ratio
MCAT	Malonyl-CoA:ACP transacylase
MCL PHAs	Medium-chain-length
mg	Milligram
mg/L	Milligram per litre

MIQE	Minimum Information for publication of Quantitative real-time PCR Experiments
mL/min	Millilitre per minute
mM	Millimolar
mm	Millimetre
Mol %	Relative molar fraction
MSM	Minimal salts medium
MT	Million tonnes
$M_w$	Molecular weight
ng/ $\mu$ L	Nanogram per microliter
NIST	National Institute of Science and Technology
nM	Nanomolar
nm	Nanometre
nmol	Nanomole
OD	Optical density
P(3HB-co-3HV)	Poly(3-hydroxybutyrate-co-3-hydroxyvalerate)
P(3HB)	Poly(3-hydroxybutyrate)
P(3HHx-co-3HO-co-3HD-co-3HDD)	Poly(3-hydroxyhexanoate-co-3-hydroxyoctanoate-co-3-hydroxydecanoate-co-3-hydroxydodecanoate)
P(3HHx)	Poly(3-hydroxyhexanoate)
P(3HO-co-3HD-co-3HDD)	Poly(3-hydroxyoctanoate-co-3-hydroxydecanoate-co-3-hydroxydodecanoate)
P(3HO)	Poly(3-hydroxyoctanoate)
P(3HV)	Poly(3-hydroxyvalerate)
PAHs	Polycyclic aromatic hydrocarbons
PBS	Phosphate buffered saline
PCBs	Polychlorinated biphenyl
PCR	Polymerase chain reaction
PE	Polyethylene
PET	Polyethylene terephthalate
PHA	Polyhydroxyalkanoate
PLA	Polylactic acid
POPs	Persistent organic pollutants

PP	Polypropylene
PpoR	<i>Pseudomonas putida</i> orphan regulator
PS	Polystyrene
PUR	Polyurethane
PVC	Polyvinyl chloride
qPCR	Quantitative PCR
RHK	Receptor histidine kinase
rpm	Revolutions per minute
R <sub>t</sub>	Retention time
SAM	S-adenosylmethionine
SCL PHAs	Short-chain-length PHAs
ScmR	Secondary metabolite regulator
SD	Standard deviation
TIC	Total ion chromatogram
Ton/year	Tonnes per year
U/μL	Enzyme unit per microlitre
v/v	Volume per volume
VVM	Volume of air, per volume of media, per unit of time
w/v	Weight per volume
X	Concentration
x g	G-force
μg	Microgram
μg/mL	Microgram per millilitre
μL	Microliter
μL/mL	Microliter per millilitre
μm	Micrometre
μM	Micromolar

## Chapter 1: Introduction

## 1.1 Plastics

Plastics are a group of materials that are synthesised through the process of polymerisation using a range of synthetic or semi-synthetic compounds. They are composed of a network of molecular monomers bound together to form macromolecules, of which most are commonly derived from petrochemicals (North and Halden, 2013). Their cost-effective price to produce in comparison to other material such as glass or metals, coupled with desirable properties (e.g., high durability and plasticity) has led to them to being used extensively in many different industries. Worldwide in 2015, the use of plastic was mostly dominated by packaging (36%) followed by building and construction (16%), textiles (12%), consumer and institutional products (10%), transportation (7%), electronics (4%), industrial machinery (1%) and other industries (14%) such as medical and leisure (**Figure 1.1**) (Geyer, Jambeck and Law, 2017). Plastics have completely revolutionised human society and brought benefits in terms of economic activity, jobs and quality of life. For example (Andrady and Neal, 2009):

- Plastic packaging protects food and goods from getting wasted and/or becoming contaminated saving resources.
- They can also be used for various medical applications, which contribute to improving our health (e.g., disposable gloves, syringes and blood pouches).
- Their lightweight properties in comparison to other materials aid in saving fuel and helps to reduce emission during transportation.

In just ~70 years the global demand for plastics has grown exponentially, considering large-scale production of plastics only began shortly after the Second World War in the 1950s, when global plastic production was only two million tonnes (MT) per year. Since then, annual production of plastics has increase almost 200-fold reaching a record high of 381 MT in 2015 (Geyer, Jambeck and Law, 2017). However, with as many benefits plastics provide, they are not without their faults. With such a tremendous increase in demand

coupled with diverse usage across many different industries has led to the accumulation and mismanagement of plastic waste, specifically within our environment. Large amounts of plastic waste can accumulate quickly due to the short life span of many plastics products, which has been estimated to be less than a month for approximately 40% of all plastic products (Hahladakis *et al.*, 2018). This type of waste has caused economic and ecological concerns around the globe and the need for a suitable, alternative material has never been greater than before.

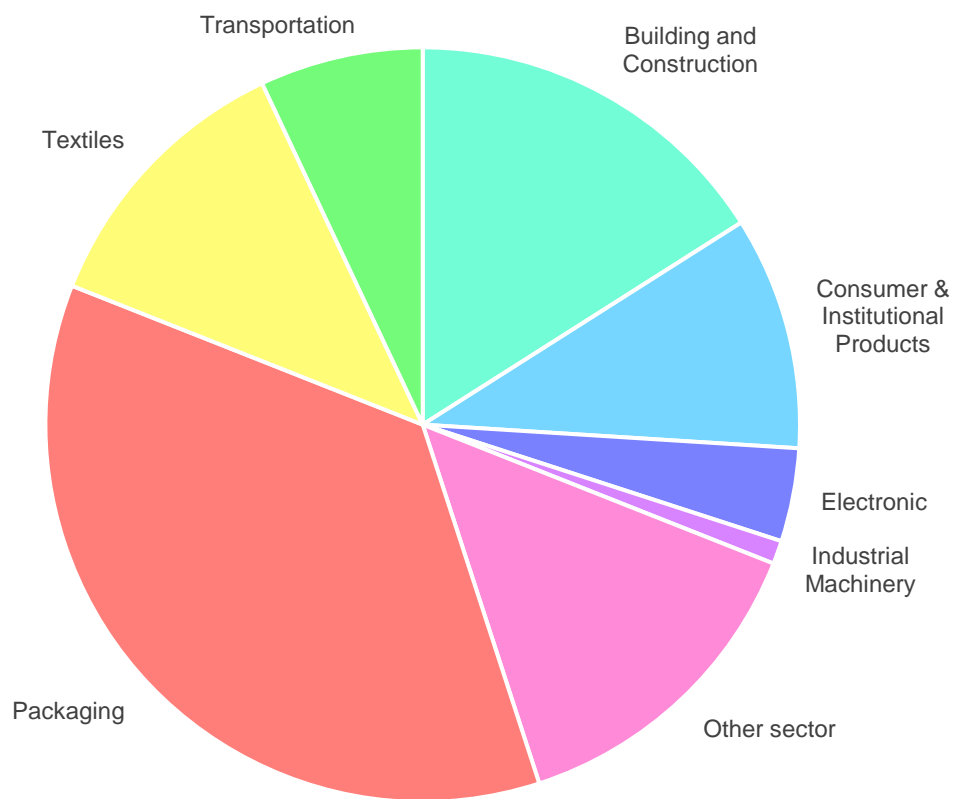


**Figure 1.1** Proportions of different industries' plastics usage worldwide in 2015, (Geyer, Jambeck and Law, 2017)

### 1.1.1 Fossil-fuel derived plastics

Fossil-fuel derived plastics (polymers) such as polyvinyl chloride (PVC), polyethylene (PE), polypropylene (PP), polystyrene (PS), and polyethylene terephthalate (PET) account for ~80% of the total global usage of plastics, and

it is this particular type of plastic that has been the greatest cause for concern **(Table 1.1) (Figure 1.2)** (Urbanek, Rymowicz and Mirończuk, 2018). These types of plastics have been derived from fossil fuels such as crude oil, a finite resource consisting of a mix of different length hydrocarbon chains. The major issue with these plastics is the negative externalities they are able to impose on the environment such as their ability to persist within the environment for many years once they have been discarded. By design fossil-fuel derived plastics are intended to be non-biodegradable, as they are unable to be decomposed and assimilated by microorganisms (biotic factors) through the process of biodegradation. Although, these plastics are affected by temperature, UV radiation and physical stress (abiotic factors), which can begin to fragment when exposed to physical factors over long periods of time (Gewert, Plassmann and MacLeod, 2015).

Fossil-fuel derived plastics are created from long, saturated hydrocarbon chains that are held together via covalent bonds and intermolecular forces such as Van der Waal's between individual chains, influencing melting and boiling points of the polymer. The chain lengths that create the polymer are often non uniform and vary in size, with most containing a variety of different length chains. In turn this affects the intermolecular forces of the polymer, and therefore begin to melt gradually over a range of temperatures as opposed to a fixed temperature. Also, since these polymers are formed from saturated chains, they are generally unreactive, thus unable to react with electrophiles, nucleophiles or undergo addition reactions. This is the primary reason as to why these plastics are considered to be non-biodegradable, as they are unable to react and be degraded by biological reagents.

Moreover, the long chain structures and high molecular weight ( $M_w$ ) of the polymers also play an important role in the resistance against biodegradation (Wilkes and Aristilde 2017). The high  $M_w$  of plastics aid in preventing biodegradation as large compounds are unable to be transported across the cellular membrane of the microorganism. Consequently, long chain polymers first have to go through a process of depolymerisation to form their smaller constituent monomers before they can be absorbed within the microorganism,

where they are then biodegraded within by intracellular enzymes (Shah *et al.*, 2008).

**Table 1.1** Uses of different fossil-fuel derived plastics

Type of plastic	Uses
PET	Food and beverage packaging, clothing, carpets, automotive parts, construction material, protective packaging
PS	Food packaging, domestic applicates, electronic goods, toys, furniture and medical equipment
PVC	Building and construction equipment ( <i>e.g.</i> , window frames, pipes, and roofing), clothing, and packaging

Abbreviations: Polyethylene terephthalate (PET), Polystyrene (PS), Polyvinyl chloride (PVC)

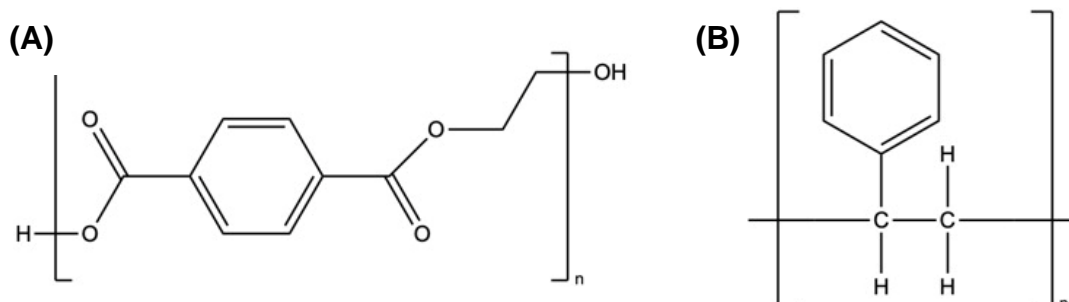


**Figure 1.2** Chemical structures of fossil-fuel derived plastics: **(A)** PET **(B)** PS

### 1.1.1.1 Disposal Methods

With fossil-fuel derived plastics having such a resistance to biodegradation, alternative methods are employed to deal with plastic waste. Currently, there are three main different methods for handling plastic waste: using landfill sites, incineration of waste and recycling. However, each of these methods have their own limitations.

#### 1.1.1.1.1 Landfill

Landfill sites are carefully designed structures that are either built into or on top of the ground where waste can be stored. These sites are usually lined with a protective plastic layer, topped with many layers of clay and soil in an

attempt to isolate the waste being contained within and preventing any leachate from leaking into surrounding groundwater (Yedla, 2005). Leachate can be defined as liquid that passes through landfill and has extracted dissolved and suspended matter from it. This results from precipitation entering the landfill from moisture that exists in the waste when it is composed (Raghab, Abd El Meguid and Hegazi, 2013). However, in many developing countries open landfill sites still exist and such thoroughly designed measures are not implemented adequately due to the lack of resources or the failure of Governments to prioritise the management of this type of waste.

A key drawback associated with this method of plastic waste disposal is the fact that the landfill sites occupy large amounts of space that could be better utilised for more productive means such as agriculture or housing developments (Webb *et al.*, 2012). Economically, this presents a significant opportunity cost as to either build landfill infrastructure to house plastic waste or utilise the land for economic benefits. As widely as they are used, ultimately landfill sites are ineffective in successfully decomposing plastic waste, with some waste taking upwards of 20 years to decompose completely and as a result, the land occupied by the landfill site remains unavailable for long periods of time and can often be described as being aesthetically unpleasing (Tansel and Yildiz, 2011). This slow rate of decomposition is associated with anaerobic conditions that are created within the landfill because of how densely packed they are with plastic waste, with any decomposition usually occurring due to the result of thermooxidative degradation (Webb *et al.*, 2012).

Unfortunately, another negative consequence of landfill sites are the plastic fragments that are created during decomposition. They act as the source of several secondary environmental pollutants such as benzene, toluene, xylenes, ethyl benzenes and trimethyl benzenes, which can be contained in leachate and released as gases into the surrounding environment, of which all are potential health hazards to humans in high concentrations (Zhang *et al.*, 2004). Finally, the protective plastic layers that are put in place to help separate the landfill from the surrounding soil and the underlying groundwater may tear or even degrade over time themselves (North and Halden, 2013).

This represents a significant long-term risk of contamination of soil and surrounding groundwater with landfill leachate that could potentially contain toxic organic pollutants, heavy metals and ammonia nitrogen compounds (Youcai, 2018).

#### **1.1.1.1.2 Incineration**

Alternatively, one of the simplest methods of dealing with plastic waste is via incineration. Upon first glance it could be hard to identify the possible benefits this method of plastic waste disposal holds over the alternatives, but the incineration of plastic waste could be favourable. One major disadvantage of landfill sites is that it requires large areas of land and infrastructure to build, which incineration does not. Additionally, there is even the possibility of being able to recover energy in the form of heat given off during the burning process (North and Halden, 2013). Although, like all methods of plastic disposal incineration has its own weaknesses, mainly due to the large amounts of toxic pollutants it produces, most of which are released directly into the atmosphere. Polycyclic aromatic hydrocarbons (PAHs), polychlorinated biphenyl (PCBs), persistent organic pollutants (POPs) such as dioxins and bisphenol A are amongst some of the pollutants released into the atmosphere that pose a great risk to human health as a result of burning plastics (**Table 1.2**) (Verma *et al.*, 2016).

Furthermore, the incineration of plastics results in the significant release of greenhouse gasses such as carbon dioxide and water vapour, which are well known to contribute to climate change (Butler, 2018). It is because of the consequences of these pollutants being released into the atmosphere that many are reluctant to adopt this method of plastic waste disposal. The significant economic and environment costs caused by incineration and even landfill far outweigh the benefits they provide, and as a result can be viewed as a driving force behind the development of many plastic recycling processes.

**Table 1.2** Summary of toxic pollutants released during the incineration of plastics and their effects (Verma *et al.*, 2016)

Toxic Compound	Effect(s)
Bisphenol A	Mimics oestrogen
POPs	Carcinogen and reproductive damage in both males and females
Dioxins	Carcinogen and interferes with testosterone
PAHs	Carcinogen, cardiovascular diseases and developmental impacts (poor foetal growth)
PCBs	Carcinogen and interferes with thyroid hormone
Phthalates	Decreased sperm count and motility

Abbreviations: Persistent organic pollutants (POPs), Polycyclic aromatic hydrocarbons (PAHs), Polychlorinated biphenyl (PCBs)

### 1.1.1.1.3 Recycling

In theory, recycling presents itself as the superior solution to handling plastic waste when compared to alternative methods, as it allows for partial recovery of the constituent monomers and energy used to produce them (North and Halden, 2013). However, there are number of considerable challenges that are associated with the recycling of plastics and as a result, not all plastics can be recycled.

The first issue that must be considered is the technicality of sorting plastics and the consequences of contaminating different types together (Hopewell, Dvorak and Kosior, 2009). In any given collection of waste there may be several different polymers as well as other materials. This must be separated carefully, as the introduction of one type of polymer into another may lead to the reduction in the desirable properties of the recycled material being produced due to the different melting points (Singh *et al.*, 2017). In turn, this contamination of different types of plastics results in the production of poor-quality recycled polymers, which is another difficulty that must be overcome. For example, the blending of polypropylene (PP) in high-density polyethylene (HDPE) can lead to an increase in the brittleness of recycled HDPE. To circumvent this issue, sophisticated techniques are employed to aid in the separation of different types of plastics such as Fourier transformed infrared technique (FTIR) or magnetic density separation (Singh *et al.*, 2017).

Yet, even with these systems in place it is often impossible to produce recycled plastics of the same quality as “new” (virgin) polymers as these systems are prone to error and the expectation that the materials used to produce the recycled plastics are impure or of poorer quality (Hopewell, Dvorak and Kosior, 2009). Consequently, although these recycled polymers are cheaper to produce, the quality of the end product is expected to decrease due to contamination with each recycling cycle, which ultimately limits their usage to only low-value applications (North and Halden, 2013). The use of these separation techniques also inadvertently drives up the cost of the recycling process, which could be detrimental to the entire recycling process.

Unfortunately, not all types of plastics are able to be completely recycled (**Figure 1.3**). This is owing to their chemical properties and whether the polymer is either thermosetting or thermoplastic. For example, the polymer polyurethane (PUR) is widely not recycled as it is a thermosetting polymer, which means it is irreversibly hardened by curing from a liquid or soft solid pre-resin (Nikje, Garmarudi and Idris, 2011). Whereas thermoplastics are much more suitable for recycling as they can be moulded into different applications once they reach a particular temperature. Yet, the price of crude oil is not high enough to incentivise producers to the use of recycled materials. However, as petroleum begins to grow scarcer, and the public becomes more educated about the environmental consequences of plastic consumption, it is more than likely that the demand for products produced using recycled plastics and alternatives to fossil-fuel derived plastic becomes mainstream.

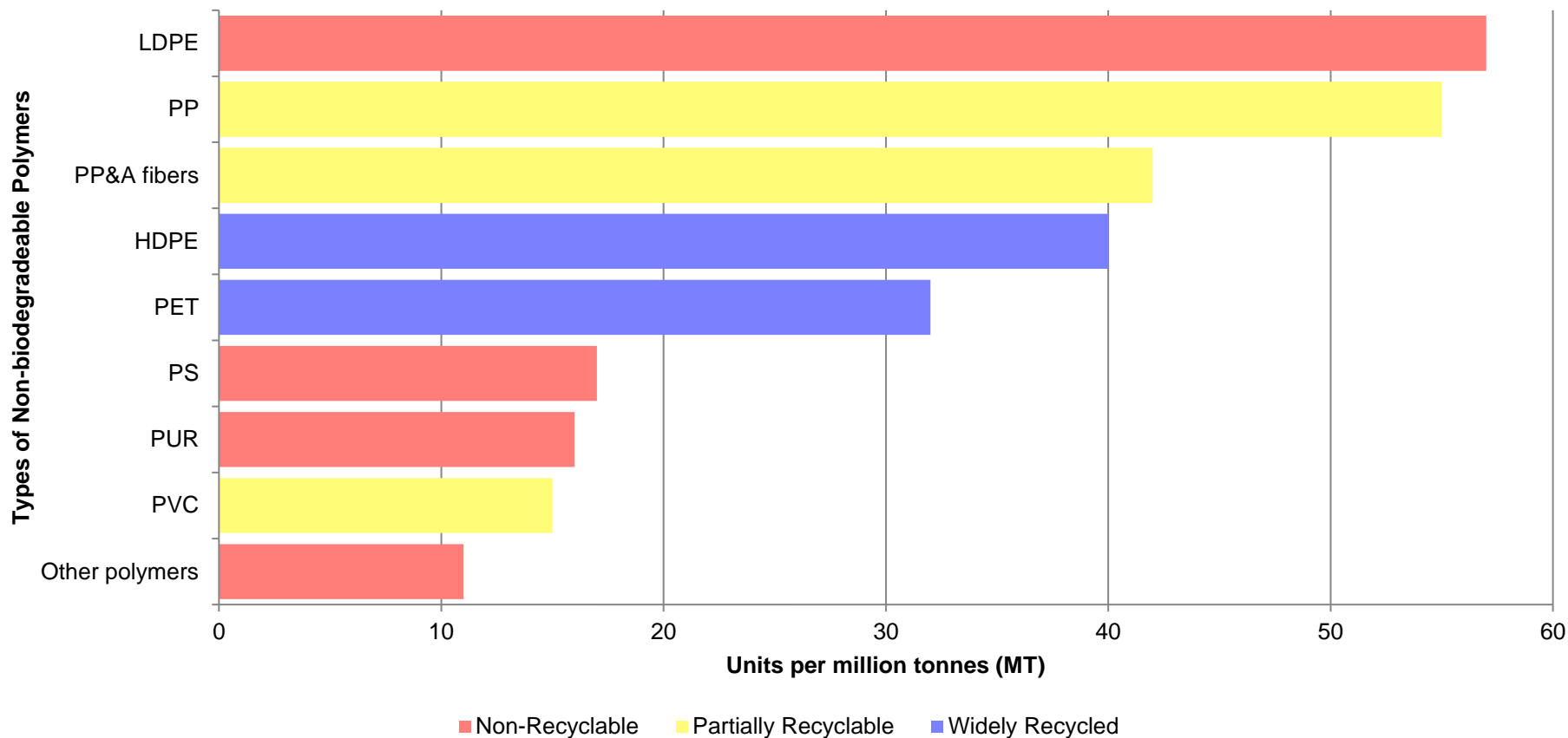


**Figure 1.3** Global primary waste generation by polymer type measured in million tonnes (MT) per year. Polymer types are as follows: LDPE (Low-density polyethylene), HDPE (High-density polyethylene), PP (Polypropylene), PS (Polystyrene), PVC (Polyvinyl chloride), PET (Polyethylene terephthalate), PUR (polyurethane) and PP&A fibres (Polyphthalamide fibres) (Geyer, Jambeck and Law, 2017)

### 1.1.2 Biopolymers

Just like fossil-fuel derived plastics, biopolymers are similar in the sense that they are formed of singular monomeric units that are covalently bonded together to form larger macromolecules. However, fundamentally there are two main difference between these types of polymers; their chemical structure and sustainability (Mohan *et al.*, 2016). Biopolymers are naturally occurring polymers that are formed during the growth the cycles of all organisms. They have well defined structures in comparison to their fossil-fuel derived counterparts, which have much simpler, stochastic structures as explained in **Section 1.1.1**. The structure of biopolymers is an important characteristic. This is because their structure directly correlates to their functions as active molecules taking part in vital cellular functions. For example, haemoglobin is a protein molecule responsible for the transportation of oxygen around the blood of vertebrates and is able to fulfil its function due to its folded quaternary structure (Elliott and Elliott, 2009). They can also be used for the conservation and expression of genetic information as well as the storage of carbon, energy or other energy nutrients (Rao, Bharathi and Akila, 2014).

Biopolymers are seen as a viable substitute to fossil-fuel derived plastics owing to their sustainability, but also carbon neutrality and biodegradability. These properties address the inherent flaws associated with synthetic polymers, given the problems faced with their disposal and the environmental consequence they impose. In many cases biopolymers such as polyhydroxyalkanoate (PHA) can be synthesised from renewable sources (*e.g.*, vegetable/coconut oil and sugar cane molasses) (Basnett *et al.*, 2020) (**Table 1.3**), which can be produced indefinitely as they are derived from plant-based materials. Thus, biopolymers can be classed as being a sustainable product. They can also be considered to be carbon neutral and biodegradable as they able to sequester atmospheric carbon dioxide during the growth of the raw materials and once disposed of can be broken down via biotic factors allowing for the raw materials to be absorbed back into the environment and used for the next generation of biopolymers (Johnson, Mwaikambo and Tucker, 2003). The advantages of biopolymers can be further attributed to

their reliance on plant-based materials over fossil fuels, which suffer from price and supply instability (Mohan *et al.*, 2016).

Bioplastics is a term that is often used in scientific literature interchangeably with biopolymers. However, the term bioplastics encompasses a large array of different polymers that may not pertain to biopolymers. The term bioplastic can be misleading to an extent as the prefix “bio” invokes thoughts of biodegradability, which refers to the process in which a material whose physical and chemical property can be completely disintegrate when exposed to microorganisms, but this is not necessarily the case with all bioplastics. Bioplastics can be defined as polymers that can be created from renewable raw materials or a material that can be biodegraded or both (Babu, O'Connor and Seeram, 2013). This definition can be broad or a sweeping generalisation as it only excludes polymers derived from fossil fuels or polymers that are not biodegradable. Bioplastics, (which can also encompass biopolymers by its definition) are created from renewable biological material, but are then often put through a process of chemical polymerisation to create the final polymer. Though, this polymer produced may not be biodegradable and as a result could mean they are able to persist within the environment causing the same economic and ecological issues as fossil fuel derived plastics. There are bioplastics such as polylactic acid (PLA) that are able to be created from renewable sources such as corn starch and can be broken down into its constituent monomers through biotic factors.

There are several different types of biopolymers that exist such as polynucleotides, polyamides, polysaccharides, polyoxoesters, polythioesters, polyanhydrides, polyisoprenoids and polyphenols, which are all potential candidates for the substitution of synthetic plastics (Steinbüchel, 1991). Amongst these, PHAs belong to the polyoxoesters group and have received much attention due to their biodegradable, thermoplastic properties (Albuquerque *et al.*, 2007).

**Table 1.3** Raw materials to produce and uses of different biopolymers

Types of biopolymers	Raw materials	Uses
PHA	Vegetable oils (e.g., coconut, groundnut, olive and corn), sugarcane and glucose	Packaging, drug delivery systems, biological medical implants and nanotechnology
PLA	Corn, cassava sugarcane, and sugar beet pulp	Films, medical devices (e.g., screws, pins, rods and plates) and upholstery
Chitosan	Shells of shrimps, lobsters, crayfish and crabs	Bandages, biopesticide and nanomaterials

Abbreviations: Polyhydroxyalkanoates (PHAs), Polylactic acid (PLA)

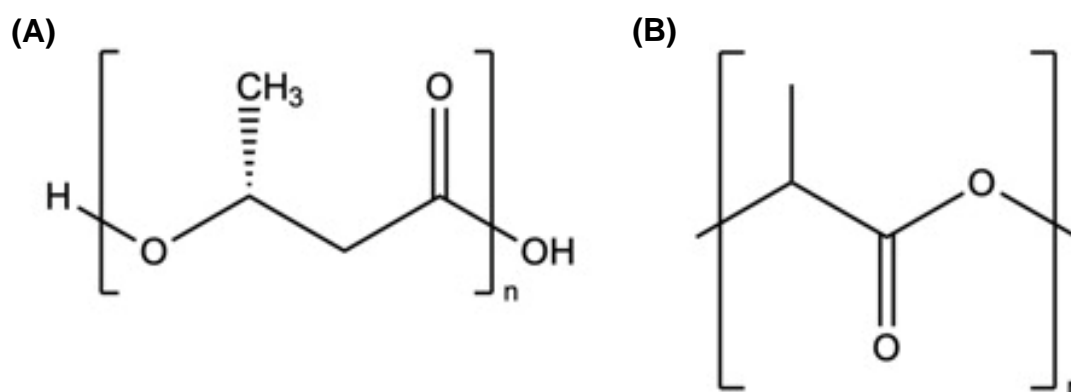


**Figure 1.4** Chemical structures of biopolymers: **(A)** PHA and **(B)** PLA

## 1.2 Polyhydroxyalkanoates (PHAs)

Polyhydroxyalkanoates (PHAs) (**Figure 1.4**) are biological polyesters produced by over 300 different bacteria, including Gram-negative and Gram-positive species (examples of which include *Bacillus*, *Methylobacterium* and *Pseudomonas* species) (Keshavarz and Roy, 2010). They are synthesised within the cytoplasm of bacteria and stored in the form of insoluble granules. These granules can be between 0.2 – 0.7 nm in diameter surrounded by a membrane layer consisting of lipids and proteins approximately 2 nm thick, with each granule containing a minimum of 1000 polymeric molecules (Braunegg, Lefebvre and Genser, 1998). They are produced when bacteria are grown under unbalanced culture conditions, for instance, when in the presence of excess carbon or under limiting conditions of essential nutrients

such as nitrogen, phosphorus, sulphur, magnesium or oxygen (Rai *et al.*, 2011).

These granules act as an ideal form of carbon and energy storage as they are insoluble within the cytoplasm aiding in the long-term survival of the bacteria. It has been observed that bacteria containing PHAs are able to survive during periods of starvation in comparison to those without this form of energy reserve, in turn slowing down the rate of cell autolysis and subsequently its own mortality (Chee *et al.*, 2010). Additionally, bacteria that harbour PHA have shown to have increased tolerance against unfavourable abiotic environmental conditions and can also serve as a sink for carbon and reducing equivalents for some species (Tan *et al.*, 2014).

### 1.2.1 Discovery of PHAs

The first type of PHA – poly(3-hydroxybutyrate) (P(3HB)) was discovered by French scientist Maurice Lemoigne in 1925, from his work with the bacterium *Bacillus megaterium*. The significance of his discovery was often overlooked by the scientific community at the time given the abundance of fossil fuels and their inexpensiveness. It was only until the mid 1970s when the oil crisis struck when there was renewed interest in Lemoigne's research, which began to gain traction within the community becoming the focus of many researchers work. This included Dawes and Senior who in 1973 noted that P(3HB) played a similar role to starch or glycogen (forms of storage compounds) within *B. megaterium* (Dawes and Senior, 1973). This production of biopolymer was only initiated when the ratio of glucose to nitrogen was high and degradation of P(3HB) occurring in the absence or scarcity of carbon or alternative suitable energy sources (Macrae and Wilkinson, 1958). Since Lemoigne's initial discovery several bacterial strains (archaeobacteria, Gram-negative and Gram-positive bacteria, photosynthetic bacteria including cyanobacteria) are now known to be able to produce and accumulate P(3HB) both aerobically and anaerobically (**Figure 1.5**).

Before 1974 the existence of copolymers (outside of/besides P(3HB)) were unheard of, however, Wallen and Rohwedder were able to extract and identify previously unknown monomer constituents from activated sewage sludge. 3-hydroxyvalerate (3HV), 3-hydroxyhexanoate (3HHx) and 3-hydroxyheptanoate (3HHp) monomers were all discovered from the sludge. 7 years later in 1983, 3HHp was discovered to be produced by *B. megaterium* and 3-hydroxyoctanoate (3HO) with trace amounts of 3HHx from *Pseudomonas oleovorans* when grown with *n*-octane (Wallen and Rohwedder, 1974). Collectively, these studies concluded that the production of different types of PHA monomers units were dependant on the carbon source used to grow the bacteria. As a result, it is now possible to be able to produce PHA copolymers of different monomeric composition with straight, branched, saturated, unsaturated and also aromatic structures. To date, more than 150 different monomer constituents of PHAs have been discovered and as previously mentioned before, 300 different types of bacterial species are known to produce PHAs.

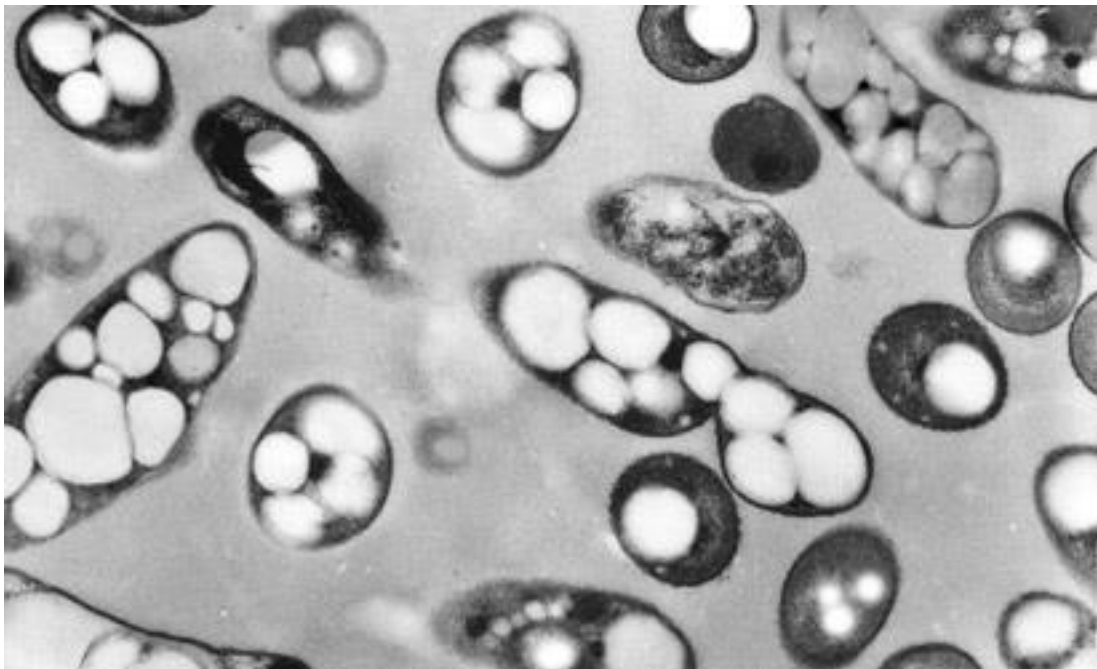


**Figure 1.5** TEM image of intracellular PHA granules in *Marichromatium bheemicum* (Higuchi-Takeuchi *et al.*, 2016)

### 1.2.2 Types and characteristics of PHAs

PHAs are a versatile biopolymer that can be described as a thermoplastic and elastomeric material. They are also able to be degraded by several different organisms found within the environment as well as enzymes within the human body and can have their structure manipulated through various genetic or physiological strategies in efforts to produce different types of PHAs each with their own unique physical and mechanical properties, which lends themselves to be used in various applications. For instance, the fermentation conditions and carbon source within the choice of medium used to grow the organism can affect the ratio, types of functional groups and monomer composition of PHA being produced (Francis, 2011).

Whereas the length and type of pendant groups, distance between the ester linkages in the polymer backbone and the number of repeating units in the polymer chain all play a role in determining the properties of PHAs. Properties such as flexibility, crystallinity, melting point and glass transition temperature of PHAs are dependent on the length and types of pendant groups of the repeating units. As the length of the side chain attached to the  $\beta$ -carbon of the PHA increases, the polymer begins to change from a glassy state to a softer, stickier material instead. The  $M_w$  of these biopolymers can also vary between 200 - 3000 kDa, which is also usually dependant on the organism producing the polymer as well as the conditions that it is cultured within (Sudesh, Abe and Doi, 2000). Consequently, with so many different factors playing a role in determining the type and characteristics of the PHAs, they can be divided into groups according to the number of carbon atoms that are present in its monomer units. There are three main groups (Chen *et al.*, 2018):

- Short-chain length PHA (SCL PHA) consist of 3-5 carbon atoms
- Medium-chain length PHA (MCL PHA) consist of 6-14 carbon atoms
- Long-chain length PHA (LCL PHA) consist of  $\geq 15$  carbon atoms

PHAs can also be further classed depending on the number of different types of copolymers within the monomer unit. Homopolymers consist of one type of

copolymer whereas heteropolymers consist of two or more copolymers within the monomer unit (Sharma *et al.*, 2017).

#### 1.2.2.1 Short-chain-length PHAs (SCL PHAs)

One of the most studied SCL PHAs is P(3HB) produced by various species of bacteria such as *Cupriavidus necator* H16 (formerly *Ralstonia eutropha*), which is widely used to produce P(3HB). It is a highly crystalline, brittle and stiff material with a melting point of between 80 – 180°C (**Table 1.4**). It has ideal biocompatibility because the polymer and its degradation product, 3-hydroxybutyric acid (3HB) is a product of cell metabolism and is present within blood and tissue. As a result, *in vitro* studies have shown that P(3HB) are highly biocompatible with various cell lines such as, osteoblasts and epithelial cells, which triggered a commercial interest in the polymer. However, due to its brittle nature and high stiffness, its applications are significantly limited. As a result of its poor physical properties, the incorporation of a second monomer unit can enhance P(3HB) properties (Chen *et al.*, 2018). The introduction of different monomer units to P(3HB) has resulted in the production of PHAs such as poly(3-hydroxybutyrate-co-3-hydroxyvalerate) (P(3HB-co-3HV)), which is more flexible and tougher than the original polymer P(3HB), and has a degree of higher biodegradability when discarded into the environment.

#### 1.2.2.2 Medium-chain-length PHAs (MCL PHAs)

MCL PHAs are polyesters accumulated by fluorescent Pseudomonads. After the discovery of MCL PHAs in 1983, more than 100 different monomer units have been characterised within MCL-PHAs, in order to achieve different physical as well as mechanical and thermal properties, to be utilized in various applications (Witholt and Kessler, 1999) (**Table 1.4**). The most common examples of MCL-PHAs are thermoplastic elastomers such as poly(3-hydroxyhexanoate) (P(3HHx)) and poly(3-hydroxyoctanoate) (P(3HO)) (Basnett, 2014). These materials have lower crystallinity, are rather flexible and soft. They have elastomeric nature which increases with the length of the side chain. These are also biodegradable, water resistant and biocompatible, which could be utilized in medical implants, such as scaffolding for the

regeneration of arteries and nerve axons (Rai *et al.*, 2011). The major advantage of the MCL PHAs is the variability in their biological as well as material properties which can be tailored by altering the culture conditions, carbon source and organism used.

**Table 1.4** Summary of physical and chemical properties of SCL PHA and MCL PHA against PP (Zinn and Hany, 2005).

Properties	SCL PHA	MCL PHA	PP
Crystallite (%)	40-80	20-40	70
Melting point (°C)	80-180	30-80	160-175
Density (g/cm <sup>3</sup> )	1.25	1.05	0.91
UV resistance	Good	Good	Poor
Solvent resistance	Poor	Poor	Good
Biodegradability	Good	Good	None
Large scale production	Partially available	Partially available	Easily available

### 1.2.3 Biosynthesis and metabolism of PHAs

As previously stated PHAs are known to play an integral role in maintaining the cells metabolism, acting as a form of energy reservoir that can be broken down during unfavourable conditions, whilst additionally increasing the cells' ability to tolerate against particular agents such as increased tolerance to heat, osmotic shock and UV radiation. The biosynthesis of PHAs tends to begin production during the logarithmic phase during its growth cycle and continues to produce PHAs till the late stages of the stationary phase (Cavalheiro, de Almeida, Grandfils and da Fonseca, 2009).

To date, 13 different metabolic pathways for the biosynthesis of PHAs have been observed and studied within wild type and genetically modified strains, possessing the ability to produce either SCL PHAs or MCL PHAs. From these 13 pathways a total of 10 result in the production of SCL PHAs, whereas a total of 4 can produce MCL PHAs (Tan *et al.*, 2014). **Sections 1.2.3.1** and **1.2.3.2** below expand upon three pathways that result in the production of either SCL PHAs or MCL PHAs.

All three of the pathways that are well known for the ability to produce PHAs are interconnected with the anabolic/catabolic pathways such as glycolysis,

Krebs Cycle,  $\beta$ -oxidation, *de novo* fatty acids biosynthesis, amino acid catabolism, Calvin Cycle, and serine pathway of the producing organism. Acetyl-CoA is the common intermediate between PHA synthesis and metabolic pathways. When there are nutrient rich conditions, acetyl-CoA is transferred into the Krebs Cycle by excessive coenzyme A (CoA) production which inhibits  $\beta$ -ketothiolase and blocks PHA synthesis (Ratledge and Kristiansen, 2001). However, when there are nutrient limiting conditions, the level of CoA is non-inhibitory which allows acetyl-CoA to be channelled into PHA synthetic pathways.

Biosynthesis of PHAs involves two main steps. The first is the synthesis of (*R*)-3-hydroxyacyl-CoA ((*R*)-3-HA-CoA) and the second is the polymerisation of (*R*)-3-HA-CoA into PHAs (Rehm, Mitsky and Steinbüchel, 2001). As mentioned above, three different pathways are involved in the production of the (*R*)-3-HA-CoA units from which, in two pathways carbohydrates are being utilised as the feedstocks for the organisms in the PHA production (Pathway I and III). While, in the final pathway, PHA production is carried out using fatty acids as the carbon source for the organisms (Pathway II).

#### **1.2.3.1 Biosynthesis of SCL PHAs**

The first pathway involves the glycosylation of sugars (Pathway I) and the use of three different enzymes;  $\beta$ -ketothiolase, acetoacetyl-coenzyme A reductase, and PHA synthase, which are involved in a three-step reaction (**Figure 1.6**). These enzymes are encoded by the *PhaA*, *PhaB* and *PhaC* genes respectively and constitute the *PhaCAB* operon (Mozes-Koch *et al.*, 2017). This reaction begins with the condensation of two molecules of acetyl-CoA to produce acetoacetyl-CoA, which is catalysed by  $\beta$ -ketothiolase (*PhaA*). Acetoacetyl-CoA is then converted to (*R*)-3-hydroxybutyryl-CoA monomers ((*R*)-3-HB-CoA) by acetoacetyl-CoA reductase (*PhaB*), which are then polymerised together by PHA synthase (*PhaC*) in the final reaction to form SCL PHAs such as P(3HB) (Numata *et al.*, 2013). This pathway has been extensively studied to take place within strains of, *Aeromonas hydrophila* and *C. necator*.

However, ultimately PHA is a storage molecule for bacteria and can be broken down to access its constituent compounds that originally helped form the final SCL PHA. The intracellular degradation of P(3HB) begins with the enzyme PHA depolymerase, encoded for by the *PhaZ* gene, resulting in the production of (*R*)-3-hydroxybutyric acid, the first depolymerisation product in this series of reactions. (*R*)-3-hydroxybutyric acid is then oxidised by the enzyme (*R*)-3-hydroxybutyrate dehydrogenase ((*R*)-3-HButDH) to form acetoacetic acid, which is subsequently catalysed by acetoacetyl-CoA synthase, encoded for by the *NphT7* gene to form acetoacetyl-CoA and converted back to an acetyl-CoA molecule by  $\beta$ -ketothiolase (*PhaA*) (Oeding and Schlegel, 1973). This allows for acetyl-CoA to re-enter the biosynthesis pathway or be used for other cellular processes such as within the citric acid cycle. PHA depolymerases are specific to either SCL PHAs or MCL PHAs. However, it has been noted that some strains such as *Comamonas* species can produce PHA depolymerases that are able to degrade both SCL PHAs and MCL PHAs (Idris, Su Yean and Kumar, 2018).

### 1.2.3.2 Biosynthesis of MCL PHAs

The second PHA synthesis pathway is related to fatty acid uptake (Pathway II) as the carbon source by microorganisms, which specifically involve *PhaJ* and *FabG* genes encoding for enoyl-CoA hydratase and 3-ketoacyl-acyl reductase respectively (**Figure 1.6**). After fatty acid  $\beta$ -oxidation, acyl-CoA enters the MCL PHA monomer synthesis process. During this process enoyl-CoA is converted into the PHA precursor (*R*)-3-HA-CoA by enoyl-CoA hydratase (*PhaJ*) as with 3-ketoacyl-CoA, which is also converted into (*R*)-3-HA-CoA by 3-ketoacyl-acyl reductase (*FabG*) for MCL PHA synthesis via PHA synthase (*PhaC*) (Chen, 2009). Bacterial species such as *P. putida* and *Pseudomonas aeruginosa* are both examples of microorganisms that are able to produce MCL PHAs via the fatty acid  $\beta$ -oxidation pathway as well as copolymers of poly(3-hydroxyoctanoate) (P(3HO)) and poly(3-hydroxyhexanoate) (P(3HHx)).

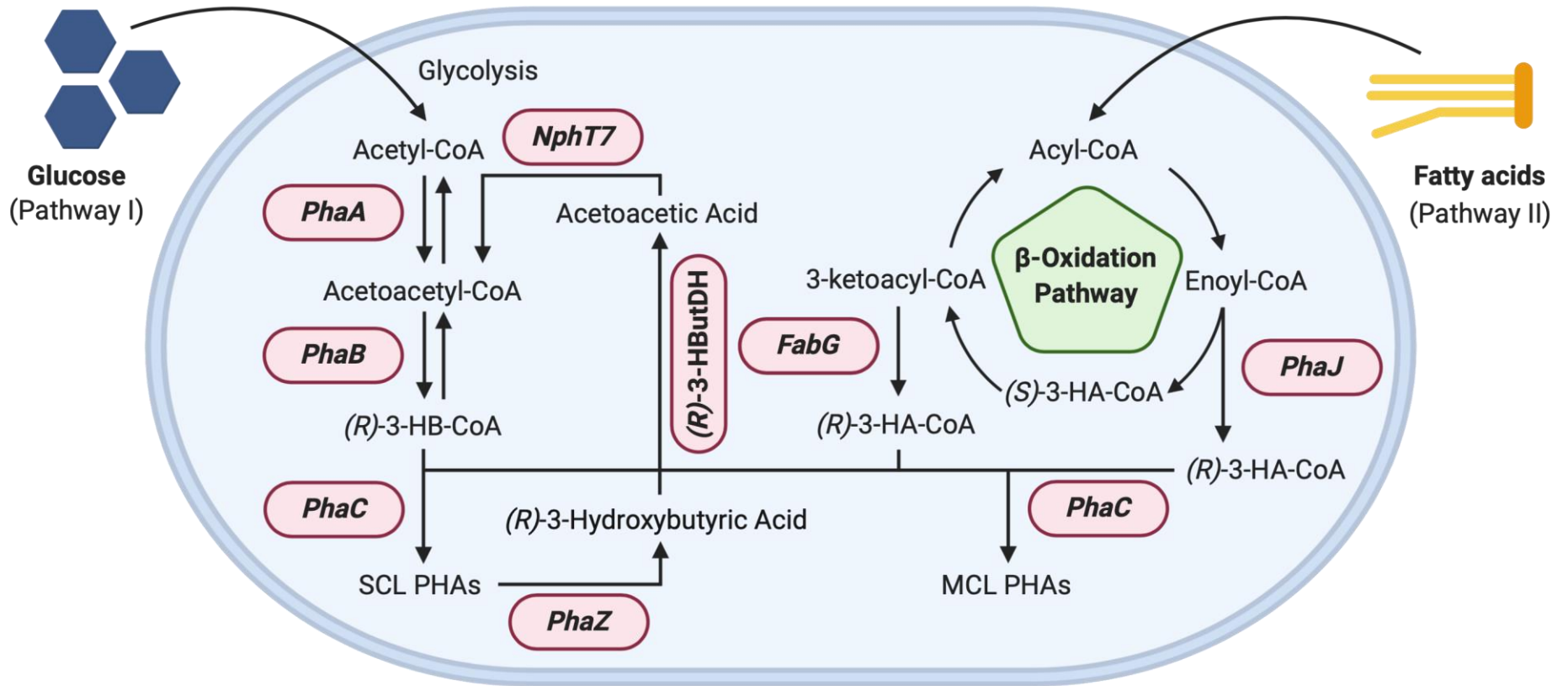


**Figure 1.6** Pathway for the biosynthesis and metabolism of PHAs in bacteria produced from sugars and fatty acids.

Alternatively, some species of bacteria such as Pseudomonads are able to utilise the third PHA pathway (Pathway III) to produce MCL PHAs from sugars, as opposed to SCL PHAs. When *P. putida* KT2442 was grown on glucose, the PHA obtained was characterised as being MCL PHA of which contained mainly copolymers of 3HO and 3HD (Huijberts *et al.*, 1992).

As stated in the first pathway, sugars are initially made to go through the process of glycolysis resulting in the production of acetyl-CoA. In turn, molecules of acetyl-CoA and bicarbonate take part in a carboxylation reaction facilitated by acetyl-CoA carboxylase, thus rendering malonyl-CoA. Subsequently, malonyl-CoA is then catalysed with an acyl carrier protein (ACP) to produce malonyl-ACP and CoA by malonyl-CoA:ACP transacylase (MCAT), encoded for by the *FabD* gene. It is at this point malonyl-ACP enters the fatty acid *de novo* biosynthesis pathway, undergoing condensation reactions with acyl-ACP, facilitated by ketoacyl synthase (KSs) to form 3-ketoacyl-ACP, which is used as a substrate for  $\beta$ -ketoacyl-ACP reductase to produce (*R*)-3-hydroxyacyl-ACP, a precursor molecule to (*R*)-3-HA-CoA, which ultimately goes on to transform into MCL PHA through a reaction involving PHA synthase (Le Meur *et al.*, 2012). It was found that the *PhaG* gene was responsible for the transformation between (*R*)-3-hydroxyacyl-ACP and (*R*)-3-HA-CoA, encoding for 3-hydroxyacyl-ACP:CoA transferase (Rehm, Mitsky and Steinbüchel, 2001).

### **1.2.3.3 Classification of PHA synthases and their genes**

Pathway I of the production of SCL PHAs naturally occurs within over 250 PHA producing bacteria. Within this pathway PHA synthase is the most important as it determines the type of PHA being synthesised. This particular type of enzyme can be classed into four major classes (I, II, III, IV) on the basis of primary structures, specificity of substrate and subunit composition (Rehm, 2003) (**Table 1.5**). All four types of PHA synthases have one conserved region of a conserved cysteine residue which is the active site of the enzyme, involved in the polymerisation reaction.

**Table 1.5** The four classes of PHA synthases (Rehm, 2003).

Class	Subunits	Size (kDa)	Substrate	Species
I	PhaC	61 - 73	3HA <sub>SCL</sub>	<i>C. necator</i>
II	PhaC	60 – 65	3HA <sub>SCL</sub>	<i>P. aeruginosa</i>
III	PhaC and PhaE	~40 and ~40	3HA <sub>SCL</sub>	<i>A. vinosum</i>
IV	PhaC and PhaR	~40 and ~20	3HA <sub>SCL</sub>	<i>B. megaterium</i>

Class I and II PHA synthases are both comprised of a singular type of subunit (*PhaC*) with  $M_W$  between 61 and 73 kDa. However, according to their *in vivo* and *in vitro* substrate specificity class I synthases (e.g., in *C. necator*) preferentially utilise CoA thioesters of various (*R*)-3- hydroxy fatty acids comprising 3 - 5 carbon atoms resulting predominantly in the production of SCL monomers, whereas in contrast to class II synthases (e.g., *P. aeruginosa* and *P. oleovorans*) that predominantly produce MCL monomers, utilising CoA thioesters of various (*R*)-3- hydroxy fatty acids comprising of 6 - 14 carbon atoms instead (Idris, Su Yean and Kumar, 2018).

Class III and IV are different to class I and II synthases as they both comprise of two different subunits as opposed to a singular one. Class III PHA synthases (e.g., in *Allochromatium vinosum*) comprise of the following two subunits: (i) the *PhaC* subunit, which has a  $M_W$  of ~40 kDa, with amino acid sequence similarity of 21 – 28% to both class I and II PHA synthases and (ii) the *PhaE* subunit, which has also has a  $M_W$  of ~40 kDa, but with no similarities with other PHA synthases (Idris, Su Yean and Kumar, 2018). This class of PHA synthase prefers CoA thioesters of (*R*)-3-hydroxy fatty acids comprising 3 - 5 carbon atoms. Class IV (e.g., in *B. megaterium*) PHA synthases resemble the class III PHA synthases, however *PhaE* is instead replaced by *PhaR* that has a  $M_W$  of ~20 kDa, and also have a substrate specificity towards CoA thioesters of (*R*)-3-hydroxy fatty acids comprising 3 - 5 carbon atoms (Rehm, 2003). A schematic diagram of the organisation of these genes encoding for different classes of PHA synthases is shown in **Figure 1.7**.

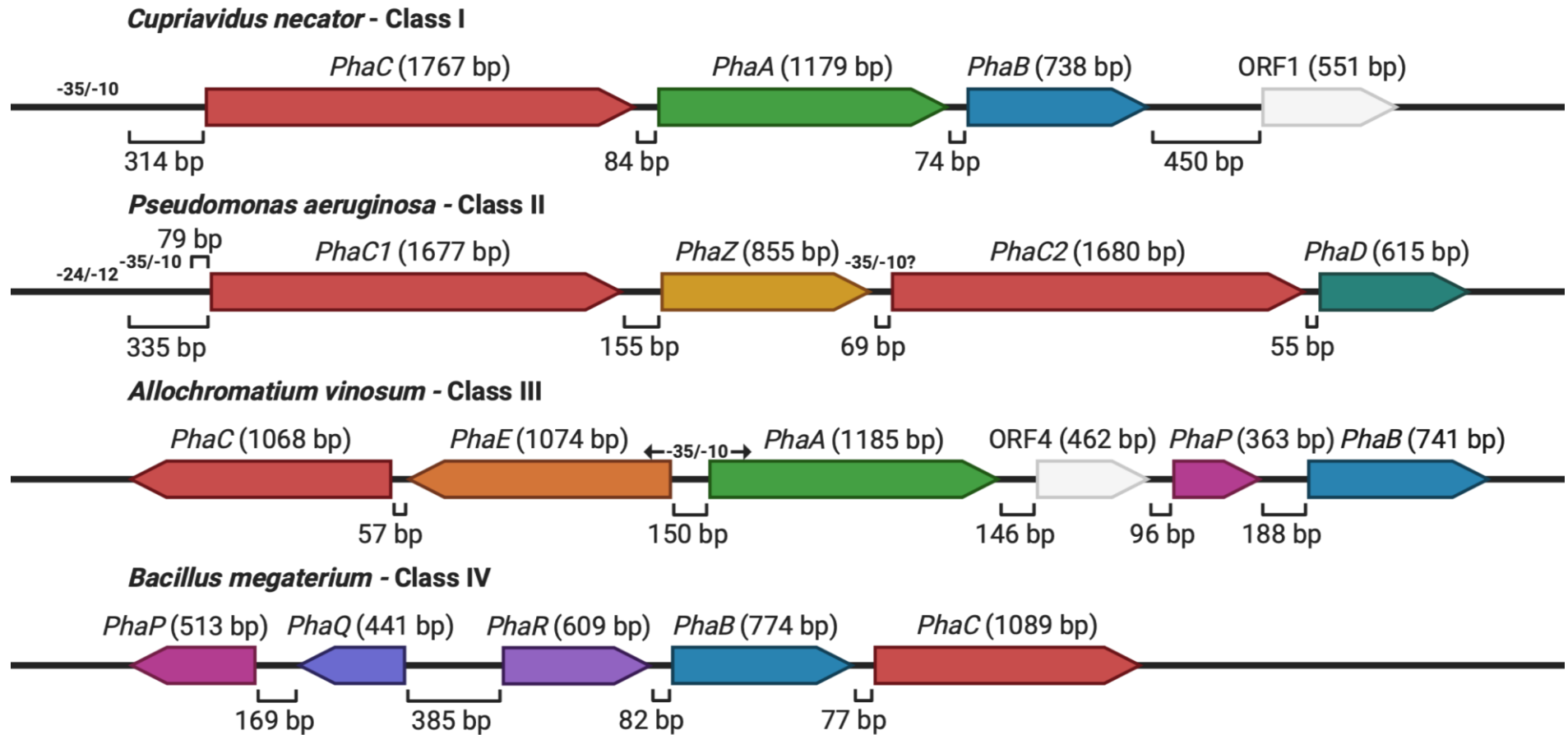


**Figure 1.7** Schematic diagram of the organisation of synthase genes encoding various classes of enzymes.

#### **1.2.4 Biodegradability of PHAs**

Biodegradation can be defined as the fragmentation or breakdown of materials by bacteria, fungi or through other biological means whether aerobically or anaerobically. As a result of this definition, PHAs can be considered as biodegradable as they are able to be degraded in biological environments through enzymatic and non-enzymatic hydrolysis as opposed to strictly thermal oxidation, photolysis or radiolysis means. The ability for PHAs to degrade naturally within the environment has made it a promising material for many applications such as within the field of biomaterials and packaging **(Section 1.5)**.

One of the biggest selling points of PHAs is its ability to biodegrade within various natural environments such as, soil, sea water and lake water. The biodegradability of PHAs can be assessed by monitoring samples within these environments and evaluating the molecular weight and mechanical strength over a period. The rate at which PHAs can biodegrade is dependent on many environmental factors, as well as factors pertaining to the PHA itself. Environmental factors that have an influence on the rate of degradation include temperature, moisture level, pH and nutrient supply, whilst simultaneously factors such as the composition of the PHA, crystallinity and surface area also have a role within the biodegradation process (Sudesh, Abe and Doi, 2000). This degradation of PHAs usually occurs at the surface via enzymatic hydrolysis. Interestingly throughout this process the molecular weight of the PHA itself remains mostly unchanged during the course of biodegradation.

The ability to breakdown PHAs is broadly carried out by microorganisms such as bacteria and fungi found within soil, sludge and sea water that are processed by microbial enzymes into organic molecules such as carbon dioxide and water under aerobic conditions or alternatively, methane and water when under anaerobic conditions. This ability possessed by microorganisms to break down PHAs depends on the release of specific

extracellular depolymerases into the surrounding environment or by the intracellular mobilisation of PHA in the accumulating strain itself (Divya, Archana and Alejandro Manzano, 2013). Both intracellular mobilisation of PHAs and extracellular degradation of PHAs differ from each other due to the difference in biophysical conformations of extracellular (denatures) PHA from those of intracellular (native) PHAs.

Intracellular PHA depolymerases can hydrolyse an endogenous carbon reservoir, which are in an amorphous state. In this state the native PHA granule's surface is layered with proteins and phospholipids, which are responsive to chemical or physical stress. This breakdown in PHA usually occurs as a method to reutilise materials used to produce the PHAs as nutrients for the cell itself. Alternatively, extracellular PHA depolymerases can degrade denatured extracellular PHA granules that are partially crystalline and lack the surface layer that covers the PHA granule when stored intracellularly.

### **1.2.5 Production strategies**

There are different variables that need to be considered in regard to the production of PHAs, including strain types, carbon and nitrogen sources and ratios, total cultivation time, and reactor volume. Optimising the process in order to obtain high product yields with a high product conversion rate is the key in process design. Various fermentation strategies and modes of fermentation (batch, fed-batch and continuous) can be used to achieve high yields of PHAs which are explored in the sections below.

#### **1.2.5.1 Raw materials**

One of the main barriers to entry to market that PHAs face is their high costs of production that is associated with them. Much of this cost is spent on the purchasing of raw materials required to produce the PHAs themselves. A strategy to help combat this issue could come in the form of being able to utilise a broad range of waste or surplus materials that can be modified for its use as feedstocks to produce PHAs. Industries such as agriculture are usually able to produce these types of materials as waste streams or by-products.

It has been estimated that the cost of carbon can account for up to 50% of the entire production costs, especially in large scale processes. This is most likely due to the fact that PHA accumulation occurs under aerobic conditions, which results in high losses of the carbon substrate by intracellular respiration. Therefore, the economic feasibility of PHA productions in large scale processes is dependent on the development of efficient fermentation processes from inexpensive carbon sources. The utilisation of waste products as carbon sources presents a twofold advantage of a decrease in the costs for disposal needs as well as the production of a value-added product (Sudesh, Abe and Doi, 2000).

Selection of an appropriate waste stream as feedstock for PHA production is mainly dependant on the global region where production is set to take place. In Europe huge amounts of surplus whey is available in the dairy industry, which provides lactose to produce lactic acid, PLA and bioethanol. The increasing production of biodiesel also generates enormous amounts of its side stream product, glycerol, which can also be used to produce PHAs or even lactic acid. Alternatively, in other parts of the globe, the waste from the sugar industry, starch, waste lipids and alcohols such as methanol are available in quantities that are appropriate for industrial process demands. Waste lipids are available from a variety of sources such as waste cooking oil, different plant oils, wastewater from olive oil and palm oil production.

#### **1.2.5.2 Batch fermentation**

The simplest and most popular mode of fermentation comes in the form of batch mode fermentation. In this mode of fermentation, all nutrients such as substrates are provided at the start of the run without the addition of more nutrients as the fermentation progresses, except for elements such as gasses, acids and bases. Ultimately, this is a closed system, which serves as an advantage as this reduces the risk of contamination as no additional components are added into the system that could potentially contaminate the entire fermentation. The fermentation period usually lasts until all the nutrients

are depleted by the microorganisms being grown before the biomass is harvested to obtain the desired product. This mode of fermentation is suitable for experiments that run for a short period of time as it is recommended that the maximum amount of carbon added at the start of the fermentation is up to 30 g/L (Raza *et al.*, 2019). This mode is also generally regarded as the easiest to operate and inexpensive, however, there are disadvantages, such as the lower biomass and product yields due to inhibited bacterial growth, which is often attributed to the limited availability of nutrients or oxygen transfer acting as limiting factors. Longer lag phases are also often observed in batch mode fermentation.

When producing PHAs the point at which a fermentation is stopped is vital as if carbon decreases to a low enough level, it could result in the bacteria producing the PHA to begin degrading the accumulated PHA, which results in decreasing the productivity of the culture. PHA accumulation begins at the start of the stationary phase of growth, thus this growth phase must be completed to allow for the maximum amount of PHA to be produced and accumulated.

### **1.2.5.3 Fed-batch fermentation**

One way of preventing nutrients from becoming a limiting factor is to constantly supply the culture with nutrients throughout the cultivation process when the concentration falls below its optimum value, which is a type of fermentation known as fed-batch fermentation, a modified version of the previous mode. This system is considered to be partly open as nutrients such as substrates are slowly added as the fermentation progresses in order to prevent nutrients becoming a limiting factor, which impedes the overall productivity of the culture. This mode of fermentation also often leads to higher product quantities overall, which favoured within industrial settings.

A major advantage of fed-batch fermentations is that cultures can be grown for an extended period as nutrients are constantly fed to the culture, as well as increasing the productivity of the culture by using various feeding

strategies. Although, with nutrients constantly being supplied into the culture comes with the increased chance of contamination. There is also the possibility that toxins and inhibitory agents could build up within the fermenter, which causes harm to the culture.

Fed-batch fermentation is one of the most suitable strategies to produce PHAs, because of its ability to reach high cell densities. For example, carbon and nitrogen are added periodically throughout the fermentation process, which are added to avoid the depletion of PHAs accumulated during the production stage until a specific biomass yield is achieved.

#### **1.2.5.4 Continuous fermentation**

The final mode of fermentation is known as continuous fermentation. During this mode of fermentation, the key feature is that fresh medium can be continuously fed into the fermenter whilst the growing culture is harvested at the same rate (chemostat). The consumed nutrients can be replenished by the fresh medium that is added as well as removing any toxic metabolites, which could be present within the culture. As fresh medium is added at the same rate the culture is removed from the fermenter a constant volume is maintained throughout the fermentation process, which eliminates the issue of maximum working volumes that the other two fermentation modes face. Continuous fermentations are known for enabling cultures to reach high productivities, especially when strains with high maximum specific growth rates are used.

Studies that used continuous fermentations to produce PHAs found that the PHA content of the cells were growth rate dependent. When dilution rate was increased, whilst biomass is also increasing, the PHA content of the cells decrease. This was shown by Preusting, Kingma and Witholt, (1991) in which they were increased the dilution rate of cultures of *P. oleovorans* from 0.09 hours<sup>-1</sup> to 0.46 hours<sup>-1</sup>, the PHA content of the cells decreased from 40% PHA yield (%DCW) to 8% PHA yield (% DCW), as well as the cell density decreasing from 2.25 g/L to 1.32 g/L. Therefore, it is important to optimise the

PHA content, biomass and productivity in continuous fermentations, which can be difficult.

### **1.3 Microbial production of PHAs**

PHA production is a trait that is widespread amongst various microorganisms, produced by over 70 genera of bacteria and *Archaea*, with the principle aim to conserve and store carbon. The specific groups mentioned will be described in the sections below.

#### **1.3.1 Gram-negative bacteria**

To date, the majority of bacteria that are able to produce PHAs can be classified as being Gram-negative bacteria. SCL PHAs can be synthesised by a variety of different Gram-negative species of bacteria; from *Azohydromonas*, *Burkholderia*, and *Cupriavidus*. According to literature, *Azohydromonas lata* possess the ability to produce between 50 – 88% dry cell weight (DCW) of P(3HB) from various different carbon substrates, including glucose, fructose and sucrose, whilst *Burkholderia* species can synthesise up to 69% DCW of P(3HB) from fatty acids (Chee *et al.*, 2010). *C. necator* is a well characterised Knallgas bacterium (hydrogen oxidising bacterium) with the ability to produce PHAs by fixing carbon dioxide through the Calvin Cycle, as well as possessing the ability to shift between heterotrophic and autotrophic modes for growth and PHA production.

Shimizu *et al.*, (2013) also suggested that both heterotrophic and autotrophic PHA biosynthesis can occur concurrently in this bacterium. Owing to *C. necator*'s distinctive physiology it also possesses the ability to utilise chemically diverse carbon sources such as carbon dioxide, sugars (*i.e.*, glucose and fructose), *n*-alkanoic acids (*i.e.*, 4-hydroxyhexanoic acid), vegetable oils (*i.e.*, olive oil, corn oil, and palm oil) for P(3HB) accumulation in the range of 67 – 88.9% DCW (Gomez *et al.*, 1996). As a result of the aforementioned bacterial species ability to high SCL PHA production capacity, wild type and mutant strains are used widely in the production of PHAs within industrial environments.

SCL PHAs have also been observed to be produced by Gram-negative methylotrophs (microorganisms that have the ability to utilise simple methyl compounds such as methane and methanol as a source of carbon and energy). *Methylobacterium extorquens* and *Paracoccus denitrificans* produced up to 46% DCW P(3HB) from menthol and up to 24% DCW poly(3-hydroxyvalerate) (P(3HV)) from *n*-pentanol respectively (Bourque, Pomerleau and Groleau, 1995). Due to the cheaper cost of methanol compared to pure sugar substrates, the use of methylotrophs for industrial SCL PHA production could potentially reduce their cost of production. However, given their lower yields in comparison to species that can utilise sugar substrates, further studies have to be conducted in order to enhance their PHA content and PHA productivity before they can be considered as inoculum alternatives for industrial scale producers of SCL PHAs.

*Pseudomonas* species are often reported as one of the main producers of MCL PHAs, usually producing PHA contents within a range between 1 – 30% DCW. However, higher MCL PHA contents have also been observed in other *Pseudomonas* species such as within *P. putida* mt-2, which reportedly could produce up to 77% DCW MCL PHAs from octanoic acid and *P. putida* KT2440, a mutant strain of *P. putida* mt-2 which lacks the TOL plasmid, can produce up to 75.4% DCW using nonanoic acid as a carbon source (Sun *et al.*, 2007). Besides from MCL PHAs, some Pseudomonad species have also been reported to synthesise SCL-MCL-PHA co-polyesters. Species such as *P. marginalis*, *P. mendocina*, *P. putida* GPo1 and *P. oleovorans*, when *n*-alkanoates and 1,3 butanediol were supplemented as carbon sources. Most of these Pseudomonad species, 3-hydroxybutyrate (3HB) typically incorporate as a minor constituent in SCL-MCL-PHAs (between less than 1 mol% and 7.8 mol%) (Lee *et al.*, 1995). Although, *P. oleovorans* cultivated on 4-hydroxyhexanoic acid resulted in a copolymer predominated by 3HB (92.4 mol%) (Valentin *et al.*, 1994). Pseudomonads are also well known for their bioremediation properties including the biodegradation recalcitrant and/or toxic aromatic carbon substrates, and have been successfully applied in the

treatment of contaminated effluents, exhaust gas and soils (Poblete-Castro *et al.*, 2012).

Nikodinovic *et al.*, (2008) were able to demonstrate that aromatic degraders *P. putida* F1, *P. putida* mt-2 and *P. putida* CA-3 possess the ability to bio-convert toxic pollutants such as benzene, toluene, ethylbenzene and xylene (BTEX) as well as styrene to MCL PHAs. *P. putida* CA-3 and other Pseudomonads including *P. aeruginosa* PAO1, *P. frederiksbergensis* GO23, *P. putida* GO16 and *P. putida* GO19 could all utilise crude pyrolysis products from different plastics (*i.e.*, PS, PE and PET) for MCL PHA production, which offers the added potential benefit to off-set waste treatment cost through PHA recovery (Guzik *et al.*, 2014).

PHA production and accumulation has also been observed in Gram-negative extremophilic bacteria. These types of bacteria can accumulate PHAs under unique conditions with either high salinity or elevated temperatures. The halophilic bacteria *Halomonas boliviensis* LC1 can grow and produce 56% DCW of SCL PHA P(3HB) from starch hydrolysate under moderate saline conditions (0.77 M NaCl), whilst the thermophilic bacteria *Thermus thermophilus* HB8 synthesised up to 35.6% DCW of SCL-MCL PHA copolymer from whey at high cultivation temperatures of 70°C (Quillaguamán *et al.*, 2005). Compared to other Gram-negative bacteria, extremophiles are advantageous in terms of their lower sterility demand as well as their potential for direct application with waste effluents originally high in salt concentrations or temperatures, eliminating the need and cost involved for pre-treatment of waste effluents.

However, the main concern with Gram-negative bacteria is the presence of lipopolysaccharide (LPS) endotoxins in the bacteria's outer cell membrane, which may co-purify with crude PHA polymer during the extraction process (Rai *et al.*, 2011). LPS endotoxin is a pyrogen, which has the potential to elicit a strong inflammatory response. As a result of this response, it could result in the PHA produced being unsuitable for biomedical applications (Ray *et al.*, 2013). The removal of LPS endotoxins can be achieved through the treatment

of PHA polymer with oxidising agents (*i.e.*, sodium hypochlorite and sodium hydroxide, ozone, hydrogen peroxide, and benzoyl peroxide) with repeated solvent extractions, or with solvent extraction followed by purification with activated charcoal (Rai *et al.*, 2011). Although, these methods result in an increase in the overall cost of production of PHAs as well as changes in the PHAs properties (*i.e.*, reduction in molecular mass and polydispersity), both which are undesirable from an industrial producer's perspective.

### 1.3.2 Gram-positive bacteria

Just as PHA production has been reported in a variety of species of Gram-negative bacteria, Gram-positive bacteria are also able to produce and accumulate PHAs. For example, PHA production has been reported in genera *Bacillus*, *Caryophanon*, *Clostridium*, *Corynebacterium*, *Micrococcus*, *Microlunatus*, *Microcystis*, *Nocardia*, *Rhodococcus*, *Staphylococcus*, and *Streptomyces* (Lu, Tappel and Nomura, 2009). When comparing the different types of bacteria, Gram-positive bacteria were found to mostly produce SCL PHAs, and at lower PHA contents (~2 – 50% DCW), which is the predominant reason as to why Gram-positive bacteria have yet to be adapted for commercial PHA production (Valappil *et al.*, 2007). Some strains have displayed the ability to synthesise MCL PHAs or SCL-MCL PHA copolymers if cultivated with suitable carbon substrates and optimum conditions provided.

A study by Shahid *et al.*, (2013) demonstrated that *B. megaterium* formed exclusively P(3HB) from glycerol and succinic acid in a mineral medium with the supplementation of nitrogen, but started to produce SCL-MCL PHAs upon subculturing to the same medium, but in the absence of nitrogen. In the same bacterium, the formation of exclusively MCL PHAs (48% DCW) was observed when it was cultivated on octanoic acid and in the absence of nitrogen (Shahid *et al.*, 2013).

However, despite Gram-positive bacteria generally producing lower amounts of PHAs in comparison to their Gram-negative counterpart, Gram-positive bacteria possess advantageous characteristics for the production of PHAs.

This comes in the form of their lack of LPS, which could potentially make Gram-positive bacteria a better source of PHAs as raw materials for biomedical applications (Valappil *et al.*, 2007). Although, it is known that some Gram-positive bacteria are known to produce lipidated macoamphiphiles including lipoglycans and lipoteichoic acids (LTA), which are known to have immunogenic properties like LPS (Ray *et al.*, 2013). The bacterial genera *Corynebacterium*, *Nocardia*, *Rhodococcus* reportedly produce lipoglycans, whereas LTA production is known to occur in the genera *Bacillus*, *Clostridium*, and *Staphylococcus*, but some PHA producing strains from these genera lack LTA, potentially making them viable candidates (Sutcliffe and Shaw, 1991). As a result of the potential immunogenic response triggered by PHA-based biomedical applications produced by Gram-positive bacteria require further investigation as to whether there are alternative lipidated macoamphiphiles in Gram-positive and PHA producing bacteria, but at present the immunogenic effects of lipidated macoamphiphiles in PHAs remains unknown.

Future *in vitro* and *in vivo* evaluation studies would be imperative to evaluate the suitability of PHAs derived from Gram-positive bacteria for use in biomedical applications.

### **1.3.3 Archaea**

To date only one group of *Archaea* species (haloarchaea) have been identified as to be able to produce PHAs. Haloarchaeal species, specifically the genera *Haloferax*, *Halalkalicoccus*, *Haloarcula*, *Halobacterium*, *Halobiforma*, *Halococcus*, *Halopiger*, *Haloquadratum*, *Halorhabdus*, *Halorubrum*, *Halostagnicola*, *Haloterrigena*, *Natrialba*, *Natrinema*, *Natronobacterium*, *Natronococcus*, *Natronomonas*, and *Natronorubrum* are all known producers of PHAs (Han *et al.*, 2010). Haloarchaea are extremely halophilic members of the archaea domain, which require high salt concentrations for normal function of enzymatic activities, and grow optimally at concentrations of up to 6 M sodium chloride (Danson and Hough, 1997).

Although haloarchaea require such extremes conditions to survive and grow they have been reported to be able to exclusively synthesis SCL PHAs from glucose, volatile fatty acids and complex carbon sources such as starch, whey hydrolysate, vinasse and crude glycerol from biodiesel production (Hermann-Krauss *et al.*, 2013). The type of PHAs produced appear to be homopolymers containing either 3HB or 3HV monomers, and/or heteropolymers containing both 3HB and 3HV monomers (Han *et al.*, 2010). However, just like Gram-positive bacteria, haloarchaea suffer from the inability to accumulate high contents of PHAs in comparison to Gram-negative bacteria, producing PHAs at lower cellular contents between 0.8 – 22.9% DCW (Han *et al.*, 2010).

The best PHA producer from the genera of haloarchaea has been identified as *Haloferax mediterranei*, which required between 2 – 5 M sodium chloride for optimal growth and can accumulate high PHA levels between 50 – 76% DCW. *H. mediterranei* has been discussed as a candidate for the production of PHA production as the hypersaline conditions, required for its growth as well as PHA cultivation means that few contaminating organisms can survive and thereby reducing the need for sterility and its associated costs (*i.e.*, process piping, instrumentation and insulation, electricity for steam generation, *etc.*) (Bhattacharyya *et al.*, 2012). However, when compared to moderately halophilic bacteria such as *H. boliviensis* LC1, the extreme salinity required by haloarchaea could be an issue in itself in regard to PHA production as the high salt concentration results in manufacturers incurring higher costs for chemicals as well as the acceleration of corrosion of stainless-steel fermenters (Quillaguamán *et al.*, 2005).

Nevertheless, haloarchaea hold advantages over halophilic bacteria due to their ease of PHA recovery. PHA recovery from halophilic bacteria usually requires the use of chemical, enzymatic or mechanical methods for cell wall disruption to release intracellular PHA granules that have accumulated within the bacteria itself, and it is these methods that can account for up to 50% or more of the overall cost of production of PHAs (Chen *et al.*, 2001). Extraction solvents such as chloroform and acetone also pose potential environmental hazards if their utilisation and disposal are mismanaged. Conversely,

haloarchaea undergo cell lysis in distilled water, resulting in the release of the intracellular PHA granules that can then be recovered by low-speed centrifugation (Poli *et al.*, 2011). Consequently, when comparing the halophilic bacteria to haloarchaea bacteria, the latter has a relatively easy, less chemical and energy intensive process, which ultimately translates to lower extraction cost and low ecological footprint.

#### **1.3.4 Detection of PHA**

Over time various methods have been developed and become available for the detection and analysis of intracellular microbial PHAs. These methods are not only useful for identifying novel PHA producing organisms, but also for routine monitoring of PHA production bioprocesses. **Table 1.6** provides a detailed summary about each method used for the detection of PHAs and the principal characteristic of the method as well as comparing the advantages and disadvantages of each method.

**Table 1.6** Methods of detection of PHAs (Tan *et al.*, 2014)

Method	Characteristic	Advantages	Disadvantages
Polymerase chain reaction (PCR) gene detection	Detection of the <i>PhaC</i> gene encoding for PHA synthase enzyme	Requires small sample size High sensitivity and high throughput	Primers are inadequate for detection of all <i>PhaC</i> genes Prone to detection errors
Nile red staining	Detection of intracellular PHA granule structures	Enables direct observation of live and actively growing cells Requires small sample size Rapid analysis Allows for the differentiation between SCL PHAs and MCL PHAs under flow cytometry analysis	Method can't discriminate between lipids and PHAs Less effective at distinguishing between PHA-negative and PHA-positive strains of Gram-positive bacteria
Transmission electron microscopy (TEM)	Detection of intracellular PHA granule structures	High throughput High magnification enables direct visualisation and size measurements of PHA granules	Tedious sample preparation involving radioactive and hazardous chemicals Cells are killed during sample preparation

<b>Method</b>	<b>Characteristic</b>	<b>Advantages</b>	<b>Disadvantages</b>
Crotonic acid assay	Quantitative determination of P(3HB)	Easy and inexpensive assay Specific for the detection of P(3HB)	Results can be interfered by other endogenous components and matrix interferences can result in over estimation of P(3HB) content
Fourier transform infrared spectroscopy (FTIR)	Cellular PHA content	Requires small sample size Short analysis time Solvent usage is optional Can be used to provide quantitative information Enables online and real-time PHA analysis High throughput	Method is limited to the detection of only P(3HB) Method can't discriminate between different PHA monomeric units Unable to distinguish between homogenous PHA and PHA copolymer Low sensitivity Quantification limited to SCL PHAs

<b>Method</b>	<b>Characteristic</b>	<b>Advantages</b>	<b>Disadvantages</b>
Liquid chromatography (LC)	PHA monomeric units	<p>Does not require cell lyophilisation</p> <p>Requires small sample size</p> <p>Short sample preparation time</p> <p>Provides both quantitative and qualitative information</p> <p>Coupling with mass spectrometer (MS) detector enables tentative identification of novel PHA monomers</p> <p>Applicable for quantitative and qualitative analysis of MCL PHA monomers</p>	<p>Low separation power that is currently limited to analysis of SCL PHA monomers unless coupled to MS detector</p> <p>Unable to distinguish between homogenous PHA and PHA copolymer</p>
Gas chromatography (GC)	PHA monomeric units	<p>High separation power and high sensitivity</p> <p>Provides both quantitative and qualitative information</p> <p>Can be applied for tentative identification of novel PHA monomers when coupled to MS detector</p>	<p>Requires cell lyophilisation</p> <p>Long sample preparation time requiring the use of hazardous and volatile solvents</p> <p>Unable to distinguish between homogenous PHA and PHA copolymer</p>

#### 1.3.4.1 Downstream recovery process methods

Downstream recovery processing refers to the process of which biosynthetic products (such as PHAs) are recovered and purified from fermentation broth. By design, downstream recovery process methods should be economical, and environmentally friendly, avoiding the use of toxic solvents. However, unfortunately, many of the traditional approaches towards polymer recovery from cellular biomass often involve large amounts of toxic solvents such as chloroform, methylene chloride or acetone, as they are effective agents at degrading the cell wall and cell membrane to release PHAs (Raza *et al.*, 2019). Although, alternative methods to extract PHAs exist, which avoid the use of toxic solvents, but they are not without their disadvantages. For example, the sodium hypochlorite method is an alternative route for the recovery of PHAs that does not involve the use of any solvent. The method works by dissolving the non-PHAs cellular mass, but in turn reduces the molecular mass of the polymer itself, rendering the PHA produced unfit for usage in particular industries such as within the medical field, as PHAs must be of high purity and contain no impurities.

Alternatively, “green solvents” have been suggested as a method to help improve the downstream recovery process method of PHAs, by using solvents such as dimethyl carbonate and various alcohols like ethanol, 1-propanol and 1-butanol), which can be used to replace traditional solvents that are harmful towards the environment (Koller, 2020). Nevertheless, linear carbonates such as dimethyl carbonate require high temperatures for efficient extraction of PHAs, which besides being energy demanding, also typically results in the reduction in the PHAs molecular mass. When transesterification between esters used as solvents as PHA takes place, which relates back to the previous issue explained when using the sodium hypochlorite method. Importantly the potential solvation of PHAs using these “green solvents” depends on the crystallinity of the PHA. Amorphous MCL PHAs are easily dissolved by these solvents as opposed to crystalline SCL PHAs. A comparison of the advantages and disadvantages of the extraction methods that can be used for the extraction of PHAs are shown in **Table 1.7** below.

**Table 1.7** Comparison of the advantages and disadvantages of various PHA extraction methods (Kunasundari and Sudesh, 2011)

Method	Recovery Method	Advantage	Disadvantage
Digestion method	Dissolve cell mess to conserve PHA granules (e.g., Alkali acid and strong oxidising agent used to non-selective digestion method)	98% purity of product	Treatment required to remove surfactant from wastewater
	Protolytic enzyme and anionic surfactant used for selective digestion of non-cell dry mass	Increase intracellular polymer content recovery	
Cell fragility	Gram-positive and Gram-negative bacteria both are used. Cell wall strength of bacteria compromised by modifying the composition	Appropriate size of PHA granule	Need to balance cell wall softening and cell integrity in order to promote microbial growth with a higher PHA content
	The accumulation of PHA in cells causes fragility	Non-cell dry mass converted to sustainable by value added way	
	Inorganic salt media was used which decrease other amino acids	Inorganic media was used to recover the polymer with greater yield and ease	
Irradiation	Gamma irradiation has shown to influence wet cells assisting in the cell disruption process	Simple, rapid and inexpensive method	
		Environmentally friendly	
		Retention of solvent solubility due to the low degree of cross-linking	Length of irradiation time
		No chemicals used	High initial investment cost

Method	Recovery Method	Advantage	Disadvantage
Solvent extraction	A solvent based recovery of PHA and collected out by precipitation method	Purity of product obtained from 95 - 97%	Non environmentally friendly
	Halogen containing solvent and other solvent also used such as methanol	Solvent extraction agent works at 100°C	Consumption of large volumes of toxic and volatile solvents
	Water can be used as a solvent too	The use of water make process cheaper	High capital and operational costs
Mechanical disruption method	Bead milling and high pressure homogenisation used for disruption	Minimum damage to the environment and polymer as there is no addition of chemicals	Lengthy process
	Purity of product was increased using surfactant in process of recovery	Less contamination	Various parameters must be controlled precisely
Heat pre-treatment	To assess the various enzyme (trypsin, lysozyme) for PHA extraction	Greater yield with 99% purity	Formation of fine cellular debris that can interfere with the downstream process
		Reutilization of nutrients released during enzymolysis	
Insect based recovery of PHA	Insects have ability to lyophilized cell with polymer granules	The cell biomass was obtained with 54% of yield	
	The larvae of <i>Tenebrio molitor</i> and mealworm beetle recover PHA by engulfing them		

Abbreviation: Polyhydroxyalkanoate (PHA)

#### 1.4 Global markets and economics of PHAs

Despite the clear environmental advantages PHAs possess over mineral-based polymers, currently their applications are unfortunately limited to small scale ventures. This is often due to the lack of available producers of PHAs in comparison to producers of traditional plastics, as opposed to limited usages. **Table 1.8** displays the different companies within the market that are producing PHAs. The main problem associated with large scale production of PHAs is their high costs, which ultimately hampers the progress for their use in mainstream products and phasing out mineral-based polymers.

Sukan, (2015) reported that 1 kg of PHA was being produced by the company Metabolix and sold under the trade name Mirel for \$11, in comparison to PET, which at the time was being sold for between \$0.50 - \$1.50 per kg. In order to tackle the biggest issue PHA producers face, a drastic reduction in cost is required for PHAs to become a viable competitor to mineral-based polymers, with an estimated cost reduction of ~86% (~\$1.60 per kg of PHA) (Philip *et al.*, 2007). This could come in the form of improving yield of PHA produced to help facilitate a reduction in costs. However, it is often difficult to compare the prices of the two different polymers due to the constant fluctuations in oil prices due to the discovery of new oil reservoirs and the over extraction of crude oil, which in 2020 lead to supply outstripping demand. As a result of this imbalance of supply and demand, in April 2020 US oil prices turned negatives for the first time in history, due to major economies shutting down because of coronavirus.

Ultimately, there are three main costs factors in the production of PHAs. In the case for production of P(3HB), Zahari *et al.*, (2015) estimated that the largest cost was attributed to raw materials (29%), followed by equipment depreciation (27%) and extraction and purification (20%). Various strategies have been explored in order to lower the price and make the entire process more efficient, including using cheaper carbon sources, design of genetically engineered strains and enhancement of downstream and upstream processes.

**Table 1.8** List of commercial companies producing PHAs (Dufour *et al.*, 2019).

Company (Country)	Product/(Commercial Name)	Substrate	Production/planned capacity (ton/year)
Bio-on (Italy)	PHB, PHBV spheres/(Minerv <sup>®</sup> - PHA)	Sugar beets	10000
Biomer (Germany)	PHB pellets/(Biomer <sup>®</sup> )	Sucrose	-
Goodfellow Cambridge Ltd. (UK)	PHA granules/(Goodfellow)	-	-
KANEKA CORPORATION (Japan)	PHB/(AONILEX <sup>®</sup> )	Fatty acids	20000
Meredian/Danimer Scientific (USA)	MCL PHA/(Nodax <sup>™</sup> )	Canola oil	13500
Metabolix (USA)	PHB pellets/(Mirel <sup>®</sup> )	Glucose	50000
Mitsubishi Gas Chemicals (Japan)	P(3HB)/(Biogreen <sup>®</sup> )	Methanol	50
Newlight Technologies (USA)	PHA/ (AirCarbon <sup>™</sup> PHA)	-	50
PHB Industrial S.A. (Brazil)	(BIOCYCLE <sup>®</sup> )	Saccharose	3000
PolyFerm (Canada)	MCL PHAs/(VersaMer <sup>™</sup> PHA)	Sugars, vegetable oils	-
Shezen Ecomann Biotechnology Co. Ltd. (China)	PHA pellets, resins, microbeads/(AmBio <sup>®</sup> )	Glucose	5000
SIRIM Bioplastic Pilot Plant (Malaysia)	Various types of PHAs	Palm oil mill effluent, crude palm kernel oil	2000
TianAn Biological Materials Co. Ltd. (China)	PHB, PHBV/(ENMAT <sup>™</sup> )	Dextrose	50000
Tianjin Green Biosciences (China)	(GreenBio)	-	10000
Tianjin Northern Food (China)	-	-	10000
TianjinGreenBio Material Co. (China)	PHB films, pellets/(Sogreen <sup>®</sup> )	Sugar	10000
Yikeman Shandong (China)	-	-	3000

Abbreviations: Polyhydroxybutyrate (PHB), Poly(3-hydroxybutyrate-co-3-hydroxyvalerate) (PHBV), Polyhydroxyalkanoate (PHA), Medium-chain-length polyhydroxyalkanoates (MCL PHAs)

## **1.5 Applications of PHAs**

PHAs are “environmentally friendly”, highly biocompatible material with desirable mechanical and thermal properties proving to be a versatile material with the potential to be commercialised and used in a plethora of industries and applications including medicine, packaging, agriculture and food technology. As a result, PHAs have generated great interest and research amongst manufactures with some suggesting PHAs as a potential material to replace existing conventional materials within the market such as metals, glass and synthetic polymers. Some of the applications of PHAs are discussed in the follow sections.

### **1.5.1 Biomedical applications of PHAs**

PHAs are natural polymers with biocompatibility, biodegradability and lack of cytotoxic properties (Valappil *et al.*, 2006). Hence, PHAs are attractive materials for biomedical applications. They have been broadly utilised to prepare some medical devices such as sutures, stents, nerve repair devices and wound dressing (Rai *et al.*, 2011). Moreover, PHAs support cell attachment, migration, differentiation and proliferation functions which make them the material of choice for biomedical applications. Some of the biomedical applications of PHAs are discussed here as follows.

#### **1.5.1.1 PHAs as the scaffold materials in wound management**

P(3HB) was first suggested as an absorbable suture in mid 1960s. P(3HB) in the form of nonwoven fibre was then investigated for wound dressing materials, such as swabs, gauze, lint or fleece, by Steel and Norton-Berry in 1986. In earlier investigations, it was observed that P(3HB) and P(3HB-co-3HV) sutures had the required strength for myofacial (skeletal muscle) wound healing (Shishatskaya *et al.*, 2004). These sutures were also compared with natural absorbable (catgut) and nonabsorbable (silk) sutures. In these investigations, P(3HB) and P(3HB-co-3HV) sutures were implanted in female wistar rats in which a prominent macrophagal stage was observed throughout the post-surgery monitoring period (Shishatskaya *et al.*, 2004). Moreover, a

prolonged 1 year in vivo investigation by Shishatskaya and colleagues also showed a positive response, including less inflammatory reactions, necrosis and carcinogenesis, when P(3HB) and P(3HB-co-3HV) sutures were used. No change was observed in test animals in their weights, internal organs, blood morphology, biochemistry and lymphoid tissue reactions after suture implantation. Therefore, these investigations have revealed that PHAs can be further explored for the development of future natural absorbable wound sutures. P(3HB) and P(3HB-co-3HV) were also assessed by Webb and Adsetts in 1986 for their use as wound plaster in case of emergency to avoid any contamination through airborne bacteria (Williams and Martin, 2005).

### **1.5.1.2 PHAs as drug delivery systems**

The traditional way of administering drugs is an either intravenous or extravascular route including oral administration. These methods have a major drawback of uncontrollable drug release at the target site. Hence, more advanced methods should be developed to overcome this problem. One such approach is to utilize biodegradable polymers as the drug delivery vehicles. Homo and copolymers of lactate and glycolate are commercially available and have shown sustained drug release over a 30 day period (Valapil *et al.*, 2007). However, they do not show controlled release which reinforced scientists' interest in developing an alternative material for controlled drug delivery systems. In early 1990s, researchers noted PHAs with biodegradability and biocompatibility properties which made them potential biomaterials for drug delivery. P(3HB) was analysed for controlled release of the 7- hydroxyethyl theophylline which showed that polymer composition and its porosity combined with molecular weight of this drug affected the controlled release of the drug. Moreover, when metoclopramide (a drug used in the treatment of cattle disease) was encapsulated in P(3HB) and implanted subdermally in cattle, long term-controlled release of this drug showed a positive response for this application (Jones *et al.*, 1994).

## 1.6 Quorum sensing

The idea that bacteria are isolated organisms is widely no longer accepted by the scientific community as they have developed a sophisticated method of communication ensuring their own survival through various means. They are able to demonstrate different behaviours when at various population densities, with certain behaviours being carried out only when the population has reached a high enough concentration threshold. This is possible through the regulatory process of quorum sensing, (originally termed autoinduction) (Turovskiy *et al.*, 2007). The mechanism behind quorum sensing is dependent on the production, release and detection of chemical signal molecules, known as autoinducers (Abisado *et al.*, 2018). Bacteria have specific receptors found on their cell surface for the detection of these signalling molecules, which are released by themselves, as well as nearby bacteria. The presence of other bacteria within the nearby environment is vital, as the chance of detecting a bacterium's own autoinducer molecule is low. Once an autoinducer molecule is bound to a receptor, the transcription of genes is activated as well as the production of more autoinducers. Initially when there are only a few of the same bacteria within an environment the secretion of these autoinducers is very low, due to the fact that diffusion reduces the concentration of autoinducers to nearly zero, and as a result very little of the signalling molecules are produced by the bacteria (Deep, Chaudhary and Gupta, 2011). However, as the density of these bacterial cells increases, so does the concentration of the autoinducers produced. In turn this creates a positive feedback loop, as more receptors are likely to become activated due to the increase in concentration of autoinducers, which results in the increased production of signalling molecules too. These bacteria can utilise quorum sensing communication circuits to regulate a wide array of physiological activities including symbiosis, antibiotic production, motility, biofilm formation as well as increasing population density (Rasamiravaka *et al.*, 2015).

Quorum sensing was first described in 1970 by Kenneth Nealson, Terry Platt, and J. Woodland Hastings, who were able to establish a link between population density of the marine bacterium *Aliivibrio fischeri* (formerly *Vibrio*

*fischeri*) and its bioluminescence ability. *A. fischeri* lives in a symbiotic relationship with various marine animals, however its particular relationship with *Euprymna scolopes* (Hawaiian bobtail squid) has been studied extensively. *A. fischeri* can be found in the squid's photophore (light organs), where they are given nutrients such as sugars and amino acids as well as protection, whilst in return the squid benefits from the bacterium's bioluminescence that aids in hiding the squids silhouette when viewed from below by matching the amount of light hitting the top of the mantle (counter illumination), which enhances its ability to evade potential predators. The specifics behind how *A. fischeri* can successfully bio-luminesce at high population densities only will be explained in **Section 1.6.1.1**.

### **1.6.1 Quorum sensing in bacteria**

Both Gram-negative and Gram-positive bacteria can communicate through the process of quorum sensing. However, the types of autoinducers they communicate through are different to each other. Gram-negative bacteria employ *N*-acyl homoserine lactones (AHLs), whereas Gram-positive bacteria utilise modified oligopeptides (Verbeke *et al.*, 2017). The mechanisms as to how these signalling molecules work within each type of bacterium have been explored in the sections below and have also been illustrated in **Figure 1.9**.

#### **1.6.1.1 Mechanisms of quorum sensing molecules in Gram-negative bacteria**

Most Gram-negative quorum sensing systems have been found to utilise the *N*-AHLs as signalling molecules, produced acyl-HSL synthase enzymes, which are encoded by the *LuxI* gene. When produced, AHL molecules accumulate within the cell's cytoplasm until a concentration gradient builds up between the inside of the cell and its surroundings. Once the concentration gradient is high enough, the AHL molecules can passively diffuse out of the cell. Depending on the number of cells, as the amount of AHL molecules outside of the cell gradually increases, the concentration gradient switches as the concentration of AHLs outside of the cells becomes greater than of the concentration inside. As a result, this allows for the AHL molecules to passively

diffuse back into the cells, where they are then able to bind to cytoplasmic transcriptional activators encoded by the *LuxR* gene and in turn induce the expression of target genes (Papenfort and Bassler, 2016).

For example, the mentioned bacterium *A. Fischeri* is Gram-negative and its ability to luminesce depends on quorum sensing. At high cell densities ( $>10^7$ CFU/mL) this bacterium has access to the ability of bioluminescence, via the production of the luciferase enzyme, which catalyses redox reactions and is solely responsible for the Hawaiian bobtail squid's ability to bio-luminesce (Deep, Chaudhary and Gupta, 2011). *A. Fischeri* produces the AHL molecule *N*-(3-oxohexanoyl)-L-homoserine lactone (3-oxo-C<sub>6</sub>-HSL) by Lux I acyl-HSL synthase and accumulates within the cytoplasm of the cell, causing a concentration gradient to be formed of quorum sensing molecules between the inside of the cell and its surroundings. As this concentration gradient steepens molecules of 3-oxo-C<sub>6</sub>-HSL can passively diffuse through the cell membrane and into its surroundings. Over time, as more quorum sensing molecules diffuse out of the cell's cytoplasm and into its surroundings, the concentration gradient begins to reverse as the concentration of quorum sensing molecules outside of the cells (within the surroundings of the cells) becomes higher than that of within the cells. Consequently, this allows for 3-oxo-C<sub>6</sub>-HSL to passively diffuse back into the cell as the threshold concentration required is reached for diffusion to occur. Once back inside of the cell, 3-oxo-C<sub>6</sub>-HSL binds to the Lux R-type transcriptional activator, which in turn binds to the *LuxCDABEG* operon increasing the expression of the targeted genes. In particular *LuxA* and *LuxB* genes produce proteins, that when combined together form the luciferase enzyme. This increased transcription of the *LuxCDABEG* operon also increases the transcription of the *LuxI* and *LuxR* genes, increasing the production of Lux I acyl-HSL synthase and in turn, 3-oxo-C<sub>6</sub>-HSL as well as Lux R-type transcriptional activator.

Similarly, *P. aeruginosa* is another example of Gram-negative bacteria that employs a LuxI/LuxR quorum sensing system to communicate. *P. aeruginosa* is an opportunistic pathogen that can chronically colonise and infect patients suffering from cystic fibrosis (Steindler *et al.*, 2009). This bacterium is able to

utilise quorum sensing for the coordination of biofilm formation as well as antibiotic production, which in turn aids in its pathogenicity. *P. aeruginosa* holds two pairs of LuxI/LuxR homologues in the form of LasI/LasR and RhII/RhIR. Both LasI and RhII are synthase enzymes that drive the production of *N*-(3-oxododecanoyl)-L-homoserine lactone (3-oxo-C<sub>12</sub>-HSL) and *N*-butanoyl-L-homoserine lactone (C<sub>4</sub>-HSL) respectively (**Figure 1.8**), which again accumulate within the cytoplasm until a concentration gradient is created between the cell and its surroundings, resulting in the quorum sensing molecule being able to passively diffuse out of the cell through the cellular membrane (Rasamiravaka *et al.*, 2015). Over time as the concentration increases outside of the cell, the AHL signalling molecules are able to diffuse back into the cell and bind and activate their cognate transcriptional activators, (LasR and RhIR) influencing the transcription of targeted genes.

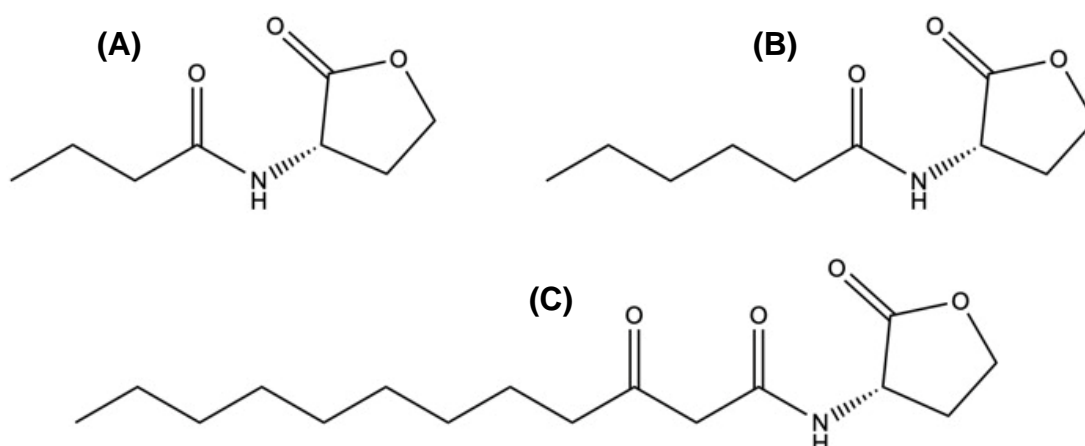


**Figure 1.8** Chemical structures of quorum sensing molecules (AHLs) produced by Gram-negative bacteria: **(A)** C<sub>4</sub>-HSL, **(B)** C<sub>6</sub>-HSL and **(C)** 3-oxo-C<sub>12</sub>-HSL

#### 1.6.1.2 Mechanisms of quorum sensing molecules in Gram-positive bacteria

In comparison Gram-positive bacteria utilise oligopeptides also known as autoinducer peptides (AIP) as autoinducers for quorum sensing as opposed to Gram-negative bacteria, which use AHLs. These peptides are synthesised by ribosomes as precursor oligopeptides and are cleaved within the cytoplasm

as a form of post-translational modification, to create functional molecules around 10 - 20 amino acids long. Unlike AHLs, AIPs are unable to freely diffuse through the cellular membrane and therefore must be actively transported out of the cell, which is facilitated by the transmembrane ATP-binding cassette (ABC) transporter (Turovskiy *et al.*, 2007).

Once a high enough concentration of AIPs has been reached outside of the cell, AIPs are able to bind to a receptor on the cell surface beginning a cascade of reactions. While Lux R-type transcriptional activators are found within the cytoplasm of Gram-negative bacteria, the receptors for AIPs molecules are embedded within the membrane of Gram-positive bacteria. A typical Gram-positive quorum sensing circuit consists of a two-component signalling mechanism. In this case it comes in the form of a receptor histidine kinase (RHK) and a cognate cytoplasmic response regulator protein, which acts as a transcriptional regulator (Deep, Chaudhary and Gupta, 2011). The binding process between the cleaved oligopeptide and RHK leads to its autophosphorylation inside of the cell, resulting in ATP-guided phosphorylation of conserved histidine residue (H) in the cytoplasm. The phosphate group is then transferred to the conserved aspartate residue (D) of a cognate response regulator protein and as a result, alters the transcription of target genes, including the AIPs and the ABC transporter and genes for the receptor kinase and response regulator.

*Staphylococcus aureus* is an example of a Gram-positive bacteria that utilises quorum sensing to regulate its pathogenesis. However, *S. aureus* manipulates quorum sensing circuits in a unique method by employing different strategies at varying cell densities to promote its pathogenesis. At low cell densities *S. aureus* expresses protein factors that promote attachment and colonisation, whereas at high densities the bacteria can repress these traits and instead switch to express genes products such as toxins and other virulence factors that cause damage to the host (Waters and Bassler, 2005). This switch in gene expression is controlled by the *Agr* quorum sensing system. *AgrD* is the gene responsible for the production of precursor AIPs specific for *S. aureus*. These precursor AIPs can interact with a transmembrane protein (*AgrB*) that then

processes and modifies the AIP, before actively transporting them out of the cell. AgrC and AgrA form the two-component signalling mechanism of RHK and response regulator protein, respectively (Yarwood and Schlievert, 2003). The binding of the extracellular AIP to the AgrC RHK leads to the phosphorylation of AgrA, and thus inducing the expression of a regulatory RNAs named RNAII and RNAIII. Of these two regulatory RNAs, RNAIII results in repressing the expression of cell adhesion factors, whilst inducing the expression of toxins such as  $\delta$ -hemolysin (via the *hld* gene) and other virulence factors, whereas RNAII promotes the expression of the *AgrBDCA* operon, resulting in the increased production of AIPs and in turn allowing for the population to switch from a low cell density state to a high cell density state (Waters and Bassler, 2005).

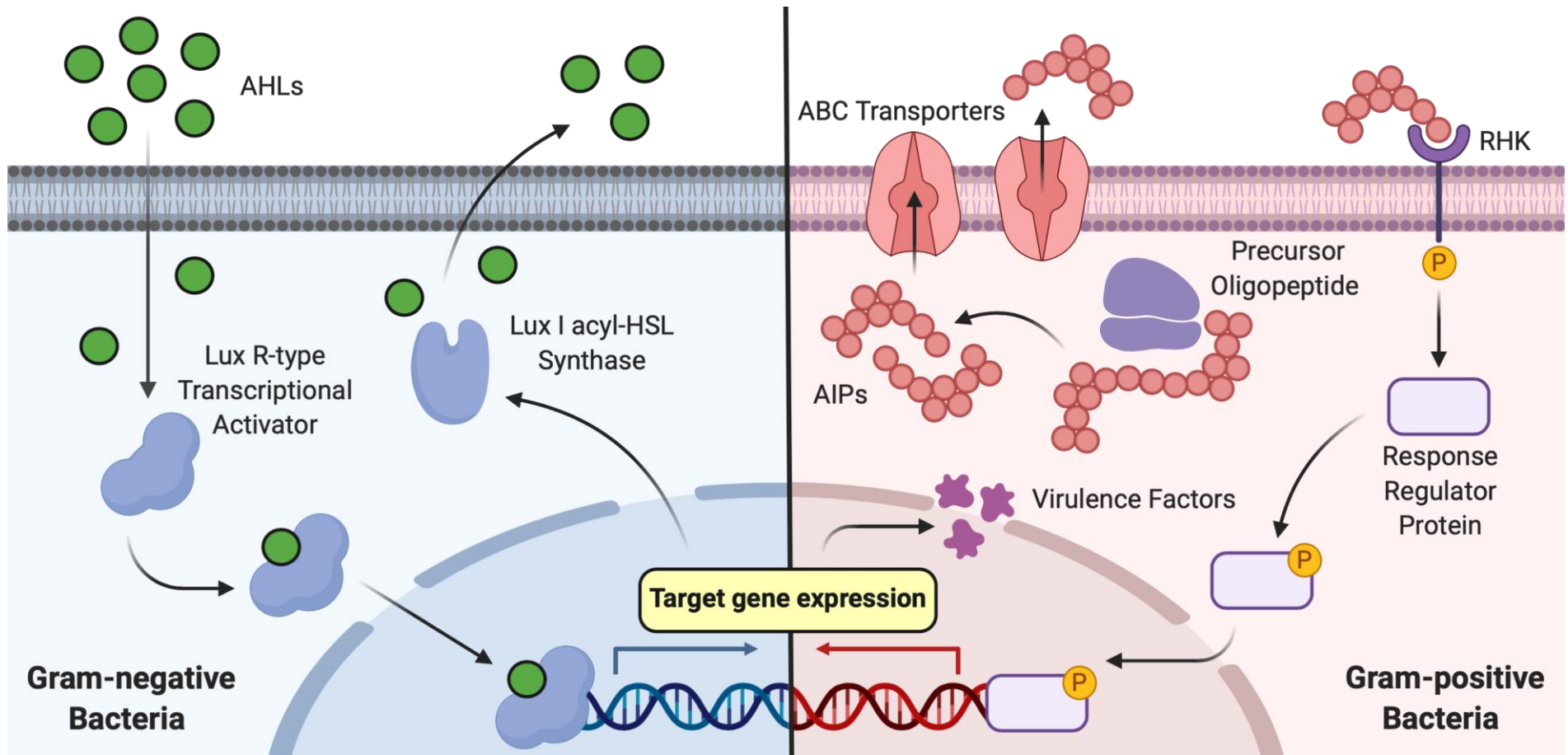


**Figure 1.9** Simplified scheme of quorum sensing networks in Gram-negative bacteria (left) and Gram-positive bacteria (right)

### 1.6.1.3 Interspecies Quorum Sensing

It has been discovered that some bacteria species are not only able to communicate with their own species, but with others too. This form of quorum sensing is known as interspecies quorum sensing. This method of communication is accomplished through the production and detection of a generic, universal signalling molecule produced by both Gram-negative and Gram-positive bacteria, known as autoinducer 2 (AI-2). This system was first discovered in the Gram-negative bacterium *Vibrio harveyi*. Its ability to luminesce is depending on two different quorum sensing systems. The first is controlled by the typical AHLs pathway, employed by Gram-negative bacteria, but it was noted that *V. harveyi* was able to recognise a second type of autoinducer, AI-2. This autoinducer was also able to induce luminescence and could be produced by 75 other species of bacteria (Miller *et al.*, 2004). AI-2 is required for the formation of biofilm in the Gram-negative bacterium *Porphyromonas gingivalis* and *Streptococcus gordonii*, which is Gram-positive. *S. gordonii* is a major cause of dental plaque and is the primary coloniser of teeth, which is a prerequisite for other subsequent colonisation by pathogens such as *P. gingivalis*. If neither of the two types of bacteria possess a functional copy of the *LuxS* gene, then they are unable to successfully form a biofilm (Xavier and Bassler, 2003). However, if either one possesses a functioning *LuxS* gene, they can proceed to colonise the tooth surface and creating a biofilm, which suggests that this molecule is able to be used as a signalling molecule between different species and types of bacteria.

The *LuxS* gene is responsible for the production the enzyme S-ribosylhomocysteinase lyase, which functions to cleave S-ribosylhomocysteine, an intermediate in the S-adenosylmethionine (SAM) pathway, into homocysteine and 4,5-dihydroxy-2,3-pentanedione (DPD) (Cao *et al.*, 2011). DPD then undergoes a series of dehydration and cyclisation reactions to produce several molecules, in which some function as the AI-2 signalling molecule. These signalling molecules can accumulate within the cells until a concentration gradient is created, where they are able to diffuse

out of the cell and into its surroundings. AI-2 is then actively transported back into the cell via the Lsr ABC transporter protein, and is phosphorylated by the AI-2 kinase, LsrK to produce AI-2 phosphate (AI-2-P) (Rezzonico, Smits and Duffy, 2012). AI-2-P is then able to bind to the transcriptional repressor protein LsrR, which is subsequently released from the promoter/operator region of the *Lsr* operon, therefore allowing for the transcription of the *Lsr* genes (Xavier and Bassler, 2004).

## **1.6.2 Quorum Sensing applications**

With our ability to understand how different types of microbes are able to communicate with each other, attention of many researchers has turned to how we can manipulate these communication circuits for our own benefits. The following section highlights the potential applications of engineering quorum sensing systems from the disruption of microbial communication (quorum quenching), to creating quorum sensing based microbial biosensors and altering secondary metabolite production such as increasing yield of PHAs.

### **1.6.2.1 Quorum sensing inhibition - Quorum quenching**

As previously stated, quorum sensing plays a major role in the regulation of vital cellular processes such as the production of virulence factors or formation of biofilms. Owing to the ever-growing problem of antibiotic resistance within bacteria (due to the misuse/over usage of antibiotics), alternative antimicrobial therapies are being researched and developed to help combat the issue on hand. One alternative therapy could come in the form of quorum quenching. Where quorum sensing is a mechanism that allows communication between microbes, quorum quenching can be defined as the inhibition of quorum sensing. This disruption or inhibition in microbial communication can be facilitated through several different mechanisms: inactivation or enzymatic degradation of signalling molecules (AHL/AIP), competing with signal molecule-receptor analogues, inhibition of signal molecule synthesis, and blocking the signal transduction cascades (Paluch *et al.*, 2020).

Of the different mechanisms that facilitate quorum quenching, the most well understood is that of enzymatic degradation of AHLs. These enzymes that catalyse AHLs can be classified into four distinct groups: lactonases and acylases operate by hydrolysing the HSL ring and amine bond of AHLs, respectively, whilst reductases and oxidases modify the activity of the AHL, but do not degrade them. To our knowledge, specific enzymes that target and degrade AIPs have not been reported, however, it has been suggested that generic peptidases would be able to degrade the oligopeptide backbone of AIPs, inhibiting microbial communication within Gram-positive bacteria (Choudhary and Schmidt-Dannert, 2010).

Inductor antagonists are another mode in which quorum quenching can be achieved, as these molecules are able to bind to the signal receptor, non-competitively, to block the inductor-mediated signal transmission into the cell. Alternatively, quorum quenching can be achieved through the inhibition of the synthesis of signalling molecules, which impeded the enzymatic activity of acyl-HSL synthases. Kinase inhibitors such as closantel, result in the inhibition of AIP production.

Finally, quorum quenching can also be achieved by the blocking of the signal transduction cascades. Savrin, a small inhibitor molecule interferes with AgrA by binding to DNA resulting in the inhibition of RNAIII production, which in turn shuts down the production of many virulence factors as RNAIII induces their expression. As the quorum quenching does not affect the cell's survival, the target bacteria will not be able to use selection pressure to develop drug resistance, thus makes quorum quenching an attractive strategy for the development of novel drugs (Choudhary and Schmidt-Dannert, 2010).

#### **1.6.2.2 Biosensors and quorum sensing**

Alternatively, whole-cell and cell-free biosensors are a new developing technology that can recognise pathogenic microbes within the environment and diseases hosts, by the means of detecting quorum sensing molecules produced by the pathogenic microbe. A biosensor can be defined as a type of

sensor that can detect and identify a component within a cell or tissue. In this case biosensors are able to detect quorum sensing molecules, which could give early indication of virulence and used to help identify the onset of an infection (Miller and Gilmore, 2020). To date, most whole-cell biosensors that have been developed are able to successfully recognise AHLs produced by Gram-negative bacteria that contains a AHL responsive transcriptional regulator and a cognate promoter, which directs the transcription of a reporter gene. It has been suggested that quorum sensing molecules alone can be used as markers for the presence of pathogenic microbes. Yet often quorum sensing deficient mutants often develop within the host after successful colonisation, rendering the biosensor ineffective and no longer fit for purpose (Kohler, Buckling and van Delden, 2009). As a result, quorum sensing molecules should not be the sole activator of biosensors. Even so quorum sensing circuits can still be used to engineer biosensing circuits to detect the presence of potentially pathogenic microbes in contaminated bodies of water, crop produce, dairy and meat products. For example, the pathogen *EHEC* (*E. coli* O157:H7) is estimated to cause more than 70000 illnesses and 60 deaths within the USA alone (Silagyi *et al.*, 2009). Genetic circuits could be designed to recognise *EHEC* cell surface antigens or the shiga toxin as an input. This information could then be linked to a quorum sensing signal amplification module, resulting into a readable output.

Furthermore, quorum sensing has been shown to potentially be a therapeutic agent against cancer. For example, the AHL 3-oxo-C<sub>12</sub>-HSL produced by *P. aeruginosa* can inhibit proliferation and induce apoptosis in human breast cancer cell lines (Li *et al.*, 2004). However, its applications in anti-cancer therapy are prevented by the possibility that the bacteria may cause virulence in immunocompromised individuals. Nevertheless, 3-oxo-C<sub>12</sub>-HSL serves as a good starting point for the development of synthetic AHL homologs that retain their anti-cancer toxicity whilst losing the ability to activate quorum sensing circuits.

### 1.6.2.3 Quorum sensing and PHA production

In theory, the manipulation of these communication circuits could have great potential, but the idea of the addition of exogenous quorum sensing molecules as a method for increasing the yield of PHAs within Gram-negative bacteria has yet to be explored, and is ultimately what this study intends to answer.

However, the specific role in which quorum sensing plays within the production of PHAs was previously unknown, until recently. Mohanan *et al.*, (2019) were able to successfully demonstrate the relationship between quorum sensing systems and the regulatory role it plays in the production of PHAs within *Pseudomonas chlororaphis* PA23. During this study a derivative strain of the wild type (*P. chlororaphis* PA23-6863) was grown on two different carbon sources to observe its ability to accumulate PHAs. This strain was chosen as it harboured a plasmid encoding for a lactonase enzyme, which subsequently would be able to degrade all AHLs produced by the bacterium and in essence eliminating the ability for quorum sensing to occur within the strain. When comparing PHA yields (% DCW) between the two strains, *P. chlororaphis* PA23-6863 was unable to synthesise high amounts of PHAs. PHA accumulation had decreased by up to 82% and 93.5% within *P. chlororaphis* PA23-6863 when grown on glucose and octanoate respectively in comparison to the wild type strain. This reduction in PHA accumulation was directly attributed due to the lack of quorum sensing within the strain, and further verified through the measurement of expression of the six genes present within the *Pha* locus (*PhaC1*, *PhaC2*, *PhaZ*, *PhaD*, *PhaF* and *PhaI*). In all six genes, expression was down regulated by as much as 14-fold, resulting in the low accumulation of PHA and thus establishing that PHA production within *P. chlororaphis* PA23 is regulated by quorum sensing.

Furthermore, a study conducted by Irorere *et al.*, (2019), was able to create a link between that of quorum sensing and the production of rhamnolipids, a secondary metabolite, in the bacterium *Burkholderia thailandensis* E264. By using mutant strains of *B. thailandensis* E264 that lacked complete quorum sensing systems, Irorere *et al.*, (2019) demonstrated the mutant's strains

ability to product significantly higher amounts of rhamnolipids in comparison to the wild type strain, which suggested that quorum sensing acted as a repressor for the production of rhamnolipids and had some influence on the production on secondary metabolites. This was further supported by the fact that the study was able to uncover that the increased production of rhamnolipids results in the decreased production of another secondary metabolite, namely PHAs. *B. thailandensis* E264 is a known producer of P(3HB) (Funston *et al.*, 2017). PHA production was observed to have accumulated in higher amounts within the wild type strain when compared to the quorum sensing deficient mutant strain. This is most likely due to the fact that both rhamnolipids and PHAs could share the same pool of lipid precursor molecules, but as quorum sensing acts as a repressor for the production of rhamnolipids within *B. thailandensis* E264, the mutant strain accumulated less PHAs, and higher amounts of rhamnolipids instead. Although the presence of quorum sensing had a negative effect on the production of rhamnolipids, it did have an influence on the type of rhamnolipid produced when supplemented exogenously to the media, favouring the synthesis of dirhamnolipids over monorhamnolipids, which could be advantageous in certain situations.

These findings were supported by Martinez *et al.*, (2020) who were able to identify the impact of secondary metabolite regulators (*ScmR*) on the production of rhamnolipids and PHAs within *B. thailandensis* E264 and its relationship with quorum sensing. During this study, it was found that quorum sensing acts as an activator of *ScmR* transcription, which in turn downregulates the production of rhamnolipids by affecting the expression of the *Rhl* operons. It was also noted that mutant strains lacking the *ScmR* gene saw a reduction in PHA biosynthesis as *ScmR* promotes the transcription of *PhaC* and *PhaZ* genes in *B. thailandensis* E264. Therefore, *ScmR* negatively affects rhamnolipid production, whilst positively impacting PHA biosynthesis, thus supporting the findings of Irorere *et al.*, (2019) that quorum sensing influenced the production of rhamnolipids as well as PHAs.

Ultimately, these three studies were able to conclude that quorum sensing had an impact on the production of PHAs and therefore opens a line of inquest that

this project pursues between the relationship of quorum sensing molecules and PHA production.

## 1.7 Hypothesis

Null Hypothesis ( $H_0$ ): The addition of exogenous quorum sensing molecules are not effective agents in the overproduction of biopolymers such as PHAs.

Alternative Hypothesis ( $H_1$ ): The addition of exogenous quorum sensing molecules are effective agents in overproduction of biopolymers such as PHAs.

## 1.8 Aim and objectives

For this study two Gram-negative bacteria species were selected due to their known ability to produce and accumulate high amounts of PHAs (%DCW): *C. necator* H16 and *P. putida* KT2440. This thesis primarily focuses on the production of PHAs, and explores the possible enhancement of their production through the manipulation of quorum sensing systems in order to establish a novel and innovative production process for commercially important polymers.

The overall aim of this project was to investigate the potential change in the production of PHAs from *C. necator* H16 and *P. putida* KT2440, through the addition of different exogenous quorum sensing molecules. In order to address the aim of this project the following objectives were investigated:

- Study the effect of the addition of quorum sensing molecules on the production of PHAs, determining which of the three different quorum sensing molecules (*N*-butanoyl-L-homoserine lactone, *N*-hexanoyl-L-homoserine and *N*-(3-oxododecanoyl)-L-homoserine lactone) selected in this study is the most effective at increasing production, if any at all. Standard growth parameters such as optical density, biomass and usage of nutrient were also monitored.

- Optimise the concentration of exogenous quorum sensing molecules added to potentially increase and maximise PHA yield (%DCW) obtained.
- Determine the specific type of PHAs produced by each bacterium (*C. necator* H16 and *P. putida* KT2440) used in this study and characterise the composition of the PHAs through the analysis of their monomer units present.
- Assess the expression of key genes related to PHA production (*PhaC* and *PhaZ*) and evaluate whether there is a change in the expression of these genes in relation to the addition of exogenous quorum sensing molecules.

## **Chapter 2: Materials and method**

## 2.1 Materials, chemicals and reagents

Materials throughout this study were purchased from the following suppliers: Cambridge Biosciences (Cambridge, UK), Merck Millipore (Hertfordshire, UK), Sigma-Aldrich (Dorset, UK), Fisher Scientific (Loughborough, UK), Thermo Fisher Scientific (Loughborough, UK), and Tocris Bioscience (Abingdon, UK). Bacterial culture media were obtained from Sigma-Aldrich (Dorset, UK).

DNA extraction kits, RNA purification reagents and qPCR kits were purchased and obtained from Qiagen Ltd. (Crawley, UK). PCR master mix (2X), TriTrack DNA loading dye (6X), GeneRuler 50 base pairs (bp) DNA ladder (50 – 1000 bp) and 96-well reaction plates for qPCR were all purchased from Thermo Fisher Scientific (Loughborough, UK). Primers for PCR and qPCR custom ordered and were obtained from Eurofins Scientific (Hamburg, Germany).

All quantitative and qualitative assays were performed using analytical grade reagents.

## 2.2 Bacterial strains

*C. necator* H16 (NCIMB 10442) and *P. putida* KT2440 (NCIMB 11950) were purchased from the National Collection of Industrial Food and Marine Bacteria (NCIMB) (Aberdeen, UK).

### 2.2.1 Long-term storage of bacterial strains

Both strains were stored as 20% glycerol stocks in cryovials at -80°C. The stocks were prepared by selective growth of a single colony in liquid broth in Nutrient Broth No. 2 (Sigma-Aldrich, Dorset, UK) (**Table 2.1**) to an optical density (OD) of ~1.00 (600 nm). A 1:1 ratio (total volume of 1 mL) of bacterial culture in 20% (v/v) glycerol was prepared and vortexed using an IKA Vortex 3 shaker (IKA, Staufen, Germany) prior to storage at -80°C.

### 2.2.2 Preparation of working stock

In order to conduct experiments, a working stock was prepared by taking a loopful of the frozen bacteria to be streaked onto nutrient agar slants (**Table 2.2**) (containing approximately 15 mL of nutrient agar), which were incubated using a Heratherm OGS series 400 standing incubator (Thermo Fisher Scientific, Loughborough, UK) at 37°C for ~18 – 24 hours and then stored at 4°C. Sub-culturing from the frozen stock was performed every two months to maintain the viability and homogeneity of the working stock.

Each bacterial strain was then transferred from slants onto petri dishes containing nutrient agar via streaking method. This was performed under aseptic conditions (either within a biological safety cabinet such as a Labcaire Genesis class II microbiological safety cabinet (PuriCore Scientific, London, UK) or by proximity to a lit Bunsen burner). The petri dishes were then incubated for 24 hours at 37°C.

Nutrient agar (Sigma-Aldrich, Dorset, UK) (**Table 2.2**) was prepared according to the manufacturer's instructions. Briefly, 28 g/L of the powder was dissolved in deionised water. In order to make sure the components of the agar were fully dissolved, the solution was heated and stirred on a hotplate (Stuart, Staffordshire, UK) prior to autoclaving the solution at 121°C for 15 minutes.

### 2.3 Media

All media selected for use in this study was prepared using deionised water and sterilised at 121°C for 15 minutes. Sugars were prepared separately and autoclaved at 110°C for 10 minutes prior to combining with the primary medium under aseptic conditions to obtain the required concentration. Additionally, if the medium required the supplementation of trace elements, the trace elements were dissolved in 1 M hydrochloric acid and filter sterilised using sterile syringe driven filter units (0.22 µm pore size, polyethersulfone membrane) (Merck Millipore, Hertfordshire, UK).

**Table 2.1** Nutrient Broth No. 2 composition (Sigma-Aldrich, Dorset, UK).

Chemicals	Concentration (g/L)
Casein peptone	4.30
Meat peptone	4.30
Sodium chloride (NaCl)	6.40

**Table 2.2** Nutrient agar composition (Sigma-Aldrich, Dorset, UK).

Chemicals	Concentration (g/L)
Agar (C <sub>14</sub> H <sub>24</sub> O <sub>9</sub> )	15.0
Meat extract	1.0
Peptone	5.0
Sodium chloride (NaCl)	5.0
Yeast extract	2.0

**Table 2.3** Modified minimal salts medium (MSM) composition for *C. necator* H16 (Rai *et al.*, 2011).

Chemicals	Concentration (g/L)
Ammonium sulphate ((NH <sub>4</sub> ) <sub>2</sub> SO <sub>4</sub> )	0.50
Magnesium sulphate (MgSO <sub>4</sub> )	0.40
Monopotassium phosphate (KH <sub>2</sub> PO <sub>4</sub> )	2.38
Sodium phosphate dibasic (Na <sub>2</sub> HPO <sub>4</sub> )	3.42
Fructose (C <sub>6</sub> H <sub>12</sub> O <sub>6</sub> )	20.0
Trace element solution	1.0 mL/L

**Table 2.4** Trace element stock solution for modified MSM composition in 1 M hydrochloric acid (HCl) (Rai *et al.*, 2011).

Chemicals	Concentration in 1 M hydrochloric acid (HCl) (g/L)
Calcium chloride (CaCl <sub>2</sub> )	7.80
Chromium chloride hexahydrate (CrCl <sub>6</sub> ·6H <sub>2</sub> O)	0.11
Cobalt (II) chloride (CoCl <sub>2</sub> )	0.22
Copper (II) sulphate hexahydrate (CuSO <sub>4</sub> ·6H <sub>2</sub> O)	0.16
Iron (III) chloride (FeCl <sub>3</sub> )	9.70
Nickle (III) chloride (NiCl <sub>3</sub> )	0.12

**Table 2.5** E2 medium composition for *P. putida* KT2440 (Le Meur *et al.*, 2012).

Chemicals	Concentration (g/L)
Ammonium sodium phosphate dibasic tetrahydrate (NaNH <sub>4</sub> HPO <sub>4</sub> ·4H <sub>2</sub> O)	3.5
Monopotassium phosphate (KH <sub>2</sub> PO <sub>4</sub> )	3.7
Potassium phosphate dibasic (K <sub>2</sub> HPO <sub>4</sub> )	7.5
Glucose (C <sub>6</sub> H <sub>12</sub> O <sub>6</sub> )	10.0
Trace element solution	1.0 mL/L
Magnesium sulphate heptahydrate (MgSO <sub>4</sub> ·7H <sub>2</sub> O)	1.0 mL/L

**Table 2.6** Trace element stock solution for E2 medium composition in 1 M hydrochloric acid (HCl) (Le Meur *et al.*, 2012).

Chemicals	Concentration in 1 M hydrochloric acid (HCl) (g/L)
Calcium chloride dihydrate (CaCl <sub>2</sub> ·2H <sub>2</sub> O)	1.47
Cobalt (II) chloride hexahydrate (CoCl <sub>2</sub> ·6H <sub>2</sub> O)	2.38
Copper (II) chloride dihydrate (CuCl <sub>2</sub> ·2H <sub>2</sub> O)	0.17
Iron (II) sulphate heptahydrate (FeSO <sub>4</sub> ·7H <sub>2</sub> O)	2.78
Manganese (II) chloride tetrahydrate (MnCl <sub>2</sub> ·4H <sub>2</sub> O)	1.98
Zinc sulphate heptahydrate (ZnSO <sub>4</sub> ·7H <sub>2</sub> O)	0.29

**Table 2.7** Magnesium sulphate heptahydrate stock solution composition (Le Meur *et al.*, 2012).

Chemicals	Concentration (g/L)
Magnesium sulphate heptahydrate (MgSO <sub>4</sub> ·7H <sub>2</sub> O)	246.50

### 2.3.1 Inoculum medium

Nutrient Broth No. 2 (**Table 2.1**) was prepared according to the manufacturer's instructions. Briefly, 15 g/L of the powder was dissolved to prepare the broth before being sterilised by autoclaving at 121°C for 15 minutes.

### 2.3.2 PHA production media

#### 2.3.2.1 *C. necator* H16 PHA production medium

A modified minimal salts medium (MSM) (**Table 2.3**) with fructose as the main carbon source was used as PHA production medium for growth of *C. necator* H16 as described by Rai *et al.*, (2011). The medium constituents were as follows:

Mineral salts such as ammonium sulphate, magnesium sulphate, monopotassium phosphate and sodium phosphate dibasic were dissolved in deionised water and subsequently sterilised by autoclaving together at 121°C for 15 minutes.

Fructose was sterilised by autoclaving separately at 110°C for 10 minutes before being added to the sterile mineral salts aseptically.

Finally, the trace element solution (**Table 2.4**) was prepared by dissolving the following chemicals in 1 M hydrochloric acid: calcium chloride, chromium chloride hexahydrate, cobalt (II) chloride, copper (II) sulphate hexahydrate, iron (III) chloride and nickel (III) chloride. 1 mL of this stock solution was then added to the sterile medium by filter sterilisation using a syringe driven filter unit (0.22 µm pore size, polyethersulfone membrane).

#### **2.3.2.2 *P. putida* KT2440 PHA production medium**

E2 medium (**Table 2.5**) supplemented with glucose as the main carbon source was used as PHA production medium for growth of *P. putida* KT2440 as described by Le Meur *et al.*, (2012). The medium constituents were as follows:

Salts for the medium such as ammonium sodium phosphate dibasic tetrahydrate, monopotassium phosphate and potassium phosphate dibasic were dissolved together using deionised water and sterilised by autoclaving at 121°C for 15 minutes.

Glucose was sterilised separately by autoclaving at 110°C for 10 minutes before being added to the sterile salts aseptically.

The trace element solution (**Table 2.6**) was prepared by dissolving the following chemicals in 1 M hydrochloric acid: calcium chloride dihydrate, cobalt (II) chloride hexahydrate, copper (II) chloride dihydrate, iron (II) sulphate, manganese (II) chloride tetrahydrate and zinc sulphate heptahydrate. 1 mL of

this stock solution was then added aseptically to the sterile medium using a syringe driven filter unit (0.22  $\mu\text{m}$  pore size, polyethersulfone membrane).

In addition, 1 mL of magnesium sulphate heptahydrate was removed from a stock solution (**Table 2.7**) created and added to the medium aseptically using a syringe driven filter unit (0.22  $\mu\text{m}$  pore size, polyethersulfone membrane) to complete the medium.

## **2.4 Experimental setup**

The following sections provide details as to how each experiment was set up and conducted, including the preparation of quorum sensing molecules and inoculum, as well as how both modes of fermentation (shaken flask and bioreactors) were set up too.

### **2.4.1 Preparation of quorum sensing molecules**

Throughout this project three different quorum sensing molecules were selected for use. *N*-butanoyl-L-homoserine lactone ( $\text{C}_4\text{-HSL}$ ) and *N*-hexanoyl-L-homoserine ( $\text{C}_6\text{-HSL}$ ) were both purchased from Cambridge Biosciences (Cambridge, UK), whereas *N*-(3-oxododecanoyl)-L-homoserine lactone (3-oxo- $\text{C}_{12}\text{-HSL}$ ) was purchased from Tocris Bioscience (Abingdon, UK).

All three quorum sensing molecules arrived as a sterile crystalline solid, which were prepared according to the manufacturer's instructions. The manufacturers stated that the quorum sensing molecule should be dissolved in 1 mL of organic solvent such as dimethyl sulfoxide (DMSO) to create a stock solution, which could then be used to produce working stocks. Prior to the addition of DMSO, the organic solvent had to be filter sterilised to maintain sterility of the quorum sensing molecules. This was achieved by passing the solvent through a syringe driven filter unit (0.22  $\mu\text{m}$  pore size, nylon membrane) (Merck Millipore, Hertfordshire, UK) under aseptic conditions. The three stock solutions created were then diluted using sterile DMSO to create working stock solutions, which would be used for the addition of quorum

sensing molecule to the respective allocated flask or bioreactor. The working stock solutions were diluted to achieve a final concentration of 1 mg/mL.

Both stock and working stock solutions of each quorum sensing molecule was then stored at -20°C when not in use.

#### 2.4.2 Preparation of inoculum for shaken flask fermentation

Inocula was prepared by aseptically transferring a loop of single colonies of either *C. necator* H16 or *P. putida* KT2440, into sterile Nutrient Broth No. 2 in shake flasks (20% total working volume). These were incubated in a New Brunswick Innova 4430 orbital shaker incubator (Thermo Fisher Scientific, Loughborough, UK) for ~16 hours and then used as inoculate for the shaken flask fermentation process. The growth conditions for the inoculum of each species of bacteria are shown in **Table 2.8**.

**Table 2.8** Inoculum growth conditions for each bacterial species.

Bacterial Species	Temperature (°C)	Revolutions per minute (rpm)
<i>C. necator</i> H16	30	130
<i>P. putida</i> KT2440	37	180

#### 2.4.3 Shake flask fermentation process

1 L shake flasks (20% total working volume) were used for this set of experiments in this study. Each contained a total of 180 mL of either sterile MSM or E2 medium, depending on the bacterial species being grown. Each flask was then inoculated with 20 mL of ~16 hour old bacterial inoculum (10% volume per volume (v/v) of the total working volume) to achieve a total working volume of 20%.

1 mg/mL stock solutions of three different quorum sensing molecules were prepared in DMSO (**Section 2.4.1**) and were each added to separate flasks to obtain a final concentration of 2 µM or 10 µM (**Table 2.9**). Quorum sensing molecules were added to the flasks at the point of inoculation. These flasks acted as the experimental group. Two additional flasks were used in this series

of experiments, which acted as the control group. The first control flask contained no amounts of quorum sensing molecules or DMSO, whereas the second control flask contained DMSO with a final concentration of 2  $\mu\text{M}$  or 10  $\mu\text{M}$ , without the addition of quorum sensing molecules.

Flasks were incubated for a total of 72 hours from inoculation with specific conditions for each bacterial species detailed in **Table 2.10**. Experiments were carried out in triplicate, with 20 mL samples being removed from each flask periodically every 24 hours, until the end of the experiment at which point the entire volume was taken and used as a sample. These samples were then analysed for various assays, which are detailed in **Section 2.5**. **Figure 2.1** illustrates the experimental set up for the shaken flask fermentation process.

**Table 2.9** Concentrations of the quorum sensing molecules throughout this project.

Quorum sensing molecules	$M_w$ (g/mol)	Concentration (mg/mL)	
		2 $\mu\text{M}$	10 $\mu\text{M}$
C <sub>4</sub> -HSL	171.20	$3.424 \times 10^{-4}$	$1.712 \times 10^{-3}$
C <sub>6</sub> -HSL	199.20	$3.984 \times 10^{-4}$	$1.992 \times 10^{-3}$
3-oxo-C <sub>12</sub> -HSL	297.39	$5.948 \times 10^{-4}$	$2.974 \times 10^{-3}$
DMSO	78.13	$1.563 \times 10^{-4}$	$7.813 \times 10^{-4}$

**Table 2.10** Shaken flask fermentation conditions for each bacterial species.

Bacterial Species	Temperature ( $^{\circ}\text{C}$ )	Revolutions per minute (rpm)
<i>C. necator</i> H16	30	130
<i>P. putida</i> KT2440	30	180

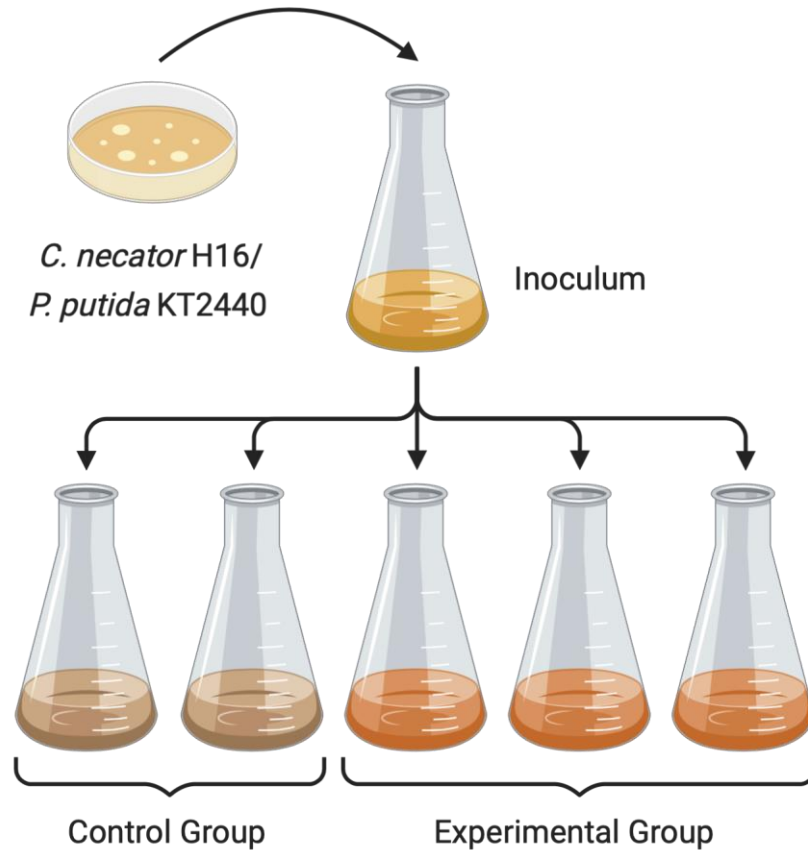


**Figure 2.1** Diagrammatic representation of the shaken flask fermentation set up.

#### 2.4.4 Preparation of inoculum for bioreactor fermentation

Inocula for bioreactors were prepared by initially growing pre-inoculum of both *C. necator* H16 and *P. putida* KT2440 in separate shake flasks. This was performed by inoculating single colonies into the required number of flasks (20% total working volume) for a run, containing sterile Nutrient Broth No. 2 under aseptic conditions. Each bacterial species was incubated in an orbital shaker for ~16 hours with specific growth conditions detailed in **Section 2.4.2**. These cultures were then used as inoculum (10% (v/v) of the total working volume) for another set of shake flasks (20% total working volume) containing either sterile MSM medium for *C. necator* H16 or E2 medium for *P. putida* KT2440. The flasks were incubated for a further 24 hours under the same conditions as before for each bacterial species, after which time, they were used as inoculum (10% (v/v) of the total working volume) to inoculate the 2 L benchtop bioreactors (75% total working volume).

#### 2.4.5 Bioreactor fermentation

Four 2 L FerMac 310/60 benchtop bioreactors and FerMac 360 Controllers (Electrolab Biotech Ltd., Gloucestershire, UK) were used in this study, with each bioreactor equipped with two six-bladed Rushton turbine impellers 7 cm apart, along with a temperature probe and heating jacket. Each bioreactor was also equipped with a F-695 autoclavable pH electrode (225 mm) and a D140 autoclavable dissolved oxygen sensor (220 mm) (Broadly-James Ltd., Bedford, UK) for the measurement of fermentation culture pH and dissolved oxygen, as well as a WOB-L pump 2511 (Welch Vacuum, Ilmenau, Germany) as a means of providing consistent aeration for the bioreactors.

Each 2 L bioreactor (75% total working volume) was autoclaved prior to use. The salts of either MSM or E2 medium were then added and autoclaved to the bioreactor, whilst trace elements and sugars were autoclaved separately and supplemented afterwards (**Section 2.3**) to complete the medium. This totalled 1350 mL of production medium per bioreactor used. Each bioreactor was then inoculated with 150 mL (10% (v/v) of the total working volume) of ~16 hour old bacterial inoculum (**Section 2.4.4**), achieving a total working volume of 75%.

1 mg/mL stock solutions of three different quorum sensing molecules were prepared in DMSO (**Section 2.4.1**) and were each added to separate bioreactors to obtain a final concentration of 10  $\mu$ M (**Table 2.9**). Quorum sensing molecules were added to the bioreactors at the point of inoculation. These bioreactors acted as the experimental group. In addition, another bioreactor was also set up, which served as the control group. This control bioreactor contained no amounts of quorum sensing molecules at all.

Bioreactors were allowed to run for a total of 72 hours from the point of inoculation of the bioreactor, with specific conditions for each bacterium detailed in **Table 2.11**. pH of the media was maintained at pH 7 through the addition of either 1 M solution of NaOH or HCl, dropwise. Experiments were repeated a minimum of three times and carried out in batch mode fermentation. 50 mL samples were withdrawn from the bioreactor every 24

hours, until the end of run where the entire volume was taken instead. These samples were then analysed for various assays, which are detailed in **Section 2.5**. **Figure 2.2** illustrates the experimental set up for the bioreactor fermentation.

**Table 2.11** Bioreactor fermentation conditions for each bacterial species.

Bacterial Species	Temperature (°C)	Revolutions per minute (rpm)	Air flow rate (VVM) (L/L/min)	Dissolved oxygen (DOT%)
<i>C. necator</i> H16	30	300	1	30
<i>P. putida</i> KT2440	30	300	1	30

Air flow rate was calculated as follows:

$$\text{Equation 1: } VVM (L/L/min) = \left( \frac{\text{Volume of air (L)}}{\text{Volume of media (L)}} \right) \div \text{Time (minutes)}$$

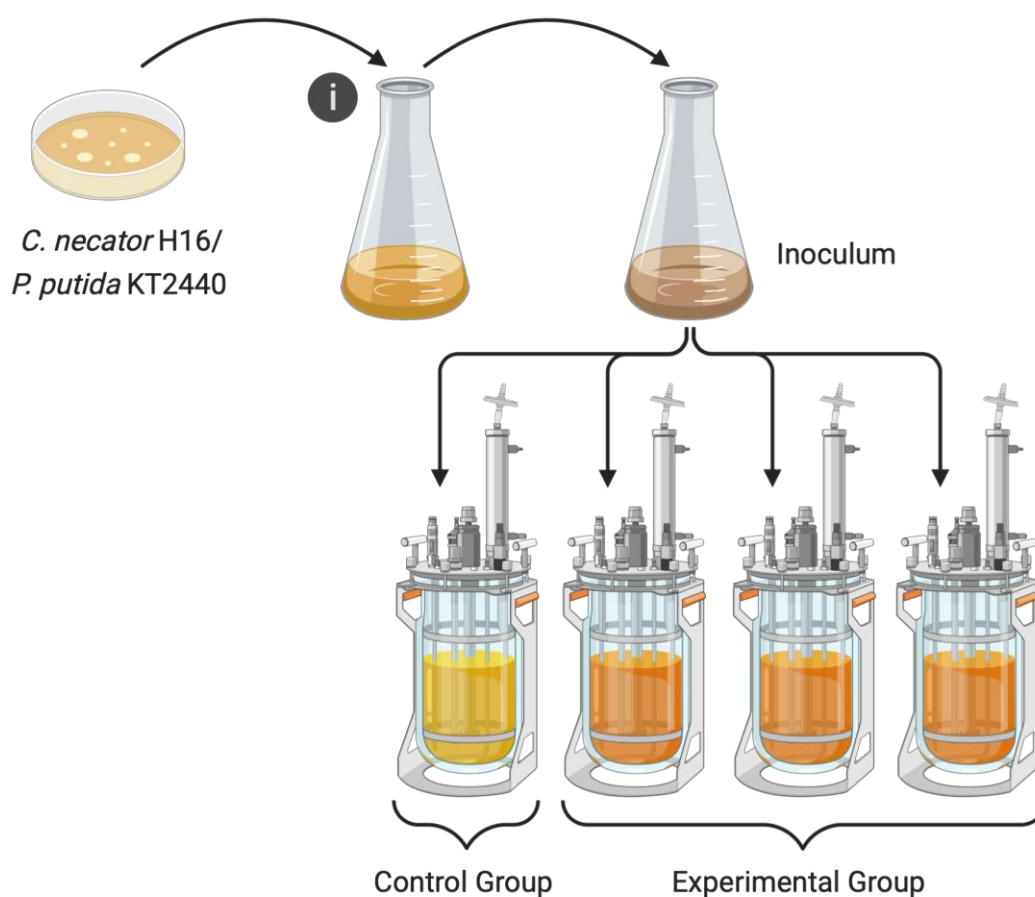


**Figure 2.2** Diagrammatic representation of the bioreactor fermentation setup. (i) represents pre-inoculum.

## **2.5 Analytical methods**

At regular time intervals samples were withdrawn from shaken flasks and bioreactors aseptically to be able to produce an overall growth profile. The OD of each sample taken was measured at a wavelength of 600 nm, whilst also being screened for the production and identification of PHAs. Samples were also centrifuged to separate biomass and supernatant. Of the two, biomass was used to calculate dry cell weights and estimate the amount of PHA produced, whereas the supernatant was used to measure the pH of the culture and to quantify the total concentration of carbohydrates and nitrogen present.

The following sections below elaborate as to how each individual assay was carried out throughout this project.

### **2.5.1 Optical density (OD) measurements**

The optical density (OD) of fermentation broth of *C. necator* H16 and *P. putida* KT2440 were measured throughout the fermentation period to give an indication of the growth of the bacteria during the fermentation. The ODs of samples taken were measured at 600 nm ( $OD_{600}$ ), with sterile MSM and E2 medium used as blanks, respectively. This procedure was carried out using a Jenway 6305 UV-vis spectrophotometer (Jenway, Staffordshire, UK). If samples produced a reading  $\geq 0.500 OD_{600}$ , then samples would be diluted 1:10 using their respective production medium.

### **2.5.2 pH measurements**

pH of samples taken periodically were measured using the Jenway 3505 pH meter (Jenway, Staffordshire, UK) with a VWR collection universal pH electrode (VWR International Ltd, Leicestershire, UK), which was submerged in 4 M potassium chloride solution when not in use. The pH meter was calibrated using a two-point calibration method. The two buffer solutions used were as follows: buffer colour coded solution pH 7.00 (yellow) (Fisher Scientific, Loughborough, UK) and buffer colour coded solution pH 4.00 (pink) (Fisher Scientific, Loughborough, UK).

### 2.5.3 Dry cell weight (DCW)

Estimation of Dry cell weight (DCW) produced by fermentation cultures was carried out by centrifuging 10 mL of the culture sample at 12,000 x *g* for 10 minutes, within pre-weighed 50 mL falcon tubes using a Heraeus Biofuge Primo R centrifuge (Thermo Fisher Scientific, Loughborough, UK). The supernatant was then either discarded or retained and used for assays. The cellular pellet was then placed in a freezer for 24 hours at -20°C, before being freeze dried using a LyoDry Compact benchtop freeze drier (LyoDry Freeze Driers, Bristol, UK) for 48 hours and weighed after.

DCW was calculated as follows:

**Equation 2:**  $DCW (g) = \text{Weight of tube containing freeze dried cells (g)} - \text{Initial weight of the tube (g)}$

### 2.5.4 Quantification of total carbohydrates

Total carbohydrates were quantified using the phenol-sulphuric acid method as described by DuBois *et al.*, (1956). However, a modified version of the phenol-sulphuric acid assay as described by Masuko *et al.*, (2005) was adopted for this study due to the convenience of performing the protocol as well as due to the numerous samples that needed to be analysed.

2 mL of culture broth samples was transferred to Eppendorf tubes and centrifuged using an Eppendorf centrifuge 5418 R (Eppendorf UK Ltd., Stevenage, UK) at 12,000 x *g* for 10 minutes from which 1 mL of supernatant was removed and diluted to a maximum concentration of  $\leq 200$  mg/L of carbohydrate using deionised water. Into glass test tubes, 200  $\mu$ L of 5% (w/v) phenol was aliquoted, followed by 200  $\mu$ L of diluted sample and mixed by swirling. Next, 1 mL of concentrated sulphuric acid (95.5% reagent grade) was rapidly added to the centre of the liquid's surface. Samples were then allowed to sit at room temperature for 30 minutes, after which each test tube was covered and vortexed briefly. From each sample 200  $\mu$ L was removed and pipetted into a 96-well plate and read at a wavelength of 490 nm using a

SPECTROstar Nano microplate reader (BMG LABCTECH, Buckinghamshire, UK).

A standard curve was constructed using known concentrations of glucose ranging from 0 – 200 mg/L (**Appendix 1**). A mixture of 200 µL of 5% (w/v) phenol and 1 mL of concentrated sulphuric acid (95.5% reagent grade) was used as a blank for this assay. The total carbohydrate concentration within samples were then calculated by using the standard curve constructed. The assay was carried out in triplicates on samples and standards that were analysed.

### **2.5.5 Estimation of nitrogen concentration**

The estimation of ammonium was carried out using the phenol hypochlorite reaction method (Rai *et al.*, 2011).

Culture samples taken were centrifuged at 12,000 x *g* for 10 minutes. The supernatant was obtained and used for the analysis by carrying out a dilution of 1:100 in deionised water. To 2.5 mL of diluted samples, 1 mL of phenol-nitroprusside buffer (**Table 2.12**) was added and mixed gently by swirling. After, 1.5 mL of the alkaline hypochlorite reagent (**Table 2.13**) was added to the sample and vortexed. The samples were then incubated at room temperature in the absence of light for 45 minutes, and absorbances of each sample was read at 635 nm.

A standard curve was constructed using known concentrations of ammonium sulphate solution ranging from 0 – 0.7 g/L (**Appendix 2**). A mixture of 1 mL phenol-nitroprusside buffer and 1.5 mL of alkaline hypochlorite reagent was used as a blank for this assay. Nitrogen concentration within samples were able to be calculated using the standard curve constructed. The assay was carried out in triplicates on samples and standards that were analysed.

The method and composition of the two reagents used for this reaction are detailed down below shown in **Table 2.12** and **Table 2.13**.

The phenol-nitroprusside buffer was created in two steps (**Table 2.12**). Firstly, 0.3 g of ethylenediaminetetraacetic acid (EDTA) with 3.0 g each of trisodium citrate and sodium phosphate tribasic dodecahydrate were dissolved in deionised water. The pH of the buffer was then adjusted to 12 using 1 M sodium hydroxide, which was added dropwise. To this buffer, 6 g of phenol and 0.02 g of sodium nitroprusside was added, and final volume was adjusted to 100 mL using deionised water. When not in use, this buffer was kept in the absence of light.

The alkaline hypochlorite reagent (**Table 2.13**) was created by adding 2.5 mL of sodium hypochlorite (10 - 15% active chlorine), mixed with 40 mL of 1 M sodium hydroxide. The final volume was then adjusted to 100 mL using deionised water.

**Table 2.12** Phenol-nitroprusside buffer (Rai *et al.*, 2011).

Chemicals	Concentration (g/100 mL)
EDTA (C <sub>10</sub> H <sub>16</sub> N <sub>2</sub> O <sub>8</sub> )	0.3
Trisodium citrate (Na <sub>3</sub> C <sub>6</sub> H <sub>5</sub> O <sub>7</sub> )	3.0
Sodium phosphate tribasic dodecahydrate (Na <sub>3</sub> PO <sub>4</sub> ·12H <sub>2</sub> O)	3.0
Phenol (C <sub>6</sub> H <sub>5</sub> OH)	6.0
Sodium nitroprusside dihydrate (Na <sub>2</sub> [Fe(CN) <sub>5</sub> NO]·2H <sub>2</sub> O)	0.02

**Table 2.13** Alkaline hypochlorite reagent (Rai *et al.*, 2011).

Chemicals	Concentration (mL/100 mL)
Sodium hypochlorite solution (10 - 15% active chlorine) (NaOCl)	2.5
1 M Sodium hydroxide (NaOH)	40.0

## 2.5.6 PHA extraction

### 2.5.6.1 Solvent dispersion/Sodium hypochlorite digestion method

Cells were harvested from culture broth by centrifugation at 4,500 x g for 15 minutes allowing for the formation of a cellular pellet. The supernatant was

removed carefully not to disturb the pellet, which was then placed in a freezer at -20°C for 24 hours. Next, the frozen pellet was lyophilised for 48 hours.

After drying, the lyophilised cells containing PHAs were extracted by treating 1 g of cells with 25 mL of a mixture containing equal parts of chloroform (99.8% reagent grade) and 30% sodium hypochlorite solution (10 - 15% active chlorine) in an orbital shaker at 100 rpm at 37°C for 1 hour. The mixture obtained was then centrifuged at 2,500 x g for 10 minutes, resulting in three separate phases appearing, of which the first phase was that of the sodium hypochlorite solution, the middle phase was that of cell debris and the bottom most phase was that of the chloroform containing dissolved PHA. The chloroform layer was carefully pipetted out and PHA recovered via precipitation using 10 volumes of ice-cold methanol (99.8% reagent grade) (ratio 1:10/) under continuous stirring.

PHA yield was calculated as a percentage of dry cell weight using the following formula:

$$\text{Equation 3: } PHA \text{ yield (\% DCW)} = \left( \frac{PHA \text{ extracted}}{DCW} \right) \times 100$$

#### 2.5.6.2 Soxhlet extraction

Fermentation broth containing cells and polymer was centrifuged at 4,500 x g for 15 minutes allowing for the formation of a cellular pellet. The harvested cells were separated from the supernatant, which was discarded and subsequently frozen for 24 hours at -20°C before then being freeze dried for a further 48 hours. Once the samples had been completely lyophilised the polymer that was contained within was extracted using a modified Soxhlet extraction method as described by Ramsay *et al.*, (1994).

The lyophilised cells were weighed, crushed into a fine powder and placed into a Whatman cellulose extraction thimble (28 x 100 mm – thickness 1.5 mm) (Sigma Aldrich, Dorset, UK) and placed inside of the Soxhlet extractor with a round bottom flask attached. The dried cells were set up in a reflux system containing 250 mL methanol (99.8% reagent grade) and boiling stones to

remove impurities from within the cells. This process was run twice at 60°C for 24 hours, allowing for a clear methanol solution to be obtained. The methanol solution was then discarded and replaced with 250 mL chloroform (99.8% reagent grade), in which another reflux system was subsequently set up. This reflux system ran for 24 hours at 45°C in order to isolate and extract the PHAs from the lyophilised biomass.

The obtained chloroform solution dissolved with PHAs was then concentrated using a Rotavapor R-210/R-215 rotary evaporator (BÜCHI Labortechnik AG, Flawil, Switzerland) and the polymer was recovered via precipitation using 10 volumes of ice-cold methanol (99.8% reagent grade) under continuous stirring with a magnetic stirrer.

PHA yield was calculated using **Equation 3** detailed under **Section 2.5.6.1**.

### **2.5.7 Crotonic acid method for PHA concentration determination**

For the estimation of the PHA concentration, a slight modification was made to the crotonic acid method of Law and Slepecky (1961). The core principle of this method is centred around the conversion of PHAs to crotonic acid, which occurs when exposed to concentrated sulphuric acid and heat. This conversion of PHAs to crotonic acid can then be measured spectrophotometrically, and is what is used as a means to assess the amount of PHA present in a sample.

100 µL of chloroform solution (containing the dissolved PHA) obtained from either extraction method (**Section 2.5.6**) was transferred into a clean glass test tube to air dry for 24 hours at room temperature, allowing for the chloroform to completely evaporate. Once 24 hours had passed, 5 mL of concentrated sulphuric acid (95.5% reagent grade) was added to the tubes and capped with glass stopper. These tubes were incubated in a water bath for 1 hour at 80°C and vortexed vigorously halfway through the incubation period. Absorbances of samples were then read at 235 nm using a UV quartz cuvette (Sigma Aldrich, Dorset, UK).

A standard curve was constructed using known concentrations of commercially standard P(3HB) (Sigma Aldrich, Dorset, UK) dissolved in chloroform (99.8% reagent grade) ranging from 0 – 500 µg/mL (**Appendix 3**). Concentrated sulphuric acid (95.5% reagent grade) in a UV quartz cuvette was used as a blank for this assay. The concentration of crotonic acid within samples were then calculated using the standard curve. The assay was carried out in triplicates on samples and standards that were analysed.

## 2.6 Kinetic growth parameters calculations

The overall performance of the fermentations was characterised by the PHA yield, PHA and biomass yields per gram of carbohydrate consumed and volumetric productivity using two different time points of the fermentation run (24 and 48 hours). These were calculated using **Equations 4 – 7**.

### 2.6.1 Growth yield

$$\text{Equation 4: } Y_{\frac{X}{S}} (g/g) = \left( \frac{\Delta X}{\Delta S} \right) = \frac{(X_2 - X_1)}{(S_1 - S_2)}$$

Where:

$\Delta X$  = Biomass concentration (g/L)

$\Delta S$  = Substrate concentration (g/L)

### 2.6.2 Product yields

**Equation 5:** Product yield from substrate consumed

$$Y_{\frac{P}{S}} (g/g) = \left( \frac{\Delta P}{\Delta S} \right) = \frac{(P_2 - P_1)}{(S_1 - S_2)}$$

**Equation 6:** Product yield from biomass produced

$$Y_{\frac{P}{X}} (g/g) = \left( \frac{\Delta P}{\Delta X} \right) = \frac{(P_2 - P_1)}{(X_2 - X_1)}$$

Where:

$\Delta P$  = Product Concentration (g/L)

### 2.6.3 Specific production rate

**Equation 7:**  $Q_p (g/L.H) = \left(\frac{1}{\bar{X}}\right) \times \left(\frac{\Delta P}{\Delta T}\right) = \left(\frac{1}{\bar{X}}\right) \times \left(\frac{(P_2 - P_1)}{(T_2 - T_1)}\right)$

Where:

$\bar{X}$  = Average biomass (g)

$\Delta P$  = Change in product concentration (g/L)

$\Delta T$  = change in time (hours)

## 2.7 Identification and structural characterisation of PHAs

To be able to ascertain the type of PHA produced, a series of experiments were carried out on culture samples taken during fermentations as well as on PHAs extracted at the end of each run. The main goal of the following set of experiments was to be able to successfully identify and characterise the type of PHA produced by each bacterium and to study whether or not the addition of exogenous quorum sensing molecules had any effect on the structure or composition of the PHA itself.

### 2.7.1 Phase contrast microscopy

Samples taken from each fermentation experiment were observed straight after sampling without any pre-treatment or staining. 5 – 10  $\mu$ L of culture broth was pipetted onto the centre of a clean microscope slide, covered with a coverslip and observed using a Nikon Eclipse Ci-L light microscope (Nikon Corporation, Tokyo, Japan) at X400 magnification, under different phase contrast settings. These settings were used as it allowed for the observation of individual cells containing PHAs (inclusion bodies) as well as the ability to track and monitor the accumulation of PHAs as the fermentation experiments were carried out.

### **2.7.2 Macroscopic observation of PHAs via Sudan Black B colony staining**

Sudan Black B (also known as Sudan Black 3/(2,2-dimethyl-1,3-dihydroperimidin-6-yl)-(4-phenylazo-1-naphthyl)diazene)) (Sigma-Aldrich, Dorset, UK) a dye for lipophilic compounds was used for the macroscopic identification of PHAs produced by the two bacteria within this study. This method allowed for inclusion bodies to be identified, highlighting the presence of bioplastics such as PHAs produced within the bacteria itself (Ghate *et al.*, 2011).

Samples of *C. necator* H16 and *P. putida* KT2440 were grown on nutrient agar plates at 37°C for 24 hours, before approximately 8 mL of Sudan Black B solution (0.02% (w/v) Sudan Black B in 96% ethanol) was poured over the plates. The plates were then incubated at 30°C for a further 30 minutes before the dye was decanted from the plates and gently rinsed with 10 mL of absolute ethanol (99.8% reagent grade) to wash off excess dye. Inclusions dyed a dark blue/black colour were regarded as positive for PHAs, which can be viewed with the naked eye.

### **2.7.3 Fluorescence microscopy and Nile red staining**

Another method to detect intracellular PHAs is through confocal microscopy using Nile red dye (also known as Nile blue oxazone/9-diethylamino-5-benzo[a]phenoxazinone) (Sigma-Aldrich, Dorset, UK). Nile red is a lipophilic fluorescent dye used for the visualisation of hydrophobic cell structures such as membranes or lipid inclusion such as PHAs (Mravec *et al.*, 2016).

To begin, a 1 mg/mL stock solution of Nile red was prepared in by dissolving the dye in DMSO and subsequently diluted using DMSO again to create a working stock solution with a final concentration of 10 µg/mL, which was used for staining the bacterial cells. Both stock solutions were kept in the absence of light at 4°C when not in use.

Bacterial samples (2 mL) of *C. necator* H16 and *P. putida* KT2440 were collected and centrifuged at 5,000 x *g* for 10 minutes resulting in the formation of a bacterial pellet. The supernatant was discarded whilst the bacterial pellet was resuspended in 1 mL of sterile phosphate buffered saline (PBS) solution (0.01 M phosphate buffer, 0.0027 M potassium chloride and 0.137 M sodium chloride) (Sigma-Aldrich, Dorset, UK) from which 20 µL was removed and pipetted into a clean Eppendorf tube, followed by the addition of 5 µL of Nile red solution (10 µg/mL in DMSO), before being vortexed briefly (Juengert, Bresan and Jendrossek, 2018). Once vortexed, the cells were kept in the absence of light at room temperature for 30 minutes to allow the cells to stain.

Afterwards, 10 µL of the stained cell suspension was pipetted directly onto a clean, dust free microscope slide and superimposed by 150 µL of 2% (w/v) aqueous agarose solution at a temperature of ~60°C to immobilise the cells on the microscope slide. A microscope coverslip was then directly placed on top of the hot agarose solution and was left to solidify for 5 minutes. The samples were then imaged on an Olympus BX41 microscope (Olympus Corporation, Tokyo, Japan).

#### **2.7.4 Fourier Transform Infrared Spectroscopy (FTIR)**

Fourier transform infrared spectroscopy (FTIR) is an analytical technique that collects spectra based on the temporal coherence measurements from an infrared source. It is primarily used for identifying unknown substances by producing an infrared absorption spectrum that can identify chemical bonds present in the molecule. As a result, FTIR was chosen as a method for the identification of the polymers produced throughout this project. Spectra produced were compared against commercial standard samples of P(3HB) to aid in the verification process of the polymer being analysed.

The FTIR system used in this study was a Spectrum Two FTIR spectrometer (PerkinElmer, Massachusetts, USA). 2 mg of PHA samples extracted were used for this analysis and were placed directly onto the diamond crystal. The force gauge was raised to a value between 100 – 120 units, and subsequently

scanned to produce an infrared absorption spectrum which measured between the wavelength region of 4000 – 450  $\text{cm}^{-1}$ . The spectral resolution was 4  $\text{cm}^{-1}$  and spectra were collated based on 4 scans.

### **2.7.5 Gas Chromatography – Mass spectroscopy (GC-MS)**

Gas chromatography – Mass spectroscopy (GC-MS) was carried out in order to identify and characterise the monomer content of the polymer obtained from bacterial cultures. Samples of polymer obtained were subjected to methanolysis, which results in the formation of volatile esters that are detectable by gas chromatography (GC) (Huijberts *et al.*, 1994).

20 mg of extracted polymer was dissolved in 2 mL of chloroform (99.8% reagent grade) within glass test tubes, before being supplemented with 2 mL of acidified methanol (15% (v/v) concentrated sulphuric acid (95.5% reagent grade) in methanol (99.8% reagent grade)) and 20  $\mu\text{L}$  of methyl benzoate (analytical standard) (Sigma Aldrich, Dorset, UK). Methyl benzoate was added as it was used as an internal standard to improve accuracy. Once added, the tubes were capped using a glass stopper and vortexed for 30 seconds and set up within a reflux system at 100°C for either 4 hours or 14 hours using an Isotemp digital dry bath/block heater (Fisher Scientific, Loughborough, UK). The time in which the extracted polymer was allowed to remain within the reflux system was entirely dependent on the specific type of polymer produced. SCL PHAs produced from *C. necator* H16 were kept within the reflux system for 4 hours, whereas MCL PHAs produced from *P. putida* KT2440 were kept in reflux for 16 hours.

Next, the glass test tubes containing the reaction mixture were cooled down on ice for 5 minutes. After cooling, 2 mL of deionised water was added to the mixture to separate the organic and aqueous phases. The test tubes were then capped and vortexed for 30 seconds, before being placed in a stand to allow phase separation. The organic phase (bottom phase), which contained the resulting methyl esters derivatives was collected and dried over 10 mg of sodium bicarbonate and sodium sulphate. The solution was gently swirled for

30 seconds and filtered into a clean test tube using Whatman qualitative filter paper (Grade 1) (Sigma Aldrich, Dorset, UK). Once filtered, the solution was pipetted into 2 mL GC vials for further analysis.

GC-MS analysis was carried out using a Trace 1300 Gas Chromatograph and an ISQ LT Single Quadrupole Mass Spectrometer (Thermo Fisher Scientific, Loughborough, UK). The Trace 1300 Gas Chromatograph was equipped with Elite-5MS capillary column (PerkinElmer, Massachusetts, USA). The dimensions of the column were 30 m in length, with 0.25 mm internal diameter and 0.25 µm film thickness. 1 µL of the organic phase was injected along with helium, which was used as the carrier gas at a flow rate of 1 mL/min. The injector temperature was 225°C and the column temperature was raised from 40°C to 240°C at 18°C/min and held at the highest temperature for 6 minutes.

The following equation was used in order to calculate the monomer compositions of the different types of PHAs produced:

$$\text{Equation 8: Monomer composition (Mol \%)} = \frac{(\text{Height of monomer peak} \times 100)}{\text{Total height of all monomers' peaks}}$$

## 2.8 Molecular biology techniques

### 2.8.1 Isolation and extraction of DNA

DNA from *C. necator* H16 and *P. putida* KT2440 was isolated using a DNeasy Blood & Tissue Kit (Qiagen Ltd., Crawley, UK). The extraction of DNA was carried out following the instructions provided by the manufacturer. Samples of both *C. necator* H16 and *P. putida* KT2440 cultures grown with or without the presence of exogenous quorum sensing molecules were taken aseptically and used for the isolation and extraction of DNA.

Cultures (1.25 mL) at an OD of 2.00 (corresponding to  $\sim 2 \times 10^9$  cells) at 600 nm were transferred to an Eppendorf tube and centrifuged at  $5,000 \times g$  for 10 minutes, to harvest bacterial cells. The supernatant was discarded, and bacterial pellet resuspended in 180 µL Buffer ATL by repeatedly pipetting. Next, 20 µL of proteinase K was added and vortexed for 30 seconds and

incubated at 56°C using a dry bath/block heater for 30 minutes. Once completed, samples were then vortexed again for another 30 seconds, before adding 200 µL of Lysis Buffer (AL) and 200 µL of absolute ethanol (99.8% reagent grade) to the samples and immediately vortexed until a homogeneous solution was created.

The obtained lysate was then transferred into a DNeasy Mini spin column in a 2 mL collection tube (provided with the kit) and centrifuged at 6000 x *g* for 1 minute. The flow-through and collection tube were both discarded after centrifugation was completed and the DNeasy mini spin column was placed into a new 2 mL collection tube with the addition of 500 µL of Washing Buffer 1 (AW1) and centrifuged once again at 6000 x *g* for 1 minute. This process was repeated once more, discarding the flow-through and collection tube as well as placing the DNeasy spin column into a new 2 mL collection tube, but with the addition of 500 µL of Washing Buffer 2 (AW2) instead, and centrifuged for 3 minutes at 20,000 x *g* to dry the DNeasy membrane. The flow-through produced was once again discarded.

Finally, the DNeasy spin column was placed into a clean Eppendorf tube and 200 µL of Elution Buffer (AE) was added directly onto the DNeasy membrane and incubated at room temperature for 1 minute and then centrifuged for the final time at 6000 x *g* for 1 minute.

DNA concentration was then evaluated as described below in **Section 2.8.2**. Samples of DNA extracted, were then subsequently stored at -20°C for future usage.

### **2.8.2 Measurement of nucleic acid concentration**

Nucleic acid purity and concentration (ng/µL) was determined by measuring the OD at 260:280 nm using a NanoDrop 1000 spectrophotometer (software version 3.8.0) (Thermo Fisher Scientific, Loughborough, UK), which required 1 µL of isolated nucleic acid. An absorbance ratio of ~1.8 – 2 between 260:280 nm ( $A_{260}/A_{280}$ ) indicated that the isolated nucleic acid (DNA or RNA) was “pure”

and absent from contamination such as proteins, phenol or other organic compounds.

### 2.8.3 Primers

Throughout this project primers were purchased from Eurofins Scientific and arrived in a lyophilised form, which were reconstituted by adding 10 µL of UltraPure DNase/RNase-free distilled water (Fisher Scientific, Loughborough, UK) for every 1 nmol of primer to create 100 µM stocks of each primer. These stocks were then vortexed for 30 seconds and diluted using UltraPure DNase/RNase-free distilled water to create 10 µM working stocks, which were then used hereafter.

Both concentrations of primer stocks were then stored at -20°C for future use. Primers for each bacterium that were used in this project have been listed below in **Table 2.14** and **Table 2.15**. as well as the reference gene, which can be found in **Table 2.16**.

**Table 2.14** Primers used for *C. necator* H16

Gene	Nucleotide sequence (5' – 3')	Source
<i>PhaC</i> (F)	CTTCTGTTCCCTTGGTGGCCTTGGTCAG	(Windhorst and Gescher, 2019)
<i>PhaC</i> (R)	CATGATTTGATTGTCTCTCTGCCGTCAC	
<i>PhaZ</i> (F)	ATGCTTAATGAATTACAACAGTTTTTAT GCGTGTGGGGCCGCACC	(York <i>et al.</i> , 2003)
<i>PhaZ</i> (R)	GCCGATCAGGTGCTGCACG GCGGGATCCCAAATCCCAGGTCCGGT GG	

**Table 2.15** Primers used for *P. putida* KT2440

Gene	Nucleotide sequence (5' – 3')	Source
<i>PhaC1</i> (F)	ACAGCGGCCTGTTACCTGGG	(Tae-Kwon <i>et al.</i> , 2003)
<i>PhaC1</i> (R)	ACGATCAGGTGCAGGAACAGC	
<i>PhaZ</i> (F)	GAAGTCATCGCCTTTGATGTGCC	(Mozejko-Ciesielska <i>et al.</i> , 2017)
<i>PhaZ</i> (R)	ATCATCCACAGCACCTTGGGCTTG	

**Table 2.16** Primers for reference gene used during qPCR

Gene	Nucleotide sequence (5' – 3')	Source
16s rRNA (F)	AGAGTTTGATCCTGGCTCAG	(Srinivasan <i>et al.</i> , 2015)
16s rRNA (R)	GGTACCTTGTTACGACTT	

### 2.8.3.1 Polymerase chain reaction (PCR)

PCR was used in this project to assess the specificity of the primers that had been selected for use as well as to verify the presence of the gene of interest itself within the extracted DNA samples.

This process was carried out in a Techne 5PrimeG Gradient Thermal Cycler (Cole-Parmer, Staffordshire, UK) using PCR Master Mix (2X) (Thermo Fisher Scientific, Loughborough, UK) in thin-walled PCR tubes, which were placed on ice.

The reaction mixture (**Table 2.17**) was prepared within a laminar flow cabinet equipped with a UV lamp, using aerosol resistant pipette tips to aid in reducing the probability of contamination of samples. Each sample was then subsequently vortexed to ensure the components of the reaction has been mixed thoroughly. In each PCR run, a non-template control was included, in which UltraPure DNase/RNase-free distilled water was used to replace the volume of template DNA. The non-template control was set up as it monitored contamination and primer-dimer formation that could produce false positive results.

**Table 2.17** PCR reaction components

Component	Volume (µL)
PCR Master Mix (2X)	12.5
Forward primer	1
Reverse primer	1
Template DNA	5
RNase-free water	5.5
<b>Total reaction volume</b>	<b>25</b>

The thin-walled PCR tubes containing the reaction mixture were then placed in the thermal cycler and run with the conditions detailed in **Table 2.18**.

**Table 2.18** PCR cycling protocol

Step	Time (minutes)	Temperature (°C)	Number of cycles
Initial denaturation	1 - 3	95	1
Denaturation	0.5	95	
Annealing	0.5	T <sub>m</sub> -5	25 - 40
Extension	1 minute per kilobase (kb)	72	
Final extension	5 - 15	72	1

Upon completion of the thermal cycler, the samples produced were ran on a 1% (w/v) TBE agarose gel (**Section 2.7.3.1.1**).

#### **2.8.3.1.1 Agarose gel electrophoresis**

To visualise the results of PCR amplification products produced, agarose gel electrophoresis was employed.

10X UltraPure TBE buffer (1 M Tris, 0.9 M boric acid and 0.01 M EDTA) (Fisher Scientific, Loughborough, UK), was used for both the production of the gel and the liquid buffer. Prior to use the 10X UltraPure TBE buffer was diluted to 1X concentration by making a 1:10 dilution using deionised water as in accordance with the manufacturer's instructions.

A 1% (w/v) agarose gel was used throughout this project and was prepared by dissolving 0.5 g of agarose (Sigma-Aldrich, Dorset, UK) in 50 mL of 1X TBE buffer by heating in a microwave until boiling. This solution was allowed to cool down before adding the nucleic acid dye, GelRed<sup>®</sup> for a final concentration of 0.02 µL/mL (Cambridge Bioscience, Cambridge, UK). The solution was swirled gently and cast into a 7 x 10 cm gel tank with an 8-well comb in place and allowed to set.

Agarose gel DNA electrophoresis was performed in a Mini-Sub Cell GT Cell (Bio-Rad, Hertfordshire, UK) powered by a PowerPac basic power supply (Bio-Rad, Hertfordshire, UK), and run in ~270 mL of 1X TBE liquid buffer.

10  $\mu$ L of each PCR sample was mixed thoroughly with 2  $\mu$ L of TriTrack DNA loading dye by vortexing for 30 seconds. Next, 6  $\mu$ L of PCR products were carefully pipetted into individual wells of a 1% (w/v) TBE agarose gel alongside 6  $\mu$ L of GeneRuler 50 bp DNA ladder, which was then allowed to run for 60 minutes at 100 volts. The GeneRuler 50 bp DNA ladder was prepared ahead of time and in accordance with the manufacturer's instructions.

The gel was then subsequently transferred to an D55 model UV-transilluminator (UVITEC, Cambridge, UK) to visualise the PCR products produced and measure their migration through the gel.

#### **2.8.4 Isolation and extraction of RNA**

RNA was extracted from cultures with the use of TRI Reagent solution (Thermo Fisher Scientific, Loughborough, UK), - a mixture of guanidine thiocyanate and phenol, which inhibits RNase activity and is able to isolate nucleic acids and proteins. The extraction of RNA was carried out using the TRI Reagent solution protocol with slight modifications as detailed below. This method was originally described by Chomczynski and Sacchi (1987) and has three distinct phases: phase separation, RNA precipitation and RNA wash resuspension.

##### **Step 1. Phase separation**

Firstly, bacterial pellets were obtained from cultures of both *C. necator* H16 and *P. putida* KT2440 at different time points (24, 48 and 72 hours) by centrifuging samples at 12,000 x *g* for 10 minutes in 1.5 mL Eppendorf tubes. The supernatant was then carefully removed and discarded. To the bacterial pellets, 1 mL of TRI Reagent solution was added and mixed carefully by pipetting repeatedly to obtain a homogenous mixture and allowed to incubate at room temperature for 5 minutes. After 5 minutes 200  $\mu$ L of chloroform (99.8% reagent grade) was added per 1 mL of TRI Reagent solution and mixed for 15 seconds and allowed to stand for 5 minutes at room temperature. The resulting mixture was then centrifuged at 12,000 x *g* for 15 minutes at 2 – 8°C,

resulting in the mixture separating into three different phases: a colourless upper aqueous phase (containing RNA), a white interphase (containing DNA), and a red organic phase (containing proteins and lipids).

### **Step 2. RNA precipitation**

Following centrifugation, the colourless upper aqueous phase (containing RNA) was transferred into a new tube. Extra care was taken by pipetting gently to avoid contamination of the solution extracted with the other phases. To the aqueous phase extracted, 500  $\mu\text{L}$  of isopropanol (2-propanol) was added per 1 mL of TRI Reagent solution that was originally added in step 1 and mixed gently and incubated at room temperature for 10 minutes. Once completed, the samples were centrifuged at 12,000  $\times g$  for 10 minutes at 2 – 8°C. As a result, RNA precipitated to form a pellet on the side and bottom of the tube.

### **Step 3. RNA wash and resuspension**

The supernatant from step 2 was removed carefully and washed with 1 mL of 75% ethanol (99.8% reagent grade) per 1 mL of TRI Reagent solution added in step 1. The samples were then vortexed and centrifuged at 7,500  $\times g$  for 5 minutes at 2 – 8°C. The supernatant was then discarded, leaving behind the RNA pellet, which was allowed to air dry for 15 minutes to allow the remaining ethanol to evaporate. Once evaporated the extracted RNA was resuspended and dissolved in 50  $\mu\text{L}$  of UltraPure DNase/RNase-free distilled water and incubated at 37°C for 15 minutes. Samples were then assessed for the concentration and purity of RNA extracted as described previously in **Section 2.8.2**. For storage, the RNA extracted from samples were then kept at -80°C for future use.

### **2.8.5 Complementary DNA (cDNA) synthesis**

RNA was purified and used for the synthesis of complementary DNA (cDNA) through the process of reverse transcription using the QuantiNova Reverse Transcription Kit (Qiagen, Crawley, UK). The kit used for this project provided

a fast and efficient method for the removal of contaminating genomic DNA (gDNA), which if not removed would affect future qPCR runs. The purification of RNA and synthesis of cDNA was carried out as per the instructions provided by the manufacturer.

The reactions that were carried out using this kit were set up in 200  $\mu$ L thin-walled PCR tubes and then incubated using a thermal cycler. To begin RNA that was extracted in **Section 2.8.4** and kept at  $-80^{\circ}\text{C}$  were thawed out on ice, alongside the gDNA removal mix and reverse transcription enzyme that both were provided with the kit. The reverse transcription mix, and RNase-free water were also thawed out, but at room temperature. All reagents were vortexed briefly for 10 seconds before use. Once all the components had thawed out, the gDNA removal reaction (**Table 2.19**) was prepared and stored on ice as detailed down below.

**Table 2.19** gDNA removal reaction components

Component	Volume ( $\mu$ L)
gDNA removal mix (Contains RNase inhibitor)	2
Template RNA (Up to 5 $\mu$ g)	Variable
RNase-free water	Variable
<b>Total reaction volume</b>	<b>14</b>

The gDNA removal reaction mix was incubated using a thermal cycler for 2 minutes at  $45^{\circ}\text{C}$  to produce template RNA and was placed on ice immediately after the reaction was complete. Whilst on ice, the reverse transcription master mix (**Table 2.20**) was prepared and added to each tube containing template RNA (14  $\mu$ L) and mixed thoroughly.

**Table 2.20** Reverse transcription reaction components

Component	Volume ( $\mu$ L)
Reverse transcription enzyme	1
Reverse transcription mix (Includes $\text{Mg}^{2+}$ and dNTPs)	4
Template RNA (Entire gDNA removal reaction)	14
<b>Total reaction volume</b>	<b>19</b>

The PCR tubes containing the template RNA and reverse transcription master mix were then placed back into the thermal cycler and incubated for 3 minutes at 25°C to allow for the annealing step to begin, followed by the reverse transcription reaction which ran for 10 minutes at 45°C, before the inactivation of the reverse transcriptase enzyme, which ran for 5 minutes at 85°C. This entire process has been summarised in **Table 2.21** down below.

**Table 2.21** gDNA elimination and reverse transcription temperature protocol using a thermal cycler

Step	Time (minutes)	Temperature (°C)
gDNA elimination reaction	2	45
<b>Pause thermal cycler</b> – Samples are removed and placed on ice, and the reverse transcription components added.		
<b>Reverse transcription reaction:</b>		
Annealing	3	25
Reverse transcription	10	45
Inactivation of reaction	5	85

cDNA samples produced were then either placed on ice and diluted 1:10 using sterile water and used directly for qPCR as detailed in **Section 2.8.6** or stored at -20°C for later use.

### 2.8.6 Quantitative PCR (qPCR)

Quantitative PCR (qPCR) was carried out in this project with the aim of being able to quantify and measure the level of gene expression of genes related to PHA synthesis. This process was carried out in an Applied Biosystems 7500 Fast Real-Time PCR system (Fisher Scientific, Loughborough, UK), using Applied Biosystems SYBR Green PCR Master Mix (Thermo Fisher Scientific, Loughborough, UK) in a 0.1 mL MicroAmp Fast Optical 96-Well Reaction Plates (Fisher Scientific, Loughborough, UK).

The reaction mixture (**Table 2.22**) was set up within a UVP UV3 HEPA PCR workstation (Analytik Jena, Jena, Germany) equipped with an UV lamp, whilst also using aerosol resistant pipette tips to help reduce the probability of contamination of samples, before being vortexed briefly to mix the

components thoroughly. In addition, each qPCR run contained a non-template control, in which UltraPure DNase/RNase-free distilled water was used to replace the volume of cDNA. The non-template control was set up as it monitored contamination and primer-dimer formation that could produce false positive results.

**Table 2.22** qPCR reaction components

Component	Volume (10 $\mu$ L per well)	Volume (50 $\mu$ L per well)	Final concentration
SYBR Green PCR Master Mix (2X)	5	25	1X
Forward primer	1	5	50 – 900 nM
Reverse primer	1	5	50 – 900 nM
Template cDNA	2	10	1 ng – 100 ng
RNase-free water	1	5	-
<b>Total reaction volume</b>	<b>10</b>	<b>50</b>	<b>-</b>

The appropriate volume of reaction mixture was then transferred to a well of the optical plate and sealed with an adhesive cover. The conditions for the reaction are shown below in **Table 2.23**. The reactions were performed in triplicate and experiments repeated with three biological replicates.

**Table 2.23** qPCR cycling protocol

Step	Time (minutes)	Temperature ( $^{\circ}$ C)	Number of cycles
AmpliTaq Gold Polymerase activation	10	95	Hold
Denature	0.25	95	40
Annealing	1	60	
Extension	1	60	

Once completed, the qPCR amplification products were separated and run on a 1% (w/v) TBE agarose gel (**Section 2.8.3.1.1**).

### 2.8.6.1 Analysis and quantification of qPCR data

The change in expression of *PhaC* and *PhaZ* genes were measured using the Livak method also referred to as the  $2^{-\Delta\Delta C_T}$  method (Livak and Schmittgen, 2001). This method allowed for the determination of the relative difference in

expression levels of the target genes of interest (GOI) in different samples against the selected reference genes.

The Livak method can be carried out in three steps, which have been explained below:

1. Normalising  $C_T$  of the GOI (*PhaC* or *PhaZ*) to the  $C_T$  of the reference gene (16s rRNA):

**Equation 9:**  $\Delta C_T(\text{Control}) = C_T(\text{GOI}, \text{Control}) - C_T(\text{Reference}, \text{Control})$

**Equation 10:**  $\Delta C_T(\text{Test}) = C_T(\text{GOI}, \text{Test}) - C_T(\text{Reference}, \text{Test})$

2. Normalise  $\Delta C_T$  of the GOI sample to the  $\Delta C_T$  of the control:

**Equation 11:**  $\Delta \Delta C_T = \Delta C_T(\text{GOI}) - \Delta C_T(\text{Control})$

3. Calculating the fold difference in expression:

**Equation 12:**  $2^{-\Delta \Delta C_T} = \text{Normalised expression ratio}$

It is important to note that the formula above is based off the assumption that both target and reference genes are amplified with efficiencies near 100% and are within 5% of each other.

## 2.9 Statistical analysis

All experiments were performed in triplicates at minimum to ensure for statistical reproducibility as well as samples being taken in triplicates too. All data for assays performed in this study were statistically analysed using one or two-way analysis of variance (ANOVA) as well as Tukey's multiple comparisons test to determine  $p$  values and establish correlation between data sets ( $p$  value < 0.05 was considered significant). These statistically analyses were carried out on GraphPad Prism (Version 9.0.1) and all graphs were plotted using the same program.

### **Chapter 3:** SCL PHA production via *C. necator* H16

### 3.1 Introduction

Polyhydroxyalkanoates have been widely explored as a group of promising biomaterials, for biomedical applications (Rai *et al.*, 2011). They represent a broad range of properties, which depends on the number of carbon atoms within the monomer unit (Laycock *et al.*, 2013). Short chain length Poly(3-hydroxyalkanoates) include PHAs with monomer length between 3 to 5 carbon atoms within the monomer unit (Verlinden *et al.*, 2007). Most of the polymers from this group of PHAs have the material properties, such as: high crystallinity, thermal properties similar to thermoplastics, as well as high stiffness and tensile strength (Pena *et al.*, 2014). However, within this group of PHAs, the P(4HB) polymer is an exception. Unlike other SCL PHAs, P(4HB) has low melting temperature, high tensile strength and is highly elastomeric. Scl-PHAs are represented by 3-hydroxypropionate (3HP), which contain 3 carbon atoms within the monomer unit, 3-hydroxybutyrate (3HB) or 4-hydroxybutyrate (4HB) with 4 carbon atoms and 3-hydroxyvalerate (3HV) with 5 carbon atoms. In addition, there are scl-PHA copolymers which include Poly(3-hydroxybutyrate-co-3-hydroxyvalerate), P(3HB-co-3HV), poly(3-hydroxybutyrate-co-4-hydroxybutyrate), P(3HB-co-4HB), which represent intermediate properties between both monomers which are dictated by the main monomer unit within the copolymer (Akaraonye *et al.*, 2010). SCL PHAs can be produced by different types of bacterial strains including *Bacillus* sp., *Cupriavidus necator*, *Cyanobacteria (Spirulina platensis)*, *Burkholderia sacchari* and *Methylobacterium* species. (Mendonca *et al.*, 2013). Each bacterial strain has different levels of polymer accumulation within the cell as well as different material properties.

### 3.2 PHA production by *C. necator* H16 in shake flasks with the addition of exogenous quorum sensing molecules at 2 $\mu$ M concentration

Investigations of PHA production from *C. necator* H16 with the supplementation of different exogenous quorum sensing molecules was first carried out at shake flask level at a final concentration of 2  $\mu$ M. This was necessary to understand if the quorum sensing molecules had any effect on

the production of PHAs as well as to gather information for the scaling up process. This also acted as a form of optimisation, by comparing the change in production of PHAs when exogenous quorum sensing molecules were supplied at two different concentrations. The process as to how the shake flasks were set up is explained in **Section 2.4.3**. The fermentation was allowed to progress for a maximum of 72 hours.

**Table 3.1** displays the results obtained from shake flasks that were supplemented with exogenous quorum sensing molecules with a final concentration of 2  $\mu\text{M}$ .

**Table 3.1** Summary of key growth parameters in relation to PHA production of *C. necator* H16 grown in 1 L shake flasks (batch mode fermentation) containing production media and exogenous quorum sensing molecules with a final concentration of 2  $\mu\text{M}$ . Results shown are from samples collected 48 hours post inoculation and expressed as means with  $\pm$  SD values (n = 9).

Quorum sensing molecules	DCW (g/L)	PHA (g/L)	PHA yield (% DCW)	% change of PHA
Control	6.95	3.242	46.65	-
DMSO	7.36	3.243	44.06	0.02 $\pm$ 0.11
C <sub>4</sub> -HSL	7.01	3.246	46.31	0.12 $\pm$ 0.15
C <sub>6</sub> -HSL	7.41	3.243	43.78	0.04 $\pm$ 0.08
3-oxo-C <sub>12</sub> -HSL	7.09	3.255	45.91	0.40 $\pm$ 0.10

### 3.3 PHA production by *C. necator* H16 in shake flasks with the addition of exogenous quorum sensing molecules at 10 $\mu\text{M}$ concentration

The concentration of exogenous quorum sensing molecule was then increased to assess whether the concentration had an impact on the change of PHA produced by *C. necator* H16. Experiments for this study were set up identically to the previous experiments (**Section 2.4.3**), but with the final concentration increased to 10  $\mu\text{M}$

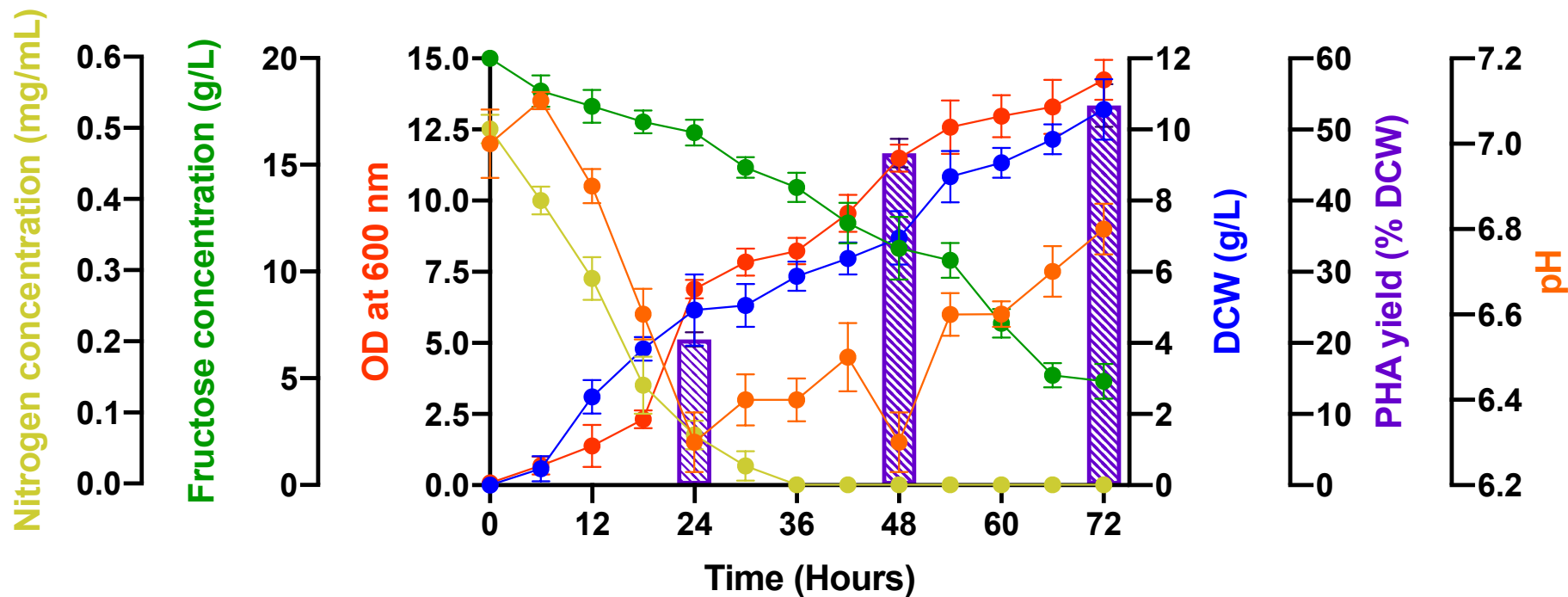


**Figure 3.1** Fermentation profile of *C. necator* H16 grown in 1 L shake flasks over a 72 hour period without the addition of exogenous quorum sensing molecules (control). Samples were taken every 6 hours throughout the fermentation run, which was run in batch mode fermentation. MSM medium was used as the production medium, containing fructose as the sole carbon source. Error bars represent  $\pm$  SD values ( $n = 9$ ).

**Figure 3.1** illustrates the growth profile of the results obtained from the control shake flasks used to grow *C. necator* H16 without the addition of exogenous quorum sensing molecules. At the start of the fermentation period, OD increases at a slow, but consistent rate in comparison to the rate of DCW accumulation. This occurs between the 0 – 18 hours, at which point OD begins to increase rapidly from 2.135 to 6.839. OD then continues to rise for the rest of the fermentation period until it reaches a maximum OD of 14.249 at 72 hours of fermentation. DCW originally increased slowly for the first 12 hours of fermentation, before increasing to a maximum DCW of 10.56 g/L. The maximum amount of PHA yielded (% DCW) accumulated at 72 hours of fermentation growth. This increased progressively as the fermentation continued, increasing every 24 hours. The biggest increase of PHA yield (% DCW) was observed between 24 and 48 hours, accumulating 20.47% and 46.65%, respectively. At 72 hours of fermentation 53.34% of PHA was yielded (% DCW), which was equivalent to 5.63 g/L of PHA.

When measure nitrogen concentration of the culture medium, within the initial 36 hours of growth, nitrogen was no longer detected within the culture. The biggest decrease in nitrogen concentration was between 12 – 18 hours, in which nitrogen decreased by 0.15 mg/mL. Fructose concentration decreased at a steady rate, however a large decrease in concentration was detected between 54 – 66 hours. Between this time period fructose concentration reduced by 5.38 g/L. Initially pH of the culture was set at pH 7.00, however this decreased to pH 6.30 within the initial 24 hours of fermentation. **Table 3.2** details the kinetic growth parameters of the culture grown without the presence of exogenous quorum sensing molecules (control).

**Table 3.2** Kinetic growth parameters of *C. necator* H16 grown in 1 L shake flasks, batch mode fermentation without the addition of exogenous quorum sensing molecules. Data from time points 24 and 48 hours were used to calculate the following parameters.

$\frac{Y_X}{\bar{S}} (g/g)$	$\frac{Y_P}{\bar{S}} (g/g)$	$\frac{Y_P}{\bar{X}} (g/g)$	$Q_p (g/L.H) (\times 10^3)$
0.373	0.412	1.105	15.664

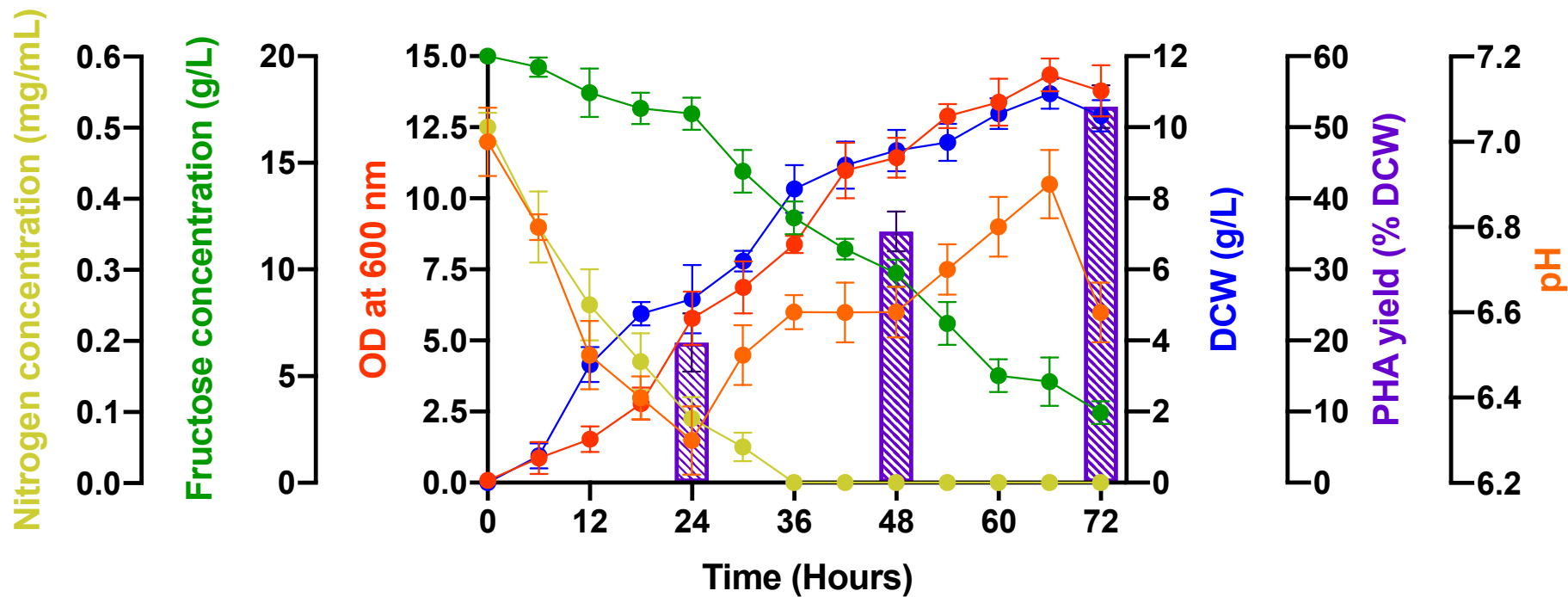


**Figure 3.2** Fermentation profile of *C. necator* H16 grown in 1 L shake flasks over a 72 hour period with addition of DMSO at a final concentration of 10  $\mu$ M. Samples were taken every 6 hours throughout the fermentation run, which was run in batch mode fermentation. MSM medium was used as the production medium, containing fructose as the sole carbon source. Error bars represent  $\pm$  SD values (n = 9).

**Figure 3.2** illustrates the growth profile the results produced from cultures grown of *C. necator* H16 in the presence of DMSO in shake flasks. OD of the fermentation increases steadily for the first 12 hours of fermentation reaching an OD of 1.537 before exponentially increasing and peaking at an OD of 14.349 at 66 hours of fermentation. DCW appeared to follow a similar pattern increasing until 66 hours of the fermentation and reaching a maximum value of 10.95 at 66 hours of fermentation, however after this point DCW begins to decrease slightly. PHA yield (% DCW) increases every 24 hours, with a maximum PHA yield coming in at 52.94% at 72 hours of growth. This was an increase of 49.67% when compared to the amount of PHA yielded (% DCW) at 48 hours.

Nitrogen concentration reduced by 82% within the first 24 hours of the fermentation beginning. As the fermentation was carried out in batch mode fermentation, nitrogen concentration with the culture media continued to decrease and as a result, by 36 hours, nitrogen was no longer detected within the fermentation culture. The concentration of fructose decreased at a consistent rate for the first 24 hours of the fermentation period, until the rate of consumed of fructose increased. As a result, between 24 – 60 hours fructose decreased by 12.28 g/L. pH of the fermentation decreased rapidly within the first 24 hours of the fermentation reaching pH 6.30 within the first 24 hours of the fermentation period. BY the end of the fermentation pH had increased to pH 6.62. **Table 3.3** details the kinetic growth parameters of the culture grown with the supplementation of DMSO.

**Table 3.3** Kinetic growth parameters of *C. necator* H16 grown in 1 L shake flasks, batch mode fermentation with the addition of DMSO. Data from time points 24 and 48 hours were used to calculate the following parameters

$\frac{Y_X (g/g)}{\bar{S}}$	$\frac{Y_P (g/g)}{\bar{S}}$	$\frac{Y_P (g/g)}{\bar{X}}$	$Q_p (g/L.H) (\times 10^3)$
0.560	0.301	0.539	12.943

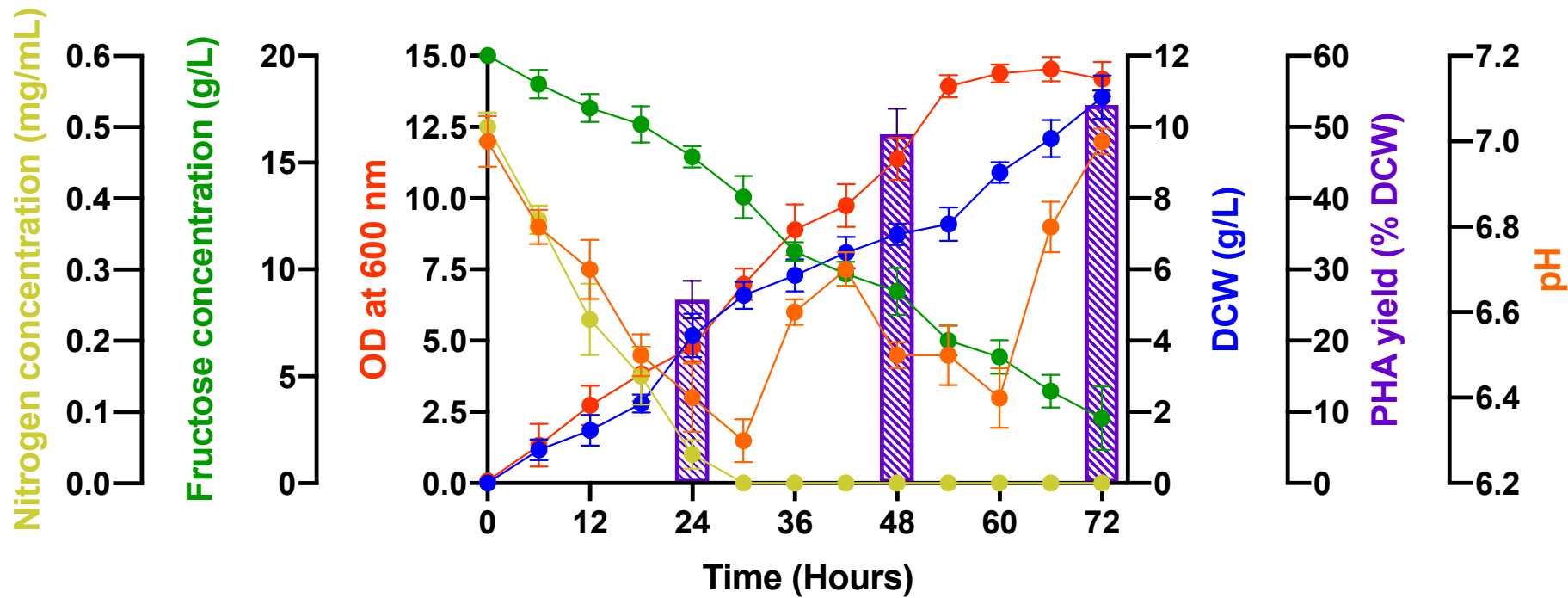


**Figure 3.3** Fermentation profile of *C. necator* H16 grown in 1 L shake flasks over a 72 hour period with addition of C<sub>4</sub>-HSL at a final concentration of 10 μM. Samples were taken every 6 hours throughout the fermentation run, which was run in batch mode fermentation. MSM medium was used as the production medium, containing fructose as the sole carbon source. Error bars represent ± SD values (n = 9).

**Figure 3.3** illustrates the growth profile of the results obtained from shake flasks used to grown *C. necator* H16 with the addition of the quorum sensing molecule C<sub>4</sub>-HSL at a final concentration of 10 µM. When observing the OD of the culture, it can be noted that there was almost no lag period observed within the culture supplemented with the exogenous quorum sensing molecules C<sub>4</sub>-HSL. OD peaked at 14.537 at 66 hours of fermentation growth, before slightly decreasing to 14.186 towards the end of the fermentation period. DCW appeared to have taken a similar growth rate, in which DCW began rising immediately with a maximum of 10.83 g/L of DCW accumulated. The culture was able to consistently accumulate DCW without decreasing at any point during the fermentation, which would suggest that there was a sufficient amount of carbon available for the culture to grow and utilise. Fructose concentration was set at 20 g/L as previously mentioned the concentration of fructose steadily decreased throughout the fermentation period, with the biggest decrease in fructose being observed between hours 30 – 36, in which fructose concentration reduced from 13.39 g/L to 10.84 g/L, a decrease of 2.55 g/L. PHA yield accumulated from 24 hours onwards of the fermentation and increased steadily throughout the entire fermentation period. A maximum of 53.10% of PHA was yielded (% DCW) at 72 hours of growth. This was an increase of 106.05%, between hours 24 and 72, from when the first PHA was detected to the end of the fermentation.

Nitrogen limiting conditions were achieved by 30 hours of fermentation growth, as nitrogen concentration was no longer detected by this time period. pH was set at pH 7 at the start of the fermentation, but decreased until 30 hours. From this point onwards, pH briefly increased and decreased again, before increasing and reaching a pH of 7.03 again. **Table 3.4** details the kinetic growth parameters of the culture grown with the supplementation of C<sub>4</sub>-HSL.

**Table 3.4** Kinetic growth parameters of *C. necator* H16 grown in 1 L shake flasks, batch mode fermentation with the addition of C<sub>4</sub>-HSL. Data from time points 24 and 48 hours were used to calculate the following parameters.

$\frac{Y_X}{\bar{S}}$ (g/g)	$\frac{Y_P}{\bar{S}}$ (g/g)	$\frac{Y_P}{\bar{X}}$ (g/g)	$Q_p$ (g/L.H) ( $\times 10^3$ )
0.444	0.367	0.827	17.299

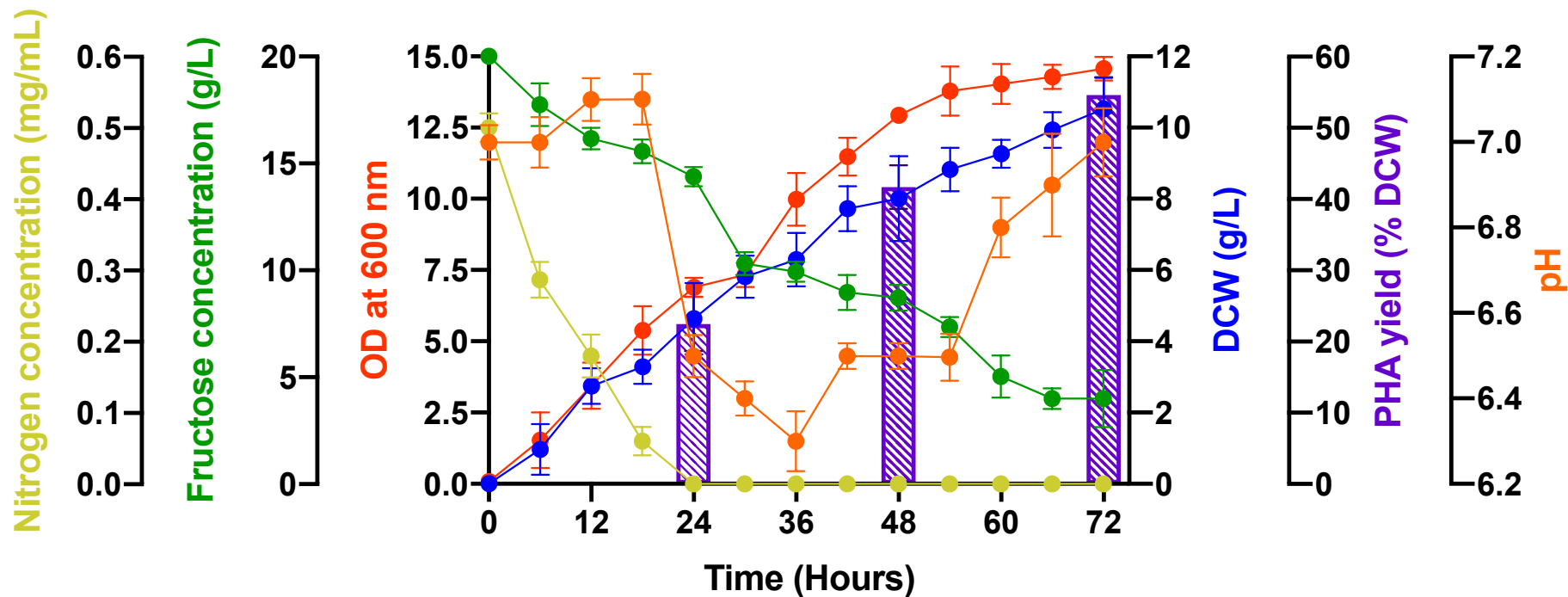


**Figure 3.4** Fermentation profile of *C. necator* H16 grown in 1 L shake flasks over a 72 hour period with addition of C<sub>6</sub>-HSL at a final concentration of 10  $\mu$ M. Samples were taken every 6 hours throughout the fermentation run, which was run in batch mode fermentation. MSM medium was used as the production medium, containing fructose as the sole carbon source. Error bars represent  $\pm$  SD values (n = 9).

**Figure 3.4** illustrates the growth profile of the results obtained from shake flasks used to grown *C. necator* H16 with the addition of the quorum sensing molecule C<sub>6</sub>-HSL at a final concentration of 10 μM. Similarly, to previous growth profiles OD began to rise rapidly and reached a maximum OD of 14.565 at the end of the fermentation period. This was also true for DCW, which accumulate a maximum of 10.52 g/L at 72 hours of fermentation. PHA yield (% DCW) started off accumulating as 22.52%, which subsequently increased to 41.7% and 54.64% every 24 hours. This resulted in 5.75 g/L of PHA being extracted at 72 hours of fermentation.

Fructose concentration decreased at a slow rate during the first 24 hours of fermentation, before a large decrease in concentration was detected between 24 and 30 hours, in which a decrease of 4.06 g/L of fructose was consumed by the culture within a 6 hour period. The largest decrease throughout the entire fermentation run. Once again, the culture was able to reach nitrogen limiting conditions by 24 hours of fermentation growth. From this point onwards nitrogen was no longer detected within the culture medium itself. Interestingly, pH of the culture remained stable for the first 6 hours growth before increasing to pH 7.11 until 18 hours of fermentation at which point pH decreased sharply to pH 6.32 at 36 hours. pH then gradually increased and reached pH 7.02 by the end of the fermentation period. **Table 3.5** details the kinetic growth parameters of the culture grown with the supplementation of C<sub>6</sub>-HSL.

**Table 3.5** Kinetic growth parameters of *C. necator* H16 grown in 1 L shake flasks, batch mode fermentation with the addition of C<sub>6</sub>-HSL. Data from time points 24 and 48 hours were used to calculate the following parameters.

$\frac{Y_X}{\bar{S}} (g/g)$	$\frac{Y_P}{\bar{S}} (g/g)$	$\frac{Y_P}{\bar{X}} (g/g)$	$Q_p (g/L.H) (\times 10^3)$
0.593	0.412	0.682	15.103

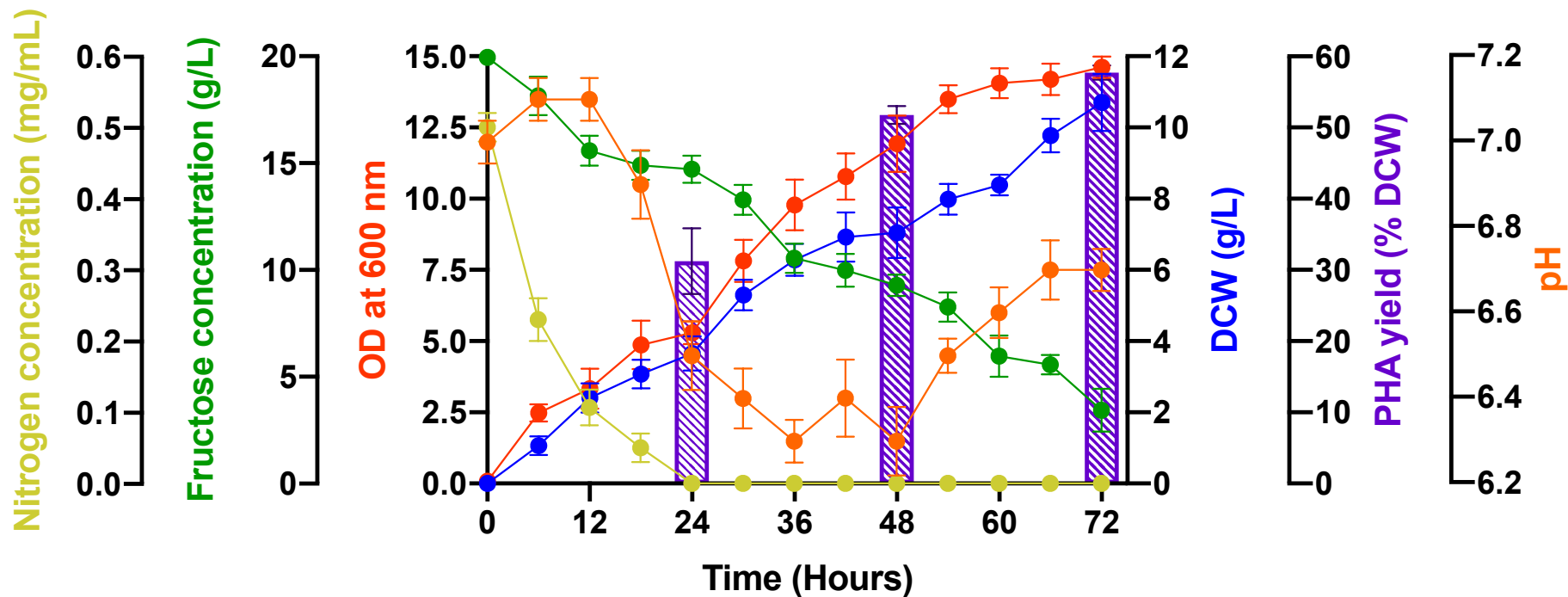


**Figure 3.5** Fermentation profile of *C. necator* H16 grown in 1 L shake flasks over a 72 hour period with addition of 3-oxo-C<sub>12</sub>-HSL at a final concentration of 10  $\mu$ M. Samples were taken every 6 hours throughout the fermentation run, which was run in batch mode fermentation. MSM medium was used as the production medium, containing fructose as the sole carbon source. Error bars represent  $\pm$  SD values (n = 9).

**Figure 3.5** illustrates the growth profile of the results obtained from shake flasks used to grown *C. necator* H16 with the addition of the quorum sensing molecule 3-oxo-C<sub>12</sub>-HSL at a final concentration of 10 µM. OD of the fermentation culture increased gradually throughout the entirety of the fermentation period reaching a maximum OD of 14.620 at 72 hours of fermentation. DCW followed a similar pattern increasing throughout the fermentation period and reaching a maximum value of 10.70 g/L. During this time period PHA yield (% DCW) increased by 65.48% between 24 and 48 hours. PHA yield (% DCW) continued to increase until the final hours of fermentation at which 57.74% of DCW was achieved as PHA, which was equal to a total of 6.18 g/L of PHA.

Fructose concentration of the fermentation decreased as the fermentation progressed, resulting in 3.49 g/L of fructose remaining within the culture medium by the end of the fermentation period, meaning 16.51 g/L of fructose was consumed by the culture during a 72 hour fermentation period. Nitrogen concentration decreased by 54% within the first 6 hours of fermentation and achieved nitrogen limiting conditions by 24 hours of fermentation growth. The pH of the culture displayed a similar pattern of previous cultured fluctuating throughout the fermentation period as a whole. Originally the pH was set at pH 7.00, which increased slightly for the first 18 hours of fermentation before rapidly decreasing to pH 6.3. After this point pH gradually increased to pH 6.73. **Table 3.6** details the kinetic growth parameters of the culture grown with the supplementation of 3-oxo-C<sub>12</sub>-HSL.

**Table 3.6** Kinetic growth parameters of *C. necator* H16 grown in 1 L shake flasks, batch mode fermentation with the addition of 3-oxo-C<sub>12</sub>-HSL. Data from time points 24 and 48 hours were used to calculate the following parameters.

$\frac{Y_X}{\bar{S}} (g/g)$	$\frac{Y_P}{\bar{S}} (g/g)$	$\frac{Y_P}{\bar{X}} (g/g)$	$Q_p (g/L.H) (\times 10^3)$
0.625	0.461	0.738	19.541

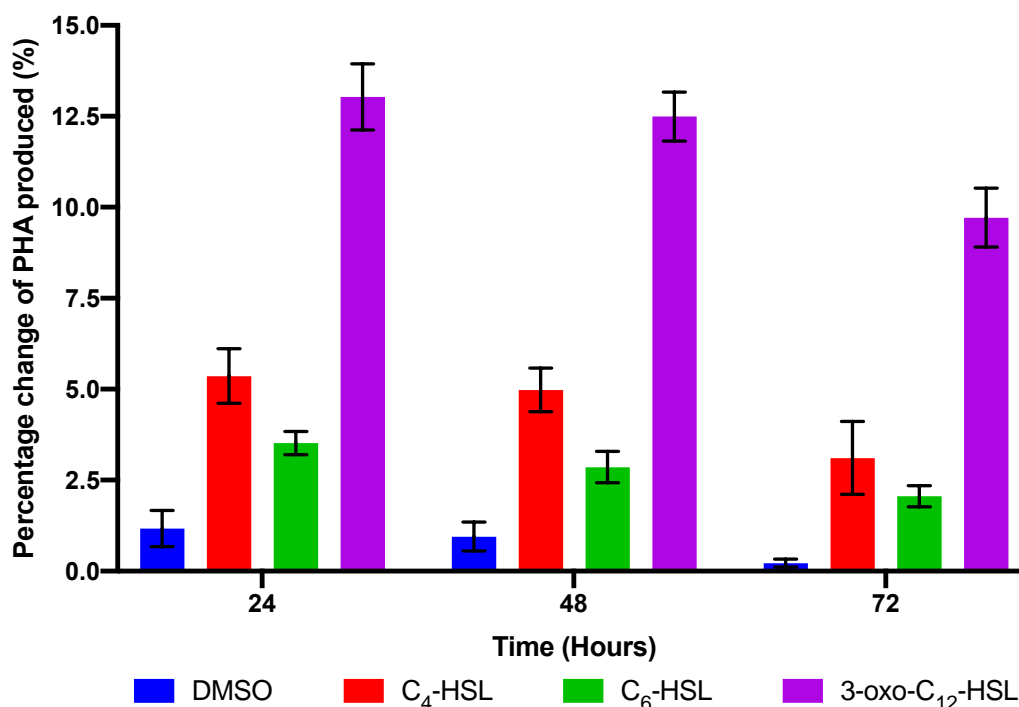


**Figure 3.6** Percentage change of PHA produced from *C. necator* H16 grown in 1 L shake flasks (batch mode fermentation) containing production media and exogenous quorum sensing molecules with a final concentration of 10  $\mu$ M. Results shown are expressed as mean percentage changes of PHA produced when compared to an untreated control (grown in the absence of exogenous quorum sensing molecules) with  $\pm$  SD values (n = 9).

**Figure 3.6** above illustrates the percentage change of PHA produced over the fermentation run within shaken flasks in *C. necator* H16. It can be observed that the greatest increase in production of PHA was by the flask that was supplemented with 3-oxo-C<sub>12</sub>-HSL, increasing the production of PHAs by a maximum of 13.03% within 24 hours of the fermentation beginning. This increase was maintained throughout the entire fermentation period, as 3-oxo-C<sub>12</sub>-HSL had the highest increase in PHA produced throughout the entirety of the run. The flask supplemented with DMSO increased in the amount of PHA produced, however this increase was below 1% for the first 48 hours, and reduced to 0.22% by 72 hours.

### 3.3.1 Characterisation and identification of SCL PHAs produced in shaken flask fermentation

The following series of experiments were carried out in order to characterise and identify the type of PHA produced by *C. necator* H16 when grown in 1 L

shake flasks (batch mode fermentation) with its respective production medium and in the presence of different exogenous quorum sensing molecules with a concentration of 10  $\mu$ M (**Section 2.4.3**).

### 3.3.1.1 Sudan Black B staining

Samples extracted were first screened for the existence of PHAs, which was confirmed by the use of Sudan Black B dye. This particular dye was chosen for its ability to dye inclusion bodies containing PHAs, which could then be observed macroscopically as described in **Section 2.7.2**. Colonies that were able to retain the dye were considered to have tested positive for inclusions containing PHAs as shown in **Figure 3.7**.



**Figure 3.7** Representative positive result of *C. necator* H16 culture grown on a nutrient agar plate and stained with Sudan Black B dye to indicate the presence of inclusion bodies. Samples of cultures were collected 48 hours post inoculation. The image shown is that of a *C. necator* H16 sample grown in the presence of the quorum sensing molecule 3-oxo-C<sub>12</sub>-HSL.

All samples examined were able to test positively for inclusion bodies as individual colonies were able to successfully retain the Sudan Black B dye, resulting in the conclusions that PHAs were being produced.

### 3.3.1.2 Nile red dye staining

Once samples of *C. necator* H16 were confirmed to have harboured PHAs in the form of inclusion bodies they were then dyed with Nile red, and fixated as

described in **Section 2.7.3**. The inclusions were able to be visualised using a fluorescence microscope as the individual cells were able to retain the dye if they contained PHAs as shown in **Figure 3.8**.

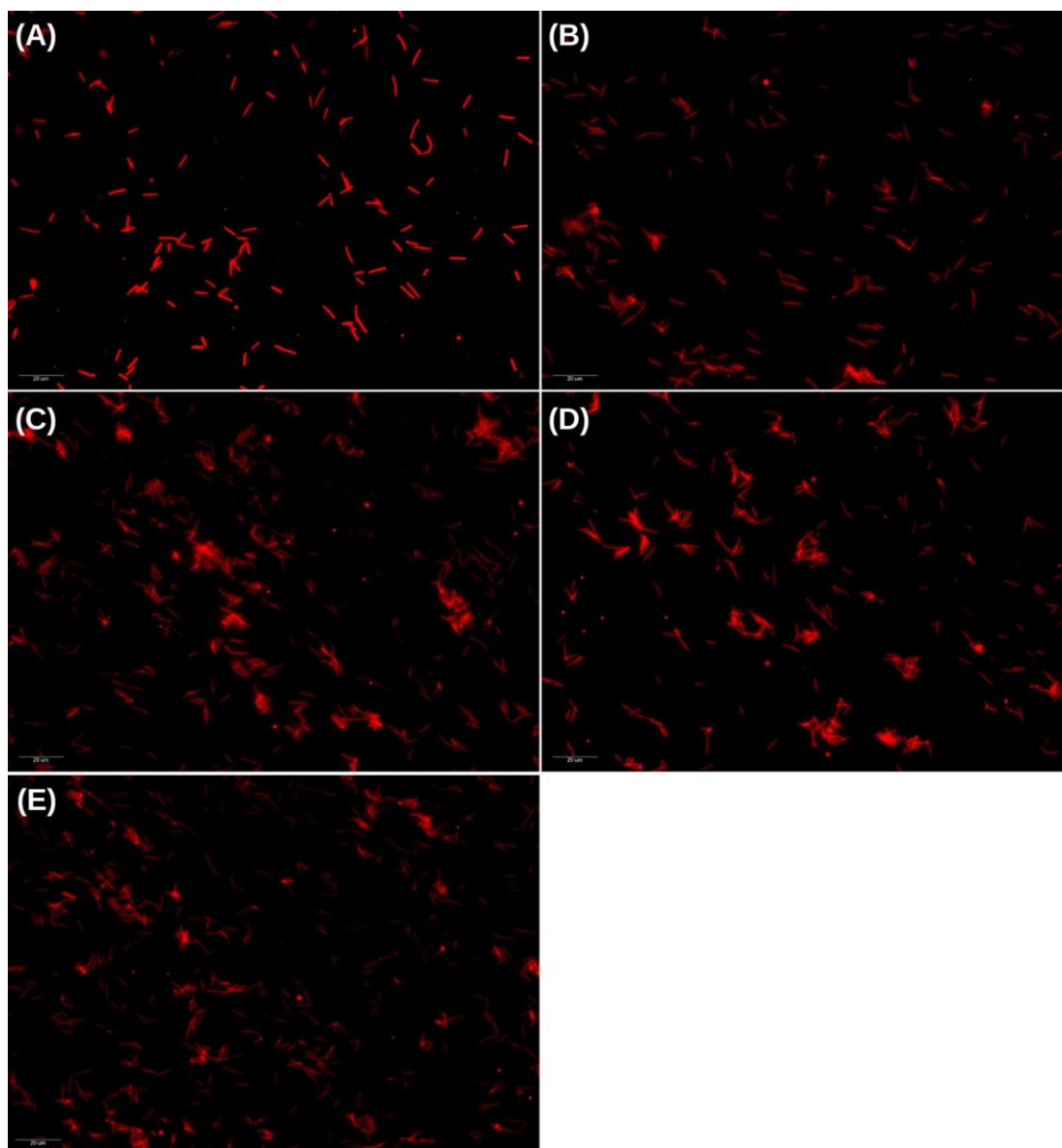


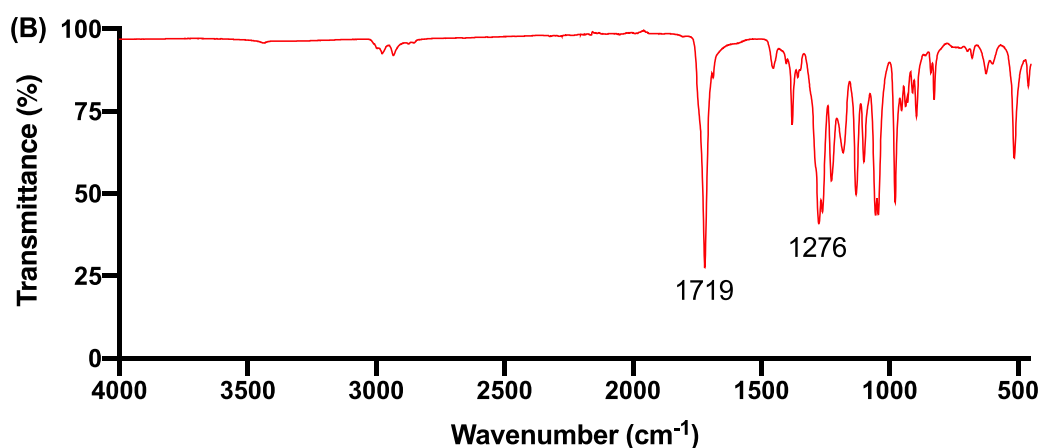
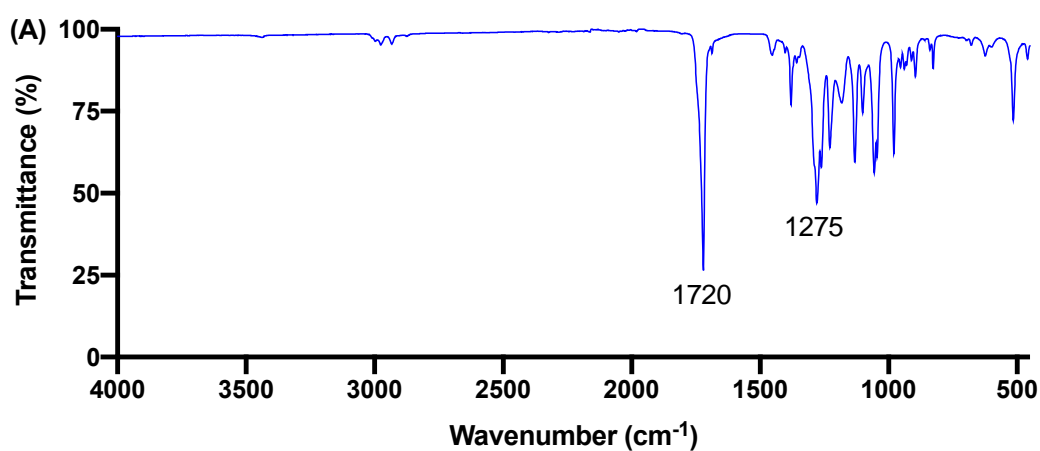
**Figure 3.8** Microscopic images of *C. necator* H16 cultures grown in 1 L shake flasks and stained with Nile red dye to indicate the presence of inclusion bodies containing PHAs. Cultures were visualised using a fluorescence microscope at X40 magnification. Images were taken of cultures 48 hours post inoculation. The images are labelled as follows: **(A)** Control, **(B)** DMSO, **(C)** C<sub>4</sub>-HSL, **(D)** C<sub>6</sub>-HSL and **(E)** 3-oxo-C<sub>12</sub>-HSL.

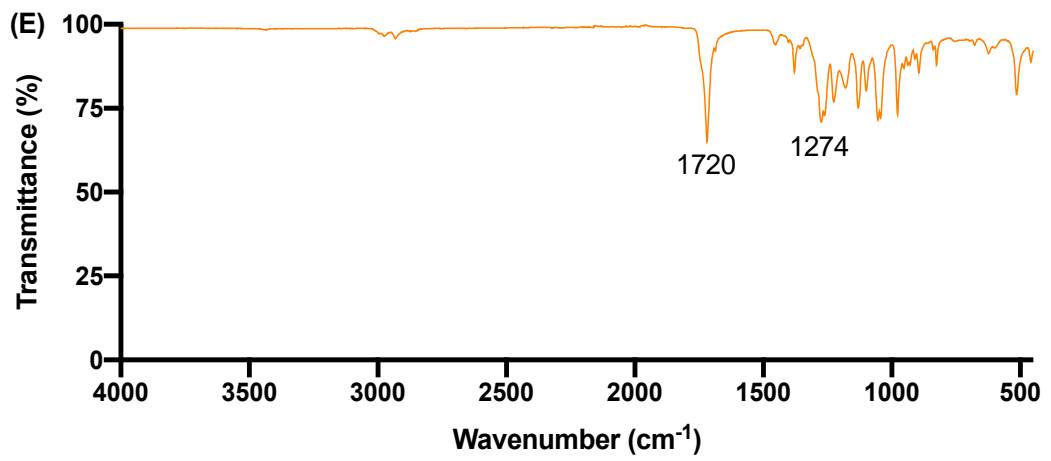
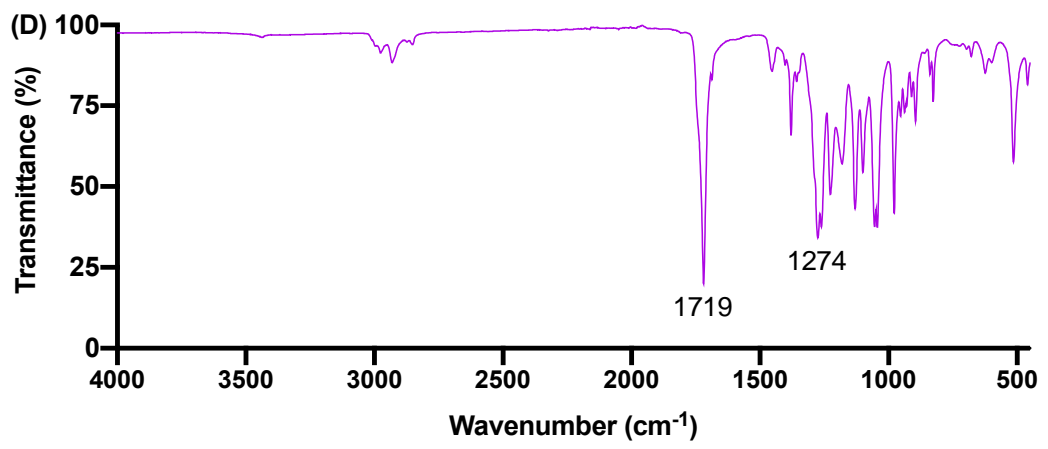
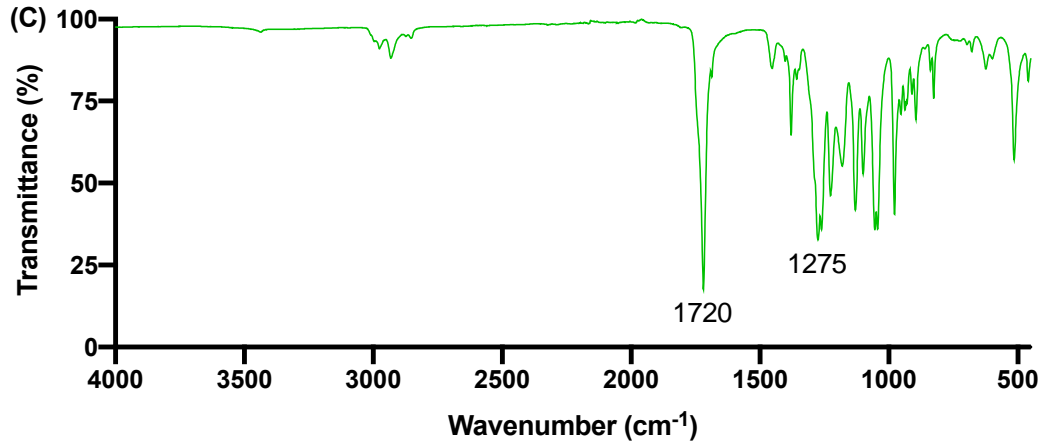
The results displayed showed that PHAs were produced by *C. necator* H16 and were harvested as an intracellular product as they were retained within the cell itself. As it is the PHA itself that retains the dye, the cells appeared as

a bright red colour when viewed under the fluorescent microscope, indicating for the presence of PHA granules within the cells.

### 3.3.1.3 FTIR

In order to initially characterise the type of polymer produced, the chemical structure of the PHA was studied using FTIR. This analytical technique produces a spectrum that can be used for the identification of signature absorption bands that are normally present within a standard sample of PHA or have been noted within literature. After 72 hours of fermentation in 1 L shake flasks, the PHA produced by the culture was extracted, purified and subsequently analysed using FTIR as described in **Section 2.7.4**. **Figure 3.9** displays the individual spectra produced by each sample, whereas **Figure 3.10** shows the combined spectra of the PHAs produced when in the presence of different quorum sensing molecules. A commercial standard of P(3HB) was also analysed via FTIR in order to compare the samples of PHAs against.





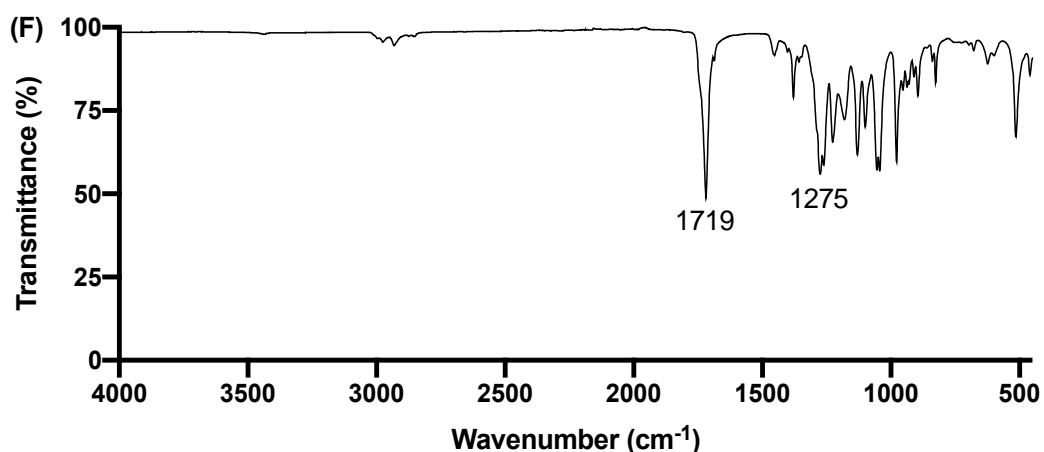


**Figure 3.9** FTIR spectra of SCL PHA produced by *C. necator* H16 grown in shaken flasks. The following spectra are labelled as follows: **(A)** Standard P(3HB) **(B)** Control, **(C)** DMSO, **(D)** C<sub>4</sub>-HSL, **(E)** C<sub>6</sub>-HSL and **(F)** 3-oxo-C<sub>12</sub>-HSL.

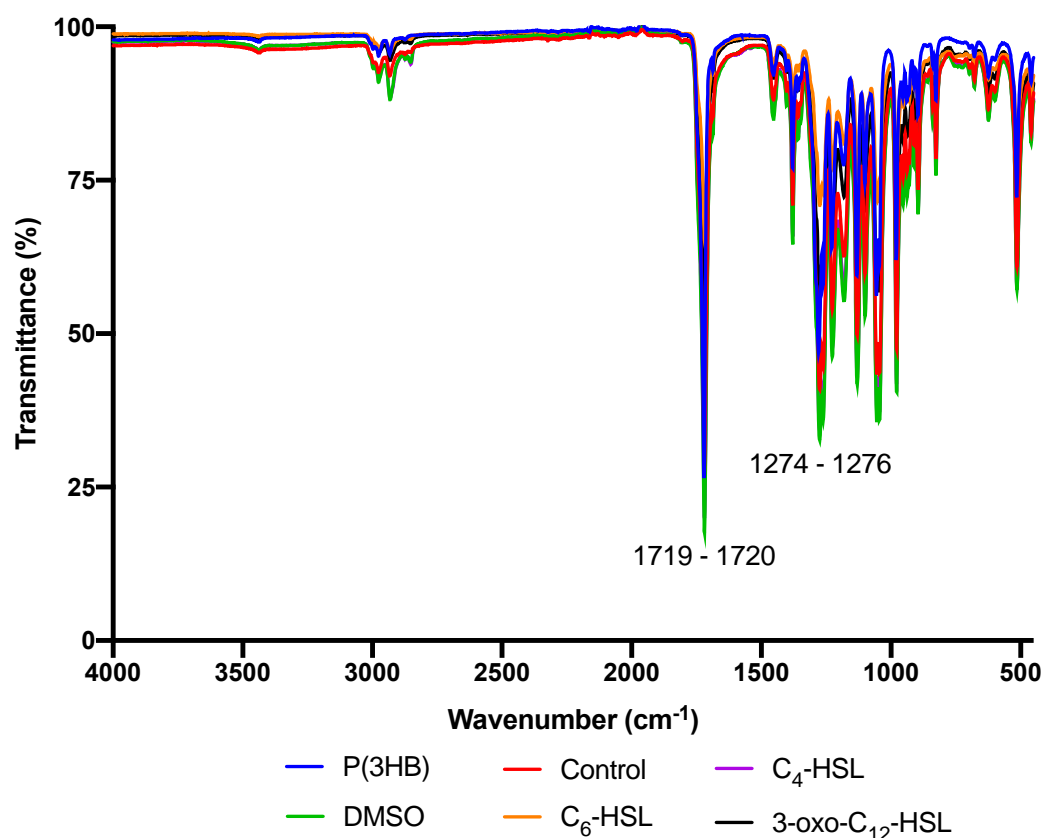


**Figure 3.10** Combined FTIR spectra of SCL PHA produced by *C. necator* H16 within shaken flasks and in the presence of different quorum sensing molecules. The graph also includes the spectrum of a commercial standard P(3HB).

FTIR analysis of the isolated PHAs revealed absorption bands at 1719 – 1720  $\text{cm}^{-1}$  and 1274 – 1276  $\text{cm}^{-1}$  corresponding to the stretching of the ester carbonyl group (C=O) and the -CH group respectively, and are characteristically present in P(3HB), an SCL PHA (Sindhu *et al.*, 2011) (**Figure 3.10**). The PHA samples extracted were also compared against a commercial standard of P(3HB) spectrum, which produced the same absorption bands as the polymers produced and no major differences were observed. In turn this confirmed the chemical structures of the PHAs produced to be that of SCL PHAs.

#### 3.3.1.4 GC-MS

For monomeric characterisation of the polymer produced in shaken flasks, GC-MS was carried out. Prior to this analysis the sample of PHA produced was made to undergo the process of methanolysis, resulting in the production of methyl esters as described in **Section 2.7.5**. A representative total ion chromatogram (TIC) of PHA produced by *C. necator* H16 when in the presence of different quorum sensing molecules is shown in **Figure 3.11**, in which two peaks of interest were generated.

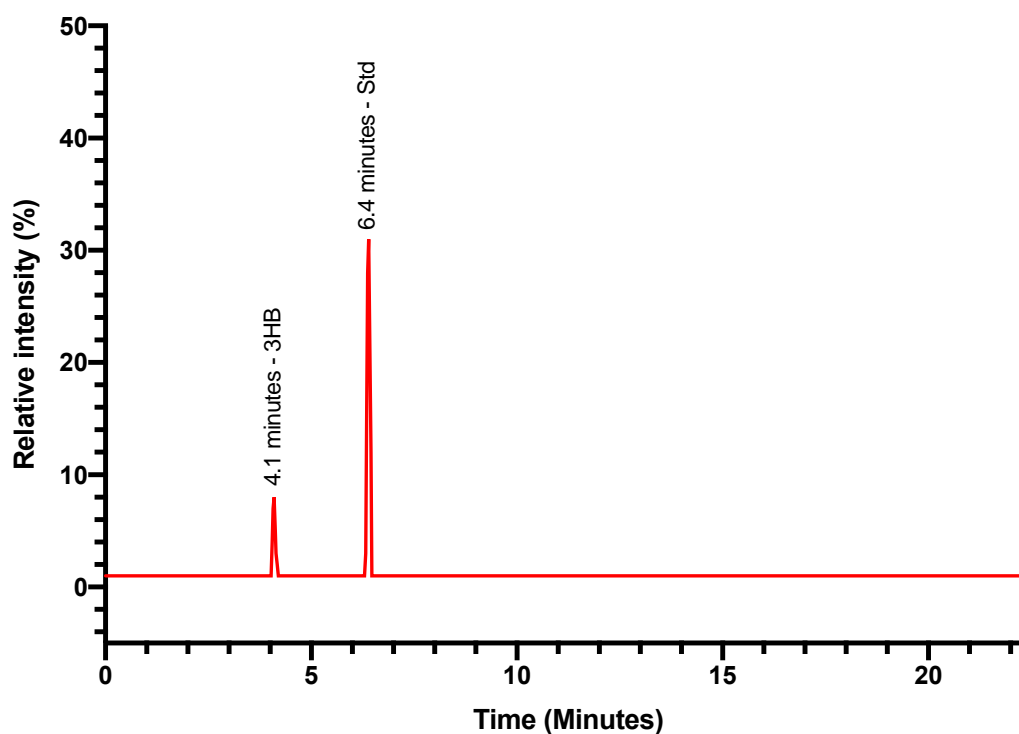


**Figure 3.11** Representative GC-MS analysis of the polymer produced when *C. necator* H16 was grown in shaken flasks. The TIC above displays the methanolysis product of the PHAs produced when grown in the presence of DMSO. Methyl Benzoate was used as an internal standard.

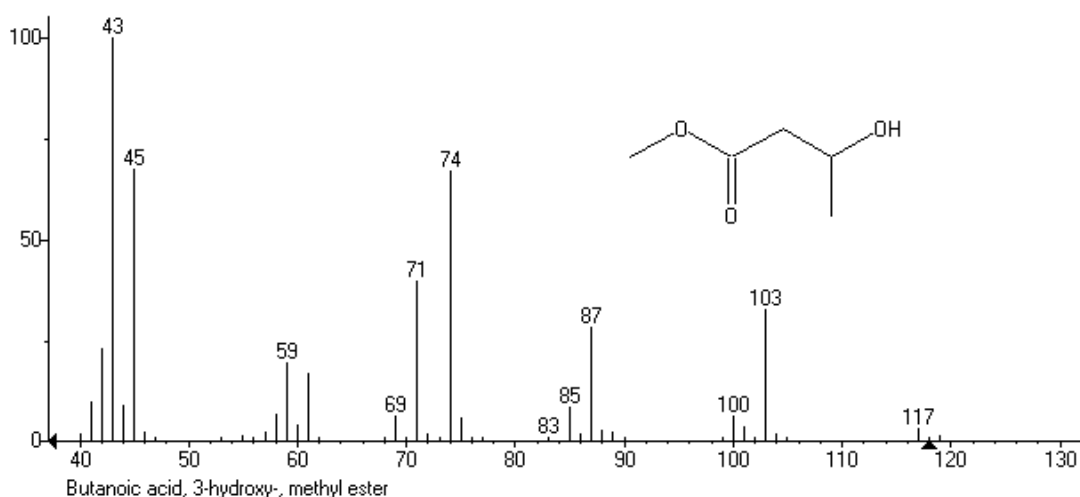


**Figure 3.12** Mass spectrum of the peak generated from GC of the methanolysis product of the PHA produced by *C. necator* H16 when grown in shaken flasks with a  $R_t$  of 4.1 minutes was identified using the NIST library as methyl ester of 3HB.

The two peaks that were produced from the methanolysis products of the isolated PHA had retention times ( $R_t$ ) of 4.1 minutes and 6.4 minutes. Of the two peaks, the one with a  $R_t$  of 6.4 was identified to be internal standard added, methyl benzoate. The mass spectrum of the peak with a  $R_t$  of 4.1 minutes was found to be comparable with the mass spectrum of the methyl ester of 3-hydroxybutyric acid in the MS library obtained from the National Institute of Science and Technology (NIST) (**Figure 3.12**).

The fragmentation pattern of 3HB showed significant peaks at mass-to-charge ratio ( $m/z$ ) 43 and 74. The  $m/z$  peak at 43 represented the hydroxyl end of the molecule, which occurred due to the cleavage of the bond between carbon atoms number 3 and 4, whereas the  $m/z$  peak at 74 represented the carbonyl end of the molecule. This also originated due to the cleavage between carbon atoms 3 and 4 following McLafferty rearrangement which involves  $\gamma$ -hydrogen rearrangement with a  $\beta$ -cleavage reaction (McLafferty, 1956).

As the methyl ester of 3HB was the only peak observed in the TIC produced across all samples of PHA produced by *C. necator* H16 in shaken flasks, when grown in the presence of different quorum sensing molecules, it was concluded that a homopolymer of P(3HB) was produced. A summary of the results of the monomeric composition of the PHA produced and the structure of the methyl ester 3HB is displayed in **Table 3.7** and **Figure 3.12** respectively.

**Table 3.7** PHA monomer composition of SCL PHAs synthesised by *C. necator* H16 when grown in shaken in the presence of different exogenous quorum sensing molecules.

Quorum sensing molecules	Monomeric composition of PHAs (Mol %) 3HB
Control	100
DMSO	100
C <sub>4</sub> -HSL	100
C <sub>6</sub> -HSL	100
3-oxo-C <sub>12</sub> -HSL	100

### 3.4 Growth profile bioreactors

Fermentations were then scaled by into 2 L bioreactors which were carried out in batch mode fermentations (**Section 2.4.5**). This was carried out in order to further optimise the production of PHA from *C. necator* H16 with the addition of three exogenous quorum sensing molecules. The PHA yield produced and PHA obtained were compared to the yield and product produced at shaken flask level to assess if there was a difference in production between the two modes.

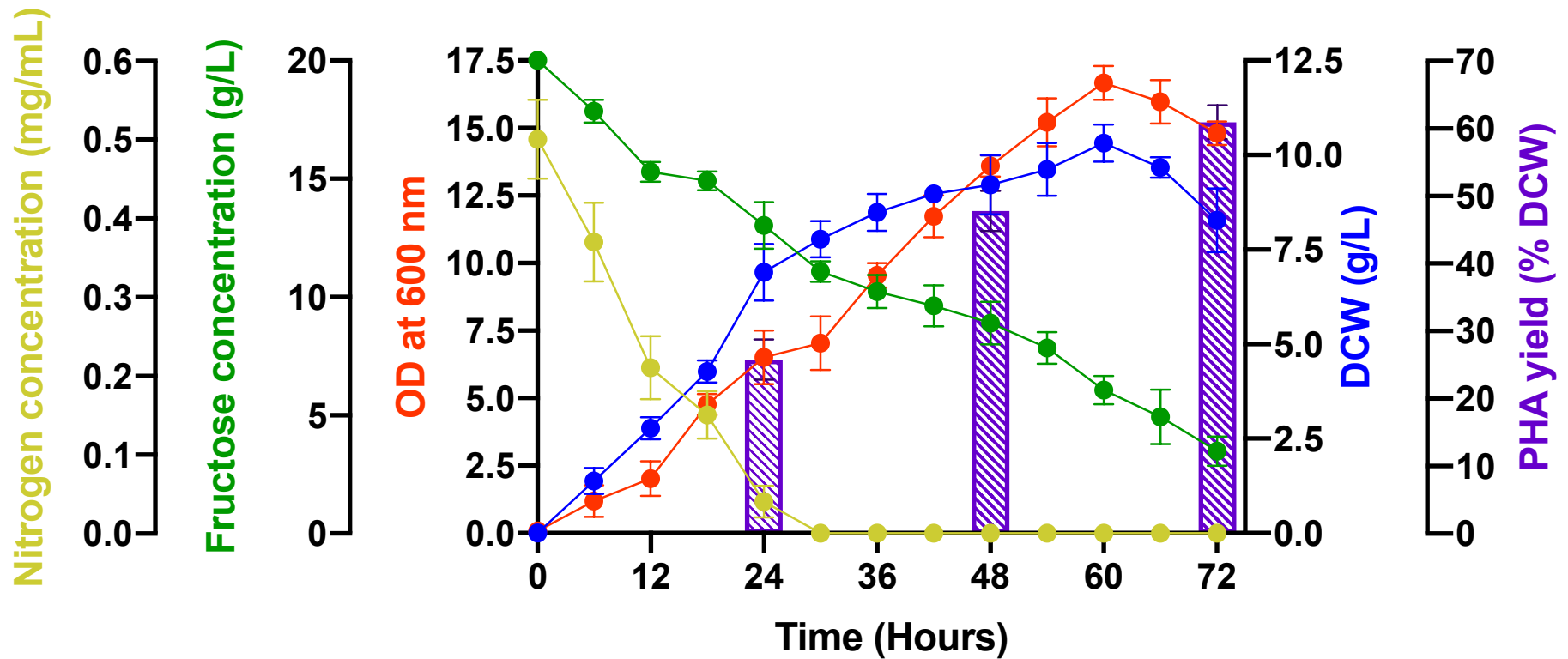


**Figure 3.13** Fermentation profile of *C. necator* H16 grown in 2 L bioreactors over a 72 hour period without the addition of exogenous quorum sensing molecules (control). Samples were taken every 6 hours throughout the fermentation run, which was run in batch mode fermentation. MSM medium was used as the production medium, containing fructose as the sole carbon source. Error bars represent  $\pm$  SD values ( $n = 3$ ).

**Figure 3.13** illustrates the growth profile of the results obtained from the control bioreactor used to grow *C. necator* H16 without the addition of exogenous quorum sensing molecules. OD of the culture grown in a bioreactor without the presence of exogenous quorum sensing molecules increased to a maximum of 16.676, which was achieved at 60 hours of fermentation. From this point onwards OD began to decrease to 14.806. DCW increased rapidly for the first 24 hours of fermentation before the rate of growth decreased. The maximum amount of DCW accumulated by the culture was observed at 60 hours, reaching 10.32 g/L. Once again from this point onwards DCW also began to decrease to reach a final DCW of 8.28 g/L. The PHA yield (% DCW) accumulated by the culture increased over the 72 hour fermentation period reaching a maximum of 5.04 g/L PHA extracted at 72 hours of fermentation, which represented 60.85% of the total DCW.

Nitrogen concentration decreased and was no longer detected at 30 hours of fermentation, which meant that nitrogen limiting conditions were achieved from this time point onwards. Fructose concentration decreased gradually throughout the entire fermentation period, however the largest decrease was observed between 6 – 12 hours in which 2.56 g/L of fructose was consumed by the culture. **Table 3.8** details the kinetic growth parameters of the culture grown without the supplementation of exogenous quorum sensing molecules.

**Table 3.8** Kinetic growth parameters of *C. necator* H16 grown in 2 L bioreactors, batch mode fermentation without the addition of exogenous quorum sensing molecules. Data from time points 24 and 48 hours were used to calculate the following parameters.

$\frac{Y_X}{\bar{S}} (g/g)$	$\frac{Y_P}{\bar{S}} (g/g)$	$\frac{Y_P}{\bar{X}} (g/g)$	$Q_p (g/L.H) (\times 10^3)$
0.532	0.603	1.133	13.542

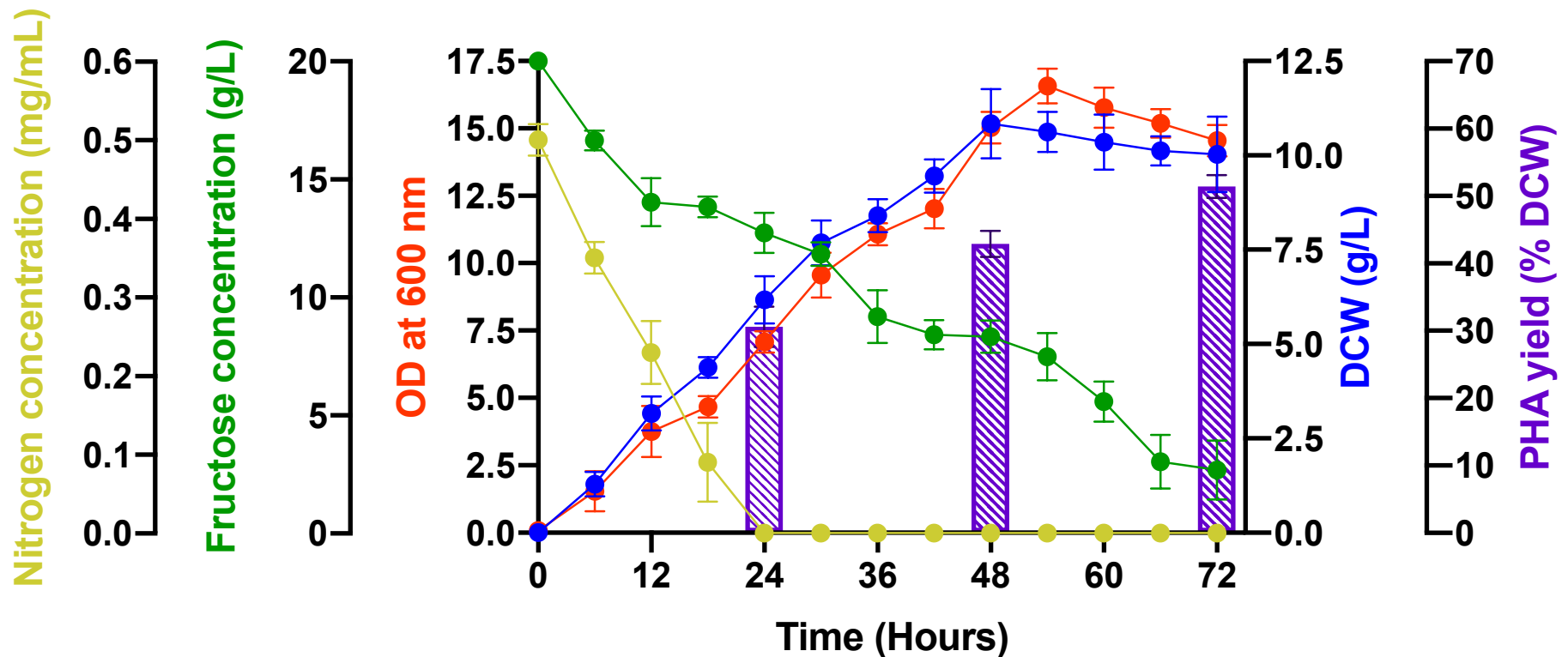


**Figure 3.14** Fermentation profile of *C. necator* H16 grown in 2 L bioreactors over a 72 hour period with addition of C<sub>4</sub>-HSL at a final concentration of 10  $\mu$ M. Samples were taken every 6 hours throughout the fermentation run, which was run in batch mode fermentation. MSM medium was used as the production medium, containing fructose as the sole carbon source. Error bars represent  $\pm$  SD values (n = 3).

**Figure 3.14** illustrates the growth profile of the results obtained from the control bioreactor used to grow *C. necator* H16 with the addition of C<sub>4</sub>-HSL. OD profile of the fermentation increased until 54 hours of growth reaching a maximum value of 16.578, before decreasing to 14.550 by the end of the fermentation period. DCW increased steadily, accumulating as the fermentation progressed until 48 hours of fermentation reaching a maximum DCW of 10.84 g/L. From this point onwards DCW began to plateau and ultimately accumulated 10.03 g/L of DCW by the end of the fermentation period. When observing PHA yield (% DCW) a maximum of 5.16 g/L of PHA was produced at 72 hours of fermentation, which was representative of 51.43% of the total DCW produced. The total increase of PHA yielded between 24 and 72 was 68.24%.

Once again nitrogen limiting conditions were achieved by 24 hours of fermentation period. After this point nitrogen was no longer detected within the culture. Fructose concentration decreased from 20 g/L to 2.68 g/L by the end of the fermentation, which resulted in 17.32 g/L of fructose being consumed by the culture. **Table 3.9** details the kinetic growth parameters of the culture grown with the supplementation of C<sub>4</sub>-HSL.

**Table 3.9** Kinetic growth parameters of *C. necator* H16 grown in 2 L bioreactors, batch mode fermentation with the addition of C<sub>4</sub>-HSL. Data from time points 24 and 48 hours were used to calculate the following parameters.

$\frac{Y_X}{\bar{S}} (g/g)$	$\frac{Y_P}{\bar{S}} (g/g)$	$\frac{Y_P}{\bar{X}} (g/g)$	$Q_p (g/L.H) (\times 10^3)$
1.060	0.628	0.592	13.536

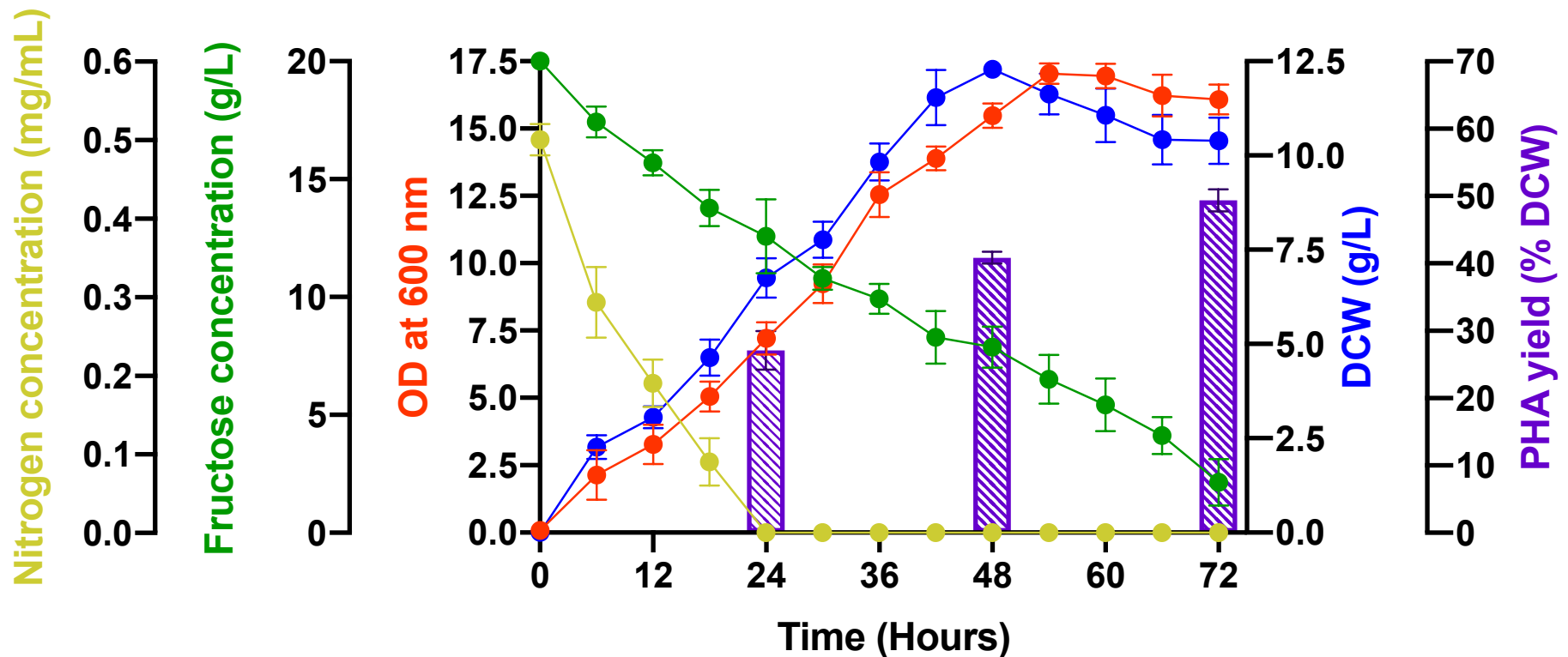


**Figure 3.15** Fermentation profile of *C. necator* H16 grown in 2 L bioreactors over a 72 hour period with addition of C<sub>6</sub>-HSL at a final concentration of 10 μM. Samples were taken every 6 hours throughout the fermentation run, which was run in batch mode fermentation. MSM medium was used as the production medium, containing fructose as the sole carbon source. Error bars represent ± SD values (n = 3).

**Figure 3.15** illustrates the growth profile of the results obtained from the control bioreactor used to grow *C. necator* H16 with the addition of C<sub>6</sub>-HSL. OD of the fermentation profile supplemented with the quorum sensing molecule C<sub>6</sub>-HSL increased reaching a maximum value of 17.034 at 54 hours of fermentation growth. After this point OD began to slowly decrease and by 72 hours of fermentation OD had reached 16.082. DCW followed a similar pattern increasing until 48 hours of fermentation reaching a maximum DCW of 12.29 g/L. PHA yield (% DCW) accumulated from 24 hours onwards, with the maximum amount of PHA accumulating at 72 hours of fermentation growth. At this point 49.36% of DCW was accumulated as PHAs, meaning a total of 5.13 g/L of PHA was extracted from the culture at 72 hours of fermentation growth.

Nitrogen concentration was completely depleted from the culture medium by 24 hours of growth from which point onwards nitrogen was no longer detected in the culture. This meant nitrogen limiting conditions had been achieved and was not replenished as the bioreactor was run in batch mode, meaning nutrients would not increase once the fermentation had begun. Fructose concentration decreased at a constant rate throughout the fermentation period with 2.14 g/L of fructose remaining in the bioreactor by the end of the fermentation period. **Table 3.10** details the kinetic growth parameters of the culture grown with the supplementation of C<sub>6</sub>-HSL.

**Table 3.10** Kinetic growth parameters of *C. necator* H16 grown in 2 L bioreactors, batch mode fermentation with the addition of C<sub>6</sub>-HSL. Data from time points 24 and 48 hours were used to calculate the following parameters.

$\frac{Y_X}{\bar{S}} (g/g)$	$\frac{Y_P}{\bar{S}} (g/g)$	$\frac{Y_P}{\bar{X}} (g/g)$	$Q_p (g/L.H) (\times 10^3)$
1.177	0.574	0.488	11.812

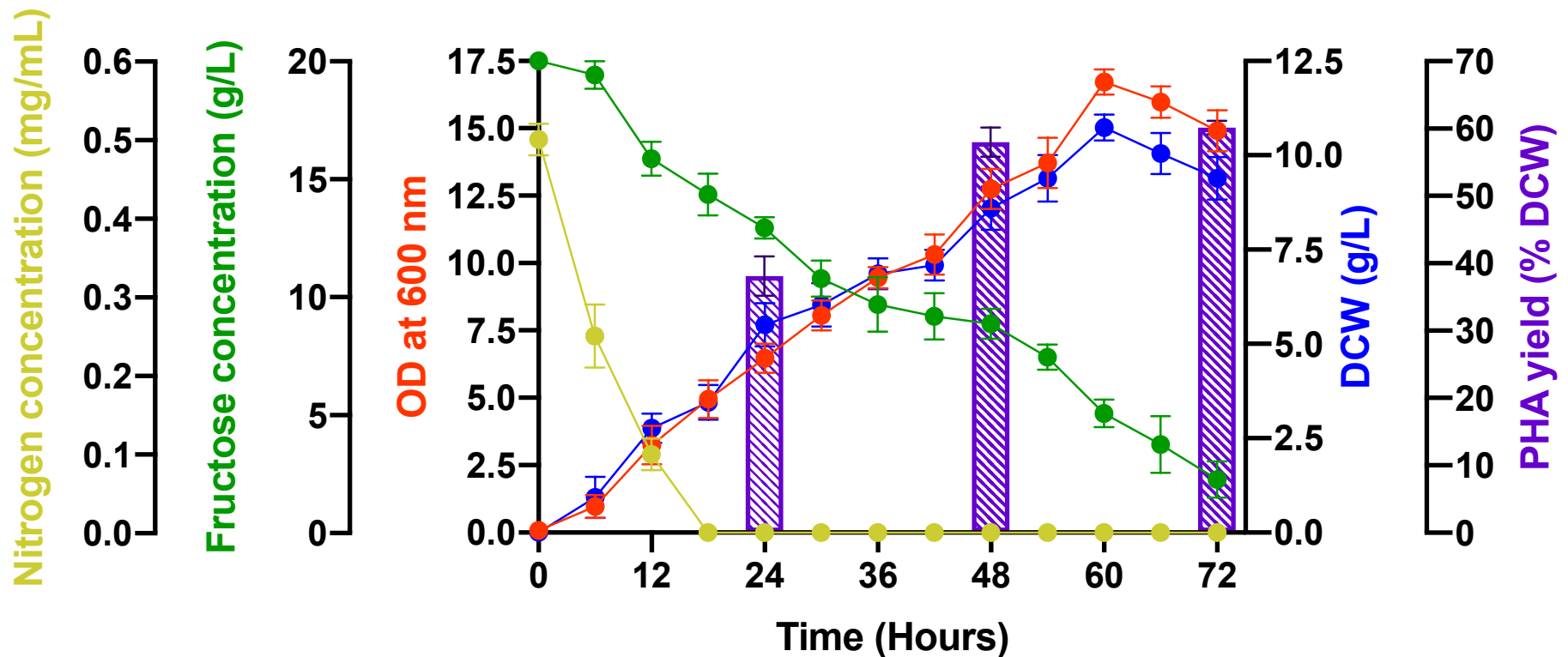


**Figure 3.16** Fermentation profile of *C. necator* H16 grown in 2 L bioreactors over a 72 hour period with addition of 3-oxo-C<sub>12</sub>-HSL at a final concentration of 10  $\mu$ M. Samples were taken every 6 hours throughout the fermentation run, which was run in batch mode fermentation. MSM medium was used as the production medium, containing fructose as the sole carbon source. Error bars represent  $\pm$  SD values (n = 3).

**Figure 3.16** illustrates the growth profile of the results obtained from the control bioreactor used to grow *C. necator* H16 with the addition of 3-oxo-C<sub>12</sub>-HSL. OD of the culture was able to reach a maximum value of 16.727 by 60 hours of fermentation at which point fermentation began to decrease resulting in the final OD reading of 14.918 at 72 hours of fermentation. DCW followed a near identical pattern of increase as OD, increasing steadily until 60 hours at which point DCW peaked with a value of 10.73 g/L. After this point DCW began to decrease as described with OD and the final DCW produced from the culture at 72 hours was 9.39 g/L. PHA yield (% DCW) increased throughout the fermentation period with a maximum amount of PHA being accumulated at the end of the fermentation run. AT this point 60.12% of DCW was extracted as PHA, thus meaning 5.65 g/L of PHA was able to be extracted from the culture at the end of the fermentation period.

Nitrogen concentration decreased to 0.00 mg/mL by 18 hours of fermentation, which meant nitrogen limiting conditions were achieved. Fructose concentration decreased to 2.26 g/L by the end of the fermentation period which mean that 17.74 g/L of fructose had been consumed by the culture. **Table 3.11** details the kinetic growth parameters of the culture grown with the supplementation of 3-oxo-C<sub>12</sub>-HSL.

**Table 3.11** Kinetic growth parameters of *C. necator* H16 grown in 2 L bioreactors, batch mode fermentation with the addition of 3-oxo-C<sub>12</sub>-HSL. Data from time points 24 and 48 hours were used to calculate the following parameters.

$\frac{Y_X (g/g)}{\bar{S}}$	$\frac{Y_P (g/g)}{\bar{S}}$	$\frac{Y_P (g/g)}{\bar{X}}$	$Q_p (g/L.H) (\times 10^3)$
0.760	0.709	0.934	17.050

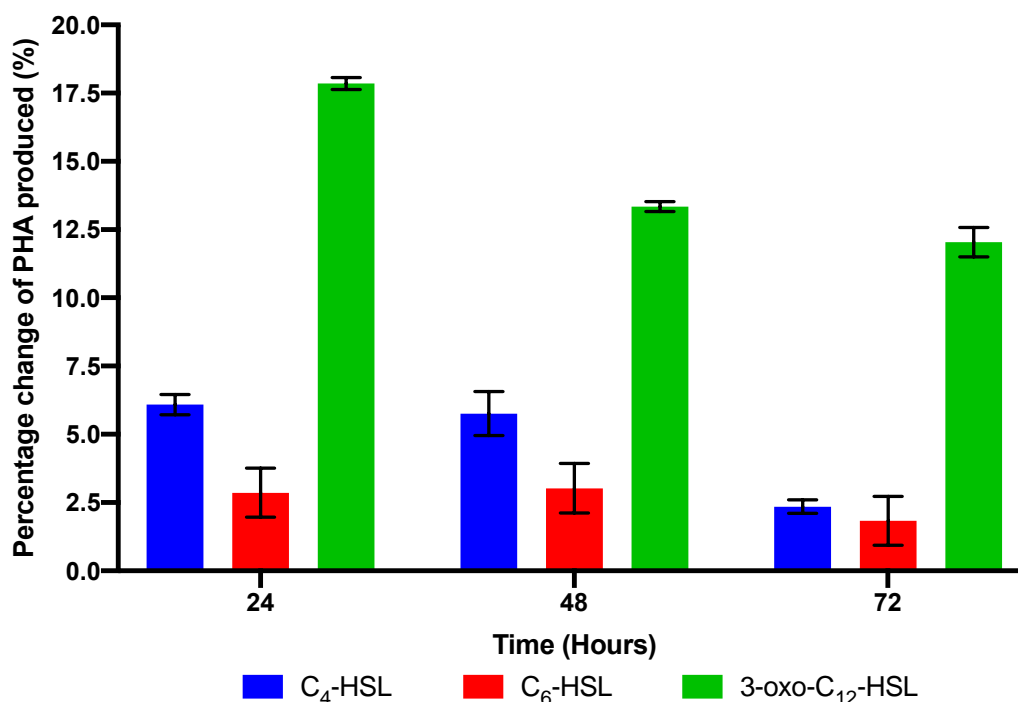


**Figure 3.17** Percentage change of PHA produced from *C. necator* H16 grown in 2 L bioreactors (batch mode fermentation) containing production media and exogenous quorum sensing molecules with a final concentration of 10  $\mu$ M. Results shown are expressed as mean percentage changes of PHA produced when compared to an untreated control (grown in the absence of exogenous quorum sensing molecules) with error bars  $\pm$  SD values (n = 3).

**Figure 3.17** displays the change of PHA produced by *C. necator* H16 in bioreactors. 3-oxo-C<sub>12</sub>-HSL resulted in the largest increase in PHA produced, with an increase of 17.85% within the first 24 hours of fermentation.

### 3.4.1 Characterisation and identification of SCL PHAs produced in 2 L bioreactor fermentation

The following series of experiments were carried out in order to characterise and identify the type of PHA produced by *C. necator* H16 when grown in 2 L bioreactors (batch mode fermentation) with its respective production medium and in the presence of different exogenous quorum sensing molecules with a concentration of 10  $\mu$ M (**Section 2.4.5**).

#### 3.4.1.1 FTIR analysis

In order to initially characterise the type of polymer produced, the chemical structure of the PHA was studied using FTIR. This analytical technique

produces a spectrum that can be used for the identification of signature absorption bands that are normally present within a standard sample of PHA or have been noted within literature. After 72 hours of fermentation in 2 L bioreactors, the PHA produced by the culture was extracted, purified and subsequently analysed using FTIR as described in **Section 2.7.4**. **Figure 3.18** the show the combined spectra of the PHAs produced when in the presence of different quorum sensing molecules. A commercial standard of P(3HB) was also analysed via FTIR in order to compare the samples of PHAs against.

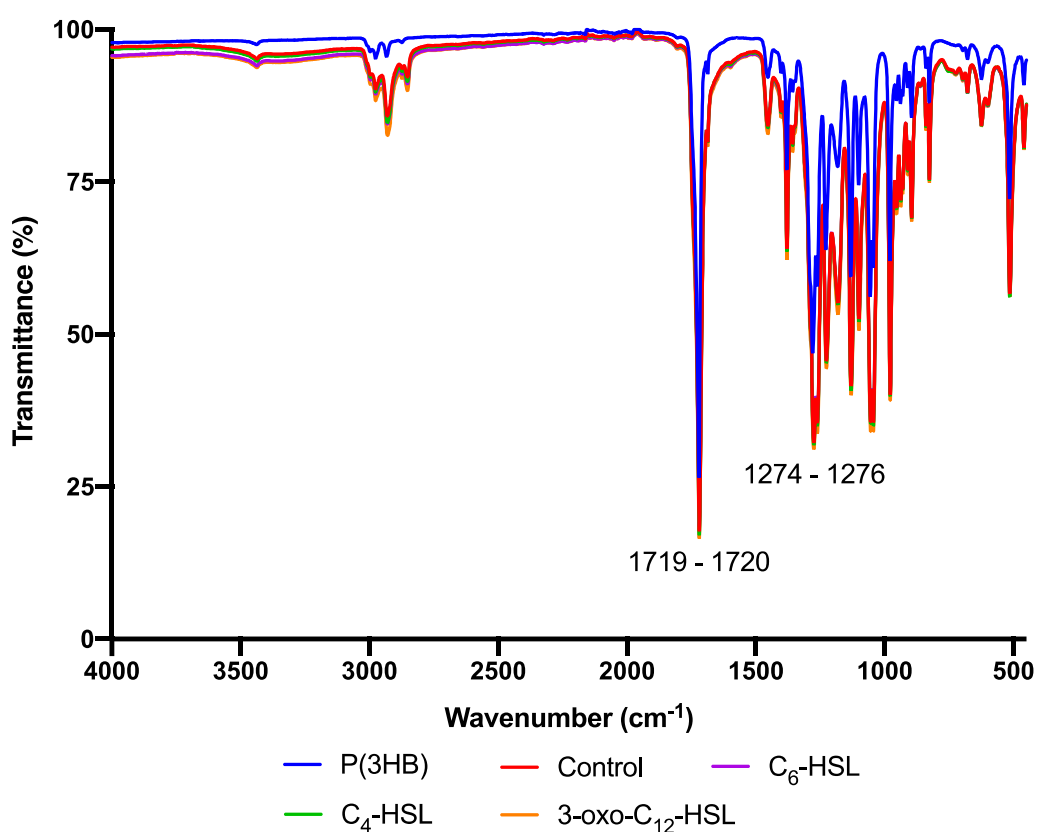


**Figure 3.18** Combined FTIR spectra of SCL PHA produced by *C. necator* H16 grown within bioreactors and in the presence of different quorum sensing molecules. The graph also includes the spectrum of a commercial standard P(3HB).

FTIR analysis of the isolated PHAs revealed absorption bands at 1719 – 1720  $\text{cm}^{-1}$  and 1274 – 1276  $\text{cm}^{-1}$  corresponding to the stretching of the ester carbonyl group (C=O) and the -CH group respectively, and are characteristically present in P(3HB), an SCL PHA (Sindhu *et al.*, 2011) (**Figure 3.18**). These absorption bands were also found to be present in PHAs

produced via shaken flask fermentation, which indicates that both PHAs produced by either mode of fermentation strategy are structurally similar. The PHA samples extracted were also compared against a commercial standard of P(3HB) spectrum, which also produced the same absorption bands as the polymers produced and no major differences were observed. In turn this confirmed the chemical structures of the PHAs produced to be that of SCL PHAs.

#### 3.4.1.2 GC-MS

For monomeric characterisation of the polymer produced in bioreactors, GC-MS was carried out. Prior to this analysis the sample of PHA produced was made to undergo the process of methanolysis, resulting in the production of methyl esters as described in **Section 2.7.5**. A representative TIC of PHA produced by *C. necator* H16 when in the presence of different quorum sensing molecules is shown in **Figure 3.19**, in which two peaks of interest were generated.

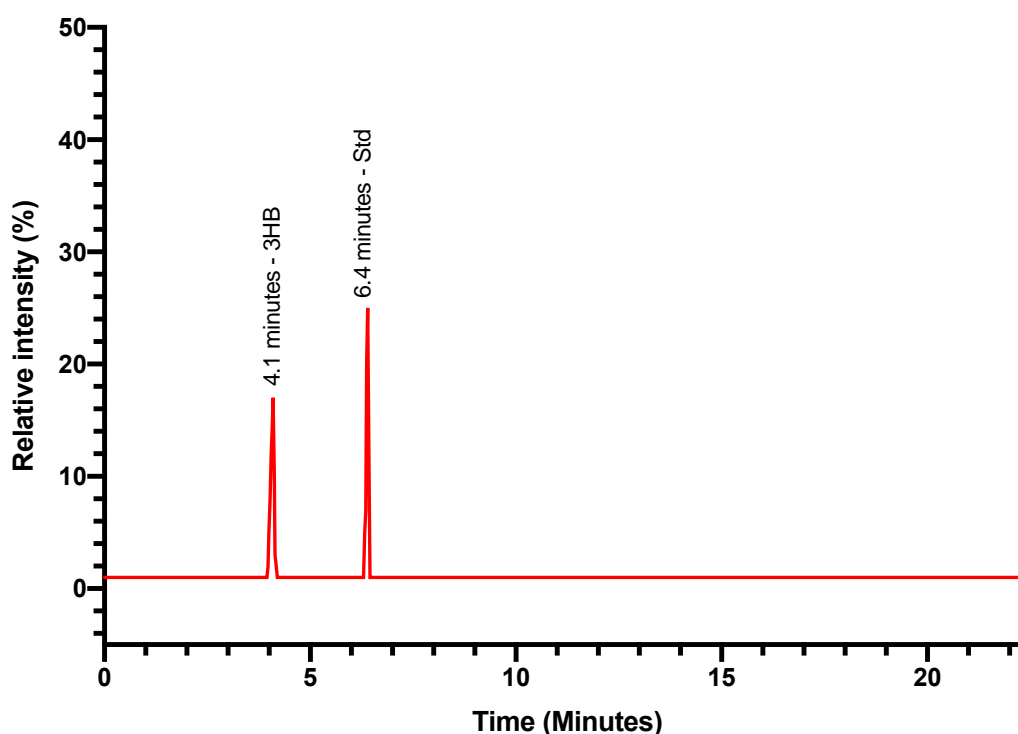


**Figure 3.19** Representative GC-MS analysis of the polymer produced when *C. necator* H16 was grown in bioreactors. The TIC above displays the methanolysis products of the PHAs produced when grown in the absence of

quorum sensing molecules. Methyl Benzoate was used as an internal standard.

The two peaks that were produced from the methanolysis products of the isolated PHA had  $R_t$  of 4.1 minutes and 6.4 minutes. Of the two peaks, the one with a  $R_t$  of 6.4 was identified to be the internal standard added, methyl benzoate. The mass spectrum of the peak with a  $R_t$  of 4.1 minutes was found to be comparable with the mass spectrum of the methyl ester of 3HB in the mass spectrum library obtained from the NIST (**Figure 3.20**). The fragmentation pattern of 3HB showed two significant peaks, which are described in **Section 3.3.1.4**.

As the methyl ester of 3HB was the only peak observed in the TIC produced across all samples of PHA produced by *C. necator* H16 in bioreactors and when grown in the presence of different quorum sensing molecules, it was concluded that a homopolymer of P(3HB) was produced. A summary of the monomeric composition of the PHA produced and the structure of the methyl ester 3HB is displayed in **Table 3.12** and **Figure 3.20** respectively.

**Table 3.12** PHA monomer composition of SCL PHAs synthesised by *C. necator* H16 when grown in bioreactors in the presence of different exogenous quorum sensing molecules.

Quorum sensing molecules	Monomeric composition of PHAs (Mol %) 3HB
Control	100
C <sub>4</sub> -HSL	100
C <sub>6</sub> -HSL	100
3-oxo-C <sub>12</sub> -HSL	100

## 3.5 Molecular biology

### 3.5.1 PCR for the confirmation of *Pha* genes in *C. necator* H16

To begin the analysis of *Pha* genes expression, PCR was first carried out to confirm the presence of GOIs within the genome itself. Primers used for this experiment can be found in **Table 2.14**, which were found in literature. These primers were applied to the primer designing tool – NCBI Primer BLAST, to check the specificity of the primers selected for this study. All samples were

able to react positively during the PCR process, therefore confirming the presence of the GOIs within the genome. The PCR resulted in two main fragments being produced with amplicon sizes of ~496 bp and ~388, respective to *PhaC* and *PhaZ* genes, which were consistent with the descriptions given by York *et al.*, (2003).

### **3.5.2 qPCR for the measurement of the expression levels of *Pha* genes in *C. necator* H16**

Following the confirmation that the GOIs (*PhaC1* and *PhaZ*) were present within the genome, the next step was to analyse the expression of the GOIs when supplemented with exogenous quorum sensing molecules over a 72 hour period. Cultures of *C. necator* H16 grown in 2 L bioreactors with production medium that was supplemented with different quorum sensing molecules at a final concentration of 10  $\mu$ M. Samples were taken every 24 hours, which were subsequently extracted for RNA as explained in **Section 2.8.4**. The results for this experiment are displayed below in **Figure 3.20**.

As previously mentioned, two *Pha* genes (*PhaC1* and *PhaZ*) were measured for the level of expression when exposed to different exogenous quorum sensing molecules. The *PhaC1* gene showed an increased level of expression when exposed to all three different quorum sensing molecules. The greatest increase in expression of the gene was observed at 24 hours when the culture was grown with the supplementation of 3-oxo-C<sub>12</sub>-HSL (**Figure 3.20A**). This finding was consistent amongst all the quorum sensing molecules supplemented, as they all resulted in the highest level of expression of *PhaC1* at 24 hours. Similarly, the expression of the *PhaZ* gene also displayed an increase when exposed to the supplementation of exogenous quorum sensing molecules. All three quorum sensing molecules showed similar expression patterns of *PhaZ*, increasing as the fermentation progressed and displaying the highest level of expression at 72 hours (**Figure 3.20B**). Throughout the fermentation, C<sub>6</sub>-HSL displayed the smallest increase in expression of this particular gene, when compared against C<sub>4</sub>-HSL and 3-oxo-C<sub>12</sub>-HSL.

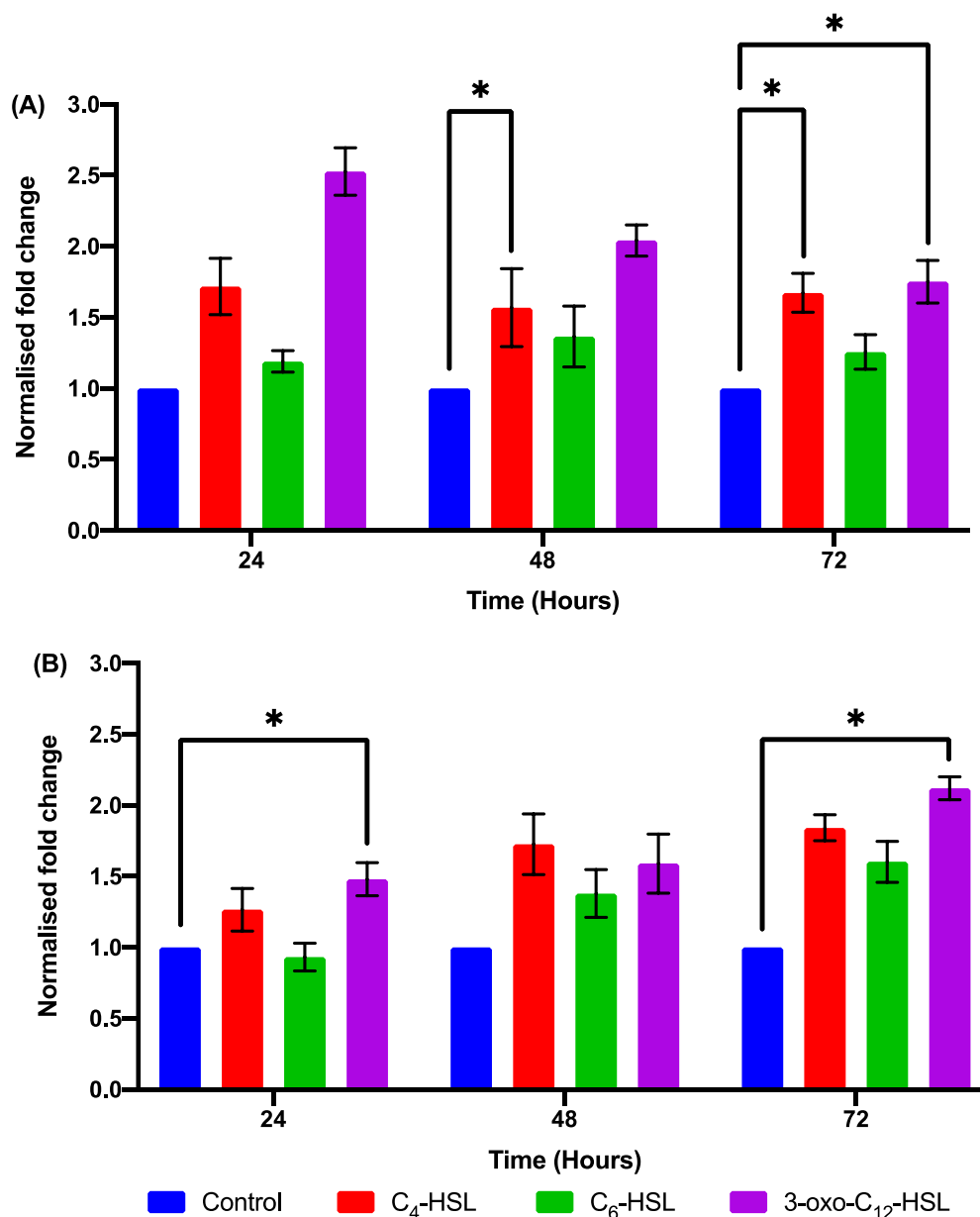


**Figure 3.20** Normalised fold change expression of **(A) *PhaC*** and **(B) *PhaZ*** in *C. necator* H16 when grown with the addition of different exogenous quorum sensing molecules, compared with an untreated control (grown without the addition of exogenous quorum sensing molecules). *C. necator* H16 cells were sampled over a 72 hour period from a 2 L bioreactor in batch mode fermentation. Results are expressed as mean fold change (control being standardised to 1.0) with error bars representing SD (n = 9). Data was analysed using a two-way ANOVA with *post hoc*. Tukey's multiple comparisons test (\* $p < 0.05$ ).

## 3.6 Discussion

### 3.6.1 Growth profile analysis

*C. necator* H16 is a gram-negative Knallgas bacterium, known for its ability to accumulate some of the highest levels of PHA (% DCW) of around 90% (Spiekermann *et al.*, 1999). Although, the effects of supplementing *C. necator* H16 with exogenous quorum sensing molecules on the production of PHAs has yet to be reported on in literature. As a result, the focus of this study to was to develop an understanding as to what the effects of exogenous quorum sensing molecules are on the production of PHAs by cultures of *C. necator* H16. This focus was established with the aim of possibility of reducing the cost of production and increasing their PHA yields, which reduces their main barriers to market. This study chose to supply cultures of *C. necator* H16 with three different quorum sensing molecules (C<sub>4</sub>-HSL, C<sub>6</sub>-HSL and 3-oxo-C<sub>12</sub>-HSL) within a specific production medium that promotes the production of PHAs. They were added at two different concentrations (2 µM and 10 µM) to best optimise fermentations. The fermentations first took place at shake flask level with the addition of exogenous quorum sensing molecules at two different concentrations, and results analysed for a change in PHA production. The concentration that had the greatest impact on the production of PHAs was then added to fermentations at a bioreactor level, to further optimise the yield of the PHA produced. The results of these studies are discussed below.

**Figure 3.1 – 3.5** display the growth profiles of *C. necator* H16 cultures that were grown in shake flasks. The maximum amount of DCW accumulate was at 72 hours, in which 10.83 g/L of DCW was accumulated by the culture that was supplemented with C<sub>4</sub>-HSL (**Figure 3.3**), whereas in contrast the lowest amount of DCW accumulated was by the culture supplemented with C<sub>6</sub>-HSL (**Figure 3.4**), producing 10.52 g/L of cellular mass. Cultures such as the untreated control, and cultures supplemented with DMSO and 3-oxo-C<sub>12</sub>-HSL produced 10.56, 10.66 and 10.70 g/L respectively of DCW. As previously mention, supplementing cultures with exogenous quorum sensing molecules and studying the effects on the production of their secondary metabolites such

as PHA production has yet to be explored. In theory, the addition of quorum sensing molecules should stimulate the production of secondary metabolites, amongst other changes in cellular functions such as the production of virulence factors or cellular densities. However, when comparing all five cultures grown at a shake flask level, statistically there was no significant difference in the amount of DCW accumulated between each culture. This meant the addition of the exogenous quorum sensing molecules did not hinder the growth of the culture itself, but it also did not promote growth, which could have come in the form of increasing cellular densities.

Unfortunately, when comparing the DCW obtained from cultures of *C. necator* H16 grown in shake flask, to other studies, the DCW was considerably lower. For example, Ertan, Keskinler and Tannriseven, (2021) were able to obtain DCW of up to 6.00 g/L within the first 24 hours of fermentation using 20 g/L of fructose as the sole carbon source. In comparison, this study was only able to produce a maximum DCW of 5.16 g/L when supplementing the culture with DMSO. However, the study mentioned previously carried out a series of experiments which increased the amount of carbon source added to the culture and the effects on the DCW. As fructose concentration increased DCW decreased considerably, decreasing from 6.00 g/L to 4.5 g/L when supplemented with 40 g/L of fructose. It was observed that as fructose concentration increased the amount of DCW decreased, which was in alignment with other studies.

Throughout this study 20 g/L of fructose was used as the carbon source in the MSM medium for the production of PHAs in batch mode fermentation from *C. necator* H16. This amount was specifically selected based off the findings of Nygaard, Yashchuk and Hermida, (2019) who were able to demonstrate that the specific growth rate of the culture significantly lowers once carbon concentration breaches 20 g/L, which in turn would have a negative impact on the production of PHAs.

When comparing the PHA yields (% DCW) of the cultures supplemented with exogenous quorum sensing molecules against the untreated control, it can be

noted that 3-oxo-C<sub>12</sub>-HSL had the greatest effect on the amount of PHA accumulated. The greatest increase was observed within the first 24 hours of fermentation, in which PHA yield (% DCW) increased by 13.03%. **Figure 3.6** displays the percentage change in amount of PHA produced by cultures that were supplemented with exogenous quorum sensing molecules. As previously stated, the greatest increase was noted in the shake flask supplemented with 3-oxo-C<sub>12</sub>-HSL when compared against the untreated control at 24 hours of growth. This was followed by C<sub>4</sub>-HSL, which increased the amount of PHA produced by 4.36%. The smallest change was observed through the addition of DMSO, which increased the amount of PHA by 1.17%. When adding DMSO to the cultures it consistently produced the lowest increase in PHA. DMSO was added to act as a negative control and to gain an understanding as to if there was a change in production, it was in relation to the addition of exogenous quorum sensing molecules as opposed to the addition of the DMSO itself. Interestingly, all the cultures accumulated similar amounts of PHAs regardless of the fact if they were supplemented with exogenous quorum sensing molecules, however, an increase in the actual amount of PHA was observed from cultures that did contain exogenous quorum sensing molecules.

An example of this can be seen when comparing the untreated control shake flask to the flask supplemented with the quorum sensing molecules C<sub>4</sub>-HSL at 24 hours of growth. The untreated control was able to produce 46.65% PHA (% DCW) which was equivalent to 3.24 g/L in comparison to the flask supplemented with C<sub>4</sub>-HSL, which accumulated 48.26% (% DCW), which was equal to 3.37 g/L of PHA. This shows that although cultures supplemented with exogenous quorum sensing molecules produced similar amounts of PHA (% DCW), the actual amount of PHA produced was significantly higher. **Table 3.13** displays the kinetic growth parameters of the cultures grown in shake flasks. When comparing the untreated control against 3-oxo-C<sub>12</sub>-HSL, it can be observed, that the culture supplemented with yielded more biomass 3-oxo-C<sub>12</sub>-HSL yielded higher amounts of biomass than the control as well as a higher amount of product too. However, at shake flasks level the control was able to yield the highest amount of product per biomass produced with a value of 1.105. This would indicate that when all three quorum sensing molecules were

added to cultures, those cultures were able to produce more substrate into biomass, however only 3-oxo-C<sub>12</sub>-HSL was the only culture to be able to produce more product from substrate consumed than the untreated control.

Ertan, Keskinler and Tanriseven, (2021) carried out a study which used *C. necator* ATCC 25207 grown on hydrolysed molasses. It was found that the amount of biomass yielded in this study was similar to the biomass yielded carried out by Ertan, Keskinler and Tanriseven, (2021). They were able to obtain a maximum value of 0.440 g/g, whereas in study a value of 0.461 g/g was obtained in the culture supplemented with 3-oxo-C<sub>12</sub>-HSL. However, in this study specific productivity was often higher than the values produced in the study previously mentioned.

**Table 3.13** PHA productions of *C. necator* H16 in batch mode fermentation using 1 L shake flasks containing production media with the addition of exogenous quorum sensing molecules at a concentration of 10 µM. Productions were calculated using data of samples collected at 24 and 48 hours.

Quorum sensing molecules	$Y_X (\text{g/g})$ $\bar{S}$	$Y_P (\text{g/g})$ $\bar{S}$	$Y_P (\text{g/g})$ $\bar{X}$	$Q_p (\text{g/L.H})$ ( $\times 10^3$ )
Control	0.373	0.412	1.105	15.664
DMSO	0.560	0.301	0.539	12.943
C <sub>4</sub> -HSL	0.444	0.367	0.827	17.299
C <sub>6</sub> -HSL	0.593	0.405	0.682	15.103
3-oxo-C <sub>12</sub> -HSL	0.625	0.461	0.738	19.541

**Figures 3.13 – 3.16** display the growth profiles of cultures grown in bioreactors. Through these modes of fermentations (shake flasks and bioreactors) PHA yield (% DCW) accumulated the most towards the end of the fermentation at 72 hours. PHA yield gradually increased throughout the entire run, which could indicate that there were sufficient levels of carbon substrate for the cultures to continuously grow and accumulate PHAs. If the cultures were in nutrient limiting conditions, such as low levels of carbon, then a decrease in PHA would have been observed at some point during the fermentation. However, this was not the case. By supplying enough carbon into the bioreactor, cultures were unlikely to break down the accumulated PHA, which in turn would reduce the overall yield.

When comparing the PHA yields (% DCW) of cultures at bioreactor level in comparison to that of shake flask level, it can be observed that cultures containing exogenous quorum sensing molecules were able to increase the accumulation of PHAs the greatest 24 hours of fermentation. This could in response to nutrient limiting conditions being achieved within the first 24 hours of fermentation as well as surplus of carbon, which promotes the production of PHAs.

Throughout this study, batch mode fermentation was used for the growth of cultures and by extension production of PHAs. However, this mode of fermentation may have hindered the growth and amount of PHA produced by the culture. As previously mentioned in **section 1.2.5.2**, batch mode fermentation is the easiest mode of fermentation to carry out, however there is one main drawback. Batch mode fermentation is associated with prolonged lag periods. A period in which no or very little growth occurs as the culture itself adapts to the new environment within the bioreactor. To help mitigate this extended lag period, the cultures were grown in the specific production medium in shake flasks first before being inoculated into the bioreactor, which also contained the same medium. However, using different fermentation strategies may have resulted in all round better yields of PHA.

For example, Santolin *et al.*, (2021) were able to demonstrate increased PHA yields (%DCW) when growing *C. necator* Re2058/pCB113 using a two-stage fed batch fermentation strategy with fructose as the main carbon source, in comparison to the batch mode fermentation method used in this study. Santolin *et al.*, (2021) were able to achieve PHA yields (%DCW) of up to a maximum of 80.12% at 72 hours of fermentation growth in comparison to a maximum of 60.12% PHA yield (% DCW) at the same timepoint, with the supplementation of 3-oxo-C<sub>12</sub>-HSL. The reason for an increase in PHA yield (% DCW) observed by Santolin *et al.*, (2021) is most likely to do the continuous replenishment of nutrients such as carbon sources, which are unable to fall below the optimum level allowing for continuous growth and in turn production of PHAs. The optimisation of fermentation carried out in the study by Santolin

*et al.*, (2021) illustrates as to how the specific mode of fermentation can greatly have an impact on the productivity and yield of PHA produced. Therefore, it could be suggested that results could potentially be further improved upon by using different modes of fermentation such as fed-batch mode.

**Table 3.14** explores the kinetic growth profiles of each bioreactor supplemented with the addition of exogenous quorum sensing molecules. As can be observed from the table below, C<sub>6</sub>-HSL produces the highest biomass yielded per substrate consumed with a value of 1.177 g/g. In turn this result means that C<sub>6</sub>-HSL was the most efficient quorum sensing molecule to promote the production of biomass from substrate consumed when compared to the other exogenous quorum sensing molecules. However, C<sub>6</sub>-HSL produced the lowest product yielded per substrate consumed value of 0.592, meaning cultures that were supplemented with C<sub>6</sub>-HSL, most likely priorities the production of biomass and cellular growth as opposed to production, which in this case was PHAs. This is true as not only did C<sub>6</sub>-HSL produce a total biomass of 11.09 g/L DCW at 48 hours, but it also produced the least amount of product in the form of PHAs, with only 4.53 g/L being produced, in comparison to C<sub>4</sub>-HSL and 3-oxo-C<sub>12</sub>-HSL, which produced 4.65 and 4.98 g/L respectively.

**Table 3.14** PHA productions of *C. necator* H16 in batch mode fermentation using 2 L bioreactors containing production media with the addition of exogenous quorum sensing molecules at a concentration of 10 µM. Productions were calculated using data of samples collected at 24 and 48 hours.

Quorum sensing molecules	$Y_{\frac{X}{S}}$ (g/g)	$Y_{\frac{P}{S}}$ (g/g)	$Y_{\frac{P}{X}}$ (g/g)	$Q_p$ (g/L.H) ( $\times 10^3$ )
Control	0.532	0.603	1.133	13.542
C <sub>4</sub> -HSL	1.060	0.628	0.592	13.536
C <sub>6</sub> -HSL	1.177	0.574	0.488	11.812
3-oxo-C <sub>12</sub> -HSL	0.760	0.706	0.934	17.050

Interestingly, when comparing product produced per unit of biomass, the control bioreactor was able to produce the highest value, which meant that the ratio between product and biomass was the highest in this particular bioreactor, even though it did not produce the most PHA as product. This can

be compared again 3-oxo-C<sub>12</sub>-HSL, which produced a product produced per unit of biomass value of 0.934 g/g. Although this value is lower, the culture supplemented with the exogenous quorum sensing molecule was able to produce 4.98 g/L of PHA in comparison to the control (untreated) bioreactor, which produced 4.40 g/L of PHA. However, 3-oxo-C<sub>12</sub>-HSL produced the highest specific growth rate value out of all the bioreactors assessed. This specific production rate was in line with previous studies carried out by Ertan, Keskinler and Tanriseven, (2021).

Ultimately, it could be concluded that the most effective agent at increasing the production of PHAs was 3-oxo-C<sub>12</sub>-HSL, as it increased the amount of PHA yielded by a maximum of 13.03% and 17.85% at shaken flask and bioreactor level respectively.

### **3.6.2 Characterisation and identification of SCL PHAs produced by *C. necator* H16**

Four different experiments were selected for the purposes of being able to accurately characterise and identify the type of PHA produced by *C. necator* H16 when from in shake flasks and bioreactors. The first two experiments (Sudan Black B and Nile red staining) ran simultaneously whilst the fermentations of cultures were ongoing, which provided a rapid assessment of whether PHAs were being produced in the cultures being grown. This also allowed for any modifications to be made to the experimental design. Once PHAs were confirmed to be harboured within the culture, they were extracted and purified, before being analysed through FTIR and GC-MS. These two experiments were carried out in order to specifically characterise the type of PHA being produced by the culture. The order in which these experiments was important as each result built upon the results of the last. Therefore, as the results from each experiment was produced, more information about the PHA produced by the culture became available.

The first of the characterisation experiments was to stain cultures of *C. necator* H16 with Sudan Black B dye as shown in **Figure 3.7**. This was used for the

identification of inclusion bodies. Each sample tested ultimately was able to provide a positive result meaning that each culture was successfully able to produce and accumulate PHAs, irrespective of the presences of exogenous quorum sensing molecules.

To follow up on this finding Nile red was then used to for the visualisation of intracellular PHAs. **Figure 3.8** illustrates the ability of *C. necator* H16 cultures to grow and accumulate PHAs in the presence of different quorum sensing molecules. Cells that successfully were able to accumulate PHAs appeared a bright red colour, which allowed for their visualisation. At this point it was confirmed the cultures were producing PHAs even in the presence of exogenous quorum sensing molecules and were extracted for characterisation examinations.

Initially FTIR was carried out, on both PHA samples extracted from either shake flask or bioreactor level. Spectra that were produced were compared against a commercial control sample which revealed the identification of absorption bands within the range of 1719 – 1720  $\text{cm}^{-1}$  and 1274 – 1276  $\text{cm}^{-1}$  these two particular bands corresponded to the stretching of the ester carbonyl group (C=O) and the -CH group respectively, and are characteristically present in P(3HB), an SCL PHA (Sindhu *et al.*, 2011). The presence of these two bands alone were able to confirm that the type of PHA being produced at either mode of fermentation was that of SCL PHA. However, when compared against the commercial standard, samples produced were almost identical, which ultimately reinforced the final finding that an SCL PHA was produced. When comparing the FTIR spectra of the PHA samples obtained, differences in peak intensities can be observed. These differences can be as a result of different clamping forces from differing sample geometries and/or inhomogeneities. The intensities of the peaks can also differ because of the sample's degree of crystallinity. Samples with higher degrees of crystallinity generally relates to greater absorbances, however when comparing the spectra produced across all samples, a similar number of bands containing speaks appear in similar locations (Vizcaino-Caston *et al.*, 2016).

To specifically find out what type of PHA was produced on a monomeric composition, GC-MS was employed. It was concluded that the type of SCL PHA produced was that of P(3HB). This PHA was produced regardless of the mode of fermentation employed, but most importantly, irrespective of the exogenous quorum sensing molecules. *C. necator* H16 is known for its ability to produce P(3HB)s, however, it also possess the ability to produce the copolymer P(3HB-co-3HV), when using propionate as a co-substrate. As reviewed in Byrom (1987 and 1992), the appearance of the monomer 3-hydroxyvalerate (3HV), is due to its structural similarity to the substrate that it is grown on. However, challenges can arise when using propionate as a co-substrate at high concentration as this compound is known to be toxic to the cell, but different fermentation strategies can be employed to decrease the negative impact of the propionate toxicity (Steinbüchel *et al.*, 2003).

Alternative substrates have been discovered to produce 3HV monomers such as valerate, levulinic acid and some fatty acids such as heptanoic and nonanoic acids. The molar fraction of the P(3HB-co-3HV) final product will depend on the choice and proportion of the 3HV precursors, along with the cultivation conditions, which will impact directly with the physical properties of the bioplastic. This final note is of importance, as the substrate used to produce PHAs dictates the monomeric composition of the PHA produced. In turn this has an influence on the PHAs properties, which could be tailored for specific niche uses within industries. However, a point to take notice of was that the presence of exogenous quorum sensing molecules, did not have an impact on the monomeric composition of the PHA produced. This meant that exogenous quorum sensing molecules could be added to culture to increase the yield, but monomeric composition would not shift. Once again, based on the **Figures 3.10** and **3.18** and the results above, it can be concluded that the PHA produced was that of (P3HB) within both shake flasks and bioreactors. This result also did not change irrespective of the presence of exogenous quorum sensing molecules or their presence either.

### 3.6.3 Molecular Biology

One of the main goals in this study is to be able to study the effects of quorum sensing molecules on the production of PHAs. IN previous sections it was determined that some exogenous quorum sensing molecules were able to have a positive influence on the production of PHAs, by increasing the cultures yield when supplemented with them. It was also understood that their addition did not affect the composition of the final PHA produced. However, quorum sensing molecules are known to alter gene expression and therefore for a change in production to occur, then a change in the expression of *Pha* Genes must have occurred, this was investigated, by study the expression of two key *Pha* genes, *PhaC* and *PhaZ*. To begin, conventional PCR was carried out to assess the presence of the two genes within the genome. This resulted in two main fragments being produced with amplicon sizes of ~496 bp and ~388, respective to *PhaC* and *PhaZ* genes, which were consistent with the descriptions given by York *et al.*, (2003).

Once the genes were confirmed to have been present, qPCR was carried out to study the expression level of the genes as fold change in comparison to the expression of said genes in the control samples. Throughout the entire fermentation period it was observed that both *PhaC* and *PhaZ*, were increased in their regulation when supplemented with exogenous quorum sensing molecules. However, of these three quorum sensing molecules 3-oxo-C<sub>12</sub>-HSL was able to increase the transcription of *PhaC* the most at 24 hours of fermentation. Expression of *PhaC* increased by 2.53-fold in comparison to the control sample, which is responsible for the transcription for PHA synthase. An increase transcription in this particular gene would result in the increased production of PHAs, which was what was observed when cultured were supplemented with exogenous quorum sensing molecules. Although this increase was only found to be statistically significant at 72 hours of fermentation.

Alternatively, when studying the expression of *PhaZ*, it was observed that its transcription also had increased, but to a lesser extent. For example, as

previously mentioned *PhaC* increased transcription at 24 hours by 2.53-fold when supplemented with 3-oxo-C<sub>12</sub>-HSL, in comparison *PhaZ*'s transcription was only increased by 1.48-fold, which was less than the previous gene. *PhaZ* is known to transcribe the enzyme PHA depolymerase, which has the ability to break down PHAs to its constituent monomers, when facing specific nutrient limiting conditions such as the shortage of carbon, as PHA itself is a carbon reservoir for the cell. Interestingly, when comparing the expression of *PhaC* and *PhaZ* at 72 hours of fermentation it can be observed that transcription of these particular genes is increased to 1.75-fold and 2.12-fold, respectively. This would indicate that this point PHAs are more likely to be broken down as opposed to produced due to the increased transcription of PHA depolymerase. This was in alignment with the PHA yield in bioreactors when supplemented with exogenous quorum sensing molecules. For example, PHA yield (% DCW) of the culture supplied with 3-oxo-C<sub>12</sub>-HSL at 48 hours was reported to be 33.4%, this value decreased to 29.84% within the next 24 hours at 72 hours of fermentation. This decrease in production could be explained by the increased transcription of *PhaZ* in comparison to PHA synthase, as the level of transcription of PHA depolymerase was higher than that of PHA synthase. Therefore, the rate of PHA breakdown was greater than that of the rate of PHA synthesis, which resulted in an overall decrease in the production of PHAs.

However, to note at shaken flask level PHA yield (% DCW) continued to increase throughout the entire run of the fermentation, with cultures accumulating the most PHAs at the end of the fermentation period. This could suggest at shaken flask level the transcription of *PhaC* is higher than that of *PhaZ*, thus the increased production at 72 hours, in comparison to bioreactors. Ultimately it was concluded that 3-oxo-C<sub>12</sub>-HSL was the most effective agent at being able to increase the production of PHAs. This conclusion was drawn because the supplementation of 3-oxo-C<sub>12</sub>-HSL was able to increase the transcription of *PhaC* (PHA synthase) responsible for the production of PHAs, which resulted in the highest levels of PHAs being accumulated (% DCW) with its addition. This was observed at two different levels. At shake flask level PHA increased by a 13.03% at 24 hours of fermentation, whereas at bioreactor level, PHA yield (% DCW) increased by 17.85% at the same time period.

**Chapter 4:** MCL PHA production by *P. putida* KT2440

## 4.1 Introduction

Polyhydroxyalkanoates are an emerging group of biomaterials, which can be an alternative to the traditional, petroleum-based plastics. PHAs are produced by a wide variety of bacterial species usually under nutrient limiting conditions with excess of carbon source. SCL PHAs have been produced and characterised as described in **Chapter 3**. The second type of PHAs is medium chain length Polyhydroxyalkanoates (MCL PHAs), which contain from 6 to 14 carbon atoms within the monomer unit (Oliveira *et al.*, 2007). This group of PHAs have different material properties in comparison to SCL PHAs. MCL PHAs are very elastomeric, have low crystallinity, low melting temperature and glass transition temperature (Rai *et al.*, 2011). The drawback of mcl-PHAs is their low Young's modulus and tensile strength values, therefore, they cannot be used in load bearing applications. Among MCL PHAs are commonly represented by 3-hydroxyhexanoate (3HHx), which has 6 carbon atoms within the monomer unit, 3-hydroxyheptanoate (3HHp) with 7 carbon atoms, 3-hydroxyoctanoate (3HO), containing 8 atoms, 3-hydroxydecanoate (3HD), containing 10 carbon atoms and 3-hydroxydodecanoate, with 12 carbon atoms within the monomer unit (Basnett *et al.*, 2017). Within MCL PHA group, a lot of different types of copolymers have been produced, such as poly(3-hydroxyhexanoate-co-3-hydroxyoctanoate) P(3HHx-3HO), poly(3-hydroxyoctanoate-co-3-hydroxydecanoate) P(3HO-3HD) and poly(3-hydroxyoctanoate-co-3-hydroxydecanoate-co-3-hydroxydodecanoate) P(3HO-3HD-3HDD) (Anderson and Dawes, 1990). MCL PHAs can be produced by different types of *Pseudomonas* sp., such as *P. aeruginosa*, *P. putida*, *P. oleovorans*, *P. mendocina*, *P. ragenesii*, *P. guezenei* and *P. stutzeri* (Simon-Collin, 2009; Simon-Collin, 2012).

## 4.2 PHA production by *P. putida* KT2440 in shake flasks with the addition of exogenous quorum sensing molecules at 2 $\mu$ M concentration

Investigations of PHA production from *P. putida* KT2440 with the supplementation of different exogenous quorum sensing molecules was first carried out at shake flask level at a final concentration of 2  $\mu$ M. This was

necessary to gain an understand as to if the quorum sensing molecules had any effect on the production of PHAs as well as to gather information for the scaling up process. This also acted as a form of optimisation, by comparing the change in production of PHAs when exogenous quorum sensing molecules were supplied at two different concentrations. The process as to how the shake flasks were set up can is explained in **Section 2.4.3**. The fermentation was allowed to progress for a maximum of 72 hours.

**Table 4.1** below displays the results obtained from shake flasks that were supplemented with exogenous quorum sensing molecules with a final concentration of 2  $\mu\text{M}$ .

**Table 4.1** Summary of key growth parameters in relation to PHA production of *P. putida* KT2440 grown in 1 L shake flasks (batch mode fermentation) containing production media and exogenous quorum sensing molecules with a final concentration of 2  $\mu\text{M}$ . Results shown are from samples collected 48 hours post inoculation and expressed as means with  $\pm$  SD values ( $n = 9$ ).

Quorum sensing molecules	DCW (g/L)	PHA (g/L)	PHA yield (% DCW)	% change of PHA
Control	2.00	0.456	22.79	-
DMSO	2.05	0.456	22.22	-
C <sub>4</sub> -HSL	1.98	0.458	23.13	0.44 $\pm$ 0.16
C <sub>6</sub> -HSL	1.96	0.456	23.27	-
3-oxo-C <sub>12</sub> -HSL	2.10	0.459	21.89	0.66 $\pm$ 0.15

#### 4.3 PHA production by *P. putida* KT2440 in shake flasks with the addition of exogenous quorum sensing molecules at 10 $\mu\text{M}$ concentration

The concentration of exogenous quorum sensing molecule was then increased to assess whether or not the concentration had an impact on the change of PHA produced by *P. putida* KT2440. Experiments for this study were set up identically to the previous experiments (**Section 2.4.3**), but with the final concentration increased to 10  $\mu\text{M}$ .

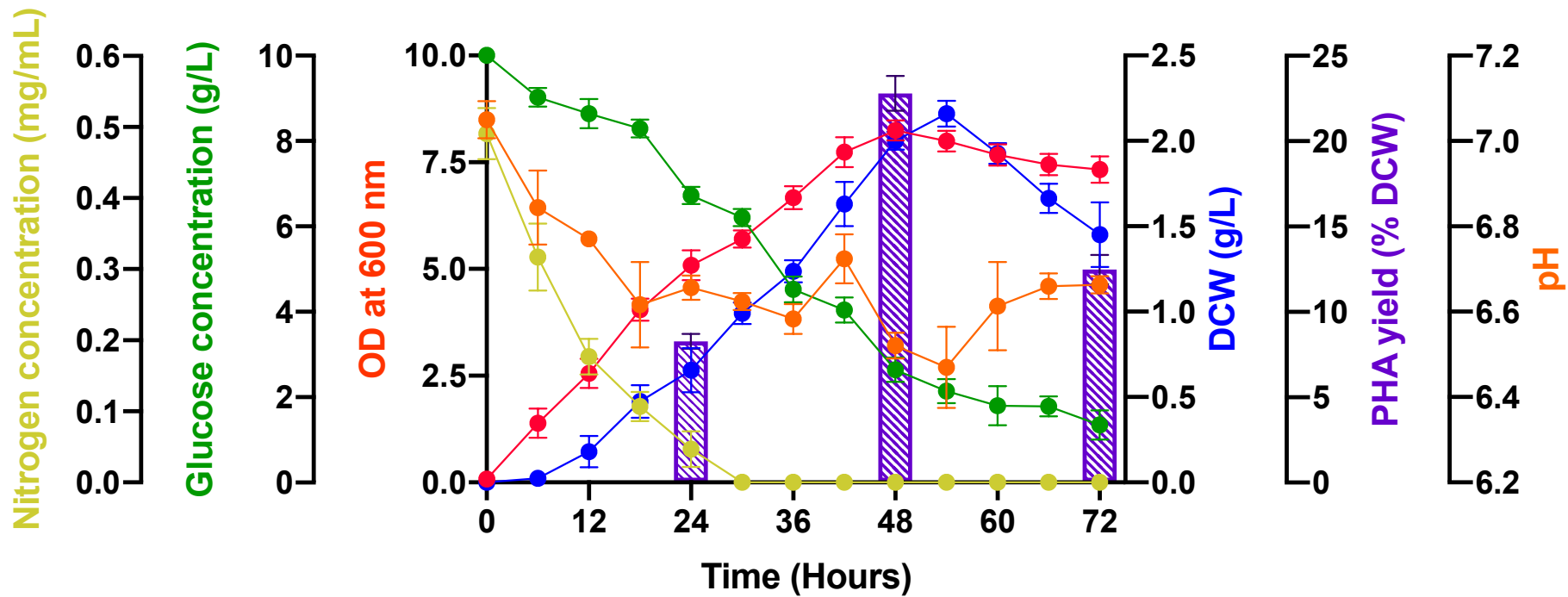


**Figure 4.1** Fermentation profile of *P. putida* KT2440 grown in 1 L shake flasks over a 72 hour period without the addition of exogenous quorum sensing molecules (control). Samples were taken every 6 hours throughout the fermentation run, which was run in batch mode fermentation. E2 medium was used as the production medium, containing glucose as the sole carbon source. Error bars represent  $\pm$  SD values (n = 9).

**Figure 4.1** illustrates the growth profile of the results obtained from the control shake flasks used to grow *P. putida* KT2440 without the addition of exogenous quorum sensing molecules. A steady increase in cellular growth can be observed up until 48 hours, after which the cells appear to enter the stationary phase of growth as OD stops increase, but over the next 24 hours slowly decreases. DCW appears to follow the same trend of cellular growth, increasing until 52 hours, but then decreasing at an increased rate in comparison to OD. The maximum DCW achieved throughout the fermentation run was achieved at 52 hours, which equated to 2.16 g/L. The maximum amount of PHA accumulated was at 48 hours, where the yield obtained was 22.79% (% DCW). PHA yield subsequently decreased as the fermentation run progressed, falling to 12.47% (% DCW) at 72 hours, a decrease of 45.28%.

The nitrogen concentration within the media decreased immediately, with concentration falling from 0.49 mg/mL to 0.32 mg/mL within the first 6 hours of the fermentation run. This decrease in nitrogen concentration continued until 30 hours, where from this point onwards nitrogen concentration fell to 0.0 mg/mL. Concentration of glucose began at 10.0 g/L and steadily decreased throughout the fermentation run. The greatest decrease in glucose concentration was observed between time points 30 and 36, where glucose fell by 1.68 g/L. The pH of the culture initially began to decrease steadily for the first 36 hours of the run, decreasing to pH 6.62. From this point onwards the pH of the culture appears to increase slightly before decreasing and increasing again. By the end of the fermentation run pH had reached 6.66.

**Table 4.2** details the kinetic growth parameters of the culture grown without the presence of exogenous quorum sensing molecules (control).

**Table 4.2** Kinetic growth parameters of *P. putida* KT2440 grown in 1 L shake flasks, batch mode fermentation without the addition of exogenous quorum sensing molecules. Data from time points 24 and 48 hours were used to calculate the following parameters.

$Y_{\bar{X}} (g/g)$	$Y_{\bar{P}} (g/g)$	$Y_{\bar{P}} (g/g)$	$Q_p (g/L.H) (\times 10^3)$
0.329	0.098	0.299	12.569

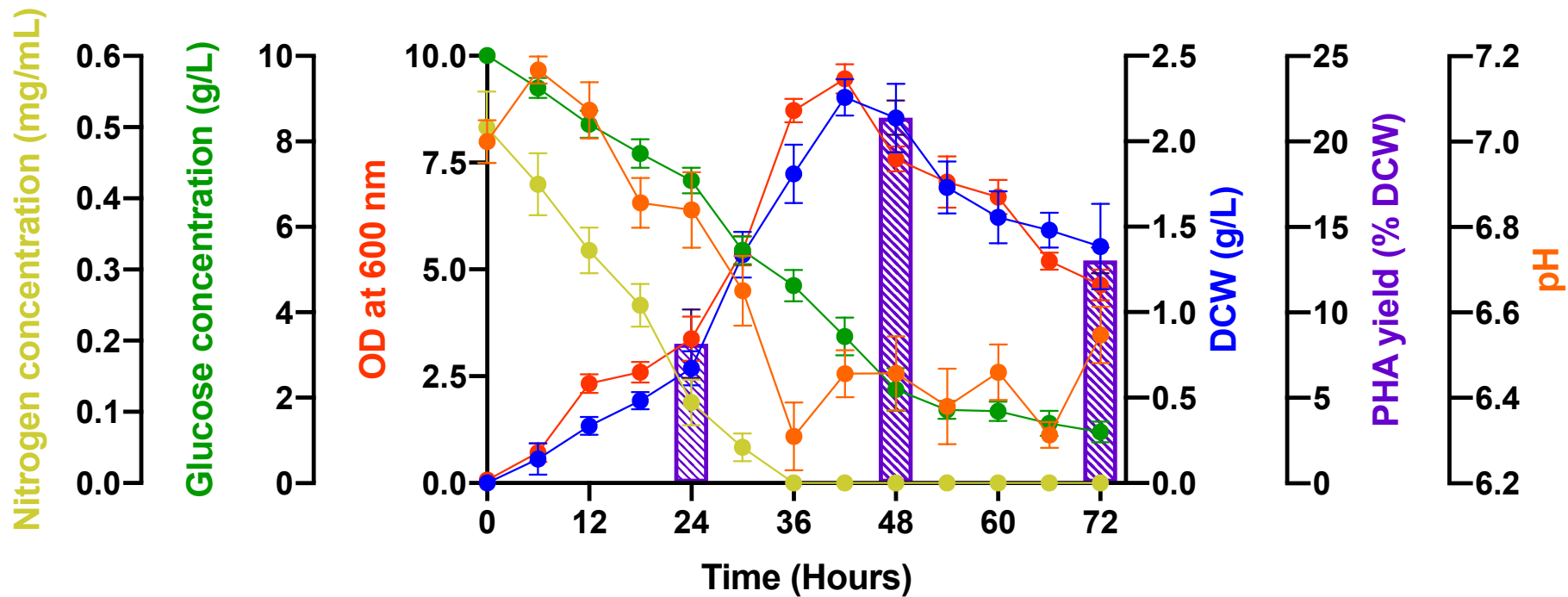


**Figure 4.2** Fermentation profile of *P. putida* KT2440 grown in 1 L shake flasks over a 72 hour period with addition of DMSO at a final concentration of 10  $\mu$ M. Samples were taken every 6 hours throughout the fermentation run, which was run in batch mode fermentation. E2 medium was used as the production medium, containing glucose as the sole carbon source. Error bars represent  $\pm$  SD values (n = 9).

**Figure 4.2** illustrates the growth profile the results produced from cultures grown of *P. putida* KT2440 in the presence of DMSO in shake flasks. A steady increase in OD can be observed up until 42 hours reaching 9.463, before steadily declining till the end of the fermentation period. DCW follows a similar pattern increasing until 42 hours and reaching a maximum DCW at this time of 2.26 g/L, and decreases by 0.88 g/L to a final DCW of 1.38 g/L by 72 hours. The maximum amount of PHA that was accumulated was observed at 48 hours, where the culture was able to accumulate 21.39% of DCW at that point during the fermentation, which is equivalent to 0.46 g/L of PHA. PHA yield decreases from this point onwards, falling to 13.04% (% DCW).

Nitrogen concentration of the culture decreased gradually over the fermentation period until it was no longer detected at 36 hours. This meant from this point onwards the fermentation was growing in nitrogen limiting conditions. Glucose concentration began at 10.0 g/L and steadily declined throughout the entire fermentation run. The biggest decrease in glucose was observed between 24 hours and 30 hours, in which 1.63 g/L of glucose was consumed by the culture. The pH of the medium supplied originally began at 7.00, but fluctuated as the fermentation progressed. pH increased slightly for the first 6 hours, before conditions became more acidic as pH decreased reaching a pH of 6.31 at 36 hours of fermentation growth. However, pH then increased and reached a final value of 6.55 by the end of the fermentation period. **Table 4.3** details the kinetic growth parameters of the culture grown with the supplementation of DMSO.

**Table 4.3** Kinetic growth parameters of *P. putida* KT2440 grown in 1 L shake flasks, batch mode fermentation with the addition of DMSO. Data from time points 24 and 48 hours were used to calculate the following parameters.

$\frac{Y_X}{\bar{S}} (g/g)$	$\frac{Y_P}{\bar{S}} (g/g)$	$\frac{Y_P}{\bar{X}} (g/g)$	$Q_p (g/L.H) (\times 10^3)$
0.300	0.082	0.274	11.946

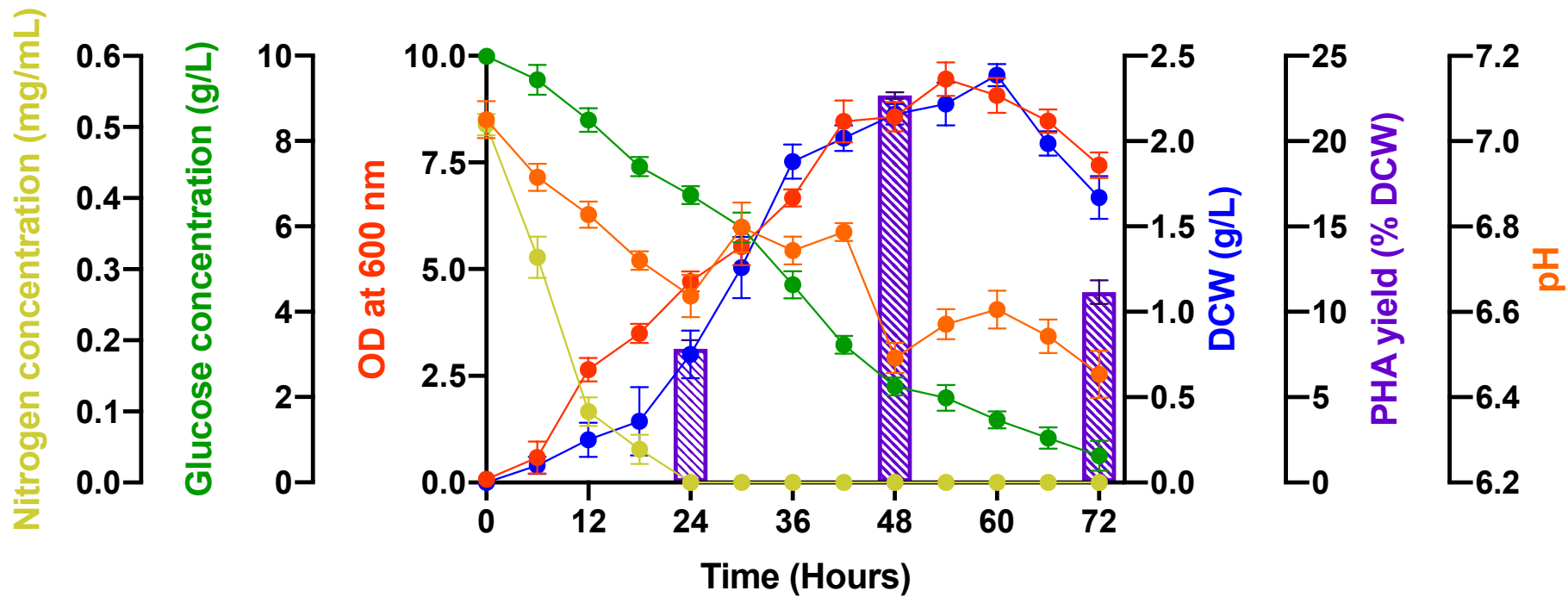


**Figure 4.3** Fermentation profile of *P. putida* KT2440 grown in 1 L shake flasks over a 72 hour period with addition of C<sub>4</sub>-HSL at a final concentration of 10  $\mu$ M. Samples were taken every 6 hours throughout the fermentation run, which was run in batch mode fermentation. E2 medium was used as the production medium, containing glucose as the sole carbon source. Error bars represent  $\pm$  SD values (n = 9).

**Figure 4.3** illustrates the growth profile of the results obtained from shake flasks used to grown *P. putida* KT2440 with the addition of the quorum sensing molecule C<sub>4</sub>-HSL at a final concentration of 10 μM. The first 6 hours of the culture appears to display a slow rate of growth with OD increasing by 0.513 from the point of inoculation. However, from 6 hours onwards, the culture appears to grow steadily increasing until 54 hours where it reaches the peak of its growth as reflected in the highest OD recorded of 9.458. The DCW follows the same pattern of growth as OD, where the first 6 hours show little difference, but after this point, there appears to be a rapid increase in DCW for the next 54 hours, reaching a maximum weight of 2.39 g/L at 60 hours. From this point onwards, DCW decreases, which was also observed with the OD. The least amount of PHA accumulated within the culture was at 24 hours, producing 0.059 g/L of PHA (7.84% (%DCW)). This later increased within the next 24 hours at 48 hours where a PHA yield of 22.67% (% DCW) was achieved.

Nitrogen concentration fell by 0.19 mg/mL within the first 6 hours of growth of the culture, and subsequently kept decreasing until 24 hours at which point there was no nitrogen detected in the media. Glucose concentration steadily decreased throughout the entire run of the fermentation, resulting in 0.63 g/L of glucose remaining at the end of the fermentation period. The biggest decrease in concentration was observed between 36 and 48 hours, in which 1.41 g/L of glucose was consumed by the culture. The culture began at a starting pH of 7.02. This decreased for the next 24 hours falling to pH 6.53, however the pH of the culture fluctuated for the next 18 hours increasing to a maximum of pH 6.72 and falling back to a final pH of 6.31 by the end of the run. **Table 4.4** details the kinetic growth parameters for this culture grown with the addition of exogenous C<sub>4</sub>-HSL molecules.

**Table 4.4** Kinetic growth parameters of *P. putida* KT2440 grown in 1 L shake flasks, batch mode fermentation with the addition of C<sub>4</sub>-HSL. Data from time points 24 and 48 hours were used to calculate the following parameters.

$\frac{Y_X (g/g)}{\bar{s}}$	$\frac{Y_P (g/g)}{\bar{s}}$	$\frac{Y_P (g/g)}{\bar{x}}$	$Q_p (g/L.H) (\times 10^3)$
0.318	0.096	0.303	12.447

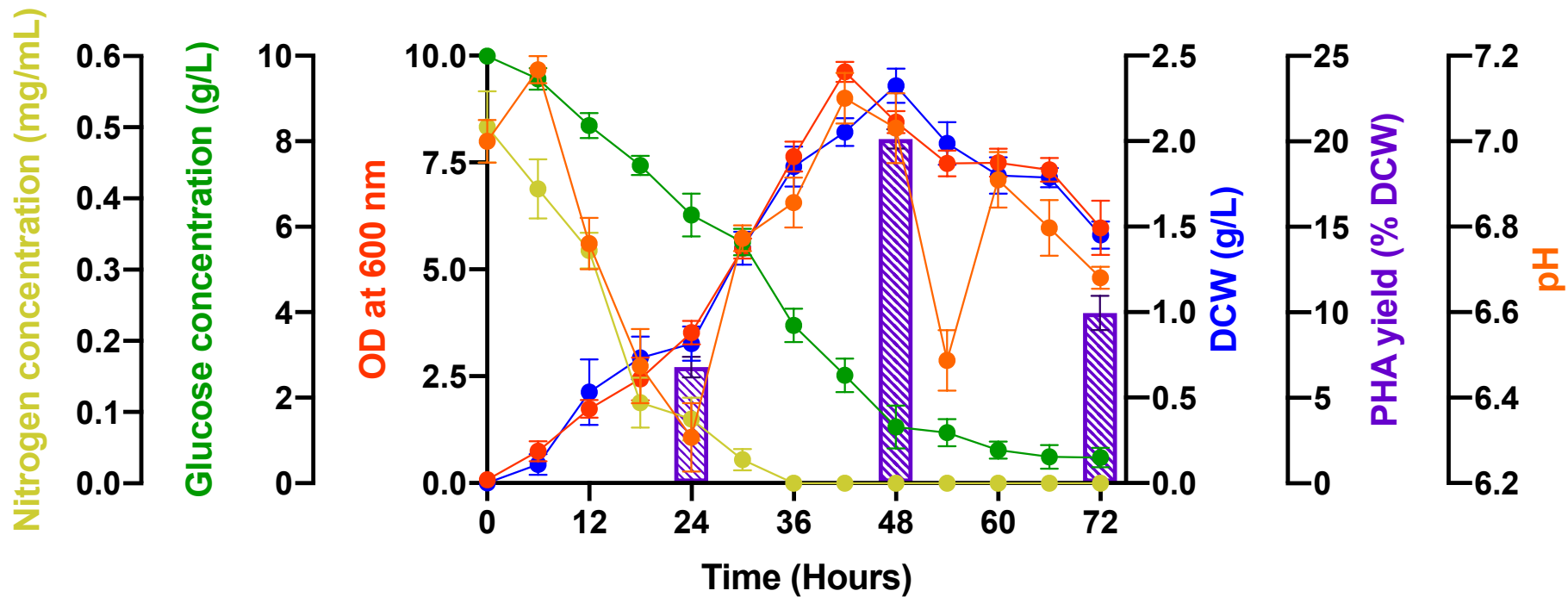


**Figure 4.4** Fermentation profile of *P. putida* KT2440 grown in 1 L shake flasks over a 72 hour period with addition of C<sub>6</sub>-HSL at a final concentration of 10  $\mu$ M. Samples were taken every 6 hours throughout the fermentation run, which was run in batch mode fermentation. E2 medium was used as the production medium, containing glucose as the sole carbon source. Error bars represent  $\pm$  SD values (n = 9).

**Figure 4.4** illustrates the growth profile of the results obtained from shake flasks used to grown *P. putida* KT2440 with the addition of the quorum sensing molecule C<sub>6</sub>-HSL at a final concentration of 10 µM. OD saw a continual and rapid increase for the first 41 hours of fermentation reaching a maximum OD of 9.618, from which point it decreased for the next 12 hours, before plateauing from 54 hours to 66 hours and decreasing to 5.975 by the end of the fermentation period. DCW followed a similar pattern, however maximum DCW was observed at 48 hours as opposed to 42 hours. At 48 hours the maximum DCW achieved by the culture was 2.32 g/L and decreased by 0.87 g/L by the end of the fermentation period. Interestingly the maximum amount of PHA yielded (% DCW) by the culture was at the same time maximum DCW weight was achieved. A maximum of 20.16% PHA (% DCW) was produced by the culture, which increased from 6.80% at 24 hours.

Within the first 6 hours of fermentation the nitrogen concentration of the medium fell by 0.10 mg/mL resulting in the medium having 0.40 mg/mL remaining. This decline was steady until 36 hours of fermentation, in which nitrogen concentration had completely depleted from the medium used to grow the culture and was no longer detected. Glucose concentration of the culture decreased between 30 and 36 hours by 1.95 g/L, which was the largest decrease within a 6 hour period throughout the entire fermentation period. During this period DCW increased by 0.48 g/L. pH of the culture fluctuated throughout the entire run, reading the lowest reading of pH 6.31 at 24 hours, however this eventually increased to pH 6.68 by the end of the fermentation period. **Table 4.5** details the kinetic growth parameters for this culture grown with the addition of exogenous C<sub>6</sub>-HSL molecules.

**Table 4.5** Kinetic growth parameters of *P. putida* KT2440 grown in 1 L shake flasks, batch mode fermentation with the addition of C<sub>6</sub>-HSL. Data from time points 24 and 48 hours were used to calculate the following parameters.

$\frac{Y_X}{\bar{S}} (g/g)$	$\frac{Y_P}{\bar{S}} (g/g)$	$\frac{Y_P}{\bar{X}} (g/g)$	$Q_p (g/L.H) (\times 10^3)$
0.301	0.083	0.275	10.937

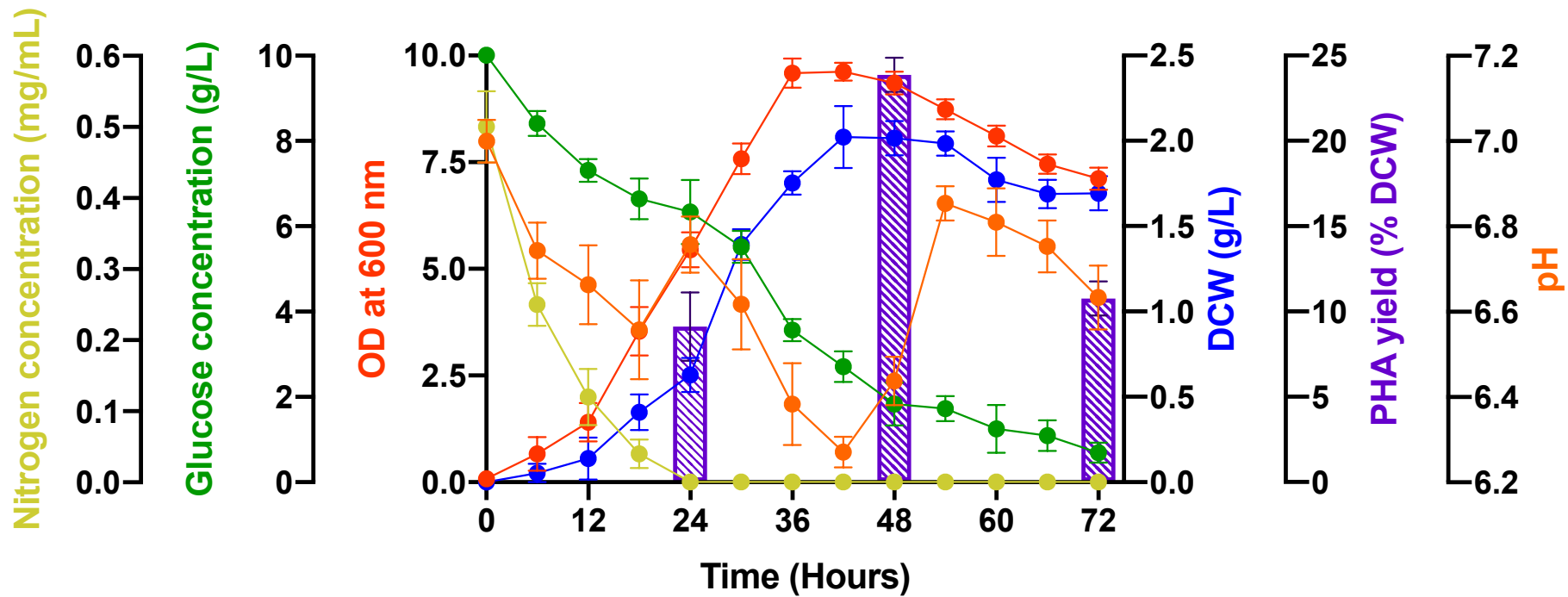


**Figure 4.5** Fermentation profile of *P. putida* KT2440 grown in 1 L shake flasks over a 72 hour period with addition of 3-oxo-C<sub>12</sub>-HSL at a final concentration of 10  $\mu$ M. Samples were taken every 6 hours throughout the fermentation run, which was run in batch mode fermentation. E2 medium was used as the production medium, containing glucose as the sole carbon source. Error bars represent  $\pm$  SD values (n = 9).

**Figure 4.5** illustrates the growth profile of the results obtained from shake flasks used to grown *P. putida* KT2440 with the addition of the quorum sensing molecule 3-oxo-C<sub>12</sub>-HSL at a final concentration of 10 µM. To begin the OD of the culture did not increase as rapidly when compared to the other growth profiles reaching an OD of 0.662 within the first 6 hours of growth, however by 36 hours of growth OD reached its maximum value of 9.589, where it remained steady for the next 12 hours and gradually fell from 48 hours onwards to 7.111. DCW followed an almost identical growth pattern as OD, reaching its maximum DCW 6 hours later OD did at 2.02 g/L, but remaining constant for the next 12 hours, before plateauing towards the end of the fermentation reaching a final DCW of 1.69 g/L. Within the first 24 hours, PHA yield (% DCW) accumulated up to 9.12%. This increased by 161.62% within the next 24 hours, from 9.12% to 23.86% at 48 hours, which was the maximum amount of PHA yielded (% DCW) throughout the entire run.

The nitrogen concentration started at 0.50 mg/mL, but rapidly decreased to the point no nitrogen was detected with the culture medium, which as a result meant that nutrient limiting conditions had been achieved. Glucose steadily decreased throughout the entire run, resulting in only 0.69 g/L of glucose remaining within the culture. The pH of the culture began at pH 7.00, but this fluctuated to reach a low pH of 6.27, before rapidly increasing to pH 6.85 at hour 54 of the fermentation period. Eventually pH decreased again and settled at pH 6.63 by the end of the fermentation period. **Table 4.6** details the kinetic growth parameters for this culture grown with the addition of exogenous 3-oxo-C<sub>12</sub>-HSL molecules.

**Table 4.6** Kinetic growth parameters of *P. putida* KT2440 grown in 1 L shake flasks, batch mode fermentation with the addition of 3-oxo-C<sub>12</sub>-HSL. Data from time points 24 and 48 hours were used to calculate the following parameters.

$\frac{Y_X}{S}$ (g/g)	$\frac{Y_P}{S}$ (g/g)	$\frac{Y_P}{X}$ (g/g)	$Q_p$ (g/L.H) ( $\times 10^3$ )
0.308	0.094	0.305	13.351

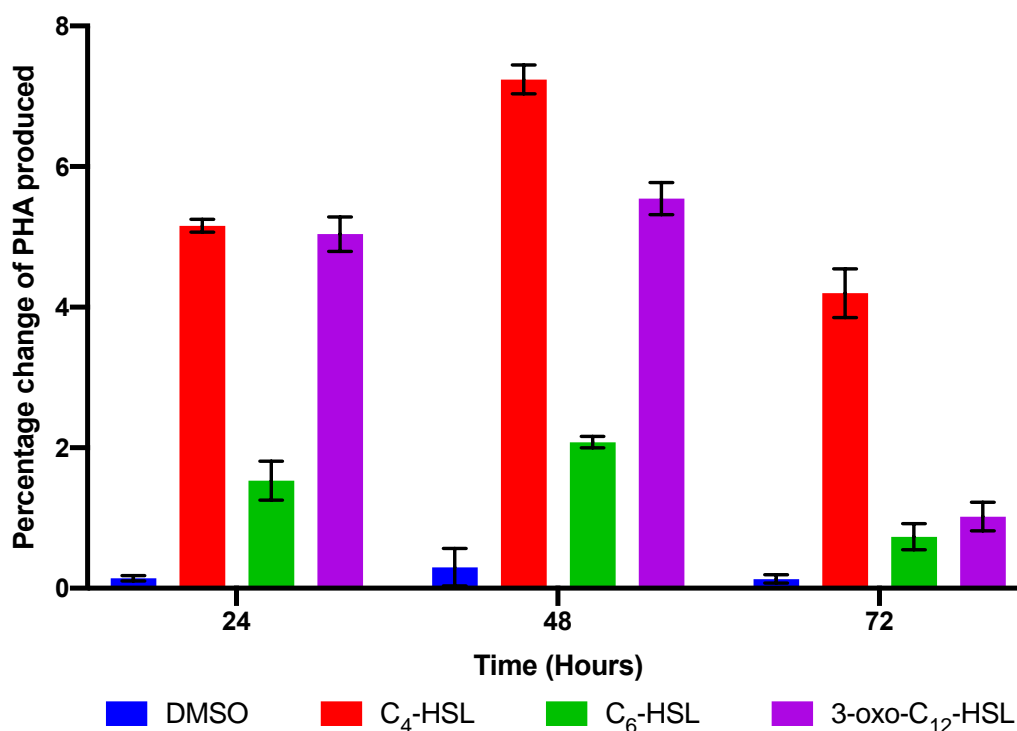


**Figure 4.6** Percentage change of PHA produced from *P. putida* KT2440 grown in 1 L shake flasks (batch mode fermentation) containing production media and exogenous quorum sensing molecules with a final concentration of 10  $\mu$ M. Results shown are expressed as mean percentage changes of PHA produced when compared to an untreated control (grown in the absence of exogenous quorum sensing molecules) with  $\pm$  SD values ( $n = 9$ ).

**Figure 4.6** displays the percentage change of PHA production of *P. putida* KT2440 when known in shake flask with exogenous quorum sensing molecules. Across the three different quorum sensing molecules supplemented, all three were able to increase the amount of PHA produced by the culture, with the maximum amount of PHA increasing until 48 hours. From this point onwards the increase in PHA produced decreased. C<sub>4</sub>-HSL appeared to have been the most effective AHL at increase production as PHA production increased by a maximum of 7.24% by 48 hours of fermentation.

#### 4.3.1 Characterisation and identification of MCL PHAs produced in shaken flask fermentation

The following series of experiments were carried out in order to characterise and identify the type of PHA produced by *P. putida* KT2440 when grown in 1 L shake flasks in batch mode fermentation with its respective production

medium and in the presence of different exogenous quorum sensing molecules with a concentration of 10  $\mu$ M (**Section 2.4.3**).

#### 4.3.1.1 Sudan Black B staining of *P. putida* KT2440

Samples extracted were first screened for the existence of PHAs, which was confirmed using Sudan Black B dye. This dye was chosen for its ability to dye inclusion bodies containing PHAs, which could then be observed macroscopically as described in **Section 2.7.2**. Colonies that were able to retain the dye were considered to have tested positive for inclusions containing PHAs as shown in **Figure 4.7**.



**Figure 4.7** Representative positive result of *P. putida* KT2440 culture grown on a nutrient agar plate and stained with Sudan Black B dye to indicate the presence of inclusion bodies. Samples of cultures were collected 48 hours post inoculation. The image shown is that of a *P. putida* KT2440 sample grown in the presence of the quorum sensing molecule C<sub>6</sub>-HSL.

All samples examined were able to test positively for inclusion bodies as individual colonies were able to successfully retain the Sudan Black B dye, resulting in the conclusions that PHAs were being produced.

#### 4.3.1.2 Nile red dye staining of *P. putida* KT2440

Once samples of *P. putida* KT2440 were confirmed to have harboured PHAs in the form of inclusion bodies they were then dyed with Nile red, and fixated as described in **Section 2.7.3**. The inclusions were able to be visualised using

a fluorescence microscope as the individual cells were able to retain the dye if they contained PHAs as shown in **Figure 4.8**.

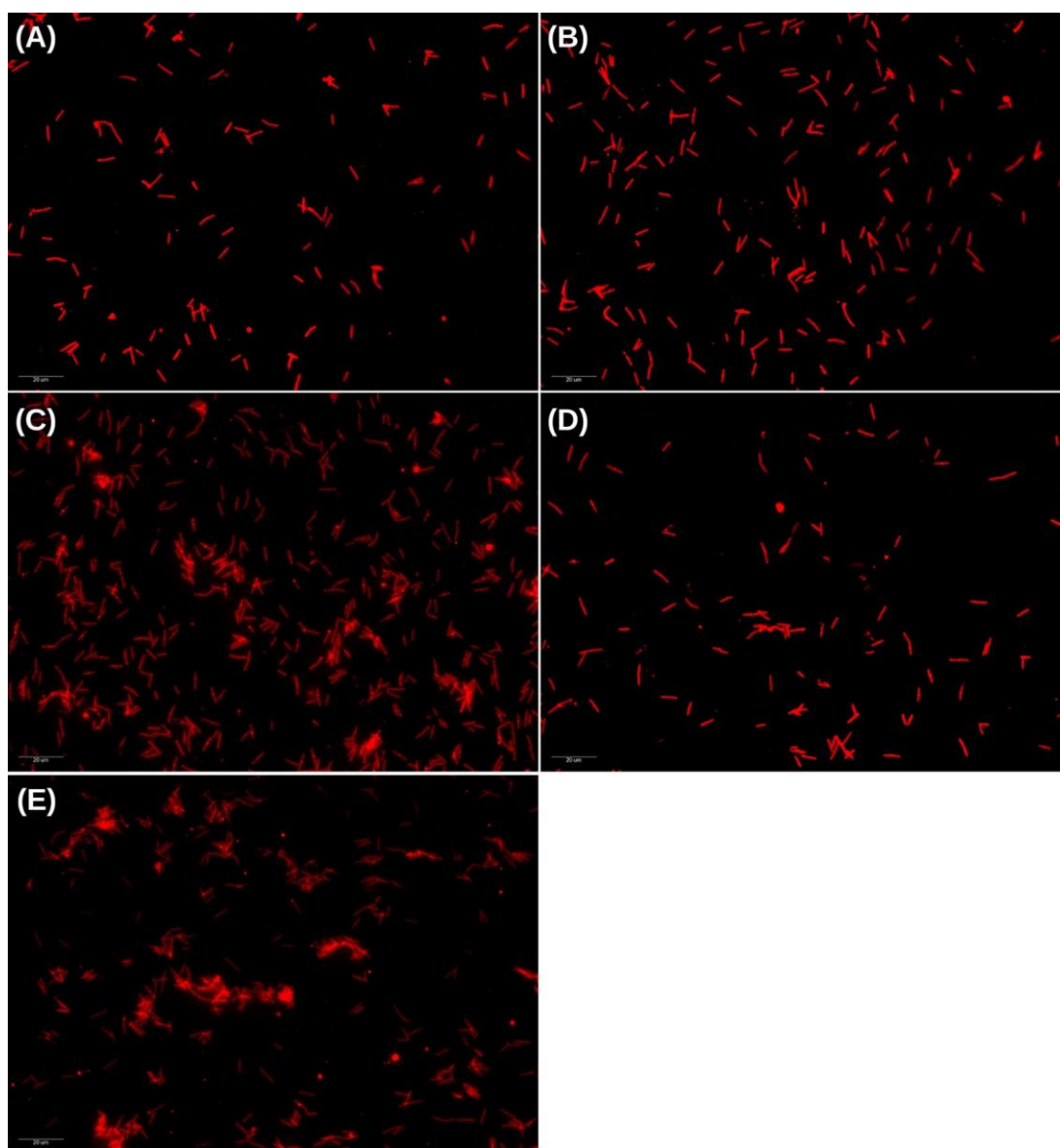


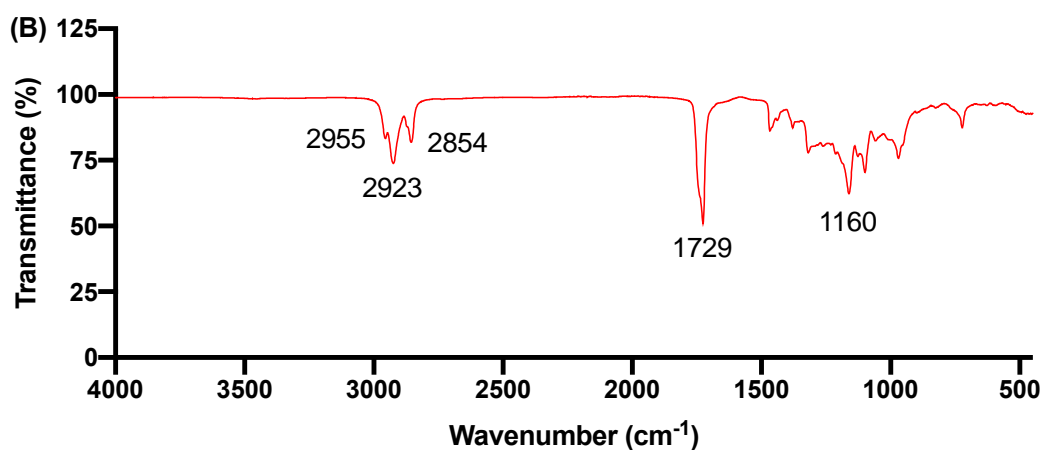
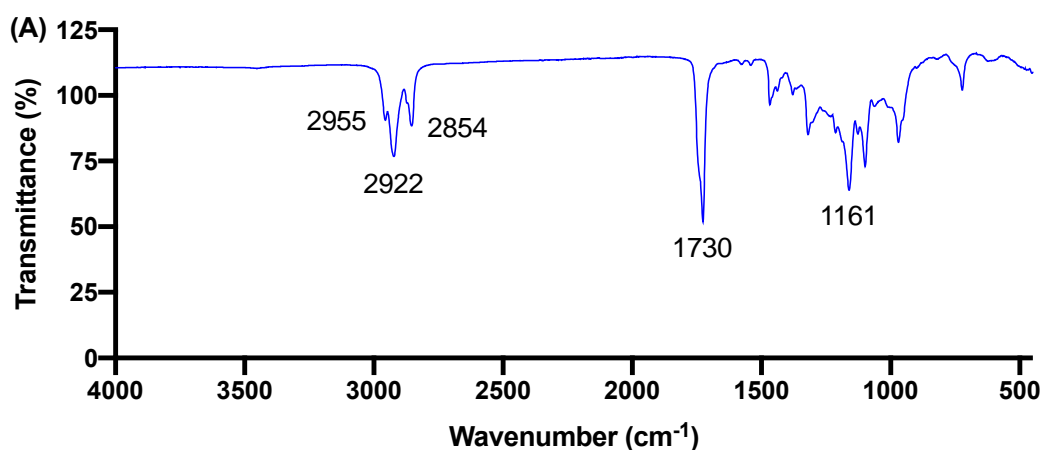
**Figure 4.8** Microscopic images of *P. putida* KT2440 cultures grown in 1 L shake flasks and stained with Nile red dye to indicate the presence of inclusion bodies. Cultures were visualised using a fluorescence microscope at X40 magnification. Images were taken of cultures 48 hours post inoculation. The images are labelled as follows: **(A)** Control, **(B)** DMSO, **(C)** C<sub>4</sub>-HSL, **(D)** C<sub>6</sub>-HSL and **(E)** 3-oxo-C<sub>12</sub>-HSL.

The results displayed showed that PHAs were produced by *P. putida* KT2440 and were harvested as an intracellular product as they were retained within the cell itself. As it is the PHA itself that retains the dye, the cells appeared as

a bright red colour when viewed under the fluorescent microscope, indicating for the presence of PHA granules within the cells.

#### 4.3.1.3 FTIR analysis of MCL PHA produced at shake flask level

In order to initially characterise the type of polymer produced, the chemical structure of the PHA was studied using FTIR. This analytical technique produces a spectrum that can be used for the identification of signature absorption bands that are normally present within a standard sample of PHA or have been noted within literature. After 72 hours of fermentation in 1 L shake flasks, the PHA produced by the culture was extracted, purified and subsequently analysed using FTIR as described in **Section 2.7.4**. **Figure 4.9** displays the individual spectra produced by each sample, whereas **Figure 4.10** shows the combined spectra of the PHAs produced when in the presence of different quorum sensing molecules.



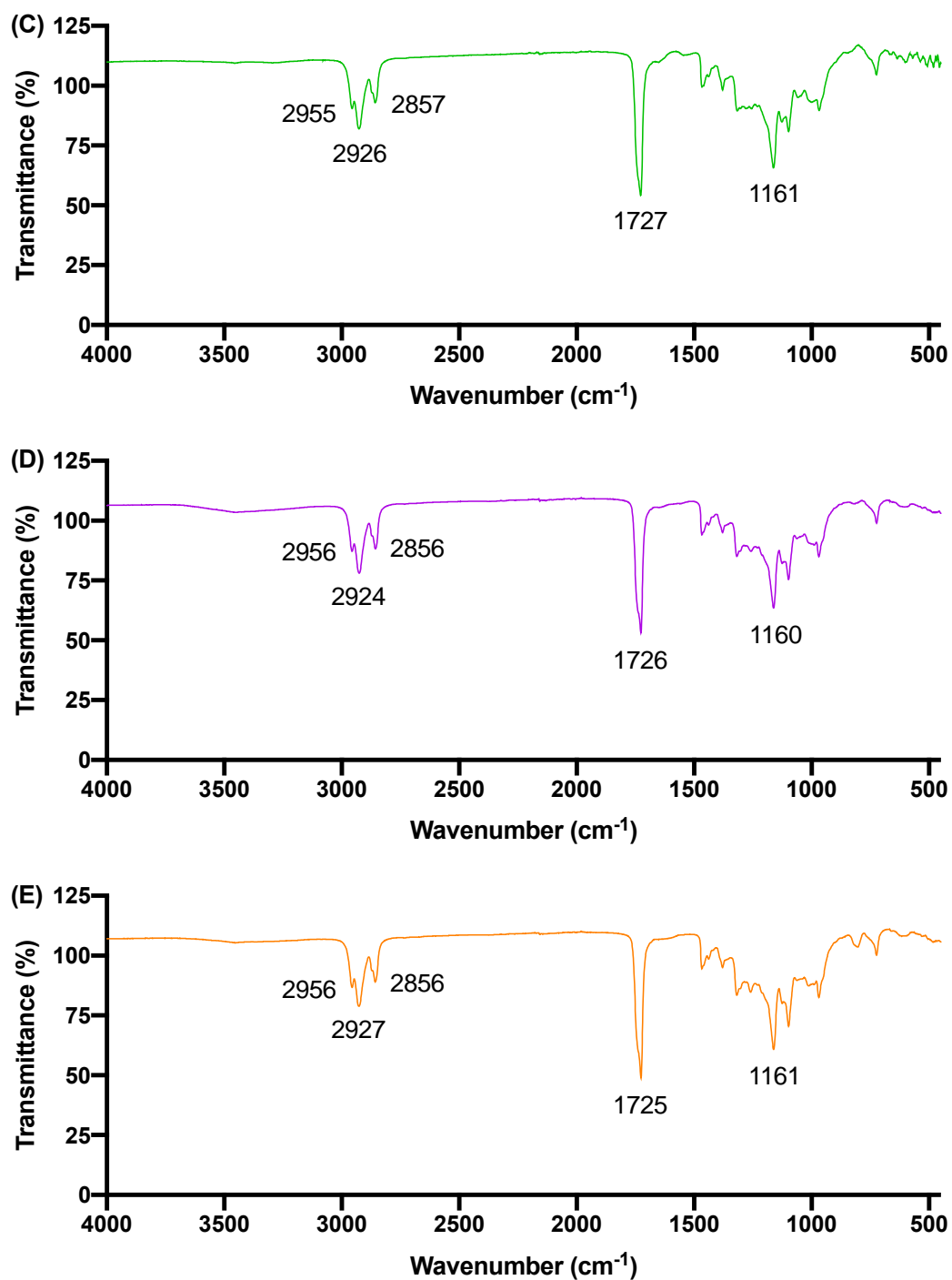


**Figure 4.9** FTIR spectra of MCL PHA produced by *P. putida* KT2440 grown within 1 L shake flasks and in the presence of exogenous quorum sensing molecules. The following spectra are labelled as follows: **(A)** Control, **(B)** DMSO, **(C)** C<sub>4</sub>-HSL, **(D)** C<sub>6</sub>-HSL and **(E)** 3-oxo-C<sub>12</sub>-HSL.

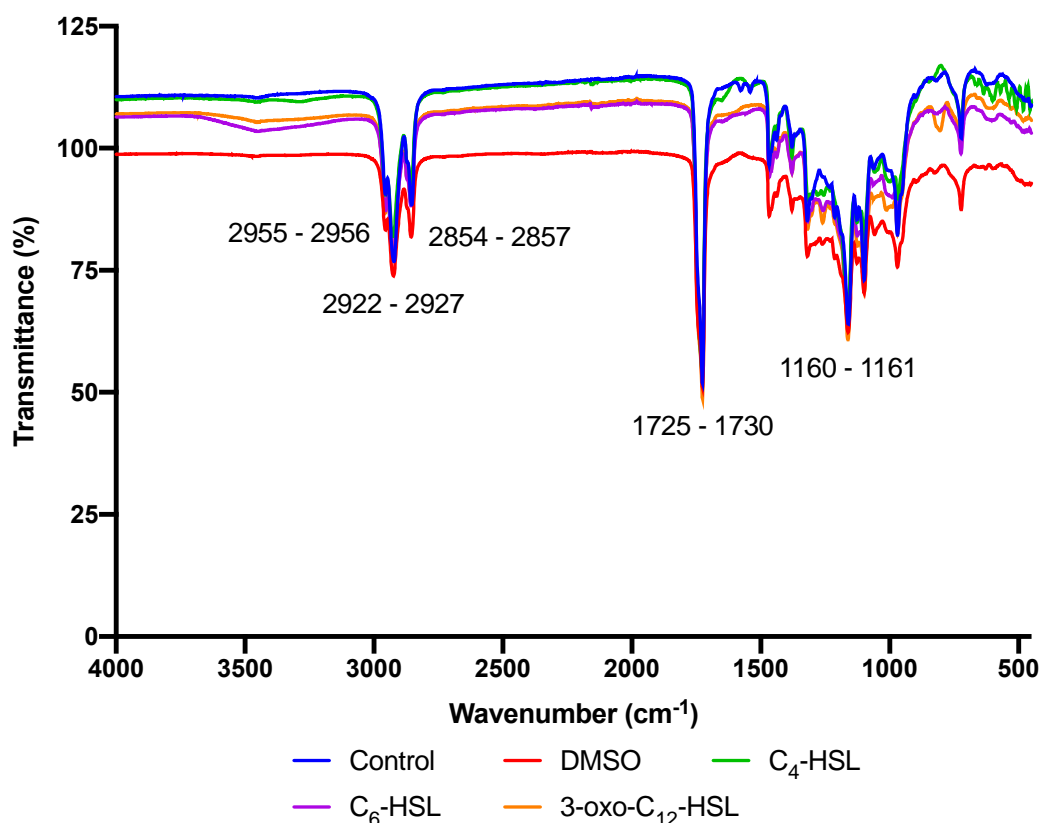


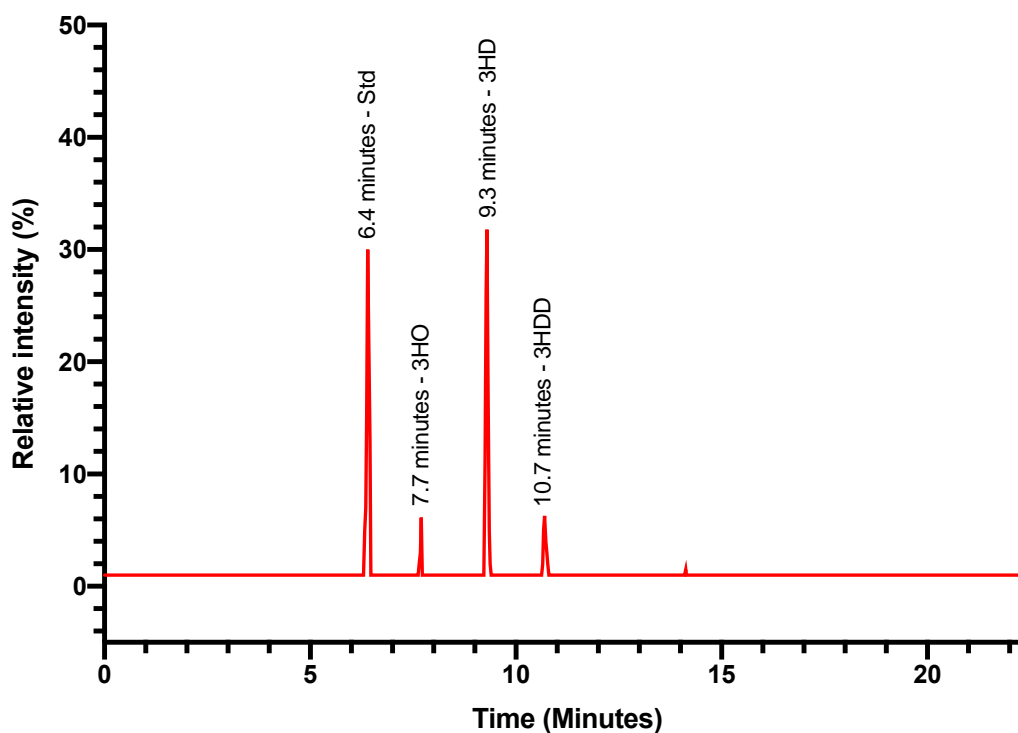
**Figure 4.10** Combined FTIR spectra of MCL PHA produced by *P. putida* KT2440 grown within 1 L shake flasks and in the presence of exogenous quorum sensing molecules.

FTIR analysis of the isolated PHAs revealed absorption bands at 1725 – 1730  $\text{cm}^{-1}$  corresponding to the stretching of the ester carbonyl group (C=O) and between 1160 – 1161  $\text{cm}^{-1}$  corresponding to the -CO stretching group, which are both characteristics of MCL PHAs. The bands at 2955 – 2956, 2922 – 2927 and 2854 – 2857  $\text{cm}^{-1}$  correspond to the aliphatic C-H group of the pendant alkyl group found in MCL PHAs (Sathiyarayanan *et al.*, 2017). As a result of the appearance of these bands, suggests that the PHA produced by *P. putida* KT2440 was MCL PHAs when in the presence of exogenous quorum sensing molecules, but also when in their absence as displayed in the control (**Figure 4.10**).

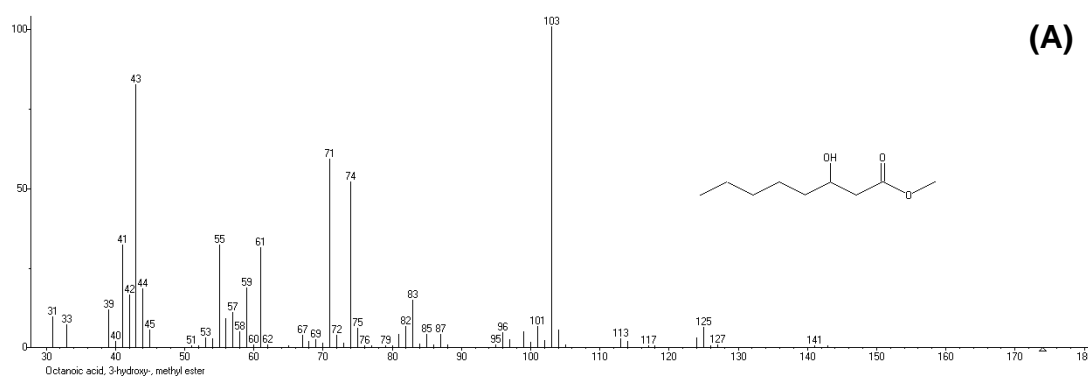
#### 4.3.1.4 GC-MS analysis of MCL PHA produced at shake flask level

For monomeric characterisation of the polymer produced in shaken flasks by *P. putida* KT2440, GC-MS was carried out. Prior to this analysis the sample of PHA produced was made to undergo the process of methanolysis, resulting in

the production of methyl esters as described in **Section 2.7.5**. TICs of PHA produced by *P. putida* KT2440 when in the presence of different quorum sensing molecules are shown in **Figure 4.11**, in which three peaks of interest were generated.



**Figure 4.11** Representative GC-MS analysis of the polymer produced when *P. putida* KT2440 was grown in 1 L shake flasks. The TIC above displays the methanolysis products of the PHAs produced when grown in the presence of 3-oxo-C<sub>12</sub>-HSL. Methyl Benzoate was used as an internal standard.



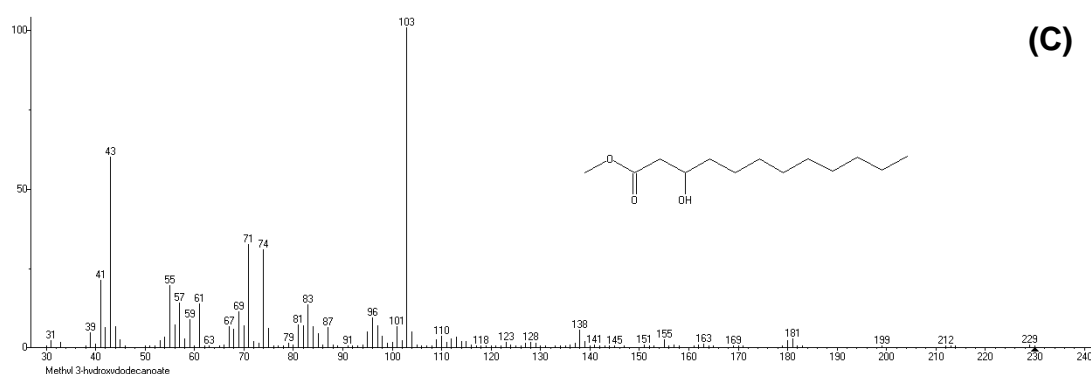
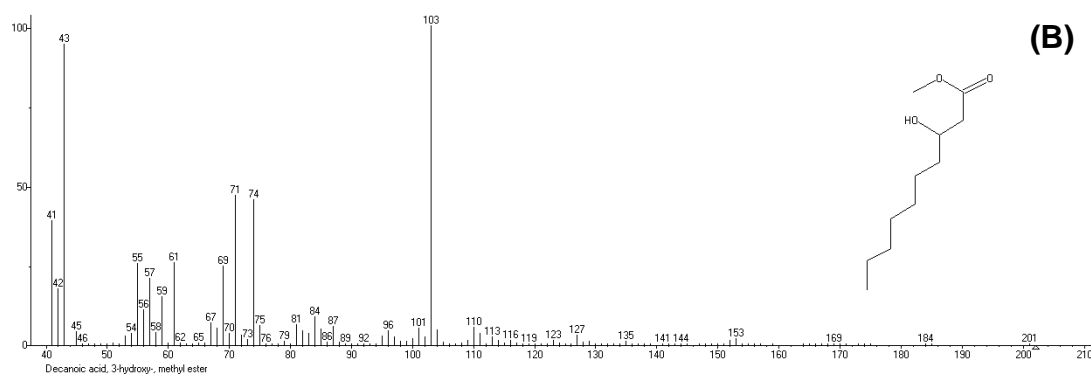


**Figure 4.12** Mass spectra of the peaks generated from GC of the methanolysis product of the PHA produced by *P. putida* KT2440 grown in shaken flasks with  $R_t$  of (A) 7.7 minutes, (B) 9.3 minutes and (C) 10.7 minutes were identified using the NIST library as methyl esters of 3HO, 3HD and 3HDD respectively.

The four peaks that were produced from the methanolysis products of the isolated PHA had  $R_t$  of 6.4 minutes, 7.7 minutes, 9.3 minutes and 10.7 minutes. Of the four peaks, the one with a  $R_t$  of 6.4 was identified to be the internal standard added, methyl benzoate. The mass spectra of the peaks with  $R_t$  of 7.7 minutes, 9.3 minutes and 10.7 minutes was found to be comparable with the mass spectra of the methyl esters of 3HO, 3HD and 3-hydroxydodecanoic acid (3HDD) respectively. Their individual mass spectra are shown in **Figure 4.12**. These comparisons were able to be drawn by using the MS library from NIST.

The fragmentation pattern of 3HO showed four significant peaks. These peaks appeared at  $m/z$  43, 71, 74 and 103. The first significant peak appeared at  $m/z$  43 which occurred due to the alkyl end of the molecule following the cleavage between carbon atoms 5 and 6. The  $m/z$  peak at 74 originated from the carbonyl end of the molecule due to the cleavage between carbon atoms 3

and 4 following McLafferty rearrangement (McLafferty, 1956). The peak at  $m/z$  103 represented the hydroxyl end of the molecule, which occurred due to the cleavage at bonds between carbon atoms 3 and 4, whereas the alkyl end of this cleavage resulted in the peak at  $m/z$  71.

The fragmentation pattern of 3HD also showed four significant peaks. These peaks also appeared at  $m/z$  43, 71, 74 and 103. The peak at  $m/z$  43 appeared due to the alkyl end of the molecule following the cleavage between carbon atoms 7 and 8, whereas the peak at  $m/z$  74 originated from the carbonyl end of the molecule due to the cleavage between carbon atoms 3 and 4 following McLafferty rearrangement (McLafferty, 1956). The peak at  $m/z$  103 occurred due to the fragmentation ion of the hydroxyl end of the molecule following the cleavage between carbon atoms 3 and 4. Similarly the alkyl end of the cleavage resulted in the peak at  $m/z$  71.

Finally, the fragmentation pattern of 3HDD was also similar, with four significant peaks appearing at  $m/z$  43, 71, 74 and 103. The peak at  $m/z$  43 occurred to the alkyl end of the molecule following cleavage between carbon atoms 9 and 10, as opposed to the peak at  $m/z$  74, which was produced from the carbonyl end of the molecule due to the cleavage between carbon atoms 3 and 4. Another peak was produced at  $m/z$  103 which originated due to the fragmentation ion of the hydroxyl end of the molecule following the cleavage between carbon atoms 3 and 4. The peak at  $m/z$  74 was produced due to the alkyl end of the cleavage.

As a result of the TICs produced, the composition of the PHA obtained from *P. putida* KT2440 when grown in shaken flasks was able to be deduced and was confirmed to be producing the copolymer poly(3-hydroxyoctanoate-co-3-hydroxydecanoate-co-3-hydroxydodecanoate) (P(3HO-co-3HD-co-3HDD)), when grown in the presence of different quorum sensing molecules. However, the ratio of the monomer composition within the PHA produced varied depending on the type of quorum sensing molecule present. **Table 4.7** displays a summary of monomeric composition of the PHA produced. The

structures of the methyl esters 3HO, 3HD and 3HDD are also displayed in **Figure 4.12 (A), (B) and (C)** respectively.

**Table 4.7** PHA monomer composition of MCL PHAs synthesised by *P. putida* KT2440 when grown in 1 L shake flasks in the presence of exogenous quorum sensing molecules.

Quorum sensing molecules	Monomeric composition of PHAs (Mol %)		
	3HO (C8)	3HD (C10)	3HDD (C12)
Control	13.5	69.7	16.8
DMSO	12.4	73.7	12.8
C <sub>4</sub> -HSL	15.3	72.7	9.8
C <sub>6</sub> -HSL	16.1	70.1	10.6
3-oxo-C <sub>12</sub> -HSL	13.7	70.6	13.9

#### 4.4 PHA production in bioreactors with the addition of exogenous quorum sensing molecules at 10 $\mu$ M concentration

Fermentations were then scaled by into 2 L bioreactors which were carried out in batch mode fermentations (**Section 2.4.5**). This was carried out in order to further optimise the production of PHA from *P. putida* KT2440 with the addition of three exogenous quorum sensing molecules. The PHA yield produced and PHA obtained were compared to the yield and product produced at shaken flask level to assess if there was a difference in production between the two modes.

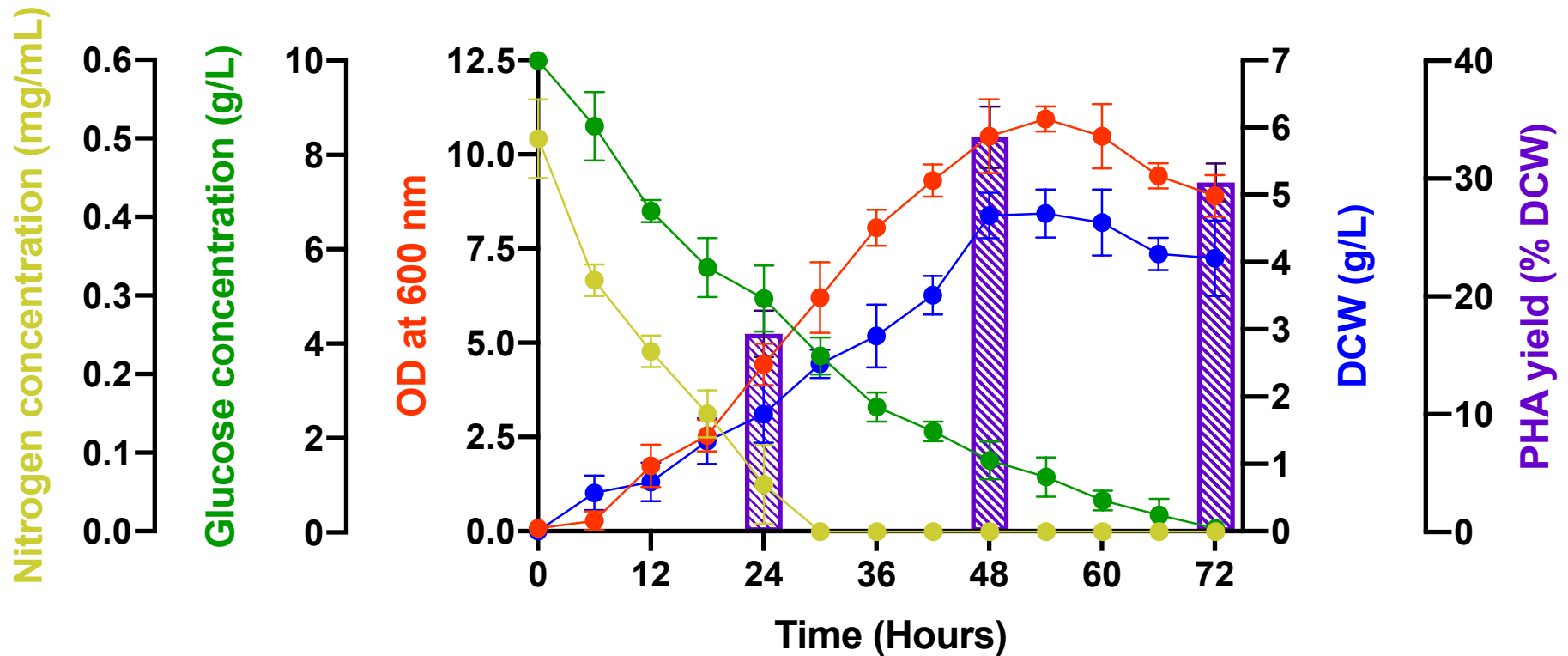


**Figure 4.13** Fermentation profile of *P. putida* KT2440 grown in 2 L bioreactors over a 72 hour period without the addition of exogenous quorum sensing molecules (control). Samples were taken every 6 hours throughout the fermentation run, which was run in batch mode fermentation. E2 medium was used as the production medium, containing glucose as the sole carbon source. Error bars represent  $\pm$  SD values ( $n = 3$ ).

**Figure 4.13** illustrates the growth profile of the results obtained from the control bioreactor used to grow *P. putida* KT2440 without the addition of exogenous quorum sensing molecules. Initially within the first 6 hours of fermentation very little growth was observed in terms of OD, however, from this point onwards OD increased rapidly and steadily until 54 hours of fermentation, in which the culture reached a maximum OD of 10.941. From this point onwards OD decreased to 8.900 by the end of the fermentation period. DCW increased in parallel with OD, increasing slowly at the start of the fermentation, but peaking at around 48 hours, instead of 54 hours. From 48 hours to 60 hours DCW remained stable, producing 4.69 to 4.59 g/L during this period of fermentation. Ultimately the final DCW produced by the culture was 4.06 g/L. PHA yield (% DCW) peaked at 48 hours producing 33.50% of PHA (% DCW). This decreased to 29.67% by 72 hours of the fermentation period.

Nitrogen limiting conditions were successfully obtained during this fermentation at 30 hours of fermentation growth. The decrease began almost immediately with nitrogen concentration falling 36% within the first 6 hours of fermentation. Medium with the bioreactor was supplemented with 10 g/L of glucose at the start of the fermentation period, which steadily decreased throughout the fermentation run. The biggest decrease in the concentration of glucose was observed between hours 12 and 18, in which glucose fell 1.8 g/L. **Table 4.8** details the kinetic growth parameters of the culture grown without the supplementation of exogenous quorum sensing molecules.

**Table 4.8** Kinetic growth parameters of *P. putida* KT2440 grown in 2 L bioreactors, batch mode fermentation without the addition of exogenous quorum sensing molecules. Data from time points 24 and 48 hours were used to calculate the following parameters.

$\frac{Y_X}{\bar{S}}$ (g/g)	$\frac{Y_P}{\bar{S}}$ (g/g)	$\frac{Y_P}{\bar{X}}$ (g/g)	$Q_p$ (g/L.H) ( $\times 10^3$ )
0.861	0.373	0.433	16.560

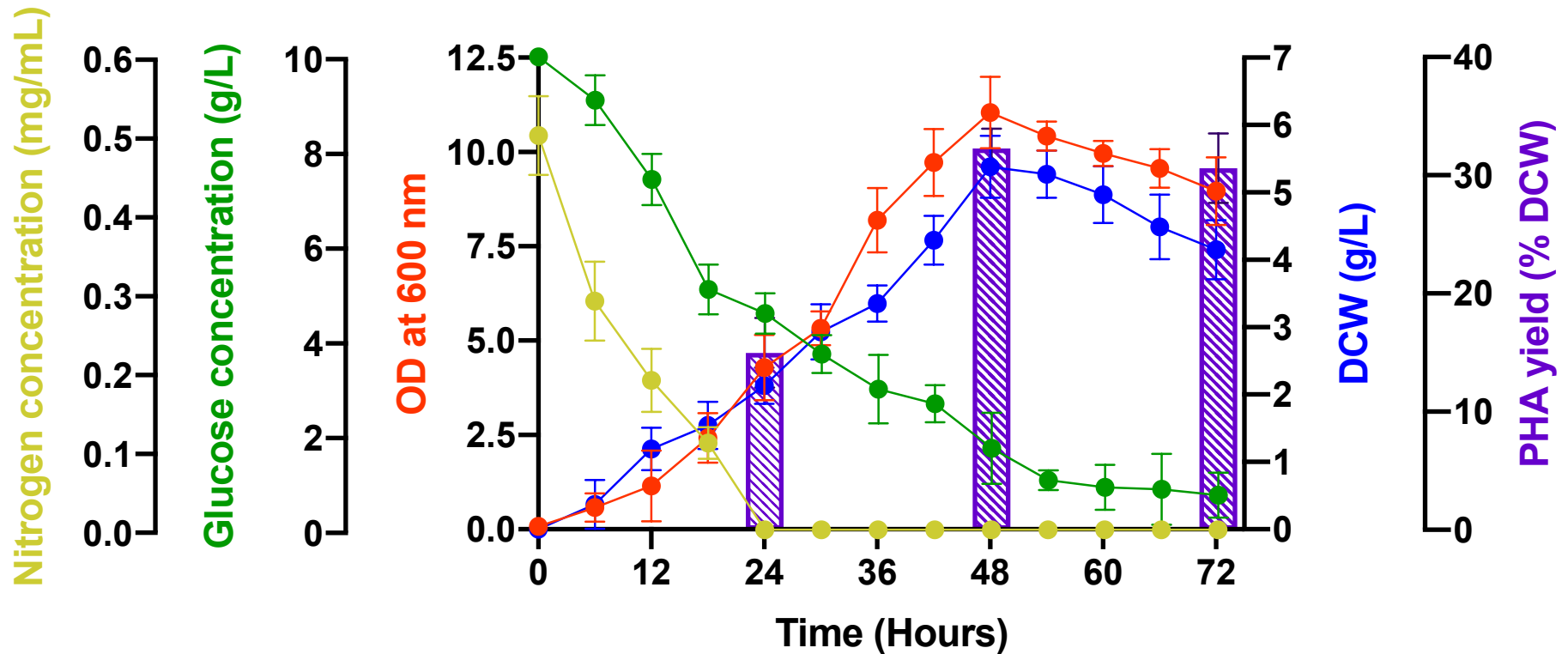


**Figure 4.14** Fermentation profile of *P. putida* KT2440 grown in 2 L bioreactors over a 72 hour period with addition of C<sub>4</sub>-HSL at a final concentration of 10  $\mu$ M. Samples were taken every 6 hours throughout the fermentation run, which was run in batch mode fermentation. E2 medium was used as the production medium, containing glucose as the sole carbon source. Error bars represent  $\pm$  SD values (n = 3).

**Figure 4.14** illustrates the growth profile of the results obtained from the control bioreactor used to grow *P. putida* KT2440 with the addition of C<sub>4</sub>-HSL. OD of the culture rose steadily until 48 hours reading a maximum OD of 11.044. During this period OD rose the highest between 30 and 36 hours increasing from 5.331 to 8.188. After this point OD decreases to 8.968. DCW followed a similar pattern in growth rising between the hours of 0 and 48 to the maximum DCW obtained of 5.38 g/L, at which point DCW began to decrease by 1.23 g/L to reach a final DCW of 4.15 g/L. At 24 hours of fermentation growth PHA yield (% DCW) of 15.03% was achieved, which was the equivalent of 0.32 g/L of PHA. This increased to a maximum PHA yield (% DCW) of 32.28% at 48 hours, but then decreased slightly 30.62%.

Nitrogen concentration began at 0.50 mg/mL at the start of the fermentation period and was no longer detected within the culture medium within the first 24 hours of growth, thus meaning that nitrogen limiting conditions had been achieved, which encourages the production of PHAs. Glucose concentration decreased slowly within the first 12 hours of growth, however from hours 18 to 24 glucose concentration decreased from 7.41 to 5.09 g/L, a decrease of 2.32 g/L of glucose within a 6 hour period. This was the largest decreased observed throughout the entire fermentation period. From hours 60 to 72, glucose concentration did not decrease as rapidly. Glucose concentration was measured at a concentration of 0.9 g/L and by the end of the fermentation a concentration of 0.74 g/L remained with the bioreactor. **Table 4.9** details the kinetic growth parameters of the culture grown with the supplementation of C<sub>4</sub>-HSL.

**Table 4.9** Kinetic growth parameters of *P. putida* KT2440 grown in 2 L bioreactors, batch mode fermentation with the addition of C<sub>4</sub>-HSL. Data from time points 24 and 48 hours were used to calculate the following parameters.

$\frac{Y_X}{\bar{S}}$ (g/g)	$\frac{Y_P}{\bar{S}}$ (g/g)	$\frac{Y_P}{\bar{X}}$ (g/g)	$Q_p$ (g/L.H) ( $\times 10^3$ )
1.141	0.500	0.438	15.771

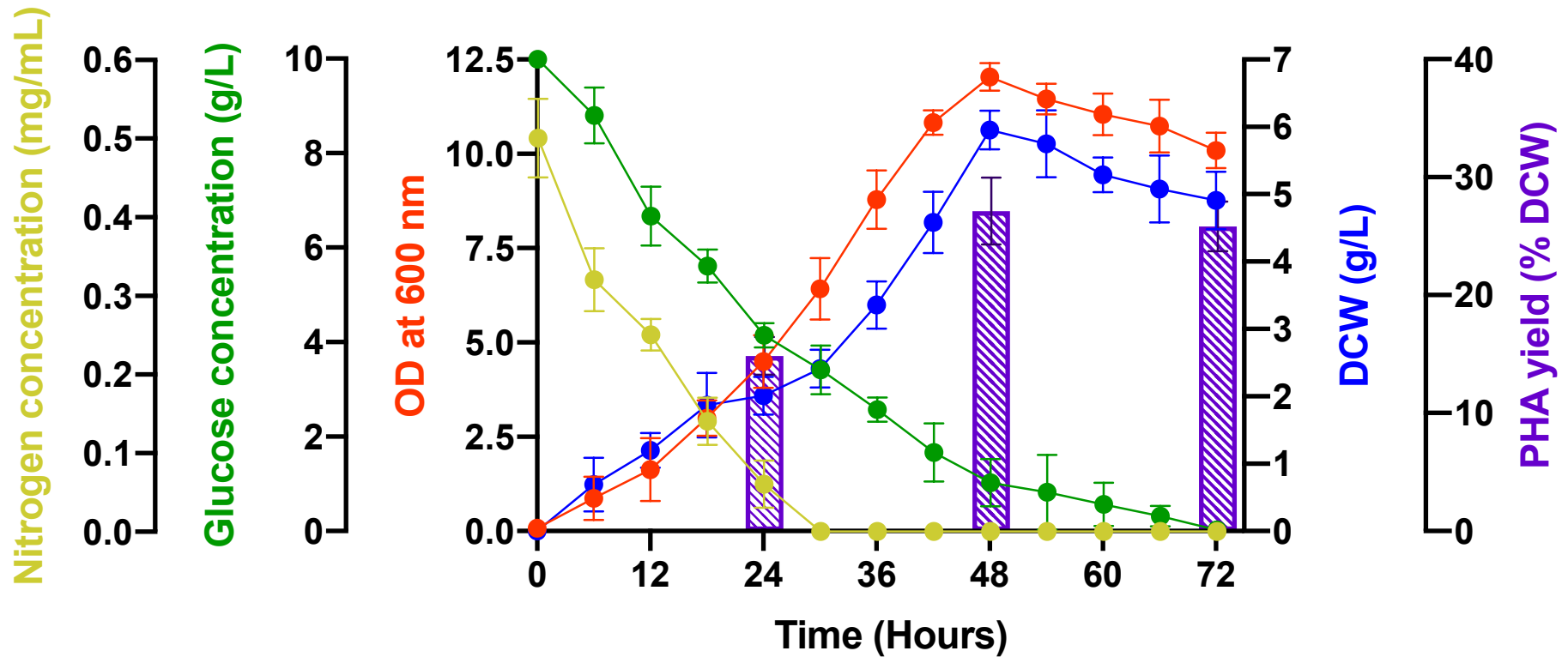


**Figure 4.15** Fermentation profile of *P. putida* KT2440 grown in 2 L bioreactors over a 72 hour period with addition of C<sub>6</sub>-HSL at a final concentration of 10 μM. Samples were taken every 6 hours throughout the fermentation run, which was run in batch mode fermentation. E2 medium was used as the production medium, containing glucose as the sole carbon source. Error bars represent ± SD values (n = 3).

**Figure 4.15** illustrates the growth profile of the results obtained from the control bioreactor used to grow *P. putida* KT2440 with the addition of C<sub>6</sub>-HSL. To begin OD appears to rise exponentially at a steady rate until 48 hours, at which OD peaks at 12.034. From this point onwards OD decreases gradually until 72 hours at which OD corresponds to 10.088. DCW increases at a steady rate between the hours of 0 and 18, but a small lag period appears in which DCW does not increase at the same rate. Nevertheless, DCW maximises at 48 hours of growth at 5.95 g/L, just like the OD readings taken. After this point DCW decreases by 1.04 g/L over the next 24 hours, achieving a DCW of 4.91 g/L. The PHA yielded by the culture initially increases, but decreases by the end of the fermentation period. PHA yield (% DCW) increases at 48 hours from 14.86% to 27.13%, but then decreases to 25.83% as mentioned by the end of the fermentation. The maximum amount of PHA obtained was 1.61 g/L.

Nitrogen concentration of the culture media depleted at 0.00 mg/mL by 30 hours of fermentation, thus meaning that nutrient limiting conditions were achieved at this point. Once again, the largest decrease in nitrogen concentration was observed within the first 6 hours of fermentation growth, decreasing by 36% from 0.50 mg/mL to 0.32 mg/mL. Glucose concentration fell throughout the entire run of the fermentation decreasing at a steady rate. As a result, by the end of the fermentation period only 0.03 g/L of glucose was detected in the remaining culture when assessed. Therefore, 9.97 g/L of glucose was consumed by the culture throughout the duration of the fermentation, the highest amount amongst all bioreactors that were supplemented with exogenous quorum sensing molecules. **Table 4.10** details the kinetic growth parameters of the culture grown with the supplementation of C<sub>4</sub>-HSL.

**Table 4.10** Kinetic growth parameters of *P. putida* KT2440 grown in 2 L bioreactors, batch mode fermentation with the addition of C<sub>6</sub>-HSL. Data from time points 24 and 48 hours were used to calculate the following parameters.

$\frac{Y_X}{\bar{S}}$ (g/g)	$\frac{Y_P}{\bar{S}}$ (g/g)	$\frac{Y_P}{\bar{X}}$ (g/g)	$Q_p$ (g/L.H) ( $\times 10^3$ )
1.262	0.421	0.334	13.791

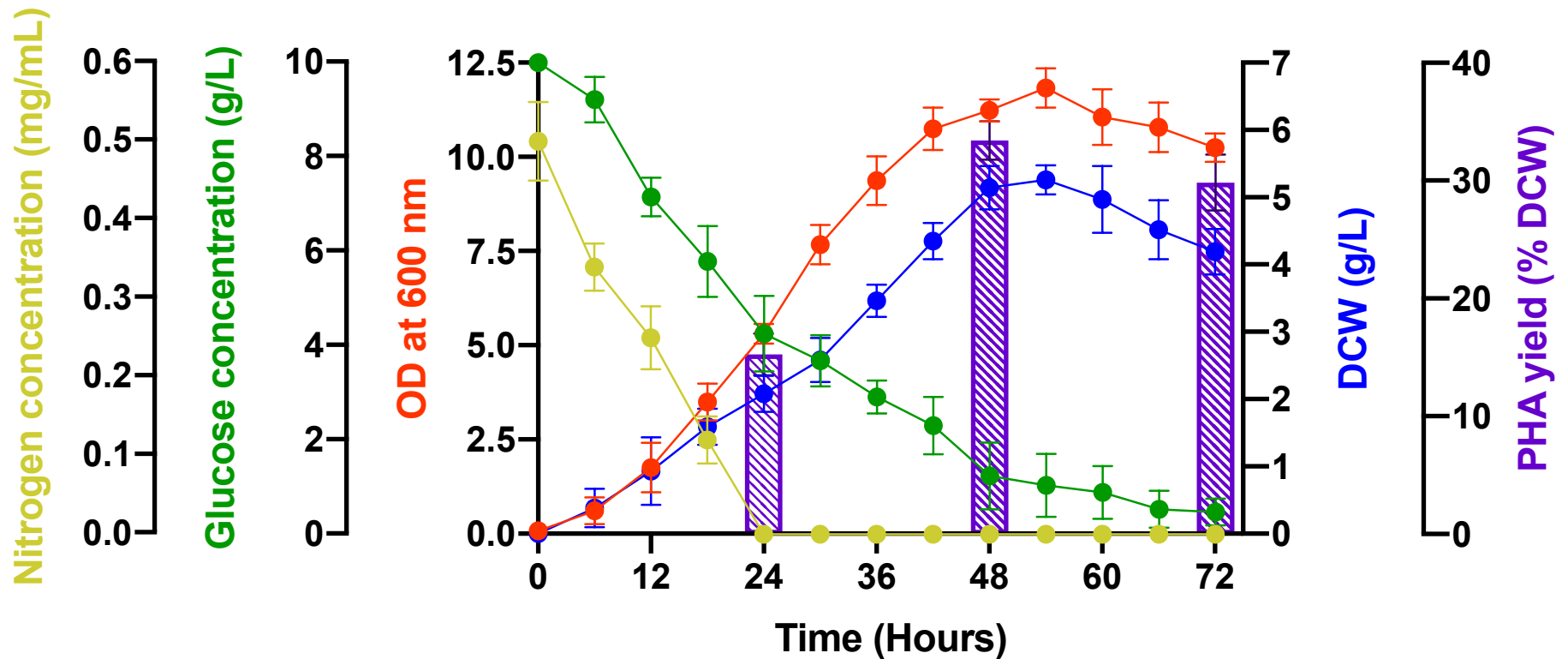


**Figure 4.16** Fermentation profile of *P. putida* KT2440 grown in 2 L bioreactors over a 72 hour period with addition of 3-oxo-C<sub>12</sub>-HSL at a final concentration of 10 μM. Samples were taken every 6 hours throughout the fermentation run, which was run in batch mode fermentation. E2 medium was used as the production medium, containing glucose as the sole carbon source. Error bars represent ± SD values (n = 3).

**Figure 4.15** illustrates the growth profile of the results obtained from the control bioreactor used to grow *P. putida* KT2440 with the addition of 3-oxo-C<sub>12</sub>-HSL. OD of the culture increased at a constant rate for the first 36 hours of fermentation, before the rate of growth decreased. OD peaked at 54 hours reaching a maximum OD of 11.831. From this point onwards, OD decreased and achieved an OD of 10.244 by the end of the fermentation period. DCW increase until 54 hours of fermentation, reaching a maximum DCW of 5.26 g/L. BY the end of the fermentation DCW had decreased slightly to 4.19 g/L, a decrease of 1.07 g/L. PHA yield (% DCW) rose 118.73% between 24 and 48 hours, increasing from 1.27% to 33.4%, which was equivalent to 0.32 g/L of PHA increasing to 1.72 g/L of PHA. However, this decreased slightly within the next 24 hours at 72 hours, producing 1.25 g/L of PHA.

Nitrogen concentration began at 0.50 mg/mL, and decreased by 32% within the first 6 hours of fermentation to 0.32 mg/mL of nitrogen. This continues at a fairly continuous rate, which resulted in nitrogen completely depleting from the culture medium by 24 hours. From this point onwards nitrogen was no longer detected. Glucose concentration decreased at a constant rate from 10.00 g/L at the start of the fermentation to 0.47 g/L by the end of the fermentation period (72 hours). The biggest decrease in glucose was observed between the hours of 6 and 12, in which 2.07 g/L of glucose was consumed by the culture. During this time period OD increase by 1.748, whereas DCW increased by 0.66 g/L. **Table 4.11** details the kinetic growth parameters of the culture grown with the supplementation of 3-oxo-C<sub>12</sub>-HSL.

**Table 4.11** Kinetic growth parameters of *P. putida* KT2440 grown in 2 L bioreactors, batch mode fermentation with the addition of 3-oxo-C<sub>12</sub>-HSL. Data from time points 24 and 48 hours were used to calculate the following parameters.

$\frac{Y_X}{S}$ (g/g)	$\frac{Y_P}{S}$ (g/g)	$\frac{Y_P}{X}$ (g/g)	$Q_p$ (g/L.H) ( $\times 10^3$ )
1.017	0.465	0.457	16.161

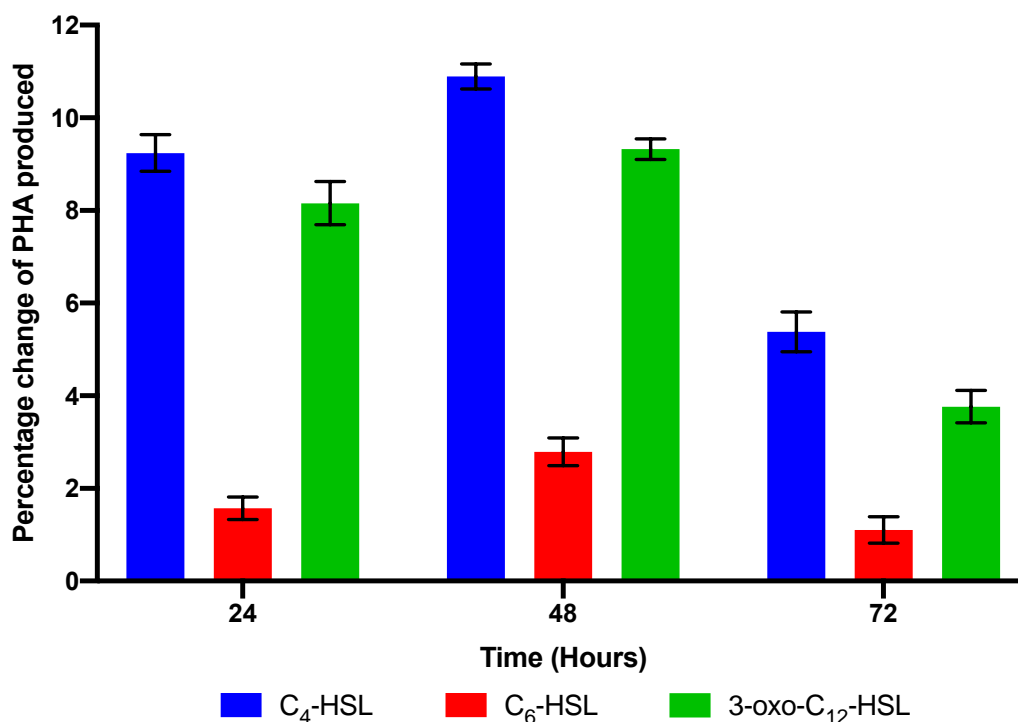


**Figure 4.17** Percentage change of PHA produced from *P. putida* KT2440 grown in 2 L bioreactors (batch mode fermentation) containing production media and exogenous quorum sensing molecules with a final concentration of 10  $\mu$ M. Results shown are expressed as mean percentage changes of PHA produced when compared to an untreated control (grown in the absence of exogenous quorum sensing molecules) with  $\pm$  SD values (n = 3).

**Figure 4.17** displays the percentage increase in PHA produced by *P. putida* KT2440 when grown in bioreactors with exogenous quorum sensing molecules. Once again, C<sub>4</sub>-HSL appeared to be the most effective AHL at increasing the amount of PHA produced, with a maximum increase of 10.89% at 48 hours, as previously observed when the grown in shake flasks (**Figure 4.6**).

#### 4.4.1 Characterisation and identification of MCL PHAs produced in 2 L bioreactor fermentation

The following series of experiments were carried out in order to characterise and identify the type of PHA produced by *P. putida* KT2440 when grown in 2 L bioreactors (batch mode) with its respective production medium and in the presence of exogenous quorum sensing molecules with a concentration of 10  $\mu$ M (**Section 2.4.5**).

#### 4.4.1.1 FTIR analysis of MCL PHA produced at bioreactor level

In order to initially characterise the type of polymer produced, the chemical structure of the PHA was studied using FTIR. This analytical technique produces a spectrum that can be used for the identification of signature absorption bands that are normally present within a standard sample of PHA or have been noted within literature. After 72 hours of fermentation in 2 L bioreactors, the PHA produced by the culture was extracted, purified and subsequently analysed using FTIR as described in **Section 2.7.4**. **Figure 4.18** the show the combined spectra of the PHAs produced when in the presence of different quorum sensing molecules.

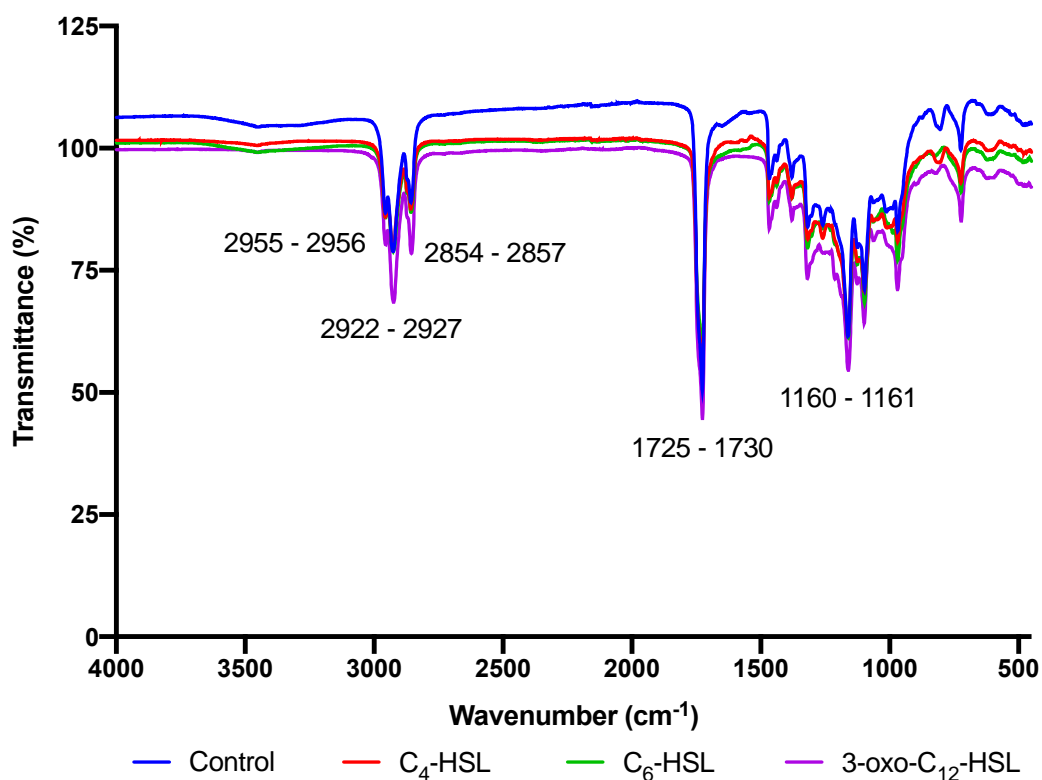


**Figure 4.18** Combined FTIR spectra of MCL PHA produced by *P. putida* KT2440 grown within 2 L bioreactors and in the presence of exogenous quorum sensing molecules.

FTIR analysis of the isolated PHAs revealed absorption bands at 1725 – 1730 cm<sup>-1</sup> corresponding to the stretching of the ester carbonyl group (C=O) and between 1160 – 1161 cm<sup>-1</sup> corresponding to the -CO stretching group, which are both characteristics of MCL PHAs. The bands at 2955 – 2956, 2922 –

2927 and 2854 – 2857  $\text{cm}^{-1}$  correspond to the aliphatic C-H group of the pendant alkyl group found in MCL PHAs (Sathiyarayanan *et al.*, 2017). As a result of the appearance of these bands, suggests that the PHA produced by *P. putida* KT2440 was MCL PHAs when in the presence of exogenous quorum sensing molecules, but also when in their absence as displayed in the control (**Figure 4.18**).

#### 4.4.1.2 GC-MS analysis of MCL PHA produced at bioreactor level

For monomeric characterisation of the polymer produced in bioreactors by *P. putida* KT2440, GC-MS was carried out. Prior to this analysis the sample of PHA produced was made to undergo the process of methanolysis, resulting in the production of methyl esters as described in **Section 2.7.5**. TICs of PHA produced by *P. putida* KT2440 when in the presence of different quorum sensing molecules is shown in **Figure 4.19**, in which four peaks of interest were generated.

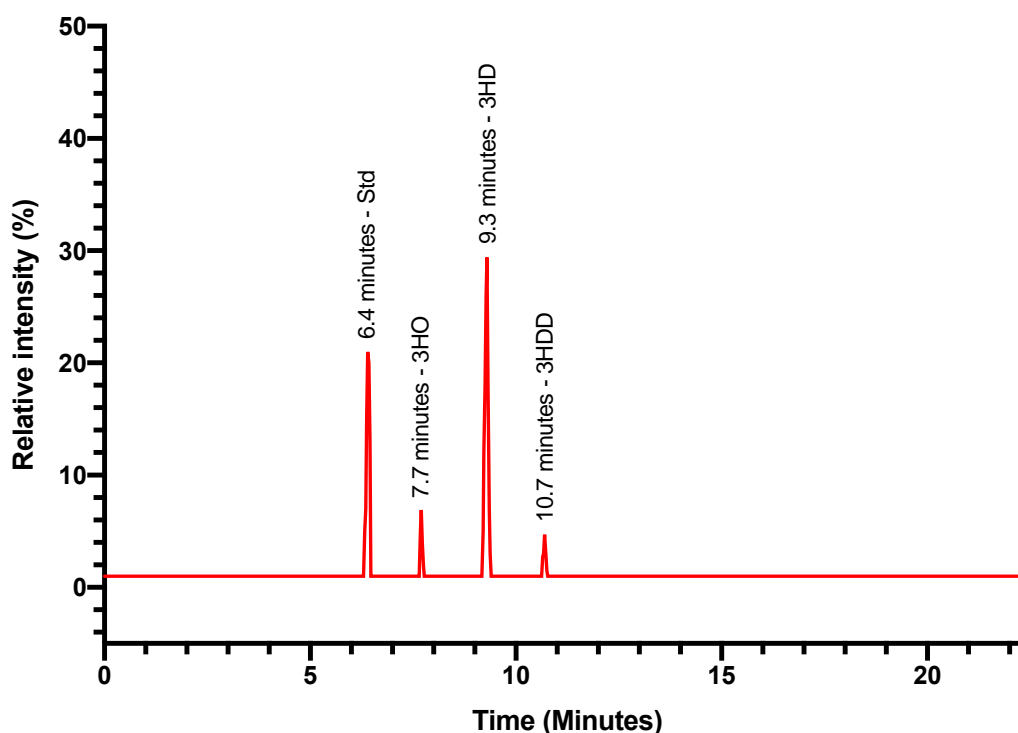


**Figure 4.19** Representative GC-MS analysis of the polymer produced when *P. putida* KT2440 was grown in 2 L bioreactors. The TIC above displays the methanolysis products of the PHAs produced when grown in the presence of C<sub>4</sub>-HSL. Methyl Benzoate was used as an internal standard.

The four peaks that were produced from the methanolysis products of the isolated PHA had Rt of 6.4 minutes, 7.7 minutes, 9.3 minutes and 10.7 minutes. Of the four peaks, the one with a Rt of 6.4 was identified to be the internal standard added, methyl benzoate. The mass spectra of the peaks with Rt of 7.7 minutes, 9.3 minutes and 10.7 minutes was found to be comparable with the mass spectra of the methyl esters of 3HO, 3HD and 3-hydroxydodecanoic acid (3HDD) respectively. Their individual mass spectra are shown in **Figure 4.12**. These comparisons were able to be drawn by using the MS library from NIST. The fragmentation patterns of 3HO, 3HD and 3HDD all showed four significant peaks, which are described in **Section 4.3.1.4**.

As a result of the TICs produced, the composition of the PHA obtained from *P. putida* KT2440 when grown in bioreactors was able to be deduced and was confirmed to also be producing the copolymer P(3HO-co-3HD-co-3HDD), when grown in the presence of different quorum sensing molecules. However, as previously mentioned the ratio of the monomer composition within the PHA produced varied depending on the type of quorum sensing molecule present. **Table 4.12** displays a summary of monomeric composition of the PHA produced. The structures of the methyl esters 3HO, 3HD and 3HDD are also displayed in **Figure 4.12 (A), (B) and (C)** respectively.

**Table 4.12** PHA monomer composition of MCL PHAs synthesised by *P. putida* KT2440 when grown in bioreactors in the presence of exogenous quorum sensing molecules.

Quorum sensing molecules	Monomeric composition of PHAs (Mol %)		
	3HO (C8)	3HD (C10)	3HDD (C12)
Control	14.9	70.8	14.3
C <sub>4</sub> -HSL	16.9	71.7	11.5
C <sub>6</sub> -HSL	15.5	73.4	10.4
3-oxo-C <sub>12</sub> -HSL	11.9	76.7	10.6

The PHAs produced in the two modes of fermentation (shake flask and bioreactors) were compared against each other to evaluate whether or not the mode of fermentation had an influence on the composition of the PHA. Results of this analysis is shown below in **Figure 4.20**. The individual PHA

compositions in both modes of fermentation are displayed in **Table 4.7** and **4.12**.

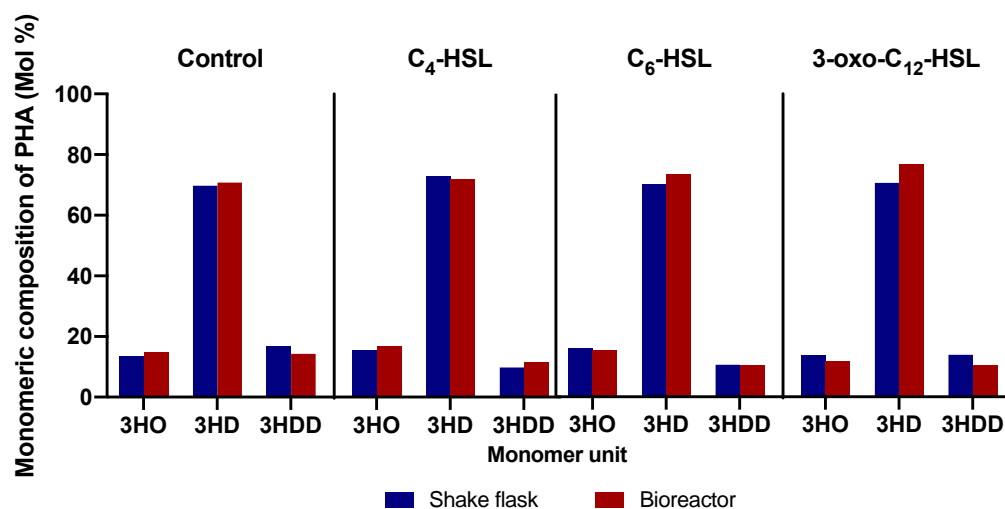


**Figure 4.20** Comparison of the monomeric composition of PHAs (Mol %) produced when supplemented with exogenous quorum sensing molecules in shake flasks and bioreactors. Data was analysed using a two-way ANOVA with *post hoc*. Tukey's multiple comparisons test ( $ns > 0.05$ ).

The compositions of the PHAs produced under different modes of fermentation were compared against each other to evaluate whether or not the mode of fermentation had an influence on the PHA produced in terms of the monomer composition, as well as if the presence of exogenous quorum sensing molecules had any effect on the composition too. It was observed that there was no significant difference between the PHAs produced in either shake flasks or bioreactors, but also no difference between the untreated control and PHAs produced with the supplementation of exogenous quorum sensing molecules. All PHAs extracted from cultures of *P. putida* KT2440 throughout this study produced MCL PHAs of P(3HO-co-3HD-co-3HDD) with the dominant monomer unit being 3HD. These findings were consistent with PHAs produced from either mode of fermentation.

#### 4.5 Molecular biology

#### 4.5.1 PCR for the confirmation of *Pha* genes in *P. putida* KT2440

To begin the analysis of *Pha* genes expression, PCR was first carried out to confirm the presence of GOIs within the genome itself. Primers used for this experiment can be found in **Table 2.15**, which were found in literature. These primers were applied to the primer designing tool – NCBI Primer BLAST, to check the specificity of the primers selected for this study. All samples were able to react positively during the PCR process, resulting in the production of fragments with amplicon sizes of ~540 bp and ~792, respective to *PhaC1* and *PhaZ* genes, which were consistent with the descriptions given by Kim Taw-Kwon *et al.*, (2003) and Devi Palraj, Ayyasamy and Kabilan, (2019).

#### 4.5.2 qPCR for the measurement of the expression levels of *Pha* genes in *P. putida* KT2440

Following the confirmation that the GOIs (*PhaC1* and *PhaZ*) were present within the genome, the next step was to analyse the expression of the GOIs when supplemented with exogenous quorum sensing molecules over a 72 hour period. Cultures of *P. putida* KT2440 grown in 2 L bioreactors with production medium that was supplemented with different quorum sensing molecules at a final concentration of 10 µM. Samples were taken every 24 hours, which were subsequently extracted for RNA as explained in **Section 2.8.4**. The results for this experiment are displayed below in **Figure 4.21**.

As previously mentioned, two *Pha* genes (*PhaC1* and *PhaZ*) were measured for the level of expression when exposed to different exogenous quorum sensing molecules. The *PhaC1* gene showed an increased level of expression when exposed to all three different quorum sensing molecules. The greatest increase in expression of the gene was observed at 48 hours when the culture was grown with the supplementation of 3-oxo-C<sub>12</sub>-HSL (**Figure 4.21A**). This finding was consistent amongst all of the quorum sensing molecules supplemented, as they all resulted in the highest level of expression of *PhaC1* at 48 hours. Similarly, the expression of the *PhaZ* gene also displayed an increase when exposed to the supplementation of exogenous quorum sensing molecules. All three quorum sensing molecules showed similar expression

patterns of *PhaZ*, increasing as the fermentation progressed and displaying the highest level of expression at 72 hours (**Figure 4.21B**). Throughout the fermentation, C<sub>6</sub>-HSL displayed the smallest increase in expression of this gene, when compared against C<sub>4</sub>-HSL and 3-oxo-C<sub>12</sub>-HSL.

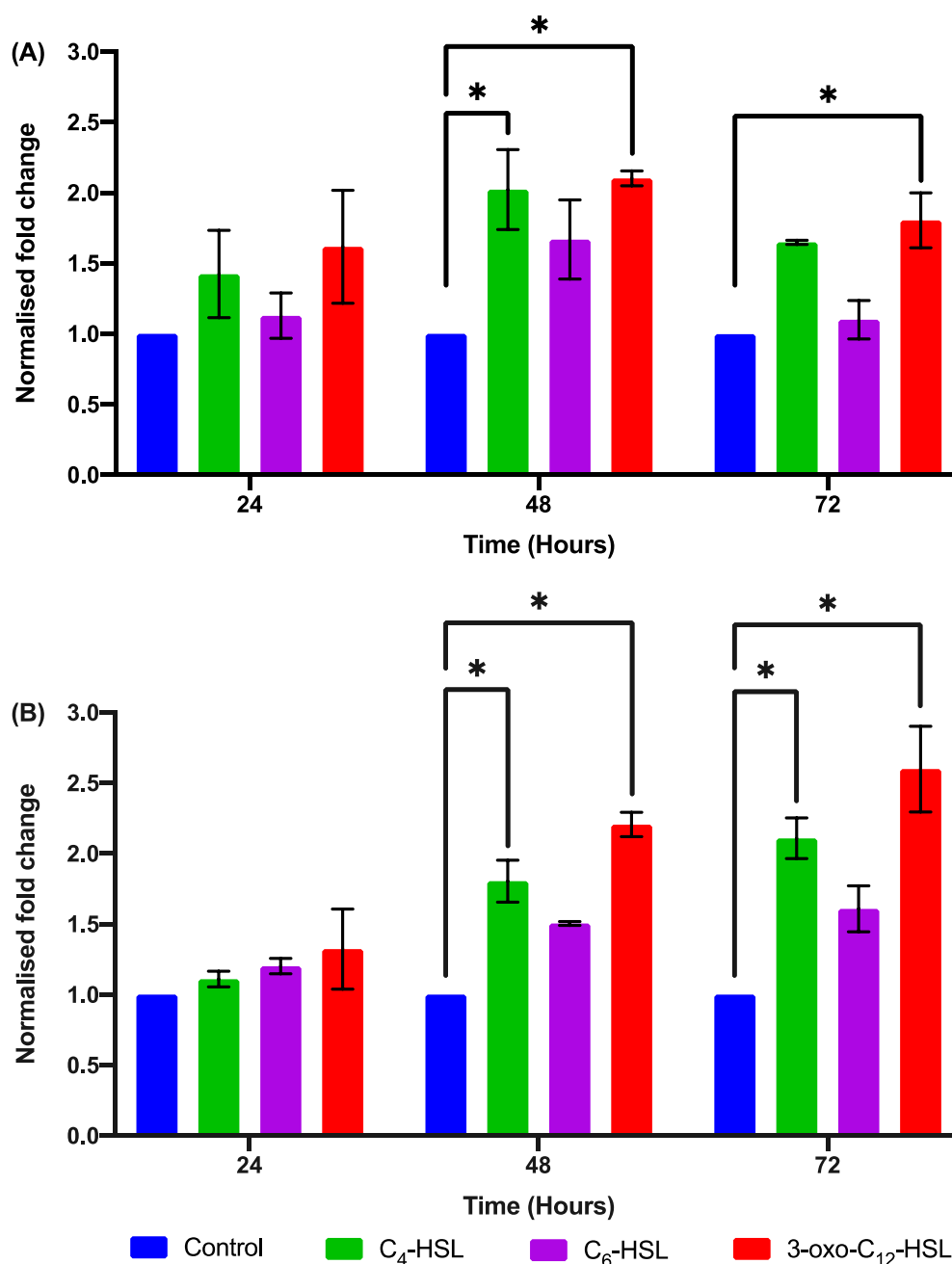


**Figure 4.21** Normalised fold change expression of **(A) *PhaC1*** and **(B) *PhaZ*** in *P. putida* KT2440 when grown with the addition of different exogenous quorum sensing molecules, compared with an untreated control (grown without the addition of exogenous quorum sensing molecules). *P. putida*

KT2440 cells were sampled over a 72 hour period from a 2 L bioreactor in batch mode fermentation. Results are expressed as mean fold change (control being standardised to 1.0) with error bars representing  $\pm$  SD (n = 9). Data was analysed using a two-way ANOVA with *post hoc*. Tukey's multiple comparisons test ( $*p < 0.05$ ).

## 4.6 Discussion

### 4.6.1 Growth profile analysis

Investigations of PHA production by the Gram-negative bacteria *P. putida* KT2440 have been extensively studied for many years well known for its ability to produce and accumulate MCL PHAs (up to 32.1% DCW when using glucose as the substrate) (Raza *et al.*, 2019). However, the impact of the supplementation of exogenous quorum sensing molecules on the production of PHAs has not been reported in literature previously. Hence this study focused on growing *P. putida* KT2440 in production medium with the supplementation of different exogenous quorum sensing molecules. One of the aims was to increase the economic viability of PHA within the marketplace by potentially increasing the yield through the addition of quorum sensing molecules. In this work, three different quorum sensing molecules (C<sub>4</sub>-HSL, C<sub>6</sub>-HSL and 3-oxo-C<sub>12</sub>-HSL) were supplemented into specific production media at two different concentrations (2  $\mu$ M and 10  $\mu$ M). The fermentations first took place at shake flask level with the addition of quorum sensing molecules at a low concentration, before increasing the concentration of quorum sensing molecules. These results were then compared against each other to assess which concentration had the greatest impact (if any) on the production and yield of PHAs. The fermentations were then scaled up into bioreactor to further optimise the yield of PHAs. Detailed results of these studies are discussed below.

As can be seen from the growth profiles displayed in **Figures 4.1 – 4.5** cultures grown with shake flasks accumulated a maximum DCW of 2.32 g/L at 48 hours, when supplemented with C<sub>6</sub>-HSL (**Figure 4.4**), whereas the lowest DCW of 2.0 g/L was accumulated by the control culture. The cultures containing DMSO, C<sub>4</sub>-HSL and 3-oxo-C<sub>12</sub>-HSL all showed similar growth,

obtaining DCWs of 2.14, 2.15 and 2.02 g/L respectively when compared to C<sub>6</sub>-HSL and the control culture. The supplementation of exogenous quorum sensing to cultures of *P. putida* KT2440 and the consequences on the production of PHAs has yet to be reported in literature. In theory the addition of exogenous quorum sensing molecules could lead to the increased regulation of various metabolic activities such as increasing cellular density, expression of virulence factors or secondary metabolites. However, when comparing the results of DCW of the cultures produced in shake flask level, it was observed that there was not a significant difference between the amount of DCW produced by each culture, regardless of the presence of exogenous quorum sensing molecules. This finding in itself was significant as it illustrated that the addition of quorum sensing molecules did not hinder the cultures' ability to replicate and produce biomass and nor did it aid the cultures ability to significantly increase in biomass.

Nevertheless, the DCW produced in this study at shaken flask level by *P. putida* KT2440 did not reach its maximum potential in regard to DCW produced. This is evident by a study carried out by Poblete-Castro *et al.*, (2014) who was able to demonstrate *P. putida* KT2440's ability to produce and accumulate a maximum of 4.23 g/L of DCW. Of this DCW, 34.5% was accumulated as PHAs resulting in 1.46 g/L of PHA being produced in shake flasks using 30 g/L of glycerol as the sole carbon source after 72 hours of fermentation growth. Yet, Davis *et al.*, (2013) were only able to accumulate 0.93 g/L of DCW from *P. putida* KT2440 when grown in shake flasks using glucose as the sole carbon source. Therefore, illustrating that potentially increasing the concentration of carbon source provided could potentially aid in increasing the DCW produced by the culture.

Despite the addition of exogenous quorum sensing molecules not having a significant impact on the DCW accumulated by the cultures, a significant change was detected between the amounts of PHA accumulated by cultures that were supplemented by exogenous quorum sensing molecules. **Figure 4.6** displays the percentage change in amount of PHA produced from cultures that were grown with the addition of quorum sensing molecules. Of the three

different quorum sensing molecules C<sub>4</sub>-HSL managed to increase the amount of PHA produced the most by 10.89% when compared to the untreated control. This was followed by 3-oxo-C<sub>12</sub>-HSL, which increased the amount of PHA by 5.55% at 48 hours. The smallest change in increase was observed from the culture supplemented with DMSO across the entire sampling period. DMSO was added to the culture to study to act an alternative negative control, which would illustrate whether any changes were occurring because of the exogenous quorum sensing molecules or because of the DMSO itself. Although, all the cultures accumulated similar amounts of PHA yields (% DCW) throughout the entire fermentation period, the cultures that were grown in the presence of exogenous quorum sensing molecules were able to produce more PHA.

For example, at 48 hours the untreated control yielded 22.79% PHA of DCW, whereas the culture supplemented with C<sub>4</sub>-HSL yielded 22.67% PHA of DCW. Ultimately, this translated to the untreated control culture producing 0.46 g/L of PHA, whereas C<sub>4</sub>-HSL was able to produce 0.49 g/L of PHA. This shows although the culture grown with exogenous quorum sensing molecules yielded less PHA (% DCW) than the control, they were still able to produce more PHA. This could be interpreted as the cultures that were grown in the presence of exogenous quorum sensing molecules were more productive and efficient at converting the carbon source into a product, which in this case was PHA. **Table 4.13** displays the kinetic growth parameters of cultures grown in shake flasks. In this example, C<sub>4</sub>-HSL had a higher ratio than the control between the amount of PHA produced and DCW as shown by the product yielded values of 0.33 and 0.299 g/g respectively. This was also true for 3-oxo-C<sub>12</sub>-HSL, but not C<sub>6</sub>-HSL. This would indicate that the presence of exogenous quorum sensing molecules has some impact on the production of PHAs as more product was being yielded per biomass. However other parameters also have an influence on the production of PHAs such as nitrogen concentration and nutrient imitating conditions that must be taken into account.

**Table 4.13** PHA productions of *P. putida* KT2440 in batch mode fermentation using 1 L shake flasks containing production media with the addition of exogenous quorum sensing molecules at a concentration of 10 µM.

Productions were calculated using data of samples collected at 24 and 48 hours.

<b>Quorum sensing molecules</b>	$Y_X (\text{g/g})$ $\bar{S}$	$Y_P (\text{g/g})$ $\bar{S}$	$Y_P (\text{g/g})$ $\bar{X}$	$Q_p (\text{g/L.H})$ ( $\times 10^3$ )
Control	0.329	0.098	0.299	12.569
DMSO	0.300	0.082	0.274	11.946
C <sub>4</sub> -HSL	0.318	0.096	0.303	12.447
C <sub>6</sub> -HSL	0.301	0.083	0.275	10.937
3-oxo-C <sub>12</sub> -HSL	0.308	0.094	0.305	13.351

Nitrogen limitation is the process in which nitrogen within culture media is driven down to a point where there is no, or very little nitrogen left within the medium and is maintained throughout the fermentation period. This is encouraged for the production of PHAs as nitrogen limitation is a known trigger for the accumulation of PHAs, as it guides cells into the stationary phase, which in leads to the production of PHAs. Throughout this study, nitrogen limiting conditions were successfully achieved, which resulted in the production of PHAs. This was in alignment with the findings of others such as Dabrowska *et al.*, (2020) who were able to confirm that nitrogen limitation had a positive effect on the production of PHAs by *P. putida* KT2440. All cultures grown in shake flasks were able to achieve nitrogen limiting conditions by 24 – 36 hours of fermentation maintained. It was during this specific time period in which PHA began to be detected within the culture as well as cultures beginning to plateau in in cellular growth indicating at this point the culture most likely would be entering the stationary phase of growth. However, this was not the case for cultures grown in bioreactors. Similarly, to cultures grown in shake flasks, nitrogen limiting conditions were achieved around 24 – 30 hours of fermentation, though cellular growth continued to progress until 48 hours. This could be owing to the fact that in bioreactors aeration of a culture can be controlled, which could attribute to increased cellular growth.

Another factor that must be taken into account is the pH of the culture itself, as this specifically affects the enzymatic activity within the cells. A medium that is set at neutral pH has been shown to accumulate more PHAs than in comparison to acidic or basic environments. This is because the fluctuations in pH slows down the fermentative process, with a reduction in cellular activity

of key enzymes related to the production of PHAs, which therefore affects the growth rate and cellular biomass (Raza *et al.*, 2019). Although it has been suggested that low pH conditions could inhibit PHA degradation that would result in the overall increase in accumulation of PHAs (Valappil *et al.*, 2007). A change in pH within a culture can generally be attributed to different ongoing types of metabolic processes by the culture itself that could lead to the secretion of different extracellular compounds (*e.g.*, rhamnolipids and citric acid), which in turn can then alter the medium's pH.

During fermentations held in shake flasks, pH was not maintained, which resulted in the erratic change in pH throughout the duration of the fermentation period. The pH of the production medium was set at pH 7.00 before beginning the fermentation, but by the end of the run the pH would generally fall to 6.72, which is not the most favourable condition for the production of PHAs. For example, in **Figure 4.4**, the culture was supplemented with C<sub>6</sub>-HSL, within the first 24 hours of the fermentation pH fell to 6.43, this then increased to pH 7.10 by 42 hours and fell to pH 6.7 by the end of the fermentation period. Similar observations were also reported by Basnett, (2014) when growing *P. mendocina* using sugarcane molasses, biodiesel waste and glycerol as the sole carbon source. The pH of the media used to grow the culture fell from 7.00 to 6.59. However, this was not the case for cultures that were grown in bioreactors as the pH was maintained at 7.00 throughout the entirety of the run. This resulted in higher amounts of PHA being produced, irrespective of the addition of quorum sensing molecules, when comparing bioreactors to their shake flask counterparts. This maintenance of pH could have helped to have increase the production of PHAs as enzymatic activity would have been kept closer to their optimum working conditions.

**Figure 4.13 – 4.16** displays the growth profiles of cultures grown in bioreactors. These cultures peaked OD between 48 – 54 hours of fermentation. However, after this point DCW steadily declined, whereas OD did not decline at the same rate. This is most likely because cells within the culture contained PHA granules, which has an influence on the cultures OD. This slow decline in OD was reflected in the PHA yield (% DCW), which was

relatively high by the end of the fermentation when compared against shake flask cultures. Shake flask cultures such as ones supplemented with C<sub>6</sub>-HSL (**Figure 4.4**) displayed a decrease of almost 50% of PHA yield (% DCW) and a simultaneous decrease in OD, whereas in bioreactors PHA yield (% DCW) only fell by 5% when supplemented with the same quorum sensing molecule (**Figure 4.15**) and OD decreased slightly. This could be a result of a longer stationary phase being maintained in cultures that are grown in bioreactors, in which cells are unable to grow further due to the depletion of nutrients in the medium. Hence, the amount of residual biomass and OD decreased due to decline in the cell growth.

However, PHA yield (% DCW) and OD was maintained due to the amount and size of the PHA granules, which increases during the early stationary phase and occupies a large proportion of the intracellular space. Hence, maximal PHA production was achieved during the stationary phase of growth and maintained throughout which resulted in higher OD being achieved even though DCW decreased, when compared to shake flask cultures. Solaiman, Ashby and Foglia, (1999) were able to observe that approximately 80% of the *P. saccharophila* cells contained PHA inclusion bodies. These results also revealed that *P. saccharophila* growing on triacylglycerol substrates continued to produce PHA granules even after an extended growth period.

*Pseudomonas* species are known for their high oxygen demands to facilitate cellular growth (Sun *et al.*, 2007). During this study when cultures grown in bioreactors were supplied with a continuous stream of air of 1 vvm with RPM set at 300. This was to ensure that oxygen limiting conditions were not achieved to help facilitate cell growth and is one of the main reasons as to why cultures grown in the bioreactor accumulated a higher amount of DCW as well as OD, when compared against cultures grown in shake flasks. In general, this should be expected as specific parameters can be well controlled in order to improve the performance of the culture, which is not as easily done in shake flasks.

The largest change in PHA accumulated when compared to the untreated control in bioreactors was observed at 48 hours of fermentation growth when the culture was supplied with C<sub>4</sub>-HSL, resulting in an increase in production of 10.89% (**Figure 4.17**). This increase in PHA translated to 1.74 g of PHA being produced or 32.38% of DCW. However, at 48 hours of fermentation growth, 3-oxo-C<sub>12</sub>-HSL was able to accumulate 33.40% of DCW as PHA, which was greater than that of C<sub>4</sub>-HSL, but this resulted in 1.72 g of PHA being produced, 0.02 g less than the culture supplemented with C<sub>4</sub>-HSL. Although the PHA yield (% DCW) was higher in the bioreactor supplemented with 3-oxo-C<sub>12</sub>-HSL, the overall product yield was slightly lower.

This can be explained through **Table 4.14**, which displays the kinetic growth parameters of *P. putida* KT2440 grown in bioreactors with the supplementation of exogenous quorum sensing molecules. C<sub>4</sub>-HSL had a higher product yield per substrate consumed value of 0.500 g/g as opposed to 3-oxo-C<sub>12</sub>-HSL, which produced a value of 0.465, this means the culture containing C<sub>4</sub>-HSL was more efficient in converting the raw substrate provided (glucose) into product (PHA), which is reflected in **Figures 4.14** and **4.16**, as by 48 hours C<sub>4</sub>-HSL consumed 8.27 g of glucose, whereas the bioreactor culture containing 3-oxo-C<sub>12</sub>-HSL consumed more glucose (8.76 g).

However, 3-oxo-C<sub>12</sub>-HSL was able to produce a higher product yield per biomass value of 0.457 g/g in comparison to the C<sub>4</sub>-HSL bioreactor that produced a value of 0.438. Product yield per biomass produced is able to show the ratio between amount of product and biomass produced, thus meaning 3-oxo-C<sub>12</sub>-HSL produced less biomass than C<sub>4</sub>-HSL, but similar amounts of PHA, which resulted in a higher product yield per biomass value. This is further supported by the fact the culture containing C<sub>4</sub>-HSL produced a higher biomass yield value of 1.141 in comparison to 3-oxo-C<sub>12</sub>-HSL, which produced a value of 1.017, thus meaning C<sub>4</sub>-HSL was able to produce more biomass between 24 and 48 hours than the culture supplemented with 3-oxo-C<sub>12</sub>-HSL.

**Table 4.14** PHA productions of *P. putida* KT2440 in batch mode fermentation using 2 L bioreactors containing production media with the addition of exogenous quorum sensing molecules at a concentration of 10 µM.

Productions were calculated using data of samples collected at 24 and 48 hours.

<b>Quorum sensing molecules</b>	$Y_{\bar{X}} (g/g)$	$Y_{\bar{P}} (g/g)$	$Y_{\bar{P}} (g/g)$	$Q_p (g/L.H)$ ( $\times 10^3$ )
Control	0.861	0.373	0.433	16.560
C <sub>4</sub> -HSL	1.141	0.500	0.438	15.771
C <sub>6</sub> -HSL	1.262	0.421	0.334	13.791
3-oxo-C <sub>12</sub> -HSL	1.017	0.465	0.457	16.161

Interestingly, although C<sub>6</sub>-HSL was unable to elicit as strong of a change in the production of PHAs when compared to the other two quorum sensing molecules, its presence was able to increase the amount of DCW accumulated, producing the highest DCW at 48 hours (5.95 g/L). This was also reflected in the kinetic growth parameters as the culture supplemented with C<sub>6</sub>-HSL produced the highest biomass yield value of 1.262 g/g. Therefore, it could be suggested that the presence of C<sub>6</sub>-HSL encourages cell growth as opposed to product production in the form of PHAs.

Across both shake flask and bioreactor fermentations, after 48 hours of fermentation polymer yield (% DCW) decreases. This finding was more pronounced in cultures grown in shake flasks than in comparison to cultures grown in bioreactors. However, this decline in PHA yield (% DCW) is most likely in response to glucose concentration within the media falling to a level in which cell growth is unsustainable and therefore PHA is utilised as a response to support growth of the culture under carbon deficient conditions. As previously stated, PHAs are accumulated intracellularly as a form of energy reservoir that can be used in the future to sustain growth. As every fermentation in this project was carried out in batch mode, the media was not replenished and therefore the culture has a higher possibility of utilising the accumulating PHA granules when facing unfavourable conditions such as carbon deficient conditions. As a result, to achieve higher yields off PHA and to prevent the utilisation of PHAs accumulated by cultures, it could be advised to explore different fermentation approached such as to step fed-batch fermentations. In this fermentation approach the first step is to achieve a high cell concentration, which is then followed by limiting the cultures growth in

order to promote the production of PHAs due to nutrient limiting conditions such as nitrogen. For example, Kim *et al.*, (1997) carried out a fermentation with this approach using *P. putida* grown on two different carbon sources (glucose and octanoate). PHA yield reached up to 40% (% DCW), which resulted in 18.6 g/L of PHA being produced.

Ultimately, the results thus have far demonstrated the supplementation of exogenous quorum sensing molecules have had a positive effect on the biosynthesis of PHAs produced by *P. putida* KT2440. Overall, through the addition of exogenous quorum sensing molecules, the amount of PHA produced increased from a minimum of 1.53% when using C<sub>6</sub>-HSL to a maximum of 7.24% when supplementing C<sub>4</sub>-HSL at shake flask level (**Figure 4.6**). Whereas in bioreactors a minimum increase of 1.57% was observed when using C<sub>6</sub>-HSL to a maximum increase of 10.89% when supplying C<sub>4</sub>-HSL exogenously to *P. putida* KT2440 cultures (**Figure 4.17**). This could possibly suggest that the addition of exogenous quorum sensing molecules when added to cultures of *P. putida* KT2440 enhances the amount of PHA produced, which aids in reducing their cost of production. However, it could be suggested that the amount of PHA yielded within shake flasks was relatively low in comparison to previous studies. This could suggest that further optimisation is required to obtain the highest levels of PHA yield possible from *P. putida* KT2440. Yet, the reason as to why the addition of quorum sensing molecules leads to an increase in the production of PHAs has not yet been understood completely and will be explored in **Section 4.6.3**.

#### **4.6.2 Characterisation and identification of MCL PHAs produced by *P. putida* KT2440**

In order to be able to accurately characterise and identify the specific type of PHA produced by *P. putida* KT2440 in shaken flask fermentations or bioreactors, four different experiments were carried out. The first two experiments (Sudan Black B and Nile red staining) were chosen due to their ability to easily identify the presence of PHAs, which would allow for any modifications to be made to the fermentation process, if the presence of PHAs

was not detected. Once the presence of PHAs was confirmed, the latter two experiments (FTIR and GC-MS) were carried out for their ability to be able to specifically characterise the type of PHA produced as well as the deduce the exact monomeric composition. These experiments were carried out in specific order, as each experiment would build upon the results of the last, whilst increasing in the power of discrimination. As a result, a characterisation profile of the PHA produced was developed simultaneously whilst the study was still ongoing.

The first of the characterisation and identification experiments was to stain cultures grown in the presence of different quorum sensing molecules with Sudan Black B dye, which was used for the indication of inclusion bodies. Each sample ultimately yielded a positive result meaning the culture was able to successfully produce and store PHAs regardless of the presence of exogenous quorum sensing molecules. However, because of the dye's affinity to lipids as well as PHAs, cultures could appear to test positive for producing and harbouring PHAs, when in reality this is not the case. This is because all bacteria are surrounded by a bacterial membrane consisting of a lipid matrix that resembles a phospholipid bilayer. As a result, it is this membrane that could be dyed resulting in the positive result. Based on findings by Ghate *et al.*, (2011) they explained that for cultures to test positive for PHAs, colonies stained should also have a dark spot in the middle of the colony itself. It was also reported that during the treatment of the plates with Sudan Black B dye, the use of solvents such as absolute ethanol would cause some cells to burst open, whilst also killing cells and removing the dye during the process.

Therefore, it is the dark spot in the middle of the colony, which is used to discriminate between whether a colony is truly producing and harbouring PHAs. **Figure 4.7** indicates the presence of these spots with the colonies themselves, however, there also is large amount of area around the culture itself stained with Sudan Black B. This could be the staining of the bacterial membrane or it could be the potential staining of a lipid-type product being secreted from the cells. Sudan Black B dye was used to stain samples from the 1 L shake flask fermentations, which was used as the primary methods for

the confirmation of PHAs. To confirm the results produced during this experiment, samples were then stained with Nile red dye and observed under a fluorescent microscope.

Nile red was used to stain cultures for the identification of intracellular PHAs, which appeared a bright red colour when visualised. **Figure 4.8** displays the ability of *P. putida* KT2440 to accumulate PHAs in the presence of the untreated control, DMSO and exogenous quorum sensing molecules. The ability for the culture to be able to produce and accumulate PHAs was expected as it was specifically grown on a production medium that had a high carbon/nitrogen ratio, which creates an environment that promotes the production of PHAs. However, when comparing **Figure 4.8C** and **4.8D** (representative of C<sub>4</sub>-HSL and 3-oxo-C<sub>12</sub>-HSL) against the other cultures also dyed with Nile red, a noticeable increase in the number of cells present within the sample can be observed. This was in line with the results gathered during the creation of the growth profiles. Both cultures supplemented with C<sub>4</sub>-HSL and 3-oxo-C<sub>12</sub>-HSL not only yielded the most PHA (% DCW) at 48 hours (22.67% and 23.86%, respectively), but were amongst the highest ODs too (8.568 and 9.355, respectively). In turn, it would have been expected that these two particular cultures, would have shown the most cellular growth and accumulation of PHA when observed under the microscope. However, as previously mentioned OD is not an accurate indication for cellular growth, particularly when a culture is able to accumulate intracellular products such as PHAs.

Once PHAs were confirmed to have been produced and accumulated by the cultures they were extracted and purified, before being analysed through two different experiments to determine what particular type of PHA was produced. As previously mentioned, the first of these experiments was through FTIR analysis. **Figures 4.9/4.10** and **4.18** display the FTIR spectra produced of each PHA sample extracted from shake flask and bioreactor respectively. Fundamentally, every sample extracted produced absorption bands in 1725 – 1730 cm<sup>-1</sup>, which corresponded to the stretching of the ester carbonyl group (C=O) and between 1160 – 1161 cm<sup>-1</sup>, which related to the -CO stretching

group. These two absorption bands are indicative that the PHA produced was that of MCL. This was further supported by the fact that three additional bands appeared in the range of 2955 – 2956, 2922 – 2927 and 2854 – 2857  $\text{cm}^{-1}$  that correspond to the aliphatic C-H group of the pendant alkyl group, which are also characteristically found in MCL PHAs.

When comparing the samples produced within the shake flasks and bioreactors there was no difference as bands appeared within the expected absorption ranges characteristic for MCL PHAs. However, the intensities of these bands varied slightly from sample to samples (**Figure 4.9B**), which was most likely due to the differing degrees of crystallinity between samples. It was also observed that the presence of exogenous quorum sensing molecules had no impact on the structural characteristics of the PHAs produced. This conclusion was able to be drawn through the comparison of the FTIR spectra produced from the untreated control and samples grown in the presence of exogenous quorum sensing molecules. When comparing the two types of spectra, there was no difference in the absorption bands detected, as they were virtually the exact same as the control's FTIR spectra. Although the general structure of the PHA was identified at this point, FTIR was unable to uncover the specific monomeric composition of the PHA. As a result, GC-MS was employed.

GC-MS analysis was used to be able to identify the specific monomeric composition of the polymers produced by *P. putida* KT2440 when grown in the presence of different quorum sensing molecules. Examining the composition of the PHAs produced was a vital step in the study as it would be able to shed light on whether the presence of the exogenous quorum sensing molecules influenced the composition of the PHA or if the opted mode of fermentation had an influence.

To begin, it was found that the PHA produced was that of the copolymer P(3HO-co-3HD-co-3HDD) with 3HD appearing as the dominant monomer component of the PHA synthesised (~70 mol %), with minor monomer units of 3HO and 3HDD. This result did not change irrespective of the addition of

quorum sensing molecules, or the specific mode of fermentation as shown in **Figure 4.20**. This was in line with the findings of previous studies, such as the one carried out by Yang, Li and Jia, (2019) who were able to produce the same type of polymer with similar monomer composition using *P. putida* KT2440 in fed-batch fermentations within bioreactors. However, others were able to conclude that *Pseudomonas* species usually produce PHAs with the main monomer unit usually comprising of 3HD when specifically grown on structurally unrelated simple sugars, such as glucose.

The monomeric composition of PHAs is strictly influenced by the carbon source utilised during the fermentation process. When in the presence of structurally related carbons (e.g., fatty acids), the final composition of the polymer reflects that of the substrate, whereas when unrelated substrates (e.g., carbohydrates) are utilised, the monomeric unit of the PHAs are independent of the structure of the carbon source (Basnett *et al.*, 2020). For example, Le Meur *et al.*, (2012) carried out a study on the effect of MCL PHA production by *P. putida* KT2440 when using different carbon sources such as xylose and octanoic acid. The study was able to uncover that the main monomeric unit of the PHA produced was that of 3HO (87 mol %) when using octanoic acid as the sole carbon source. Notably, the PHA monomer unit 3HD was not detected in the final product, which is usually produced if carbohydrates are present. The appearance of 3HO as the dominant monomer unit as well as the absence of 3HD aided in confirming that the PHA was produced from solely octanoic acid, as the presence of any carbohydrates within the media would have been expected to result in the appearance of 3HD monomer units, even as a minor component. The ability of being able to influence the monomeric composition of PHAs produced using specific carbon sources is important, as ultimately the final mechanical and physical properties of the polymer are dependent on the ratios of the monomeric units that comprise the entire PHA.

As previously mentioned, during this study glucose was opted as the sole carbon source, which is classified as an unrelated substrate. *Pseudomonas* species possess the ability to convert sugars into PHAs through the fatty acid

*de novo* biosynthesis pathway (Pathway III) as explained in **Section 1.2.3.2**. One of the two enzymes (3-hydroxyacyl-ACP dehydratases and acyl:ACP desaturase) involved in this pathway is required to catalyse the dehydration of 3-hydroxyacyl-ACP and is restricted to substrates with 10 carbons (Poblete-Castro *et al.*, 2014). As a result of this restriction, the nature of the PHA synthesis pathway - fatty acid *de novo* biosynthesis pathway - determines the pool of unsaturated fatty acids, which finally yields the high content of 3HD present in the final polymer when glucose is used as the carbon source. Once again, this study agreed with previous studies, as the MCL PHA produced was shown to possess a high content of 3HD.

Although not all *Pseudomonas* species are able to accumulate MCL PHA which can be observed within *Pseudomonas extremaustralis* (Catone *et al.*, 2014). When grown on structurally unrelated carbon sources such as glucose, the organism must first be able to metabolise the carbohydrate into acetyl-CoA, which would then go on to enter the fatty acid *de novo* biosynthesis pathway to produce MCL PHAs. It is in this pathway where the enzyme 3-hydroxyacyl-ACP:CoA transferase, encoded for by the *PhaG* gene links the fatty acid *de novo* biosynthesis pathway with MCL PHA production. Therefore, the inability of an organism to produce MCL PHAs could be ascribed due to the lack of this transferase activity, and thus results in *P. extremaustralis* producing exclusively PHB.

Three unique monomeric units were able to be identified within the PHAs produced in this study, leading to the conclusion that the PHA produced was that of P(3HO-co-3HD-co-3HDD). However, some studies were able to indicate the presence of an additional monomer unit. The monomer unit 3HHx was found in PHAs produced from *Pseudomonas* species such as *P. putida* KT2442. Huijberts *et al.*, (1992) was able to produce a copolymer of poly(3-hydroxyhexanoate-co-3-hydroxyoctanoate-co-3-hydroxydecanoate-co-3-hydroxydodecanoate) (P(3HHx-co-3HO-co-3HD-co-3HDD)) when grown on unrelated carbon sources such as glucose and glycerol. This PHA produced had 6.9 mol % and 21.4 mol % of 3HHx present when grown using glucose and glycerol respectively. However, the dominant monomeric unit of the PHA

remained as 3HD with molar fractions of 74.3 mol % and 63.6 mol % respectively.

This could indicate the need for further analysis of the PHA produced in this study as it is possible that the monomer unit of 3HHx was present in such low amounts that it was unable to be detected via GC-MS. Alternatively, there could be a possibility of the MS spectrum of methyl ester 3HHx was not present in the NIST, hence the monomer could not be matched in the library and detected, but this is highly unlikely as the NIST library is one of the most expansive MS spectra library available. Alternative methods could have also been employed to help to determine the monomeric composition of the PHA produced such as proton nuclear magnetic resonance ( $^1\text{H}$  NMR) as this method has a greater separation power and works at a higher sensitivity (Rijk *et al.*, 2005). There is also the possibility that the monomer of 3HHx was not present at all within the polymer produced and thus as to why a peak was not produced during GC-MS analysis.

Ultimately, the composition of the PHA produced remained the same, with 3HD appearing as the dominant monomer unit (~70 mol %) irrespective of the addition of quorum sensing molecule or mode of fermentation utilised. This was to be expected because as previously stated, monomer composition is strictly influenced solely by carbon source and thus meaning that quorum sensing molecules could potentially be added to fermentations that produce PHAs, without having the monomer composition of the PHA changing. As a result, this allows for the production of specific PHAs with unique monomer compositions to be produced, depending on carbon sources, whilst simultaneously increasing the yield when adding exogenous quorum sensing molecules.

#### **4.6.3 Molecular biology**

Throughout this study the main aim has always been to investigate as to whether the supplementation of exogenous quorum sensing molecules has any effect at all on the production of PHAs. However, for a change in

production to occur there must be a change at a molecular level to trigger this change, which is the reason as to why this specific line of investigation was carried out. This investigation set out to explore the expression of key genes related to the production of PHAs and study if their expression changed when in the presence of exogenous quorum sensing molecules throughout the fermentation period. The genes that were examined were *PhaC1* and *PhaZ*. The MCL PHA gene cluster (*PhaC1ZC2D*) is well conserved amongst MCL PHA producers such as *P. putida* KT2440 (Catone *et al.*, 2014), which encodes for two class II PHA synthase genes (*PhaC1* and *PhaC2*), flanking a PHA depolymerase gene (*PhaZ*) with a transcriptional activator at the end (*PhaD*) as shown in **Figure 1.4**. As previously mentioned in **Section 4.5.1**, all samples reacted positively and produced a PCR fragment with amplicon sizes of ~540 bp and ~792 bp, respective to *PhaC1* and *PhaZ* genes to confirm the presence of the genes within the genome itself. Samples were then analysed for the change of expression of these two genes every 24 hours over a 72 hour period via qPCR.

Gene expression studies were carried out, which showed an increase in the regulation of the genes *PhaC1* and *PhaZ* throughout the entire 72 hour fermentation period when cultures were supplemented with all three different quorum sensing molecules. However, of these three quorum sensing molecules, C<sub>4</sub>-HSL was able to elicit a statistically significant increase in regulation of *PhaC1* at 48 hours, whereas 3-oxo-C<sub>12</sub>-HSL increased regulation significantly of *PhaC1* at 48 and 72 hours of fermentation. This indicates that C<sub>4</sub>-HSL and 3-oxo-C<sub>12</sub>-HSL are both effective at actively increasing the regulation of the *PhaC1* gene, which is responsible for the production of PHA. Though, all of the quorum sensing molecules also had an effect on the regulation of *PhaZ*, which encodes for PHA depolymerase. By 48 hours of fermentation the addition of C<sub>4</sub>-HSL and 3-oxo-C<sub>12</sub>-HSL were able to result in a significant increase of the transcription of *PhaZ*. This increase continued till the end of the fermentation, with 3-oxo-C<sub>12</sub>-HSL eliciting the highest level of fold change. C<sub>6</sub>-HSL was also able to increase the transcription of both PHA synthase and PHA depolymerase throughout the fermentation period,

however these increases were not statistically significant when compared against the untreated control sample.

Although, it has been well documented that *P. putida* KT2440 does not possess a complete functioning quorum sensing system as its genome sequence does not encode for a LuxI homologue. However, this is not uncommon with strains belonging to this species as one third of the strains do not have a complete quorum sensing system. As a result, *P. putida* KT2440 is unable to produce quorum sensing molecules itself, but still retains the ability to recognise AHLs through the solo LuxR homolog, designated as PpoR (*Pseudomonas putida* orphan regulator) (Fernández-Piñar *et al.*, 2011). This is a highly conserved gene and has been shown to be present amongst a various number of strains within the species itself, thus suggesting that it forms part of the core genome of *P. putida*. Subramoni and Venturi, (2009) were able to demonstrate that PpoR has the ability to bind to AHLs like 3-oxo-C<sub>6</sub>-HSL and other structurally similar quorum sensing molecules such as 3-oxo-C<sub>12</sub>-HSL, which was then shown to regulate several loci, but interestingly not the colonisation of rhizosphere, which is what is usually promoted when this particular type of AHL is produced. For example, *P. putida* IsoF possess orthologues of Ppul and PpuR, which are responsible for the synthesis and response to 3-oxo-C<sub>12</sub>-HSL, which has been shown to have an influence on the development of structural biofilm. Alternatively, *P. putida* WCS358 also possesses the same orthologues, but to date no Ppul/PpuR regulated phenotype has been found for this strain yet (Veselova, 2010). This pair of orthologues shares the highest identity (~50%) with the LasI and LasR system of *P. aeruginosa*.

Even though *P. putida* KT2440 does not possess the ability to synthesis AHLs through the traditional route of LuxI homologues. It is still able to produce a variety of different of AHLs such as C<sub>4</sub>-HSL, C<sub>6</sub>-HSL and *N*-(3-hydroxy-tetradecanoyl)-L- homoserine lactone (3-OH-C<sub>14</sub>-HSL) because of a HdtS homologue present within its genome sequence. It has been reported that *Pseudomonas fluorescens* F113 can synthesise certain AHLs as by-products resulting from the activity of HdtS, an acyltransferase involved in phosphatidic

acid biosynthesis and can be considered another protein family that is capable of AHL biosynthesis (Laue *et al.*, 2000). The presence of these quorum sensing molecules was verified by Fernández-Piñar *et al.*, (2011) who grew *P. putida* KT2440 using a range of different media and carried out ethyl acetate extractions of whole cells from cultures. The organic extracts were then analysed using liquid chromatography - mass spectroscopy (LC-MS) resulting in the identification of AHLs. Interestingly, both C<sub>4</sub>-HSL and C<sub>6</sub>-HSL were produced when grown on minimal salts media using glucose as the sole carbon source. Nevertheless, despite *P. putida* KT2440 not retaining a functional LuxI homolog within its genome, it is still able to recognise exogenous quorum sensing molecules because of its solo LuxR homolog (PpoR). This solo response regulator could be activated through the addition of the exogenous quorum sensing molecules that are supplemented into the production media such as 3-oxo-C<sub>12</sub>-HSL. In turn, this could begin the quorum sensing circuit, which goes on to trigger the increased production of PHAs.

Interestingly throughout this study C<sub>4</sub>-HSL has shown to have the greatest effect on the production of PHAs, increasing the amount of PHA produced by a maximum of 7.24% in shake flasks and 10.89% in bioreactors. This AHL could have possibly been recognised by the PpoR homolog, due to the similarities in structure observed between 3-oxo-C<sub>12</sub>-HSL and C<sub>4</sub>-HSL as shown in **Figure 1.8**. An explanation for this increase in production of PHAs could come in the simplest form of when cultures of *P. putida* KT2440 are supplemented with exogenous quorum sensing molecules there is a change in the transcription of *PhaC1* genes and *PhaZ* genes as shown in **Figure 4.21**.

However, an alternative theory that needs investigation could be that C<sub>4</sub>-HSL is known to increase rhamnolipid synthesis, which shares the same pool of precursor molecules as PHAs. As previously mentioned, Martinez *et al.*, (2020) was able to explain that quorum sensing circuits can control the production of both rhamnolipids and PHAs through the regulation of *ScmR*. Mohanan *et al.*, (2019) was also able to show that PHA production was under the influence of quorum sensing molecules. The potential increase in rhamnolipid production in response to the addition of C<sub>4</sub>-HSL to culture of *P.*

*putida* KT2440 could have led to an increase in rhamnolipid precursor molecule production, which in turn was then converted into PHAs due ScmR regulation, which in turn increases production of PHAs as ScmR promotes the transcription of both *PhaC1* and *PhaZ*. As a result, the production of rhamnolipids could be investigated when cultures of *P. putida* KT2440 are supplemented with exogenous quorum sensing molecules.

Ultimately, this study was able to identify the change in transcription of two key *Pha* genes, which could be attributed to the reason as to why an increase in PHA was observed when supplementing exogenous quorum sensing molecules to cultures of *P. putida* KT2440. Of the three quorum sensing molecules C<sub>4</sub>-HSL and 3-oxo-C<sub>12</sub>-HSL were the most effective at increasing the amount of PHA produced, as the change in the level of transcription of the two genes examined were the highest. C<sub>6</sub>-HSL was able to have an influence on the transcription of the two genes, however this was less pronounced. Interestingly, cultures supplemented with C<sub>6</sub>-HSL saw a noticeable increase in DCW (shake flask 2.31 g/L, bioreactors 5.95 g/l) , which was greater than that was observed with C<sub>4</sub>-HSL and 3-oxo-C<sub>12</sub>-HSL (shake flask 2.16 and 2.02 g/L, respectively, bioreactors 5.38 and 5.14 g/L, respectively), thus suggesting C<sub>6</sub>-HSL promoted increasing cellular density as opposed to PHA production, which could be a further line of investigation.

## **Chapter 5:** General Discussion and conclusions

Across the two cultures, it can be observed that cultures grown in the medium supplemented with quorum sensing molecules displayed a slightly longer lag period at the start of the fermentation regardless of if they were grown in shaken flask or bioreactors. This could be attributed to the fact that the exogenous quorum sensing molecules were dissolved in DMSO, which is a known bacteriostatic agent that inhibits the growth of bacteria. To circumvent this issue, exogenous quorum sensing molecules could be dissolved into aqueous buffers such as PBS, but this reduces the usability of the quorum sensing molecule as it can only be stored for up to a day.

It should also be noted that OD was an inaccurate method for the estimation of growth under the conditions employed throughout this study as they promoted the production of PHAs. This is because both *C. necator* H16 and *P. putida* KT2440 were able to synthesis significant amounts of PHAs, which are stored within the cell itself, which has an impact on the morphology of each individual cell. This factor affects the light scattering and thus makes OD values unsuitable for the estimation of growth throughout the fermentation (Martinez and Déziel, 2020).

As shown in **Figure 3.8** and **4.8** both species of bacteria were successfully dyed with Nile red and visualised using a fluorescent microscope. The Nile red dye was able to dye cellular structures as well as lipid inclusions such as PHA granules that were stored within the cell itself. The majority of PHA granules observed were localised against or close to the cytoplasmic membrane, but some PHA granules can be observed to be localised in the centre of the cells. The morphology and location of the PHA granule within the cell plays an important role in the cells ability to survive as it as an influence on the overall cell's morphology and diameter (Jendrossek, Selchow and Hoppert, 2006). Changes with a cell's morphology and diameter, can directly result in a change in the cell's volume or surface area, which in turn affects the cell's metabolic flux, biosynthetic capacity and nutrient exchange. Therefore, as a result bacterium must be able to precisely control their sizes and shapes in order to efficiently import nutrients, meet the requirements imposed by cell division, be able to attach to external surfaces to take advantage of passive dispersal

mechanisms, move purposefully to pursue nutrients or avoid inhibitors and avoid predation by other organisms (Mravec *et al.*, 2016). This expands upon the role of PHAs play within the cell, maintaining and regulating cellular function as opposed to strictly being a form of energy storage for the cell.

As previously mentioned, when comparing PHAs produced in medium supplemented with the addition of exogenous quorum sensing molecules against PHAs produced in the untreated control, it was found that there was no difference in the monomeric composition of the PHAs produced by either *C. necator* H16 or *P. putida* KT2440. It was also determined that the mode of fermentation did not have a significant difference on the type of PHA produced (**Figure 4.20**). As a result, it can be concluded that quorum sensing does not influence the structural properties of PHA produced as both PHB and P(3HO-co-3HD-co-3HDD) were both identified as the types of PHA produced by *C. necator* H16 and *P. putida* KT2440 respectively. Instead, the type of substrate utilised by the culture acts as the main influencing factor for the composition of PHAs produced. The conclusion that quorum sensing does not have a role in the determination of the monomeric composition of the PHA produced was further supported by the study previously mentioned in **Section 1.6.2.3**. Irorere *et al.*, (2019), found that there was no difference in the structure of PHAs produced between two strains of *B. thailandensis* E264. Of these two strains, one was genetically modified, so that it was unable to successfully utilise quorum sensing molecules, but it was still able to produce and accumulate PHAs. The PHAs produced by each strain were compared against each other via FTIR and GC-MS. It was concluded that there was no difference in the structure and composition of either type of PHA produced between the two strains, thus further supporting the conclusion made earlier that of quorum sensing has no significant effect on the monomeric composition of the PHA produced.

During this study a single reference gene was used to normalise the data produced during qPCR experiments to aid in quantifying the data obtained. This particular reference gene was chosen because of its ability to be continually expressed regardless of the environmental conditions it was grown

in. However, although the experiment could take place with a singular reference gene, it was not recommended by the Minimum Information for publication of Quantitative real-time PCR Experiments (MIQE) guidelines, which states a minimum of two reference genes should be used for normalisation of data. This is because a single reference gene could lead to erroneous expression differences of more than the actual value (Bustin *et al.*, 2009). As a result, it is strongly recommended that in the future multiple reference genes are used to help improve the accuracy of the qPCR data obtained. Furthermore, during this study the Livak method was also used as described in **Section 2.8.6.1**, which is unable to consider multiple reference genes and was also based off the assumption that the GOIs and reference genes are amplified with efficiencies near 100% and are within 5% of each other. To be able to use multiple reference genes to calculate the change in gene expression of GOIs, the Vandesompele method could be used, as it uses the geometric mean of the reference genes instead of the arithmetic mean. The use of the geometric mean helps to reduce the potential variance in the data provided if there are significant outliers.

In conclusion, this was the first time that a study had been able to demonstrate the effect of the supplementation of quorum sensing molecules and PHA production in *C. necator* H16 and *P. putida* KT2440. An increase in production was observed when cultures were supplemented with exogenous quorum sensing molecules at both shake flask and bioreactor level. However, this increase was greater in bioreactors than in comparison to shake flasks, which is most likely since physiological parameters can be better controlled in bioreactors such as aeration. The two types of PHAs were able to be successfully identified, and examined for any differences between their monomeric composition, in which no difference appeared. This was because monomeric structure of the PHA produced was strictly influenced by the carbon source utilised as opposed to the presence of exogenous quorum sensing molecules. Finally, qPCR was carried out to investigate as to why there was a change in the production of PHAs when the addition of quorum sensing molecules was added. It was observed that across all three quorum sensing

molecules, a change in transcription was observed in two key *Pha* genes, which are directly involved in the synthesis and breakdown of PHAs.

This work has been able to uncover a unique and novel method to aid in the increased production of PHAs, in which these observations can be exploited and used in the first instance for improving large scale production of PHAs. This concept can also be extended to other bacterial cultures. These findings not only have an impact on industry with regards to the enhance of production of PHAs, but also in terms of broadening research knowledge and understanding in the interaction of quorum sensing and the regulation of PHA production.

**Section 1.7** set out a hypothesis and it can be said that the null hypothesis can be rejected, whereas the alternative hypothesis can be accepted as the addition of exogenous quorum sensing molecules were effective agents in the overproduction of biopolymers such as PHAs.

## Chapter 6: Future Works

Results obtained during this study demonstrated the possibility of increasing the production of SCL and MCL PHAs through the addition of exogenous quorum sensing in *C. necator* H16 and *P. putida* KT2440 respectively. Based on the data, the following areas can be explored in order to improve further achieved outcomes.

## **6.1 Optimisation of fermentations for the production of PHAs**

Ultimately, the main goal of this project was to be able to increase the production of PHAs from two different bacteria that are well known for the ability to produce high amounts of PHAs. This was carried out to be able to create an economically viable route for the production of PHAs, which currently have a high cost of production associated with them when compared to their mineral based polymer counterparts. This study was able to successfully demonstrate the ability to increase the production of PHAs in both bacteria through the supplementation of exogenous quorum sensing molecule, however, further optimisation could take place to help reduce the costs further and potentially increase production even further. For example, during this study the maximum PHA yielded (% DCW) in *P. putida* KT2440 was in bioreactors using glucose as the sole carbon source, accumulating 33.4 (% DCW).

However, Xu *et al.*, (2021) were able to improve upon this result with the same bacteria accumulating 37.5% PHA yield (% DCW) using glycerol and lignin derivatives as carbon sources. Glycerol is a major byproduct in the manufacturing of biodiesel, of which 10.3 billion litres was produced between 2013 and 2018 (IEA, 2019). The large-scale production of biodiesel and in turn the glycerol generated may pose an issue regarding environment as large amounts of glycerol cannot be discarded safely in the environment (Quispe, Coronado and Carvalho Jr., 2013). Therefore, finding an alternative use such as being used to produce PHAs serves as a method to help discard the solvent, whilst aiding in reducing the cost of production by using a relatively inexpensive carbon source.

Alternatively, different fermentation strategies can be investigated to see if the production of PHA increases through the supplementation of exogenous quorum sensing molecules. Throughout this project batch mode fermentation was chosen as the mode of fermentation due to its ease and low maintenance. However, fed-batch mode could potentially aid in increasing the yield of PHAs as PHAs serve as a reservoir of carbon for the bacteria that are producing them which can be broken down when in nutrient limiting conditions such as low carbon concentrations. By increasing the concentration of carbon periodically the amount of PHA produced and accumulated could increase as the need to degrade PHAs is reduced, due to the supplementation of carbon throughout the fermentation period.

Furthermore, new strategies involving the addition of exogenous quorum sensing molecules could be adopted. During this study exogenous quorum sensing moles were added at the start of the fermentation within the production medium, with no further additions. However, given that *P. putida* KT2440 does not contain a LuxI homolog within its genome a potential research avenue could be to explore the addition of exogenous quorum sensing molecules over time. The addition of exogenous quorum sensing molecules at specific time points could potentially have an influence on the expression of key genes, such as the ones explored during this study (*PhaC1* and *PhaZ*), in which a change in their expression could result in higher yields of PHAs.

## **6.2 Further characterisation of PHAs**

During this study, the PHAs produced were able to be characterised using various different analytical techniques, resulting in the identification of the specific type of PHA produced by each bacterium. However, the properties of each PHA produced remains unknown and therefore limits their scope of usage within different industries and applications. To aid in increasing their viability within specific industries such as the healthcare sector, further analysis will be required. Characteristics such as the PHA's thermal properties and tensile strength are integral pieces of information as they allow for the

PHA produced to be used for specific applications that may require heat tolerance or high durability.

For examples, medical applications are often required to be heat tolerant for purposes of sterilisation. To assess the thermal properties of the PHAs produced, differential scanning calorimetry (DSC) could be employed. DSC is an analytical technique that can measure the heat flow rate to or from a sample as it is subjected to a controlled temperature program within a controlled atmosphere. In turn, through this analysis the heat capacity of the PHA can be determined as well as the thermal transition properties such as glass transition temperature and melting points.

Furthermore, the specific mechanical properties of the PHAs produced can be deduced through tensile tests. With known measurements of the PHAs dimensions such as length and cross-sectional area information about the PHA's tensile strength and Young's modulus can be defined. The amount of force required to physically break the PHA and the extent to which the polymer stretches or elongates to its breaking point can also be defined through this test. With this type of further characterisation, the PHAs produced in this study could be used to fulfil niche uses currently occupied by mineral-based plastics.

### **6.3 Analysis of alternative *Pha* gene expressions via qPCR**

Gene expression of arguably the most important *Pha* genes (*PhaC* and *PhaZ*) were analysed in both strains of bacteria used in this study, when supplemented with exogenous quorum sensing molecules. Although a change in gene expression was observed in these two genes, there are a multitude of other *Pha* genes that could have also shown a difference in gene expression that were not analysed.

For example, *PhaD*, is found downstream within the *Pha* gene cluster, encoding for a protein (PhaD) that acts as a transcriptional regulator belonging to the TetR family of regulators, activating the transcription of the phasin-encoding genes *PhaF* and *PhaI*, which are transcribed divergently to the other

*Pha* genes (de Eugenio *et al.*, 2010). *PhaD* plays an important role in the biosynthesis of PHAs, affecting the size and number of granules produced. Studies have shown mutant strains deficient of the *PhaD* gene accumulated less PHA, which were also smaller in size too. Therefore, an investigation could be undertaken to understand the expression of the *PhaD* gene when exposed to exogenous quorum sensing molecules. By ascertaining whether there is a change in expression of the gene, which has an influence on the size and number of granules, could help to build upon the results of this study, as although there were changes in expression of *PhaC* and *PhaZ* that resulted in an increase in production of PHAs, *PhaD* could also have played a role in increasing the amount of PHA produced.

#### **6.4 Increasing production of secondary metabolites from other species of bacteria when supplemented with exogenous quorum sensing molecules**

This study was able to identify the increased production of PHAs, when cultures were grown with the supplementation of exogenous quorum sensing molecules. This is because quorum sensing molecules act as signalling molecules that promote the production of secondary metabolites or virulence factors. Different bacteria possess the ability to produce a variety of secondary metabolites, in which the change in production could be altered if supplemented with exogenous quorum sensing molecules. For example, *P. aeruginosa* is a model species of bacteria for the production of rhamnolipids, however as with many other bacteria capable of producing a useful secondary metabolite, *P. aeruginosa* produces rhamnolipids at such low yields that is difficult to scale up owing to their high cost of production. The AHL 3-oxo-C<sub>12</sub>-HSL could alleviate this problem, as it is recognised by the LasR response regulator, which induces the transcription of the RhlR/I pathway. This pathway results in the production of C<sub>4</sub>-HSL that in turn leads to the increased production of rhamnolipids via rhamnolipid synthase (rhlAB). Alternatively, C<sub>4</sub>-HSL could be supplemented from the beginning, which could lead to the same result of increased production of the secondary metabolite, rhamnolipids. Therefore, the potential for increasing yields of metabolites produced by

various bacteria throughout the supplementation of exogenous quorum sensing molecules, could provide a route for high yield production that previously may not have been possible otherwise.

### **6.5 Production and addition of “crude” quorum sensing molecules**

The main principle of this project was to assess whether the addition of exogenous quorum sensing molecules would result in an increased production of PHAs, in a bid to develop a novel strategy that would aid in reducing the overall cost of production of PHAs, so that they are able to compete within the marketplace with their mineral-based polymer counterparts. This project was able to show that the presence of exogenous quorum sensing molecules is successful in increasing the production of PHAs, however the cost of the exogenous quorum sensing molecules must also be considered, which adds to the total cost of production. To reduce costs, a new strategy could be developed, spawned from this study. Developing a method to produce, harvest and purify quorum sensing molecules from spent culture medium that could contain quorum sensing molecules could potentially help to reduce the overall cost of production of PHAs. This also helps in creating a sustainable cycle within the process itself as the need to purchase exogenous quorum sensing molecules is eliminated.

### **6.6 Effect of PHA production on Gram-positive bacteria when in the presence of exogenous quorum sensing molecules**

*C. necator* H16 and *P. putida* KT2440 were both selected for as they are well known for their ability to produce and accumulate high amounts of SCL and MCL PHAs respectively. They were also chosen due to their ability to interact with the same types of quorum sensing molecules owing to their classification of being Gram-negative bacteria. This study was able to successfully demonstrate the impact quorum sensing has on the regulation of PHA production and change in yield, which was previously unclear.

However, the relationship between quorum sensing and PHA production has yet to be established within Gram-positive bacteria, who utilise AIPs as a form

of quorum sensing molecule. *Bacillus subtilis* is well known for its ability to produce SCL PHA with a wide range of different compositions and high yields of PHAs, with some species yielded up to a maximum of 69% (% DCW). The potential to increase yield is a desirable prospect with the advantage of being able to produce different compositions of SCLs as they have different mechanical and thermal properties, expanding the viability of PHAs within the market. ComQXPA and Rap-Phr, are two different quorum sensing systems utilised by *B. subtilis* resulting in the coordination of biofilm formation, production of proteases and surfactins, but as previously stated, the impact of these quorum sensing systems has yet to be explored in relation to the production of PHAs (Kalamara *et al.*, 2018). The core principle of this study could be easily applied to Gram-positive bacteria such as *B. subtilis*, by supplementing exogenous quorum sensing molecules (AIPs) within production media that specifically promotes the production of PHAs and assessing whether the presence of these exogenous AIPs has an impact on the production of PHAs.

## Chapter 7: References

Abisado, R., Benomar, S., Klaus, J., Dandekar, A. and Chandler, J. (2018). Bacterial Quorum Sensing and Microbial Community Interactions. *mBio*, 9 (5), 1-13.

Albuquerque, M., Eiroa, M., Torres, C., Nunes, B. and Reis, M. (2007). Strategies for the development of a side stream process for polyhydroxyalkanoate (PHA) production from sugar cane molasses. *Journal of Biotechnology*, 130 (4), 411-421.

Andrady, A. and Neal, M. (2009). Applications and societal benefits of plastics. *Philosophical Transactions of the Royal Society B: Biological Sciences*, 364 (1526), 1977-1984.

Babu, R., O'Connor, K. and Seeram, R. (2013). Current progress on bio-based polymers and their future trends. *Progress in Biomaterials*, 2 (1), 8.

Basnett P (2014). Biosynthesis of polyhydroxyalkanoates, their novel blends and composites for biomedical applications. School of Life Sciences, University of Westminster, London.

Basnett, P., Marcello, E., Lukasiewicz, B., Nigmatullin, R., Paxinou, A., Ahmad, M., Gurumayum, B. and Roy, I. (2020). Antimicrobial Materials with Lime Oil and a Poly(3-hydroxyalkanoate) Produced via Valorisation of Sugar Cane Molasses. *Journal of Functional Biomaterials*, 11 (2), 24.

Bhattacharyya, A., Pramanik, A., Maji, S., Haldar, S., Mukhopadhyay, U. and Mukherjee, J. (2012). Utilization of vinasse for production of poly-3-(hydroxybutyrate-co-hydroxyvalerate) by *Haloferax mediterranei*. *AMB Express*, 2 (1), 34.

Bourque, D., Pomerleau, Y. and Groleau, D. (1995). High-cell-density production of poly- $\beta$ -hydroxybutyrate (PHB) from methanol by *Methylobacterium extorquens*: production of high-molecular-mass PHB. *Applied Microbiology and Biotechnology*, 44 (3-4), 367-376.

Braunegg, G., Lefebvre, G. and Genser, K. (1998). Polyhydroxyalkanoates, biopolyesters from renewable resources: Physiological and engineering aspects. *Journal of Biotechnology*, 65 (2-3), 127-161.

Bustin, S., Benes, V., Garson, J., Hellemans, J., Huggett, J., Kubista, M., Mueller, R., Nolan, T., Pfaffl, M., Shipley, G., Vandesompele, J. and Wittwer, C. (2009). The MIQE Guidelines: Minimum Information for Publication of Quantitative Real-Time PCR Experiments. *Clinical Chemistry*, 55 (4), 611-622.

Butler, C. (2018). Climate Change, Health and Existential Risks to Civilization: A Comprehensive Review (1989–2013). *International Journal of Environmental Research and Public Health*, 15 (10), 2266.

Cao, M., Feng, Y., Wang, C., Zheng, F., Li, M., Liao, H., Mao, Y., Pan, X., Wang, J., Hu, D., Hu, F. and Tang, J. (2011). Functional definition of LuxS, an autoinducer-2 (AI-2) synthase and its role in full virulence of *Streptococcus suis* serotype 2. *The Journal of Microbiology*, 49 (6), 1000-1011.

Catone, M., Ruiz, J., Castellanos, M., Segura, D., Espin, G. and López, N. (2014). High Polyhydroxybutyrate Production in *Pseudomonas extremaustralis* Is Associated with Differential Expression of Horizontally Acquired and Core Genome Polyhydroxyalkanoate Synthase Genes. *PLoS ONE*, 9 (6).

Cavalheiro, J., de Almeida, M., Grandfils, C. and da Fonseca, M. (2009). Poly(3-hydroxybutyrate) production by *Cupriavidus necator* using waste glycerol. *Process Biochemistry*, 44 (5), 509-515.

Chee, J., Tan, Y., Samian, M. and Sudesh, K. (2010). Isolation and Characterization of a *Burkholderia* sp. USM (JCM15050) Capable of Producing Polyhydroxyalkanoate (PHA) from Triglycerides, Fatty Acids and Glycerols. *Journal of Polymers and the Environment*, 18 (4), 584-592.

Chee, J., Yoga, S., Lau, N., Ling, S., M. M. Abed, R. and Sudesh, K. (2010). *Current Research, Technology And Education Topics In Applied Microbiology And Microbial Biotechnology*. 2nd ed. Badajoz, Spain: Formatex Research Center.

Chen, G. (2009). Plastics Completely Synthesized by Bacteria: Polyhydroxyalkanoates. *Microbiology Monographs*, 14 (1), 17-37.

Chen, G., Zhang, G., Park, S. and Lee, S. (2001). Industrial scale production of poly(3-hydroxybutyrate-co-3-hydroxyhexanoate). *Applied Microbiology and Biotechnology*, 57 (1-2), 50-55.

Chen, Y., Hung, S., Chou, E. and Wu, H. (2018). Review of Polyhydroxyalkanoates Materials and other Biopolymers for Medical Applications. *Mini-Reviews in Organic Chemistry*, 15 (2), 105-121.

Chistoserdova, L., Kalyuzhnaya, M. and Lidstrom, M. (2009). The Expanding World of Methylotrophic Metabolism. *Annual Review of Microbiology*, 63 (1), 477-499.

Chomczynski, P. and Sacchi, N. (1987). Single-step method of RNA isolation by acid guanidinium thiocyanate-phenol-chloroform extraction. *Analytical Biochemistry*, 162 (1), 156-159.

Choudhary, S. and Schmidt-Dannert, C. (2010). Applications of quorum sensing in biotechnology. *Applied Microbiology and Biotechnology*, 86 (5), 1267-1279.

Dabrowska, D., Mozejko-Ciesielska, J., Pokój, T. and Ciesielski, S. (2020). Transcriptome Changes in *Pseudomonas putida* KT2440 during Medium-Chain-Length Polyhydroxyalkanoate Synthesis Induced by Nitrogen Limitation. *International Journal of Molecular Sciences*, 22 (1), 152.

Danson, M. and Hough, D. (1997). The Structural Basis of Protein Halophilicity. *Comparative Biochemistry and Physiology Part A: Physiology*, 117 (3), 307-312.

Davis, R., Kataria, R., Cerrone, F., Woods, T., Kenny, S., O'Donovan, A., Guzik, M., Shaikh, H., Duane, G., Gupta, V., Tuohy, M., Padamatti, R., Casey, E. and O'Connor, K. (2013). Conversion of grass biomass into fermentable sugars and its utilization for medium chain length polyhydroxyalkanoate (mcl-PHA) production by *Pseudomonas* strains. *Bioresource Technology*, 150 (1), 202-209.

Dawes, E. and Senior, P. (1973). The Role and Regulation of Energy Reserve Polymers in Micro-organisms. *Advances in Microbial Physiology*, 10, 135-266.

de Eugenio, L., Galán, B., Escapa, I., Maestro, B., Sanz, J., García, J. and Prieto, M. (2010). The PhaD regulator controls the simultaneous expression of the phages involved in polyhydroxyalkanoate metabolism and turnover in *Pseudomonas putida* KT2442. *Environmental Microbiology*, 12 (6), 1591-1603.

Deep, A., Chaudhary, U. and Gupta, V. (2011). Quorum sensing and bacterial pathogenicity: From molecules to disease. *Journal of Laboratory Physicians*, 3(1), 4.

Devi Palraj, N., Ayyasamy, M. and Kabilan, S. (2019). PCR validation of gene specific primer to detect intracellular MCL polyhydroxyalkanoates degrading bacteria from environmental samples. *Journal of Emerging Technologies and Innovative Research*, 6 (3), 483-490.

Divya, G., Archana, T. and Alejandro Manzano, R. (2013). Polyhydroxy Alkanoates - A Sustainable Alternative to Petro-Based Plastics. *Journal of Petroleum & Environmental Biotechnology*, 4 (3), 1-8.

- DuBois, M., Gilles, K., Hamilton, J., Rebers, P. and Smith, F. (1956). Colorimetric Method for Determination of Sugars and Related Substances. *Analytical Chemistry*, 28(3), 350-356.
- Dufour, J., Melero, J., Olivares, J. and Puyol, D. (2019). *Wastewater Treatment Residues As Resources for Biorefinery Products and Energy*, 1st ed. San Diego: Elsevier.
- Elliott, D. and Elliott, W. (2009). *Biochemistry and Molecular Biology*. 4th ed. New York City: Oxford University Press, 62-63.
- Ertan, F., Keskinler, B. and Tanriseven, A. (2021). Exploration of *Cupriavidus necator* ATCC 25207 for the Production of Poly(3-hydroxybutyrate) Using Acid Treated Beet Molasses. *Journal of Polymers and the Environment*, 15 (3), 1-15.
- Fernández-Piñar, R., Cámara, M., Soriano, M., Dubern, J., Heeb, S., Ramos, J. and Espinosa-Urgel, M. (2011). PpoR, an orphan LuxR-family protein of *Pseudomonas putida* KT2440, modulates competitive fitness and surface motility independently of N-acylhomoserine lactones. *Environmental Microbiology Reports*, 3 (1), 79-85.
- Francis, L. (2011). Biosynthesis of Polyhydroxyalkanoates and their medical applications. Ph.D. University of Westminster.
- Funston, S., Tsaousi, K., Smyth, T., Twigg, M., Marchant, R. and Banat, I. (2017). Enhanced rhamnolipid production in *Burkholderia thailandensis* transposon knockout strains deficient in polyhydroxyalkanoate (PHA) synthesis. *Applied Microbiology and Biotechnology*, 101 (23-24), 8443-8454.
- Gewert, B., Plassmann, M. and MacLeod, M. (2015). Pathways for degradation of plastic polymers floating in the marine environment. *Environmental Science: Processes & Impacts*, 17(9), 1513-1521.
- Geyer, R., Jambeck, J. and Law, K. (2017). Production, use, and fate of all plastics ever made. *Science Advances*, 3(7), 1-5.
- Ghate, B., Prashant, P., Kulkarni, C., Mungi, D. D., Patel, T. S., (2011), P(3HB) production using novel agro-industrial sources from different *Bacillus* species. *International Journal of Pharma and Bio Sciences* 2(3), 242-249.
- Gomez, J., Rodrigues, M., Alli, R., Torres, B., Netto, C., Oliveira, M. and da Silva, L. (1996). Evaluation of soil gram-negative bacteria yielding

polyhydroxyalkanoic acids from carbohydrates and propionic acid. *Applied Microbiology and Biotechnology*, 45 (6), 785-791.

Guzik, M., Kenny, S., Duane, G., Casey, E., Woods, T., Babu, R., Nikodinovic-Runic, J., Murray, M. and O'Connor, K. (2014). Conversion of post consumer polyethylene to the biodegradable polymer polyhydroxyalkanoate. *Applied Microbiology and Biotechnology*, 98 (9), 4223-4232.

Hahladakis, J., Velis, C., Weber, R., Iacovidou, E. and Purnell, P. (2018). An overview of chemical additives present in plastics: Migration, release, fate and environmental impact during their use, disposal and recycling. *Journal of Hazardous Materials*, 344(1), 179-199.

Han, J., Hou, J., Liu, H., Cai, S., Feng, B., Zhou, J. and Xiang, H. (2010). Wide Distribution among Halophilic Archaea of a Novel Polyhydroxyalkanoate Synthase Subtype with Homology to Bacterial Type III Synthases. *Applied and Environmental Microbiology*, 76 (23), 7811-7819.

Hermann-Krauss, C., Koller, M., Muhr, A., Fasl, H., Stelzer, F. and Brauneegg, G. (2013). Archaeal Production of Polyhydroxyalkanoate (PHA) Co- and Terpolyesters from Biodiesel Industry-Derived By-Products. *Archaea*, 2013, 1-10.

Higuchi-Takeuchi, M., Morisaki, K., Toyooka, K. and Numata, K. (2016). Synthesis of High-Molecular-Weight Polyhydroxyalkanoates by Marine Photosynthetic Purple Bacteria. *PLOS ONE*, 11 (8), 1-17.

Hopewell, J., Dvorak, R. and Kosior, E. (2009). Plastics recycling: challenges and opportunities. *Philosophical Transactions of the Royal Society B: Biological Sciences*, 364(1526), 2115-2126.

Huijberts, G., de Rijk, T., de Waard, P. and Eggink, G. (1994). <sup>13</sup>C nuclear magnetic resonance studies of *Pseudomonas putida* fatty acid metabolic routes involved in poly(3-hydroxyalkanoate) synthesis. *Journal of Bacteriology*, 176 (6), 1661-1666.

Huijberts, G., Eggink, G., de Waard, P., Huisman, G. and Witholt, B. (1992). *Pseudomonas putida* KT2442 cultivated on glucose accumulates poly(3-hydroxyalkanoates) consisting of saturated and unsaturated monomers. *Applied and Environmental Microbiology*, 58 (2), 536-544.

Idris, Z., Su Yean, O. and Kumar, S. (2018). Polyhydroxyalkanoates. *Kirk-Othmer Encyclopedia of Chemical Technology*, 27 (5), 1-26.

IEA (2019). *Renewables 2019*. Paris: IEA.

Jendrossek, D., Selchow, O. and Hoppert, M. (2006). Poly(3-Hydroxybutyrate) Granules at the Early Stages of Formation Are Localized Close to the Cytoplasmic Membrane in *Caryophanon latum*. *Applied and Environmental Microbiology*, 73 (2), 586-593.

Johnson, R., Mwaikambo, L. and Tucker, N. (2003). Biopolymers. *Rapra Review Reports*, 14(3), 3-24.

Kalamara, M., Spacapan, M., Mandic-Mulec, I. and Stanley-Wall, N. (2018). Social behaviours by *Bacillus subtilis*: quorum sensing, kin discrimination and beyond. *Molecular Microbiology*, 110 (6), 863-878.

Keshavarz, T. and Roy, I. (2010). Polyhydroxyalkanoates: bioplastics with a green agenda. *Current Opinion in Microbiology*, 13 (3), 321-326.

Kim, G., Lee, I., Yoon, S., Shin, Y. and Park, Y. (1997). Enhanced yield and a high production of medium-chain-length poly(3-hydroxyalkanoates) in a two-step fed-batch cultivation of *Pseudomonas putida* by combined use of glucose and octanoate. *Enzyme and Microbial Technology*, 20 (7), 500-505.

Kohler, T., Buckling, A. and van Delden, C. (2009). Cooperation and virulence of clinical *Pseudomonas aeruginosa* populations. *Proceedings of the National Academy of Sciences*, 106 (15), 6339-6344.

Koller, M. (2020). Established and advanced approaches for recovery of microbial polyhydroxyalkanoate (PHA) biopolyesters from surrounding microbial biomass. *The EuroBiotech Journal*, 4 (3), 113-126.

Kunasundari, B. and Sudesh, K. (2011). Isolation and recovery of microbial polyhydroxyalkanoates. *Express Polymer Letters*, 5 (7), 620-634.

Laue, B., Jiang, Y., Chhabra, S., Jacob, S., Stewart, G., Hardman, A., Downie, J., O'Gara, F. and Williams, P. (2000). The biocontrol strain *Pseudomonas fluorescens* F113 produces the Rhizobium small bacteriocin, N-(3-hydroxy-7-cis-tetradecenoyl)homoserine lactone, via HdtS, a putative novel N-acylhomoserine lactone synthase The GenBank accession number for the sequence determined in this work is AF286536. *Microbiology*, 146 (10), 2469-2480.

Law, J. and Slepecky, R. (1961). Assay of poly- $\beta$ -hydroxybutyric acid. *Journal of Bacteriology*, 82 (1), 33-36.

Le Meur, S., Zinn, M., Egli, T., Thöny-Meyer, L. and Ren, Q. (2012). Production of medium-chain-length polyhydroxyalkanoates by sequential feeding of xylose and octanoic acid in engineered *Pseudomonas putida* KT2440. *BMC Biotechnology*, 12 (1), p.53.

Lee, E., Jendrossek, D., Schirmer, A., Choi, C. and Steinbüchel, A. (1995). Biosynthesis of copolyesters consisting of 3-hydroxybutyric acid and medium-chain-length 3-hydroxyalkanoic acids from 1,3-butanediol or from 3-hydroxybutyrate by *Pseudomonas* sp. A33. *Applied Microbiology and Biotechnology*, 42 (6), 901-909.

Li, L., Hooi, D., Chhabra, S., Pritchard, D. and Shaw, P. (2004). Bacterial N-acylhomoserine lactone-induced apoptosis in breast carcinoma cells correlated with down-modulation of STAT3. *Oncogene*, 23 (28), 4894-4902.

Livak, K. and Schmittgen, T. (2001). Analysis of Relative Gene Expression Data Using Real-Time Quantitative PCR and the  $2^{-\Delta\Delta CT}$  Method. *Methods*, 25 (4), 402-408.

Lu, J., Tappel, R. and Nomura, C. (2009). Mini-Review: Biosynthesis of Poly(hydroxyalkanoates). *Polymer Reviews*, 49 (3), 226-248.

Macrae, R. and Wilkinson, J. (1958). Poly- -hydroxybutyrate Metabolism in Washed Suspensions of *Bacillus cereus* and *Bacillus megaterium*. *Journal of General Microbiology*, 19 (1), 210-222.

Martinez, S. and Déziel, E. (2020). Changes in polyhydroxyalkanoate granule accumulation make optical density measurement an unreliable method for estimating bacterial growth in *Burkholderia thailandensis*. *Canadian Journal of Microbiology*, 66 (3), 256-262.

Martinez, S., Humery, A., Groleau, M. and Déziel, E. (2020). Quorum Sensing Controls Both Rhamnolipid and Polyhydroxyalkanoate Production in *Burkholderia thailandensis* Through ScmR Regulation. *Frontiers in Bioengineering and Biotechnology*, 8, 1-15.

Masuko, T., Minami, A., Iwasaki, N., Majima, T., Nishimura, S. and Lee, Y. (2005). Carbohydrate analysis by a phenol–sulfuric acid method in microplate format. *Analytical Biochemistry*, 339 (1), 69-72.

McLafferty, F. (1956). Mass Spectrometric Analysis Broad Applicability to Chemical Research. *Analytical Chemistry*, 28 (3), 306-316.

Miller, C. and Gilmore, J. (2020). Detection of Quorum-Sensing Molecules for Pathogenic Molecules Using Cell-Based and Cell-Free Biosensors. *Antibiotics*, 9 (5), 259-282.

Miller, S., Xavier, K., Campagna, S., Taga, M., Semmelhack, M., Bassler, B. and Hughson, F. (2004). *Salmonella typhimurium* Recognizes a Chemically Distinct Form of the Bacterial Quorum-Sensing Signal AI-2. *Molecular Cell*, 15(5), 677-687.

Mohan, S., Oluwafemi, O., Kalarikkal, N., Thomas, S. and Songca, S. (2016). Biopolymers – Application in Nanoscience and Nanotechnology. *Recent Advances in Biopolymers*, 1(1), 47-66.

Mohanan, N., Gislason, A., Sharma, P., Ghergab, A., Plouffe, J., Levin, D. and de Kievit, T. (2019). Quorum sensing and the anaerobic regulator (ANR) control Polyhydroxyalkanoate (PHA) production in *Pseudomonas chlororaphis* PA23. *FEMS Microbiology Letters*, 366 (18), 1-10.

Mozejko-Ciesielska, J., Dabrowska, D., Szalewska-Palasz, A. and Ciesielski, S. (2017). Medium-chain-length polyhydroxyalkanoates synthesis by *Pseudomonas putida* KT2440 relA/spoT mutant: bioprocess characterization and transcriptome analysis. *AMB Express*, 7 (1).

Mozes-Koch, R., Tanne, E., Brodezki, A., Yehuda, R., Gover, O., Rabinowitch, H. and Sela, I. (2017). Expression of the entire polyhydroxybutyrate operon of *Ralstonia eutropha* in plants. *Journal of Biological Engineering*, 11(1).

Mravec, F., Obruca, S., Krzyzanek, V., Sedlacek, P., Hrubanova, K., Samek, O., Kucera, D., Benesova, P. and Nebesarova, J. (2016). Accumulation of PHA granules in *Cupriavidus necator* as seen by confocal fluorescence microscopy. *FEMS Microbiology Letters*, 363(10).

Nealson, K., Platt, T. and Hastings, J. (1970). Cellular Control of the Synthesis and Activity of the Bacterial Luminescent System. *Journal of Bacteriology*, 104(1), 313-322.

Nikje, M., Garmarudi, A. and Idris, A. (2011). Polyurethane Waste Reduction and Recycling: From Bench to Pilot Scales. *Designed Monomers and Polymers*, 14(5), 395-421.

Nikodinovic, J., Kenny, S., Babu, R., Woods, T., Blau, W. and O'Connor, K. (2008). The conversion of BTEX compounds by single and defined mixed

cultures to medium-chain-length polyhydroxyalkanoate. *Applied Microbiology and Biotechnology*, 80 (4), 665-673.

North, E and Halden, R. (2013). Plastics and the environment health: the road ahead. *Reviews on Environmental Health*, 28(1), 1-8.

Numata, K., Morisaki, K., Tomizawa, S., Ohtani, M., Demura, T., Miyazaki, M., Nogi, Y., Deguchi, S. and Doi, Y. (2013). Synthesis of poly- and oligo(hydroxyalkanoate)s by deep-sea bacteria, *Colwellia* s, *Moritella* s, and *Shewanella* s *Polymer Journal*, 45(10), 1094-1100.

Nygaard, D., Yashchuk, O. and Hermida, É. (2019). Evaluation of culture medium on poly(3-hydroxybutyrate) production by *Cupriavidus necator* ATCC 17697: application of the response surface methodology. *Heliyon*, 5 (3), 1-18

Oeding, V. and Schlegel, H. (1973).  $\beta$ -Ketothiolase from *Hydrogenomonas eutropha* H16 and its significance in the regulation of poly- $\beta$ -hydroxybutyrate metabolism. *Biochemical Journal*, 134(1), 239-248.

Paluch, E., Rewak-Soroczyńska, J., Jędrusik, I., Mazurkiewicz, E. and Jermakow, K. (2020). Prevention of biofilm formation by quorum quenching. *Applied Microbiology and Biotechnology*, 104 (5), 1871-1881.

Panchal, B. (2016). Production of Polyhydroxyalkanoates by *Pseudomonas mendocina* using vegetable oils and their characterisation. Ph.D. University of Westminster.

Papenfort, K. and Bassler, B. (2016). Quorum sensing signal–response systems in Gram-negative bacteria. *Nature Reviews Microbiology*, 14(9), 576-588.

Philip S., Keshavarz T., Roy I., 2007. Polyhydroxyalkanoates: biodegradable polymers with range of applications. *Journal of Chemical Technology and Biotechnology*, 82(3), 233-247.

Poblete-Castro, I., Becker, J., Dohnt, K., dos Santos, V. and Wittmann, C. (2012). Industrial biotechnology of *Pseudomonas putida* and related species. *Applied Microbiology and Biotechnology*, 93 (6), 2279-2290.

Poblete-Castro, I., Binger, D., Oehlert, R. and Rohde, M. (2014). Comparison of mcl-Poly(3-hydroxyalkanoates) synthesis by different *Pseudomonas putida* strains from crude glycerol: citrate accumulates at high titer under PHA-producing conditions. *BMC Biotechnology*, 14 (1), 1-11.

Poblete-Castro, I., Rodriguez, A., Lam, C. and Kessler, W. (2014). Improved Production of Medium-Chain-Length Polyhydroxyalkanoates in Glucose-Based Fed-Batch Cultivations of Metabolically Engineered *Pseudomonas putida* Strains. *Journal of Microbiology and Biotechnology*, 24 (1), 59-69.

Poli, A., Di Donato, P., Abbamondi, G. and Nicolaus, B. (2011). Synthesis, Production, and Biotechnological Applications of Exopolysaccharides and Polyhydroxyalkanoates by Archaea. *Archaea*, 2011, 1-13.

Preusting, H., Kingma, J. and Witholt, B. (1991). Physiology and polyester formation of *Pseudomonas oleovorans* in continuous two-liquid-phase cultures. *Enzyme and Microbial Technology*, 13 (10), 770-780.

Quillaguamán, J., Hashim, S., Bento, F., Mattiasson, B. and Hatti-Kaul, R. (2005). Poly( $\beta$ -hydroxybutyrate) production by a moderate halophile, *Halomonas boliviensis* LC1 using starch hydrolysate as substrate. *Journal of Applied Microbiology*, 99 (1), 151-157.

Quispe, C., Coronado, C. and Carvalho Jr., J. (2013). Glycerol: Production, consumption, prices, characterization and new trends in combustion. *Renewable and Sustainable Energy Reviews*, 27, 475-493.

Raghab, S., Abd El Meguid, A. and Hegazi, H. (2013). Treatment of leachate from municipal solid waste landfill. *HBRC Journal*, 9(2), 187-192.

Rai, R., Boccaccini, A., Knowles, J., Mordon, N., Salih, V., Locke, I., Moshrefi-Torbati, M., Keshavarz, T. and Roy, I. (2011). The homopolymer poly(3-hydroxyoctanoate) as a matrix material for soft tissue engineering. *Journal of Applied Polymer Science*, 122(6), 3606-3617.

Rai, R., Keshavarz, T., Roether, J., Boccaccini, A. and Roy, I. (2011). Medium chain length polyhydroxyalkanoates, promising new biomedical materials for the future. *Materials Science and Engineering: R: Reports*, 72 (3), 29-47.

Rai, R., Yunos, D. M., Boccaccini, A. R., Knowles, J. C., Barker, I. A., Howdle, S. M., Tredwell, G. D., Keshavarz, T. & Roy, I. 2011. Poly-3-hydroxyoctanoate P (3HO), a medium chain length polyhydroxyalkanoate homopolymer from *Pseudomonas mendocina*. *Biomacromolecules*, 12(1), 2126-2136.

Ramsay, J., Berger, E., Voyer, R., Chavarie, C. and Ramsay, B. (1994). Extraction of poly-3-hydroxybutyrate using chlorinated solvents. *Biotechnology Techniques*, 8(8), 589-594.

Rao, M., Bharathi, P. and Akila, R. (2014). A Comprehensive Review on Biopolymers. *Scientific Reviews and Chemical Communications*, 4(2), 61-66.

Rasamiravaka, T., Labtani, Q., Duez, P. and El Jaziri, M. (2015). The Formation of Biofilms by *Pseudomonas aeruginosa*: A Review of the Natural and Synthetic Compounds Interfering with Control Mechanisms. *BioMed Research International*, 2015(1), 1-17.

Ratledge, C. and Kristiansen, B. (2001). *Basic Biotechnology*, 2nd ed. Cambridge: Cambridge University Press.

Ray, A., Cot, M., Puzo, G., Gilleron, M. and Nigou, J. (2013). Bacterial cell wall macroamphiphiles: Pathogen-/microbe-associated molecular patterns detected by mammalian innate immune system. *Biochimie*, 95 (1), 33-42.

Raza, Z., Tariq, M., Majeed, M. and Banat, I. (2019). Recent developments in bioreactor scale production of bacterial polyhydroxyalkanoates. *Bioprocess and Biosystems Engineering*, 42 (6), 901-919.

Rehm, B. (2003). Polyester synthases: natural catalysts for plastics. *Biochemical Journal*, 376 (1), 15-33.

Rehm, B., Mitsky, T. and Steinbüchel, A. (2001). Role of Fatty Acid De Novo Biosynthesis in Polyhydroxyalkanoic Acid (PHA) and Rhamnolipid Synthesis by Pseudomonads: Establishment of the Transacylase (PhaG)-Mediated Pathway for PHA Biosynthesis in *Escherichia coli*. *Applied and Environmental Microbiology*, 67 (7), 3102-3109.

Rezzonico, F., Smits, T. and Duffy, B. (2012). Detection of AI-2 Receptors in Genomes of Enterobacteriaceae Suggests a Role of Type-2 Quorum Sensing in Closed Ecosystems. *Sensors*, 12 (5), 6645-6665.

Rijk, T.C., van de Meer, P., Eggink, G., Weusthuis, R. (2005) Methods for Analysis of Poly(3-hydroxyalkanoate) (PHA) Composition. *Biopolymers Online*. 1-12.

Santolin, L., Waldburger, S., Neubauer, P. and Riedel, S. (2021). Substrate-Flexible Two-Stage Fed-Batch Cultivations for the Production of the PHA Copolymer P(HB-co-HHx) With *Cupriavidus necator* Re2058/pCB113. *Frontiers in Bioengineering and Biotechnology*, 9.

Sathiyarayanan, G., Bhatia, S., Song, H., Jeon, J., Kim, J., Lee, Y., Kim, Y. and Yang, Y. (2017). Production and characterization of medium-chain-length polyhydroxyalkanoate copolymer from Arctic psychrotrophic bacterium

*Pseudomonas* sp. PAMC 28620. *International Journal of Biological Macromolecules*, 97 (1), 710-720.

Shah, A., Hasan, F., Hameed, A. and Ahmed, S. (2008). Biological degradation of plastics: A comprehensive review. *Biotechnology Advances*, 26 (3), 246-265.

Shahid, S., Mosrati, R., Ledauphin, J., Amiel, C., Fontaine, P., Gaillard, J. and Corroler, D. (2013). Impact of carbon source and variable nitrogen conditions on bacterial biosynthesis of polyhydroxyalkanoates: Evidence of an atypical metabolism in *Bacillus megaterium* DSM 509. *Journal of Bioscience and Bioengineering*, 116 (3), 302-308.

Sharma, P., Munir, R., Blunt, W., Dartiailh, C., Cheng, J., Charles, T. and Levin, D. (2017). Synthesis and Physical Properties of Polyhydroxyalkanoate Polymers with Different Monomer Compositions by Recombinant *Pseudomonas putida* LS46 Expressing a Novel PHA SYNTHASE (PhaC116) Enzyme. *Applied Sciences*, 7 (3), 242.

Shimizu, R., Chou, K., Orita, I., Suzuki, Y., Nakamura, S. and Fukui, T. (2013). Detection of phase-dependent transcriptomic changes and Rubisco-mediated CO<sub>2</sub> fixation into poly (3-hydroxybutyrate) under heterotrophic condition in *Ralstonia eutropha* H16 based on RNA-seq and gene deletion analyses. *BMC Microbiology*, 13 (1), 169.

Silagyi, K., Kim, S., Martin Lo, Y. and Wei, C. (2009). Production of biofilm and quorum sensing by *Escherichia coli* O157:H7 and its transfer from contact surfaces to meat, poultry, ready-to-eat deli, and produce products. *Food Microbiology*, 26 (5), 514-519.

Sindhu, R., Ammu, B., Binod, P., Deepthi, S., Ramachandran, K., Soccol, C. and Pandey, A. (2011). Production and characterization of poly-3-hydroxybutyrate from crude glycerol by *Bacillus sphaericus* NII 0838 and improving its thermal properties by blending with other polymers. *Brazilian Archives of Biology and Technology*, 54 (4), 783-794.

Singh, N., Hui, D., Singh, R., Ahuja, I., Feo, L. and Fraternali, F. (2017). Recycling of plastic solid waste: A state of art review and future applications. *Composites Part B: Engineering*, 115 (1), 409-422.

Solaiman, D., Ashby, R. and Foglia, T. (1999). Medium-Chain-Length Poly( $\beta$ -Hydroxyalkanoate) Synthesis from Triacylglycerols by *Pseudomonas saccharophila*. *Current Microbiology*, 38 (3), 151-154.

Spiekermann, P., Rehm, B., Kalscheuer, R., Baumeister, D. and Steinbüchel, A. (1999). A sensitive, viable-colony staining method using Nile red for direct screening of bacteria that accumulate polyhydroxyalkanoic acids and other lipid storage compounds. *Archives of Microbiology*, 171 (2), 73-80.

Srinivasan, R., Karaoz, U., Volegova, M., MacKichan, J., Kato-Maeda, M., Miller, S., Nadarajan, R., Brodie, E. and Lynch, S. (2015). Use of 16S rRNA Gene for Identification of a Broad Range of Clinically Relevant Bacterial Pathogens. *PLOS ONE*, 10 (2), 1-22.

Steinbüchel, A. (1991). Polyhydroxyalkanoic acids. In: D. Byrom, ed., *Biomaterials*, 1st ed. London: Palgrave Macmillan, 123-213.

Steindler, L., Bertani, I., De Sordi, L., Schwager, S., Eberl, L. and Venturi, V. (2009). LasI/R and RhII/R Quorum Sensing in a Strain of *Pseudomonas aeruginosa* Beneficial to Plants. *Applied and Environmental Microbiology*, 75 (15), 5131-5140.

Subramoni, S. and Venturi, V. (2009). PpoR is a conserved unpaired LuxR solo of *Pseudomonas putida* which binds N-acyl homoserine lactones. *BMC Microbiology*, 9 (1), 125.

Sudesh, K., Abe, H. and Doi, Y. (2000). Synthesis, structure and properties of polyhydroxyalkanoates: biological polyesters. *Progress in Polymer Science*, 25 (10), 1503-1555.

Sukan, A. (2015). Dual Biopolymer Production and Separation from Cultures of *Bacillus* spp.. Ph.D. University of Westminster.

Sun, Z., Ramsay, J., Guay, M. and Ramsay, B. (2007). Carbon-limited fed-batch production of medium-chain-length polyhydroxyalkanoates from nonanoic acid by *Pseudomonas putida* KT2440. *Applied Microbiology and Biotechnology*, 74 (1), 69-77.

Sutcliffe, I. and Shaw, N. (1991). Atypical lipoteichoic acids of gram-positive bacteria. *Journal of Bacteriology*, 173 (22), 7065-7069.

Tae-Kwon, K., Dong Shin, H., Cheol Seo, M., Lee, J. and Lee, Y. (2003). Molecular structure of PCR cloned PHA synthase genes of *Pseudomonas putida* KT2440 and its utilization for medium-chain length polyhydroxyalkanoate production. *Journal of Microbiology and Biotechnology*, 13 (2), 182-190.

Tan, G., Chen, C., Li, L., Ge, L., Wang, L., Razaad, I., Li, Y., Zhao, L., Mo, Y. and Wang, J. (2014). Start a Research on Biopolymer Polyhydroxyalkanoate (PHA): A Review. *Polymers*, 6 (3), 706-754.

Tansel, B. and Yildiz, B. (2011). Goal-based waste management strategy to reduce persistence of contaminants in leachate at municipal solid waste landfills. *Environment, Development and Sustainability*, 13(5), 821-831.

Turovskiy, Y., Kashtanov, D., Paskhover, B. and Chikindas, M. (2007). Quorum Sensing: Fact, Fiction, and Everything in Between. *Advances in Applied Microbiology*, 62(1), 191-234.

Urbanek, A., Rymowicz, W. and Mirończuk, A. (2018). Degradation of plastics and plastic-degrading bacteria in cold marine habitats. *Applied Microbiology and Biotechnology*, 102(18), 7669-7678.

Valappil, S., Boccaccini, A., Bucke, C. and Roy, I. (2007). Polyhydroxyalkanoates in Gram-positive bacteria: insights from the genera *Bacillus* and *Streptomyces*. *Antonie van Leeuwenhoek*, 91 (1), 1-17.

Valentin, H., Lee, E., Choi, C. and Steinbüchel, A. (1994). Identification of 4-hydroxyhexanoic acid as a new constituent of biosynthetic polyhydroxyalkanoic acids from bacteria. *Applied Microbiology and Biotechnology*, 40 (5), 710-716.

Verbeke, F., De Craemer, S., Debunne, N., Janssens, Y., Wynendaele, E., Van de Wiele, C. and De Spiegeleer, B. (2017). Peptides as Quorum Sensing Molecules: Measurement Techniques and Obtained Levels In vitro and In vivo. *Frontiers in Neuroscience*, 11(1), 1-13.

Verma, R., Vinoda, K., Papireddy, M. and Gowda, A. (2016). Toxic Pollutants from Plastic Waste- A Review. *Procedia Environmental Sciences*, 35(1), 701-708.

Veselova, M. (2010). Quorum sensing regulation in *Pseudomonas*. *Russian Journal of Genetics*, 46 (2), 129-137.

Irorere, V., Kwienzien, M., Tripathi, L., Cobice, D., McClean, S., Marchant, R. and Banat, I. (2019). Quorum sensing as a potential target for increased production of rhamnolipid biosurfactant in *Burkholderia thailandensis* E264. *Applied Microbiology and Biotechnology*, 103 (16), 6505-6517.

Vizcaino-Caston, I., Kelly, C., Fitzgerald, A., Leeke, G., Jenkins, M. and Overton, T. (2016). Development of a rapid method to isolate

polyhydroxyalkanoates from bacteria for screening studies. *Journal of Bioscience and Bioengineering*, 121 (1), 101-104.

Wallen, L. and Rohwedder, W. (1974). Poly- $\beta$ -hydroxyalkanoate from activated sludge. *Environmental Science & Technology*, 8(6), 576-579.

Waters, C. and Bassler, B. (2005). QUORUM SENSING: Cell-to-Cell Communication in Bacteria. *Annual Review of Cell and Developmental Biology*, 21(1), 319-346.

Webb, H., Arnott, J., Crawford, R. and Ivanova, E. (2012). Plastic Degradation and Its Environmental Implications with Special Reference to Poly(ethylene terephthalate). *Polymers*, 5(1), 1-18.

Wilkes, R. and Aristilde, L. (2017). Degradation and metabolism of synthetic plastics and associated products by *Pseudomonas* sp.: capabilities and challenges. *Journal of Applied Microbiology*, 123(3), 582-593.

Windhorst, C. and Gescher, J. (2019). Efficient biochemical production of acetoin from carbon dioxide using *Cupriavidus necator* H16. *Biotechnology for Biofuels*, 12 (1).

Xavier, K. and Bassler, B. (2003). LuxS quorum sensing: more than just a numbers game. *Current Opinion in Microbiology*, 6(2), 191-197.

Xavier, K. and Bassler, B. (2004). Regulation of Uptake and Processing of the Quorum-Sensing Autoinducer AI-2 in *Escherichia coli*. *Journal of Bacteriology*, 187(1), 238-248.

Xu, Z., Pan, C., Li, X., Hao, N., Zhang, T., Gaffrey, M., Pu, Y., Cort, J., Ragauskas, A., Qian, W. and Yang, B. (2021). Enhancement of polyhydroxyalkanoate production by co-feeding lignin derivatives with glycerol in *Pseudomonas putida* KT2440. *Biotechnology for Biofuels*, 14 (1), 1-23.

Yang, S., Li, S. and Jia, X. (2019). Production of medium chain length polyhydroxyalkanoate from acetate by engineered *Pseudomonas putida* KT2440. *Journal of Industrial Microbiology & Biotechnology*, 46 (6), 793-800.

Yarwood, J. and Schlievert, P. (2003). Quorum sensing in *Staphylococcus* infections. *Journal of Clinical Investigation*, 112(11), 1620-1625.

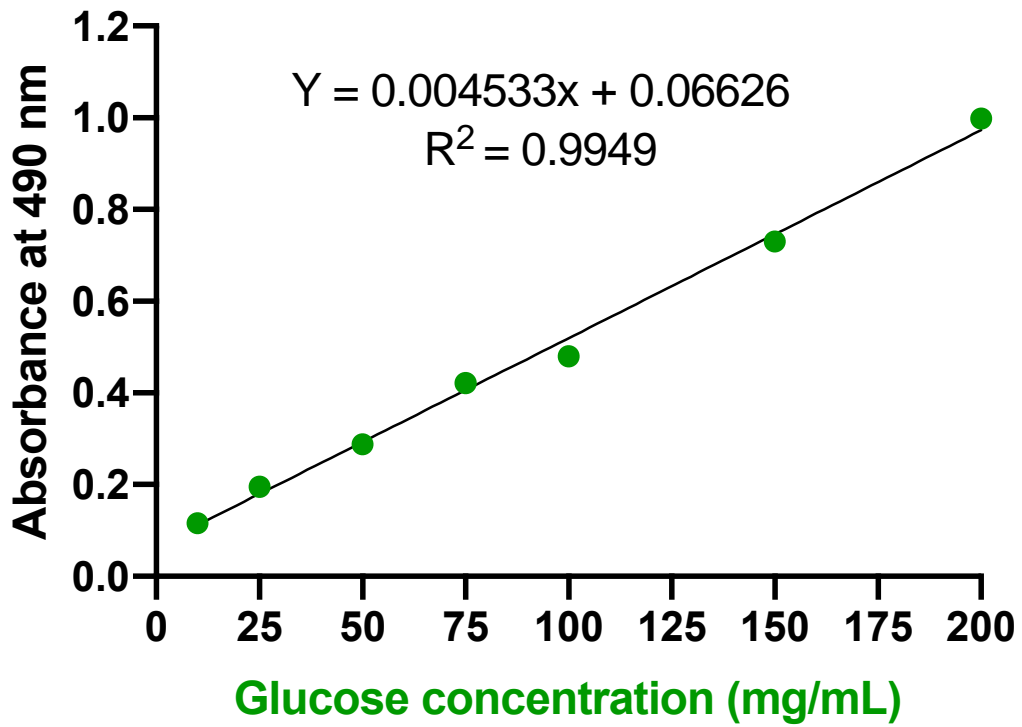
York, G., Lupberger, J., Tian, J., Lawrence, A., Stubbe, J. and Sinskey, A. (2003). *Ralstonia eutropha* H16 Encodes Two and Possibly Three Intracellular

Poly[d-(-)-3-Hydroxybutyrate] Depolymerase Genes. *Journal of Bacteriology*, 185 (13), 3788-3794.

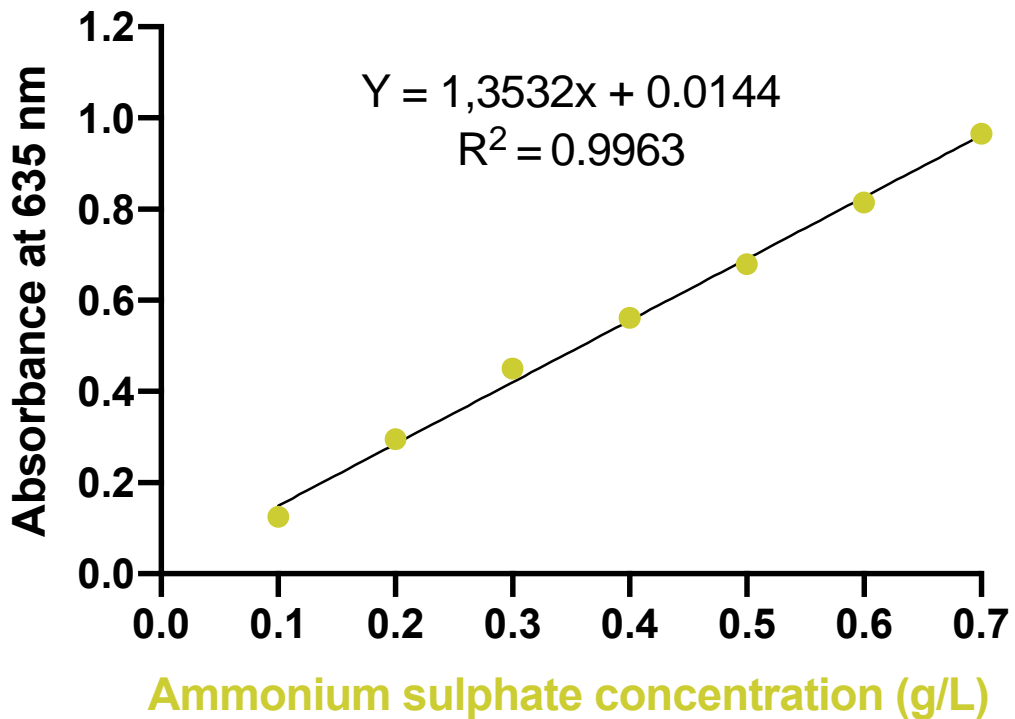
Zahari, M. A. K. M., Ariffin, H., Mokhtar, M. N., Salihon, J., Shirai, Y., and Hassan, M. A. 2015. Case study for a palm biomass biorefinery utilizing renewable non-food sugars from oil palm frond for the production of poly (3-hydroxybutyrate) bioplastic. *Journal of Cleaner Production*, 87, 284-290.

## Appendix

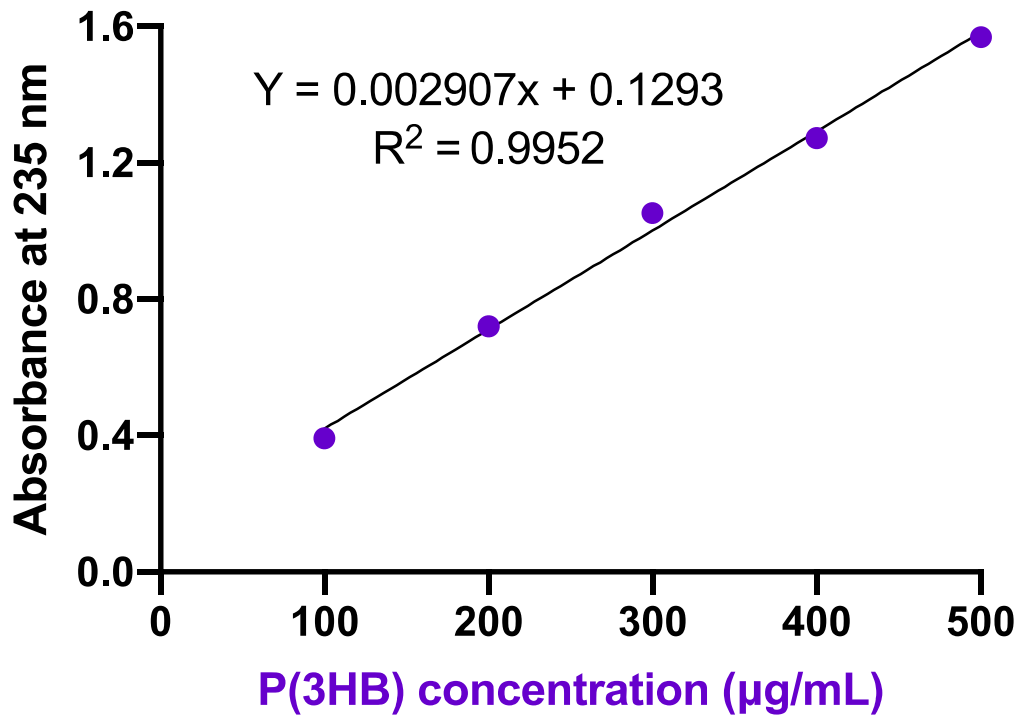
Calibration curves



Appendix 1: Total carbohydrates calibration curve



Appendix 2: Nitrogen concentration calibration curve



Appendix 3: Crotonic acid calibration curve